A. Hahne, J. Callies, A. Lefebvre & B. Christensen
ERS Project Division, ESTEC, Noordwijk, The Netherlands

R. Hoekstra, L. Fontijn, C. Olij, E. Zoutman & G. Nützel
TPD-TNO, Delft, The Netherlands

Calibration of the GOME Instrument for ERS-2

Abstract

The Global Ozone Monitoring Experiment (GOME) is an optical spectrometer to be flown on the second European Remote-Sensing Satellite, ERS-2 [1]. Its main task will be to measure the ozone content of the atmosphere and to monitor its long-term variation. Ozone is a trace gas of vital importance to mankind, as it absorbs the harmful ultraviolet radiation emitted by the Sun and prevents it from reaching the Earth's surface. This absorption occurs in an ozone layer concentrated in the stratosphere, at altitudes of between 18 and 40 km, which is threatened by human activities, in particular by the release of Chloro-Fluoro-Carbons (CFCs) used in spray cans, refrigerators and foams, and as a cleaning agent. Ozone depletion is believed to be taking place at a rate of about 0.3% per year.

The reliable measurement of such a small global trend against the background of normal spatial and temporal variability, places high demands on the instrument's accuracy and stability. To meet with these requirements, the instrument needs thorough calibration and characterisation, both on the ground and in orbit.

The breadboard model of the GOME instrument – which is functionally fully representative including the on-board means of calibration – has been subjected to a dry calibration run on the ground, and the test results are reported here.

1. Calibration requirements and the on-board calibration concept

The conventional approach for measuring ozone, which is the underlying principle of the American SBUV and TOMS instruments, is the monitoring of upwelling backscattered radiance at a number of discrete wavelengths. To yield meaningful results, the radiometric response of an instrument used in this mode must be known to better than 1%. Because the space environment is known to change the radiometric response of the instrument (e.g. by radiation-induced darkening of transmissive optics), the means for carrying out on-board calibration with the necessary stability have to be provided to enable re-calibration at regular intervals.

This is normally done by looking at the Sun, which is a rather stable light source for the wavelength range in question. However, because the solar irradiance is several orders of magnitude higher than the radiance coming from the Earth, the Sun cannot be used directly, but only via a diffuser. This diffuser attenuates the light to a level that falls within the dynamic range of the detection system, and also makes the measurement path insensitive to the variations in the line-of-sight to the Sun as function of the seasonal change in the Earth–Sun distance.

As GOME is intended to achieve continuity with the long-term records of ozone concentrations already accrued by the SBUV and TOMS instruments, this concept has been adopted for GOME also. There is, however, an alternative measurement principle known as 'Differential Optical Absorption Spectroscopy', which is made possible by the availability of multi-pixel array detectors capable of recording a continuous spectrum over a large wavelength range. With this technique, a recorded atmospheric spectrum is divided by a solar spectrum, thereby compensating for the Sun's variability (which, of course, also appears in the backscattered light), as well as for the variations in the optical throughput. To the divided spectrum obtained in this way, the absorption spectra of ozone and possibly other trace gases are then fitted, thus providing the means to retrieve the amounts of the target (absorbing) species.

For this technique to work, the wavelength observations (for both the solar spectrum and the backscattered spectrum from the atmosphere) have to be very accurate*. However, launch effects and temperature variations around the orbit prevent this stability from being achieved. Thus with GOME it is proposed to measure the wavelength shifts with the aid of a calibration lamp, which provides a sufficient number of sharp atomic emission lines in each channel to map wavelength shifts around the orbit and correct for them in the ground processing (Fig. 1).

* Ideally, the wavelength stability between recordings should be 1/100 th of a pixel.

Figure 1. The spectrometer optics of the GOME instrument

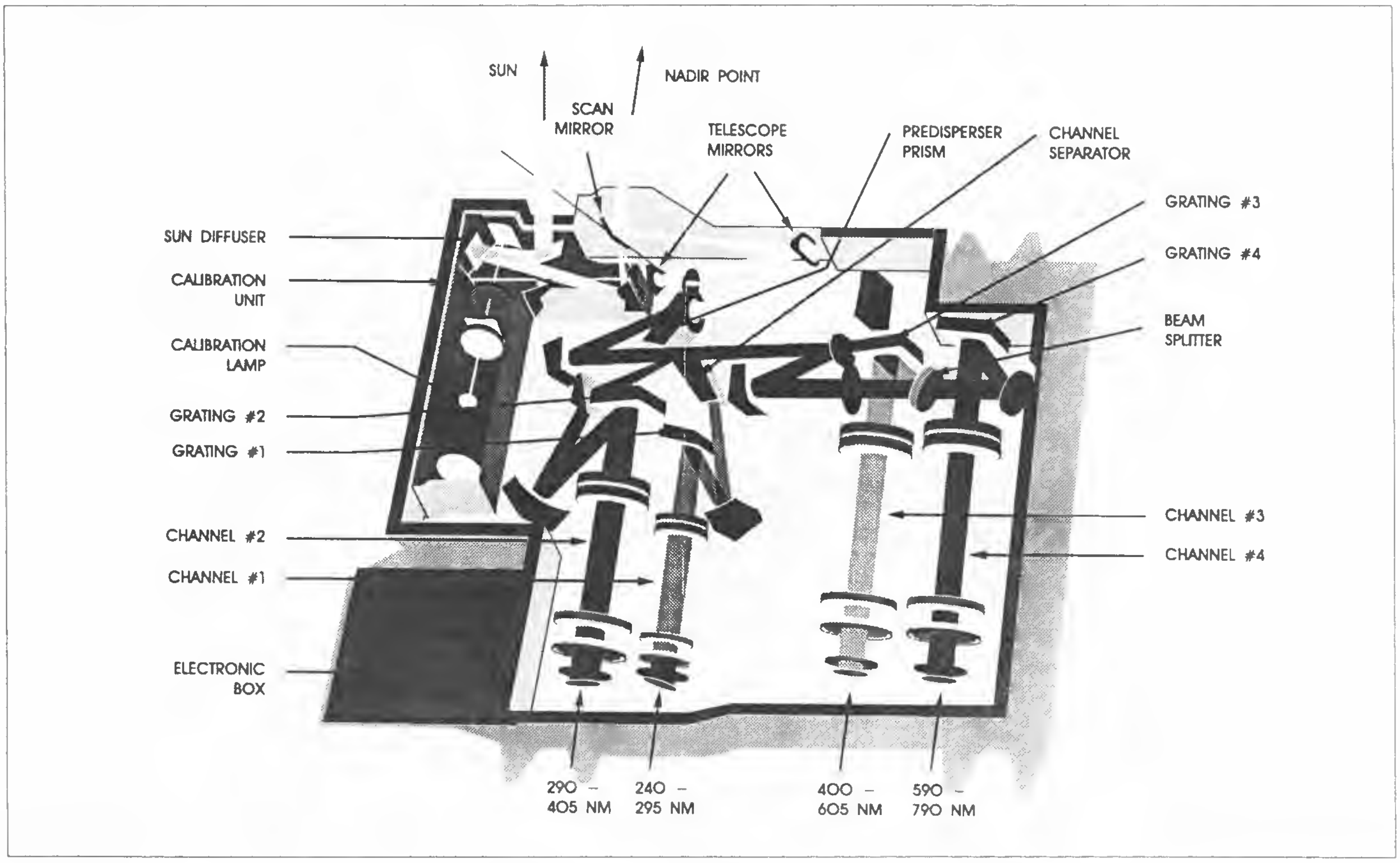

In addition to this basic calibration facility, there are in-flight provisions for:
- measuring the dark current and fixed pattern noise of the detectors and the readout chain
- calibrating the Analogue-to-Digital Converters (ADCs)
- monitoring pixel-to-pixel variability by illuminating the detectors with Light-Emitting Diodes (LEDs) built into the optical objectives of the four channels
- monitoring the reflectance of the Sun diffuser, by channelling the light from the wavelength calibration lamp via the diffuser and ratioing the measurements with the corresponding ones made when the lamp is observed directly
- finally, by tilting the scan mirror to an angle between 70° and 85° with respect to nadir, it is possible to use the Moon as a calibration target.

2. The on-board calibration unit

Almost all on-board calibration facilities (except the LEDs mentioned in the previous section) are grouped in the Calibration Unit, which is shown in Figure 2. Its two key elements are:
- the calibration lamp, and
- the Sun diffuser.

2.1. The calibration lamp

Key requirements for the calibration lamp are:
- a number of sharp spectral lines spanning the entire wavelength range observed by GOME
- a lifetime compatible with the mission (500 h, with at least 1000 on/off cycles)
- low power consumption: less than 5 W, including DC/DC conversion losses
- a rugged design, as the lamp must be able to withstand both the launch and in-orbit environments.

The lamp selected is a hollow-cathode type, which has already been flown in a similar configuration on several NASA missions. The fill-gas is neon, with a platinum cathode with 10% chromium in order to provide some additional lines needed to span the GOME wavelength range.

A small life-test programme has been conducted, operating one lamp continuously for 1500 h and another intermittently, with 5 min on and 5 min off, for 6000 cycles. The lamp current was regulated to 10 mA. The test showed very satisfactory results, as did the environmental (vibration and thermal vacuum) test programme.

Figure 3a shows the 'naked' lamp, and Figure 3b the lamp in the suspension used in the calibration unit. Figure 4 shows the spectrum of the lamp used in the GOME Breadboard Model (BBM).

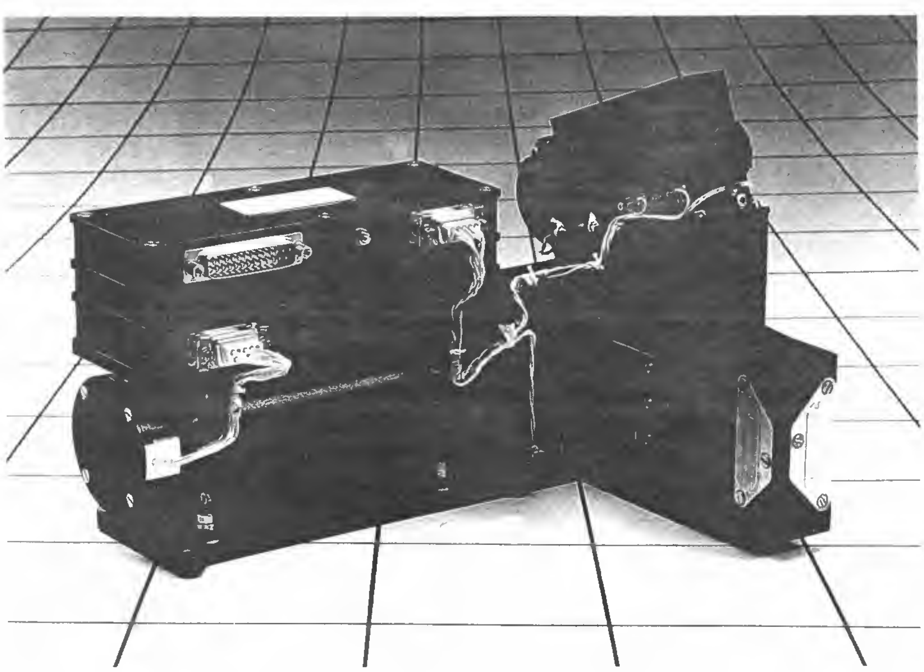

Figure 2. The on-board calibration unit

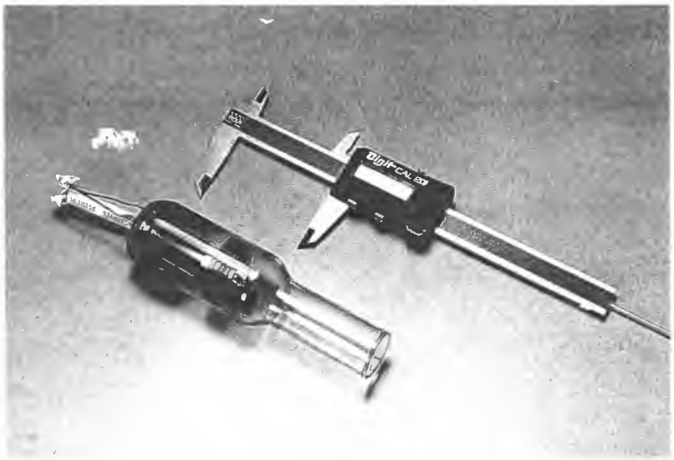

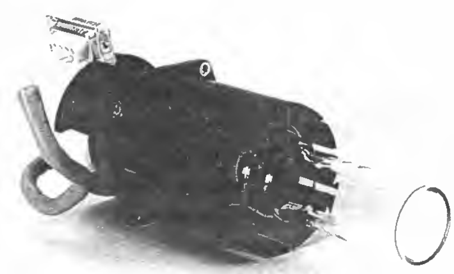

Figure 3a. The 'naked' wavelength calibration lamp

Figure 3b. The calibration lamp in its calibration-unit mount

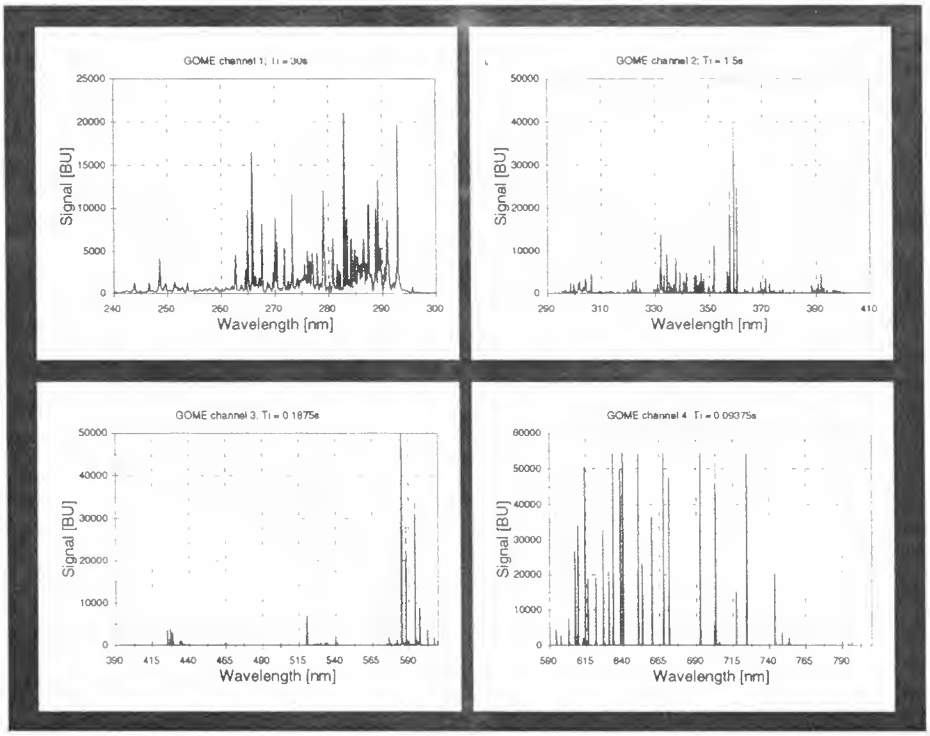

Figure 4. Spectrum of the calibration lamp, as measured for the GOME breadboard model (BBM)

2.2. The diffuser

The purpose of the Sun diffuser is to enable a calibration to be carried out with the standard system without the need for an accurate Sun acquisition and tracking mechanism. In order to obtain a reliable Sun calibration, the diffuser must have:
- a well-known Bi-Directional Scattering Function (BSDF)
- good uniformity over the illuminated surface
- a smooth and well-known wavelength response for the wavelength range of interest
- excellent in-orbit stability.

A short technology-development programme has been conducted at TPD/TNO Delft (NL) to select the most suitable material/process for the diffuser. Materials that have been investigated include aluminium oxide, quartz, magnesium oxide, titanium dioxide, barium sulphate, and aluminium with various surface treatments and coatings. Mainly for in-orbit stability reasons, a wet-blasted Aluminium 6082 with a 5 nm chromium and a 100 nm aluminium vacuum-deposited coating have been selected.

Figure 5 shows the diffuser produced with this technology, and Figure 6 the measured BSDF with the angular range of interest indicated.

2.3. The calibration unit

Aside from the lamp (with its housing) and the Sun diffuser, the Calibration Unit comprises:

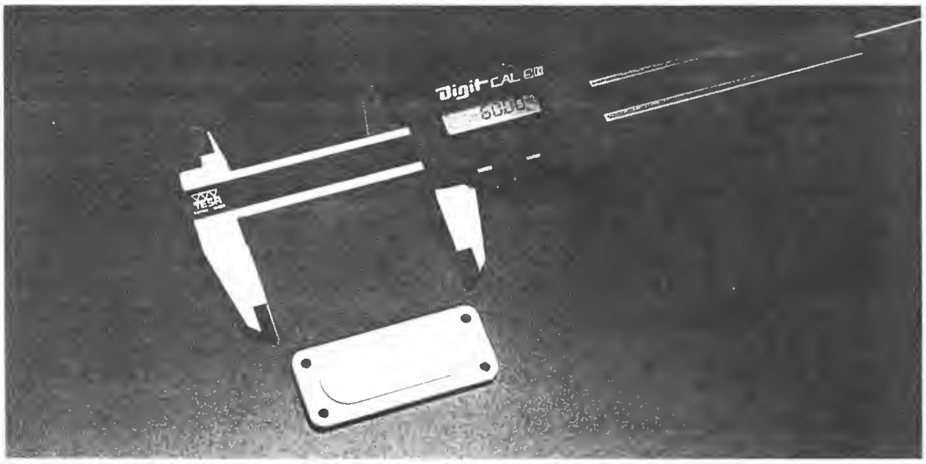

Figure 5. Wet-blasted aluminium diffuser

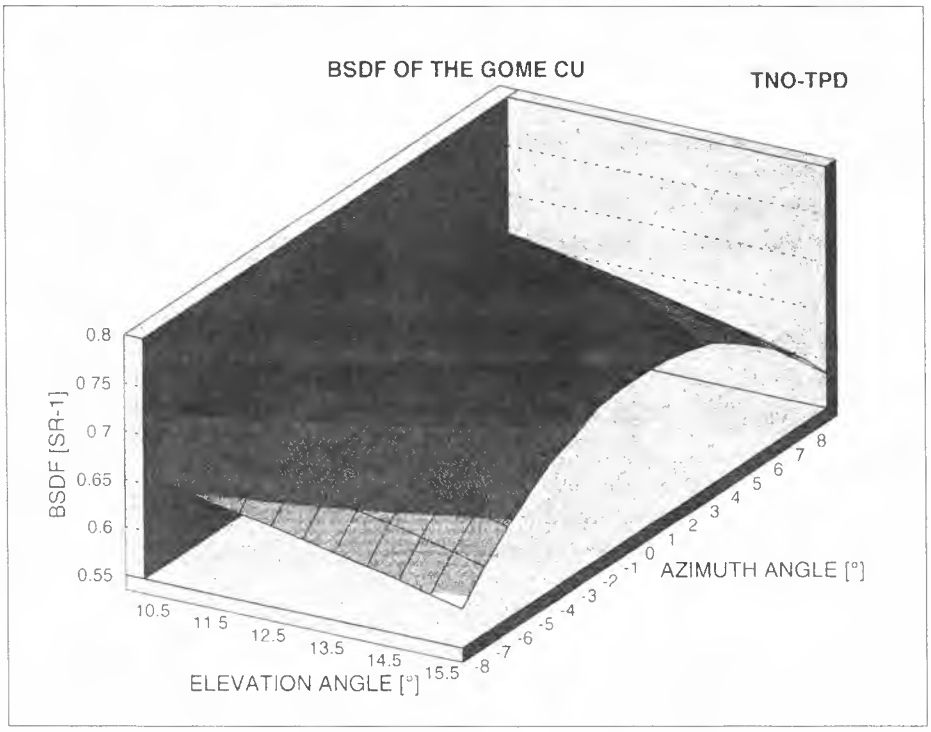

Figure 6. BSDF for the angular range of interest

- the power supply for the lamp, providing a voltage ramp to supply the ignition voltage of about 300 V and a stabilised current across the lamp of 10 mA
- the optical elements needed to ensure that the spectrometer slit and pupil are fully illuminated for both the lamp-calibration and Sun-calibration modes
- a shutter, which protects the diffuser when it is not being used for Sun calibration
- a mesh between shutter and diffuser, providing further protection to the diffuser and an additional attenuation of the light level received from the Sun.

The latter two items have been implemented based on NASA experiences which have shown that diffuser degradation is directly correlated with the time of exposure to sunlight (probably due to polymerisation of deposited contaminants caused by hard ultraviolet light).

3. The ground-calibration programme

Although a number of means for on-board calibration are included in GOME, they do not provide access to all the necessary parameters. These parameters are measured during the on-ground calibration programme and are not anticipated to change from ground to orbit.

The most important measurements to be conducted on the ground are:

- the measurement of the diffuser BSDF over the GOME wavelength range

– the characterisation of the polarisation response of the instrument as a function of the optical path (normal observation path and Sun observation path), scan mirror position (the scan mirror reflectivity for *s*- and *p*-polarisation is a function of the mirror angle), and wavelength.

On top of this, there are a number of additional measurements used for various purposes: more comprehensive instrument characterisation, consistency cross-checking, backup measurement for the case of lamp failure, and generation of test data for processing-algorithm checking.

In particular, the programme comprises:

Radiance/irradiance measurements: By illuminating the normal observation path and the Sun observation path with known radiance/irradiance, the radiometric calibration concept can be checked.

Wavelength calibration: During instrument-level thermal-vacuum testing, spectra of the calibration lamp have been recorded at different temperatures to measure wavelength shifts as a function of the temperature and the air/vacuum difference.

Detector characterisation: Dark current, readout noise, pixel-to-pixel sensitivity variations, and electronic chain performances including response linearity have been measured.

Straylight characterisation: This includes intra-channel (from high-intensity end to low-intensity end), inter-channel (from one channel to the other), and out-of-field and out-of-band straylight measurements.

Field-of-view characterisation: The variability, if any, in the radiometric response and spectral shift in the along-slit direction is measured. This is of particular interest for the lunar calibration, as the Moon only partially fills the spectrometer slit.

Measurement of the slit function: The slit function (i.e. the modulation transfer function of the entire optical system from the slit up to and including the detector) is determined. This is used to convolute high-resolution reference spectra of atmospheric species to the resolution of GOME.

4. The breadboard-model calibration programme

Recognising that this is quite a demanding programme, preparations for the calibration started as early as 1991. After agreement in principle on the scope of the programme with the scientists involved in GOME, TPD in Delft (NL) proceeded with the design, manufacturing, procurement and testing of all the necessary elements:
– turntable and fixtures to accommodate the instrument during the measurements
– calibrated lamps, diffusers and reference detectors procured from the National Institute of Standards
– monochromator and polariser covering the entire GOME wavelength range
– a temperature-controlled room to host the whole setup, clean room class 10.000, all black-painted (even including storage cabinet and water sink and tap) to suppress external straylight
– computer and software to control all the settings and provide them to the GOME Electrical Ground-Support Equipment (EGSE), to enable correlation between the GOME measurement data and the settings of the calibration setup
– algorithms and software to analyse the data, e.g. for noise correction, wavelength shift detection, BSDF computation, etc.
– procedures for setting up, aligning and performing the measurements
– calibration error budgets to establish the expected accuracy and precision of the measurements.

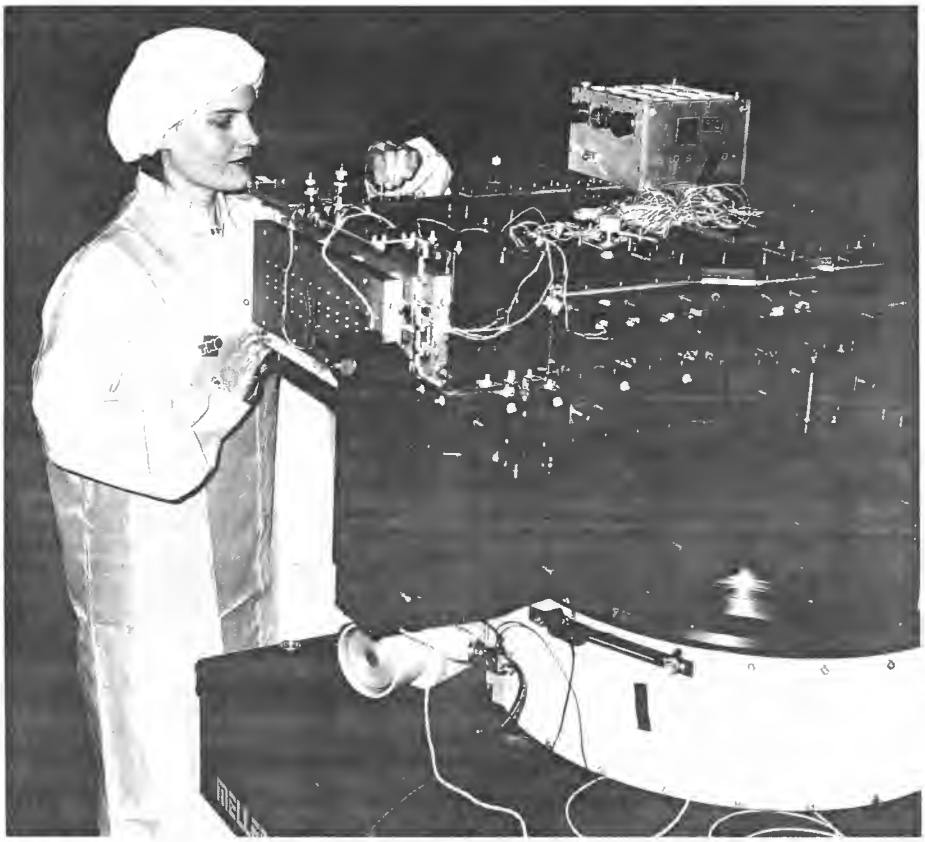

Figure 7. GOME on the turntable in the calibration facility

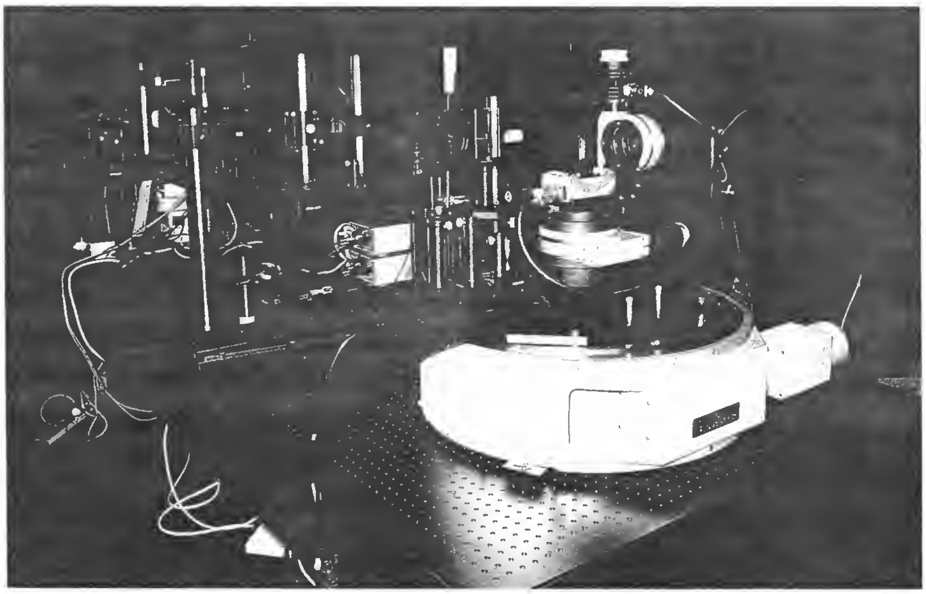

Figure 8. Part of the GOME calibration setup. Note the black environment for reducing external straylight

It was realised that to perform this exercise on only the flight model would be very risky and schedule-critical. A dry run involving all the steps and procedures has therefore been carried out on the GOME breadboard model which, since the negotiation of the main GOME development contract (Phase-C/D), has evolved into a fully-fledged de-facto engineering model, being very representative of the final flight-model configuration.

Figure 7 shows the GOME BBM mounted on the turntable in the TPD facility, while Figure 8 shows part of the optical instrumentation for performing the calibration.

First, wavelength characterisation and radiometric stability checking were carried out during the thermal-vacuum test at instrument level in the vacuum chamber of the instrument's prime contractor, Officine Galileo (I). This was then followed by two calibration periods, April–August 1993 and November–December 1993, with an intermediate review to scrutinise the results. A final review in March 1994 then concluded the BBM calibration, and the modifications necessary for the flight-model programme were agreed.

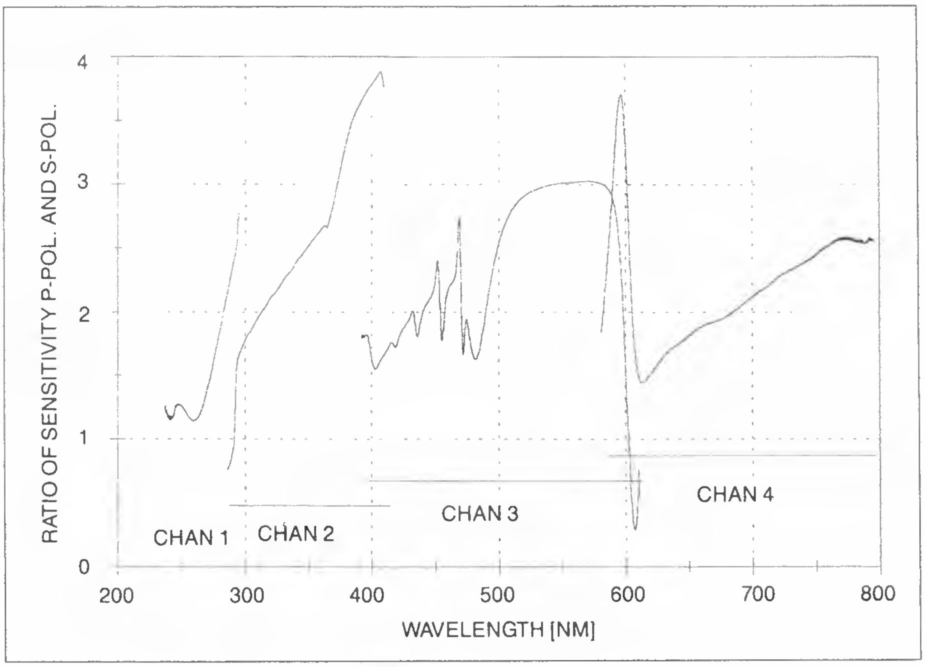

Figure 9. Polarisation response of the breadboard model (BBM)

5. Results of the BBM calibration/characterisation

BSDF: The BSDF as measured on the flight diffuser is a smooth function of both the azimuth/elevation angles and the wavelength (see Fig. 6).

Polarisation response: As expected, the instrument shows a pronounced polarisation response. In particular, channel 3 shows some narrow structure in the polarisation ratio (s over p), which is believed to be due to the combined effects of the dichroic beam-splitter and grating (Fig. 9).

Radiance/irradiance measurements: For schedule reasons, the BSDF of the BBM calibration unit could not be measured prior to integration into the BBM, so that a proper consistency check was not possible.

Wavelength calibration: During instrument- and payload-level thermal-vacuum and thermal-balance tests, the spectral stability as a function of temperature was verified. Spectral shifts in all channels were less than 0.02 pixel/°C. With an orbital temperature swing of about ±1°C, an excellent spectral stability for a passive thermal design is achieved. Figure 10 shows the instrument mounted in the Galileo thermal-vacuum chamber.

Detector characterisation: Both the dark current and its noise proved to be very low (also due to the good stability of the detector cooling loop). Pixel-to-pixel sensitivity variations across the 1024-pixel arrays were, at less than 2%, much better than the detector manufacturer had envisaged. Some electronic noise was detected in certain

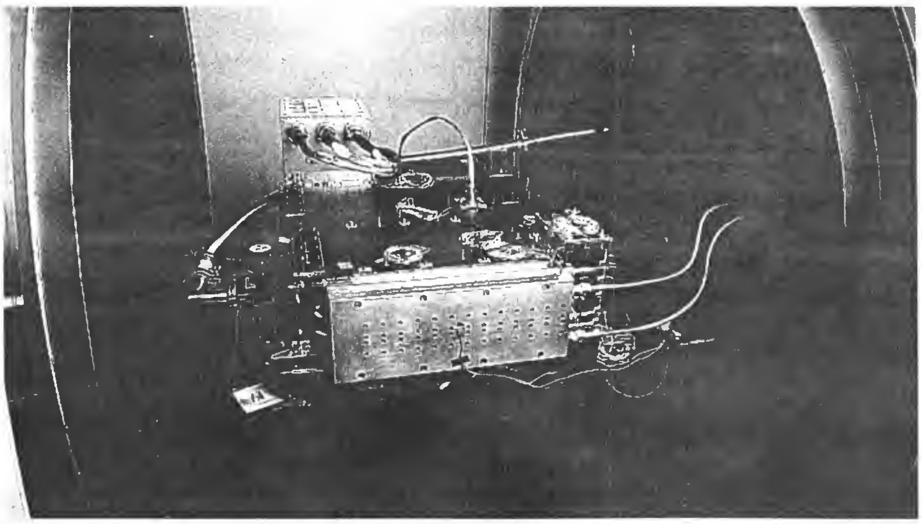

Figure 10. GOME breadboard model (BBM) during the TV test

readout situations. This was due to the ringing of the leading edge of the strobe pulse and to interference with the read-out of a temperature sensor. Both problems have been fed back into the instrument design and should be solved for the flight model.

Straylight characterisation: Quite detailed investigations were necessary to clarify the observed levels of straylight. A path for external straylight was identified and the problem solved via more and improved instrument internal baffling. Inter-channel straylight proved to be low and presented no problem.

More crucial was the intra-channel straylight, particularly that in channel 2, where at the short-wavelength end a roll-off of the signal level (by three orders of magnitude) presented a significant problem. Multiple reflections between the detector and the objective lenses and the gratings, respectively, were identified as the major cause. In channels 3 and 4 the problem could be resolved by the provision of improved anti-reflection coatings on the lenses and by slightly tilting the gratings. For channel 2, this would not have been sufficient and so, in consultation with the GOME scientists, it was decided to move the wavelength split between channels 1 and 2 to a higher value, thereby safeguarding the important channel 2, but sacrificing the performance of channel 1 slightly. The problem was alleviated by measuring straylight levels on some (so far unused) pixels, enabling some correction to be made for straylight in the ground processing.

Field-of-view characterisation

The design parameters for the GOME FOV are 0.14° x 2.8°. Under normal observational conditions, the entire slit and the entire GOME pupil are illuminated. However, when the Moon is observed, only a fraction of the slit is illuminated. For that reason, several scans have been made of the FOV by using collimated light as input for the GOME telescope. These measurements provide information on:
- actual dimensions of the FOV
- out-of-field scattered light
- influence on radiometric response and on wavelength scale when only a fraction of the FOV is illuminated.

Figure 11 shows the radiometric output of GOME for channel 3 when the FOV is scanned along the 2.8° axis of the FOV.

Slit function

This function represents the spectral line shape output for monchromatic input. It is a convolution of entrance slit width as imaged onto the spectral plane, detector pixel

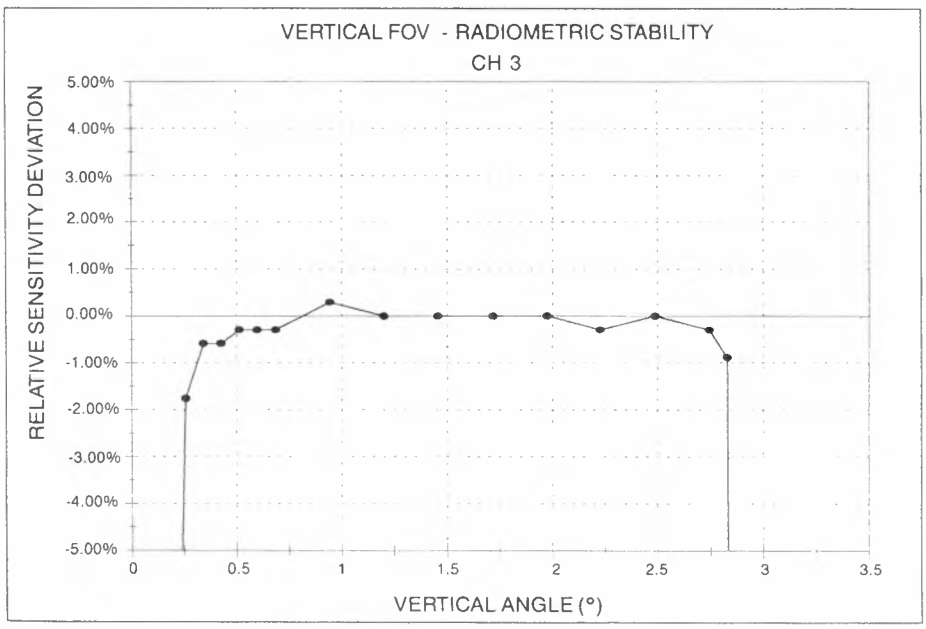

Figure 11. Radiometric response variation along the field of view

Figure 12. Slit function approximation in channel 4. The thin line is an approximation with a rectangular slit function,the thick line with a sixth-order polynomial

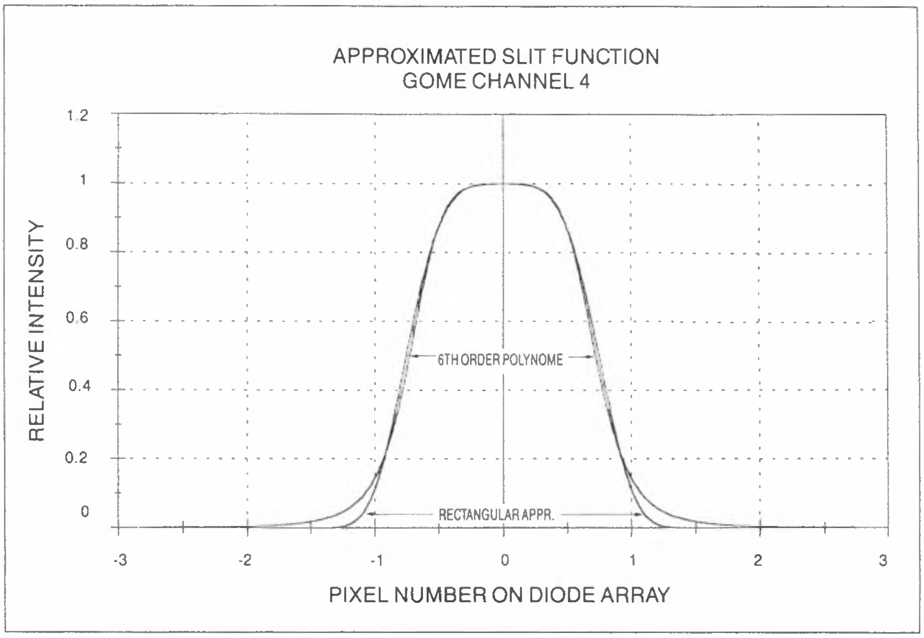

width, optical aberrations and residual effects, superimposed by straylight. Selected spectral lines from the on-board wavelength calibration lamp can be used as a test case for different mathematical approximations. In addition, observations have also been made using an external mercury lamp, providing spectral lines that are less crowded (and thus better isolated) than the lines of the on-board PtCr/Ne lamp. Two examples of approximated slit functions are shown in Figure 12.

6. Further programme

Scientists involved with the GOME instrument are presently using the breadboard model to measure the reference spectra of ozone, nitrogen dioxide and sulphur dioxide. These spectra will subsequently be used for the retrieval of ozone concentrations.

An irritating feature in atmospheric radiative transfer is the so-called 'ring effect', which fills in some of the strong Fraunhofer lines in the solar spectrum when it is viewed through the atmosphere. This will be measured as a quasi-absorption spectrum for use in the ground processing.

In consultation with the scientists, priorities have been agreed for the conduct of the flight-model calibration, which will be performed after GOME has undergone satellite-level vibration/acoustic testing, in June 1994. Evaluation and processing of the acquired data will then follow. These data will be made available to DLR (D), which is responsible for the ground processing and the installation and maintenance of the calibration database.

Reference

1. Hahne A. et al. 1993, GOME: A New Instrument for ERS-2, *ESA Bulletin No. 73*, pp. 22–29.

Manuscript received 18 January 1994

A. Hahne, J. Callies, A. Lefebvre & B. Christensen
ERS Project Division, ESTEC, Noordwijk, The Netherlands

R. Hoekstra, L. Fontijn, C. Olij, E. Zoutman & G. Nützel
TPD-TNO, Delft, The Netherlands

Calibration of the GOME Instrument for ERS-2

Abstract The Global Ozone Monitoring Experiment (GOME) is an optical spectrometer to be flown on the second European Remote-Sensing Satellite, ERS-2 [1]. Its main task will be to measure the ozone content of the atmosphere and to monitor its long-term variation. Ozone is a trace gas of vital importance to mankind, as it absorbs the harmful ultraviolet radiation emitted by the Sun and prevents it from reaching the Earth's surface. This absorption occurs in an ozone layer concentrated in the stratosphere, at altitudes of between 18 and 40 km, which is threatened by human activities, in particular by the release of Chloro-Fluoro-Carbons (CFCs) used in spray cans, refrigerators and foams, and as a cleaning agent. Ozone depletion is believed to be taking place at a rate of about 0.3% per year.

The reliable measurement of such a small global trend against the background of normal spatial and temporal variability, places high demands on the instrument's accuracy and stability. To meet with these requirements, the instrument needs thorough calibration and characterisation, both on the ground and in orbit.

The breadboard model of the GOME instrument – which is functionally fully representative including the on-board means of calibration – has been subjected to a dry calibration run on the ground, and the test results are reported here.

1. Calibration requirements and the on-board calibration concept

The conventional approach for measuring ozone, which is the underlying principle of the American SBUV and TOMS instruments, is the monitoring of upwelling backscattered radiance at a number of discrete wavelengths. To yield meaningful results, the radiometric response of an instrument used in this mode must be known to better than 1%. Because the space environment is known to change the radiometric response of the instrument (e.g. by radiation-induced darkening of transmissive optics), the means for carrying out on-board calibration with the necessary stability have to be provided to enable re-calibration at regular intervals.

This is normally done by looking at the Sun, which is a rather stable light source for the wavelength range in question. However, because the solar irradiance is several orders of magnitude higher than the radiance coming from the Earth, the Sun cannot be used directly, but only via a diffuser. This diffuser attenuates the light to a level that falls within the dynamic range of the detection system, and also makes the measurement path insensitive to the variations in the line-of-sight to the Sun as function of the seasonal change in the Earth–Sun distance.

As GOME is intended to achieve continuity with the long-term records of ozone concentrations already accrued by the SBUV and TOMS instruments, this concept has been adopted for GOME also. There is, however, an alternative measurement principle known as 'Differential Optical Absorption Spectroscopy', which is made possible by the availability of multi-pixel array detectors capable of recording a continuous spectrum over a large wavelength range. With this technique, a recorded atmospheric spectrum is divided by a solar spectrum, thereby compensating for the Sun's variability (which, of course, also appears in the backscattered light), as well as for the variations in the optical throughput. To the divided spectrum obtained in this way, the absorption spectra of ozone and possibly other trace gases are then fitted, thus providing the means to retrieve the amounts of the target (absorbing) species.

For this technique to work, the wavelength observations (for both the solar spectrum and the backscattered spectrum from the atmosphere) have to be very accurate . However, launch effects and temperature variations around the orbit prevent this stability from being achieved. Thus with GOME it is proposed to measure the wavelength shifts with the aid of a calibration lamp, which provides a sufficient number of sharp atomic emission lines in each channel to map wavelength shifts around the orbit and correct for them in the ground processing (Fig. 1).

* Ideally, the wavelength stability between recordings should be 1/100 th of a pixel.

Figure 1. The spectrometer optics of the GOME instrument

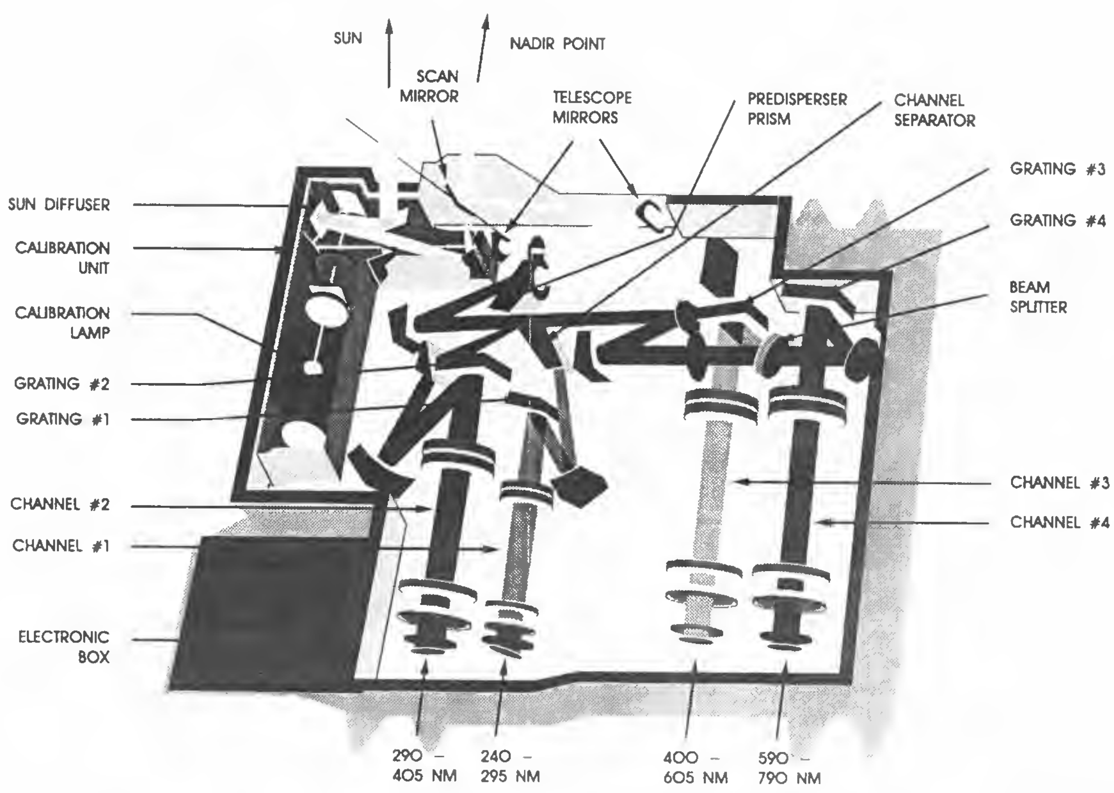

In addition to this basic calibration facility, there are in-flight provisions for:
- measuring the dark current and fixed pattern noise of the detectors and the readout chain
- calibrating the Analogue-to-Digital Converters (ADCs)
- monitoring pixel-to-pixel variability by illuminating the detectors with Light-Emitting Diodes (LEDs) built into the optical objectives of the four channels
- monitoring the reflectance of the Sun diffuser, by channelling the light from the wavelength calibration lamp via the diffuser and ratioing the measurements with the corresponding ones made when the lamp is observed directly
- finally, by tilting the scan mirror to an angle between 70° and 85° with respect to nadir, it is possible to use the Moon as a calibration target.

2. The on-board calibration unit

Almost all on-board calibration facilities (except the LEDs mentioned in the previous section) are grouped in the Calibration Unit, which is shown in Figure 2. Its two key elements are:
- the calibration lamp, and
- the Sun diffuser.

2.1. The calibration lamp

Key requirements for the calibration lamp are:
- a number of sharp spectral lines spanning the entire wavelength range observed by GOME
- a lifetime compatible with the mission (500 h, with at least 1000 on/off cycles)
- low power consumption: less than 5 W, including DC/DC conversion losses
- a rugged design, as the lamp must be able to withstand both the launch and in-orbit environments.

The lamp selected is a hollow-cathode type, which has already been flown in a similar configuration on several NASA missions. The fill-gas is neon, with a platinum cathode with 10% chromium in order to provide some additional lines needed to span the GOME wavelength range.

A small life-test programme has been conducted, operating one lamp continuously for 1500 h and another intermittently, with 5 min on and 5 min off, for 6000 cycles. The lamp current was regulated to 10 mA. The test showed very satisfactory results, as did the environmental (vibration and thermal vacuum) test programme.

Figure 3a shows the 'naked' lamp, and Figure 3b the lamp in the suspension used in the calibration unit. Figure 4 shows the spectrum of the lamp used in the GOME Breadboard Model (BBM).

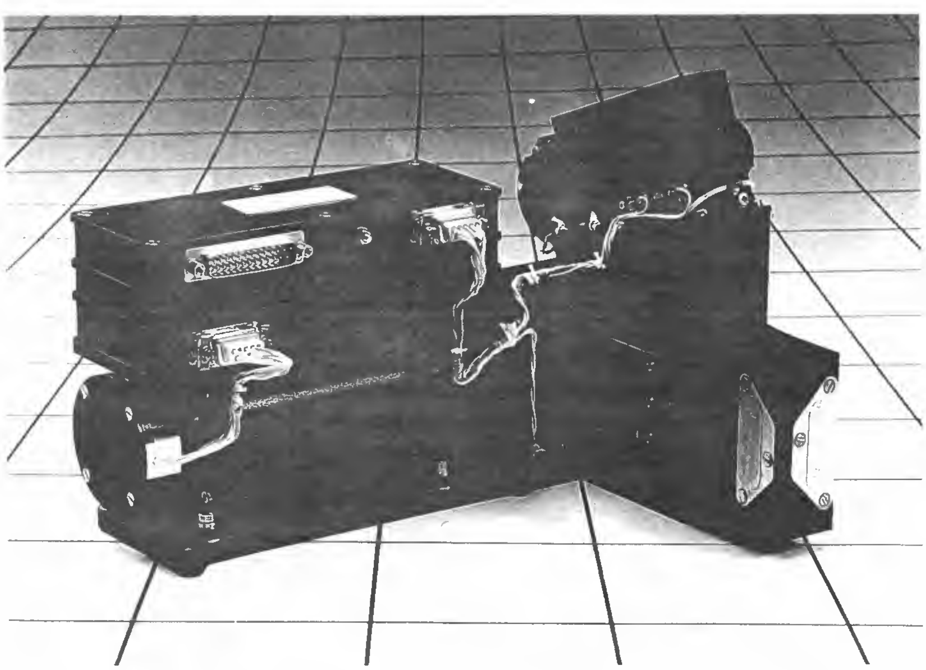

Figure 2. The on-board calibration unit

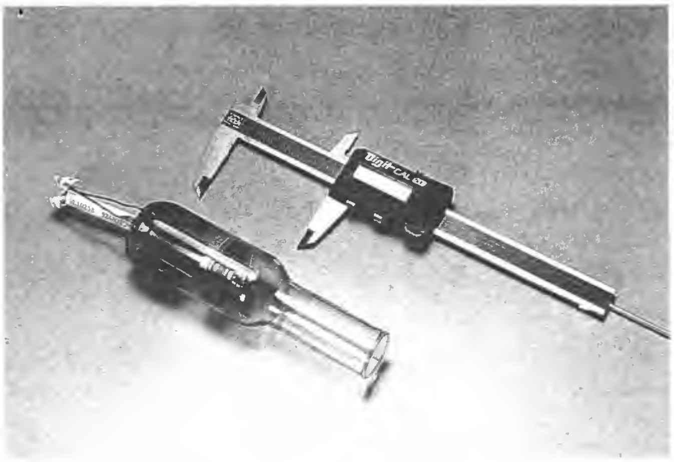

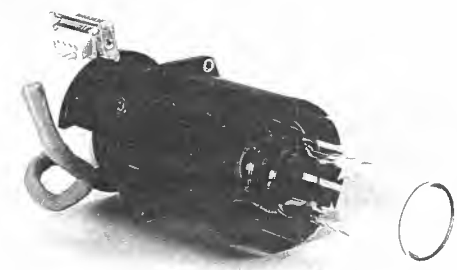

Figure 3a. The 'naked' wavelength calibration lamp

Figure 3b. The calibration lamp in its calibration-unit mount

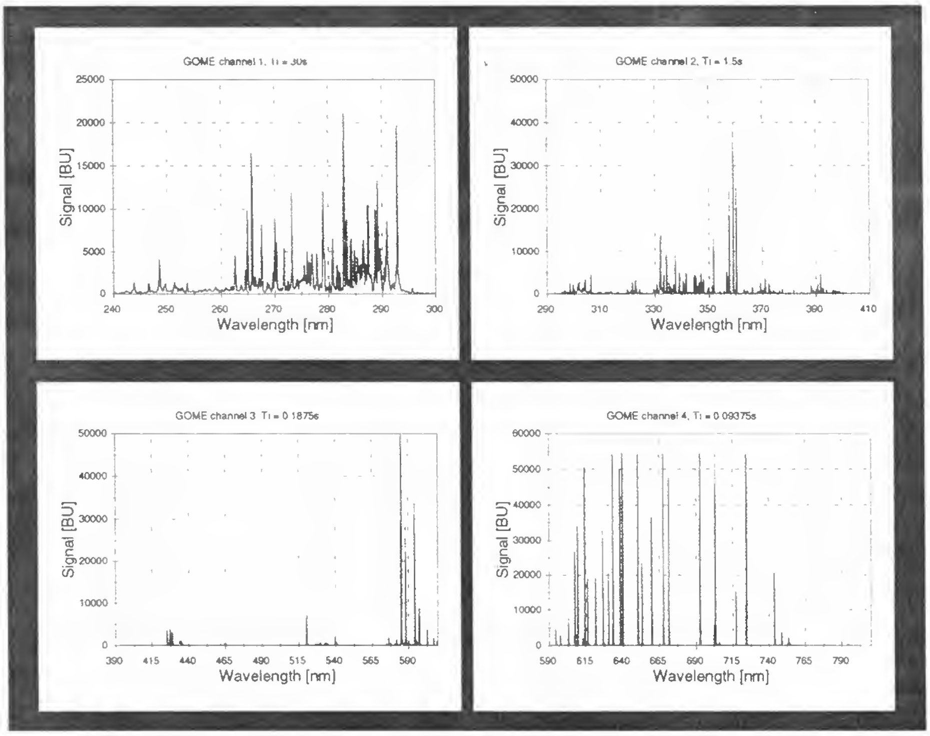

Figure 4. Spectrum of the calibration lamp, as measured for the GOME breadboard model (BBM)

2.2. The diffuser

The purpose of the Sun diffuser is to enable a calibration to be carried out with the standard system without the need for an accurate Sun acquisition and tracking mechanism. In order to obtain a reliable Sun calibration, the diffuser must have:

- a well-known Bi-Directional Scattering Function (BSDF)
- good uniformity over the illuminated surface
- a smooth and well-known wavelength response for the wavelength range of interest
- excellent in-orbit stability.

A short technology-development programme has been conducted at TPD/TNO Delft (NL) to select the most suitable material/process for the diffuser. Materials that have been investigated include aluminium oxide, quartz, magnesium oxide, titanium dioxide, barium sulphate, and aluminium with various surface treatments and coatings. Mainly for in-orbit stability reasons, a wet-blasted Aluminium 6082 with a 5 nm chromium and a 100 nm aluminium vacuum-deposited coating have been selected.

Figure 5 shows the diffuser produced with this technology, and Figure 6 the measured BSDF with the angular range of interest indicated.

2.3. The calibration unit

Aside from the lamp (with its housing) and the Sun diffuser, the Calibration Unit comprises:

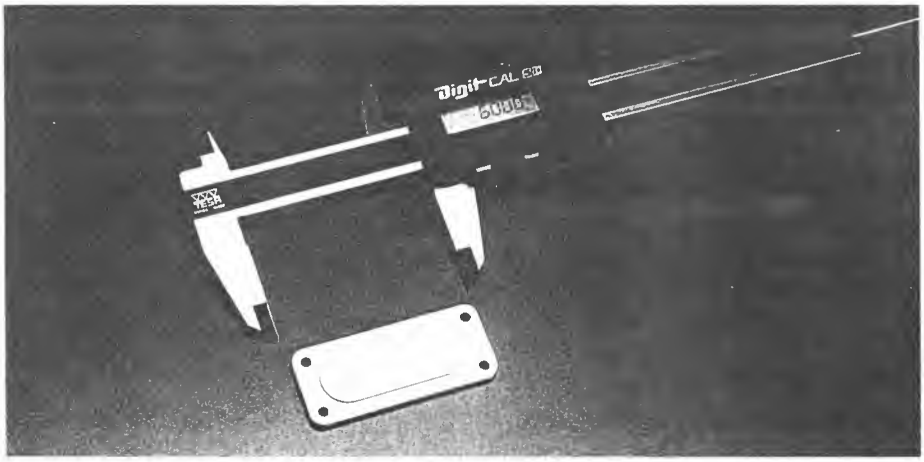

Figure 5. Wet-blasted aluminium diffuser

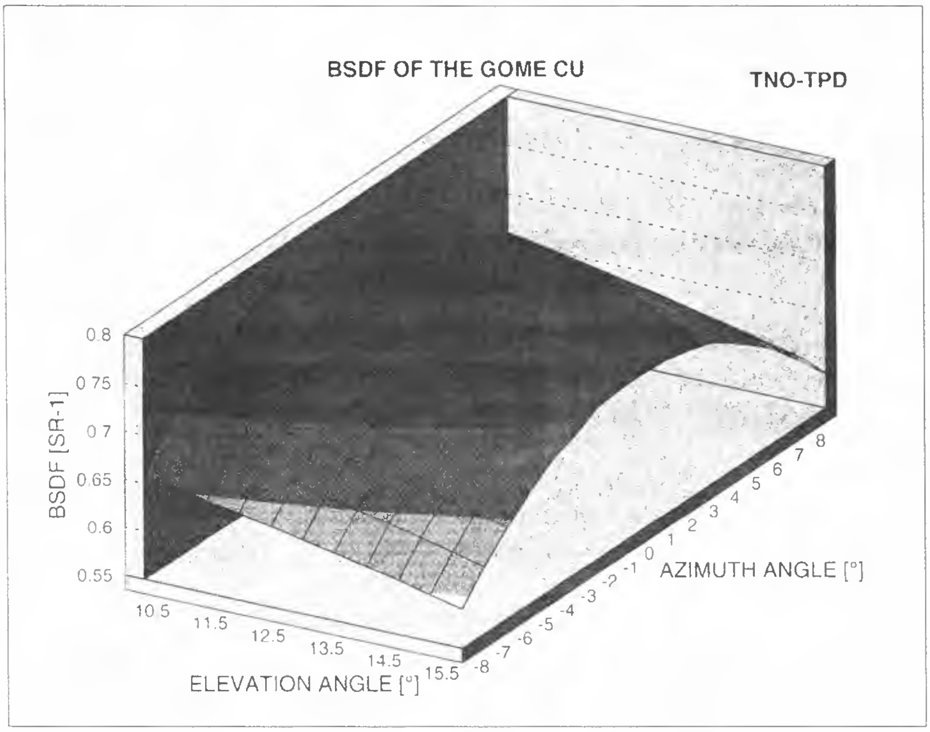

Figure 6. BSDF for the angular range of interest

– the power supply for the lamp, providing a voltage ramp to supply the ignition voltage of about 300 V and a stabilised current across the lamp of 10 mA
– the optical elements needed to ensure that the spectrometer slit and pupil are fully illuminated for both the lamp-calibration and Sun-calibration modes
– a shutter, which protects the diffuser when it is not being used for Sun calibration
– a mesh between shutter and diffuser, providing further protection to the diffuser and an additional attenuation of the light level received from the Sun.

The latter two items have been implemented based on NASA experiences which have shown that diffuser degradation is directly correlated with the time of exposure to sunlight (probably due to polymerisation of deposited contaminants caused by hard ultraviolet light).

3. The ground-calibration programme

Although a number of means for on-board calibration are included in GOME, they do not provide access to all the necessary parameters. These parameters are measured during the on-ground calibration programme and are not anticipated to change from ground to orbit.

The most important measurements to be conducted on the ground are:
– the measurement of the diffuser BSDF over the GOME wavelength range

– the characterisation of the polarisation response of the instrument as a function of the optical path (normal observation path and Sun observation path), scan mirror position (the scan mirror reflectivity for s- and p-polarisation is a function of the mirror angle), and wavelength.

On top of this, there are a number of additional measurements used for various purposes: more comprehensive instrument characterisation, consistency cross-checking, backup measurement for the case of lamp failure, and generation of test data for processing-algorithm checking.

In particular, the programme comprises:

Radiance/irradiance measurements: By illuminating the normal observation path and the Sun observation path with known radiance/irradiance, the radiometric calibration concept can be checked.

Wavelength calibration: During instrument-level thermal-vacuum testing, spectra of the calibration lamp have been recorded at different temperatures to measure wavelength shifts as a function of the temperature and the air/vacuum difference.

Detector characterisation: Dark current, readout noise, pixel-to-pixel sensitivity variations, and electronic chain performances including response linearity have been measured.

Straylight characterisation: This includes intra-channel (from high-intensity end to low-intensity end), inter-channel (from one channel to the other), and out-of-field and out-of-band straylight measurements.

Field-of-view characterisation: The variability, if any, in the radiometric response and spectral shift in the along-slit direction is measured. This is of particular interest for the lunar calibration, as the Moon only partially fills the spectrometer slit.

Measurement of the slit function: The slit function (i.e. the modulation transfer function of the entire optical system from the slit up to and including the detector) is determined. This is used to convolute high-resolution reference spectra of atmospheric species to the resolution of GOME.

4. The breadboard-model calibration programme

Recognising that this is quite a demanding programme, preparations for the calibration started as early as 1991. After agreement in principle on the scope of the programme with the scientists involved in GOME, TPD in Delft (NL) proceeded with the design, manufacturing, procurement and testing of all the necessary elements:

– turntable and fixtures to accommodate the instrument during the measurements
– calibrated lamps, diffusers and reference detectors procured from the National Institute of Standards
– monochromator and polariser covering the entire GOME wavelength range
– a temperature-controlled room to host the whole setup, clean room class 10.000, all black-painted (even including storage cabinet and water sink and tap) to suppress external straylight
– computer and software to control all the settings and provide them to the GOME Electrical Ground-Support Equipment (EGSE), to enable correlation between the GOME measurement data and the settings of the calibration setup
– algorithms and software to analyse the data, e.g. for noise correction, wavelength shift detection, BSDF computation, etc.
– procedures for setting up, aligning and performing the measurements
– calibration error budgets to establish the expected accuracy and precision of the measurements.

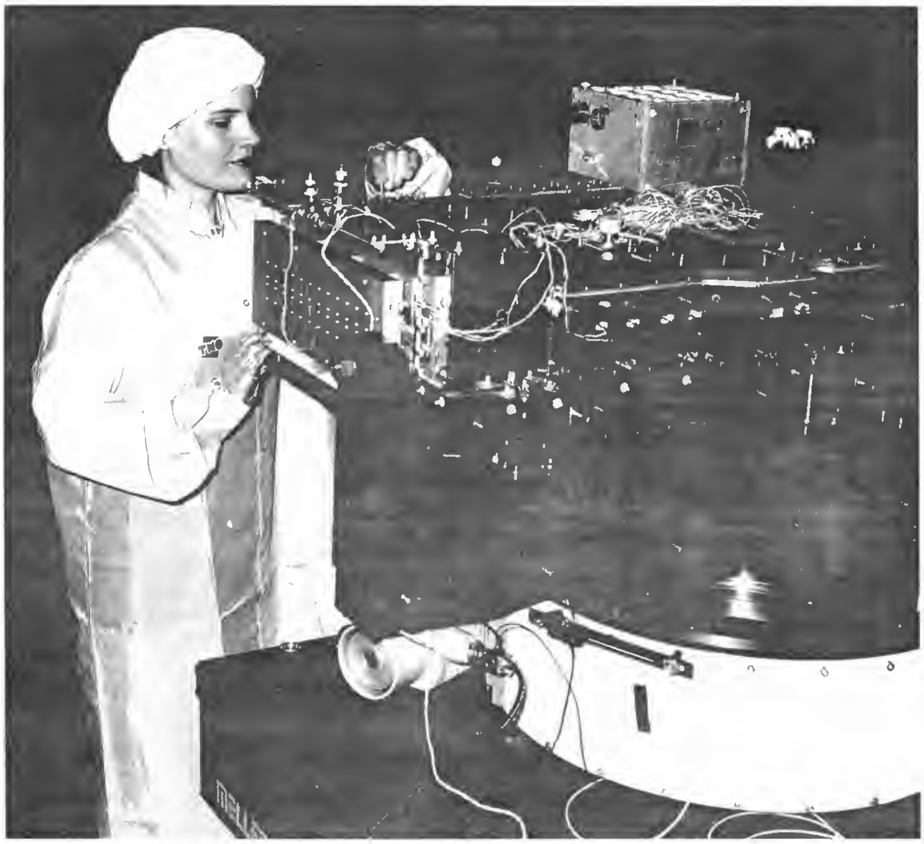

Figure 7. GOME on the turntable in the calibration facility

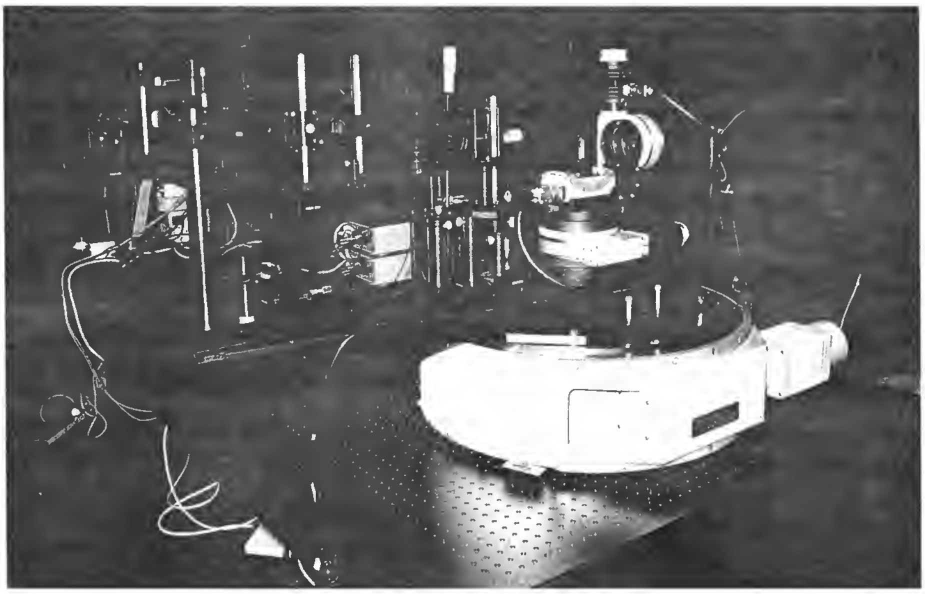

Figure 8. Part of the GOME calibration setup. Note the black environment for reducing external straylight

It was realised that to perform this exercise on only the flight model would be very risky and schedule-critical. A dry run involving all the steps and procedures has therefore been carried out on the GOME breadboard model which, since the negotiation of the main GOME development contract (Phase-C/D), has evolved into a fully-fledged de-facto engineering model, being very representative of the final flight-model configuration.

Figure 7 shows the GOME BBM mounted on the turntable in the TPD facility, while Figure 8 shows part of the optical instrumentation for performing the calibration.

First, wavelength characterisation and radiometric stability checking were carried out during the thermal-vacuum test at instrument level in the vacuum chamber of the instrument's prime contractor, Officine Galileo (I). This was then followed by two calibration periods, April–August 1993 and November–December 1993, with an intermediate review to scrutinise the results. A final review in March 1994 then concluded the BBM calibration, and the modifications necessary for the flight-model programme were agreed.

Figure 9. Polarisation response of the breadboard model (BBM)

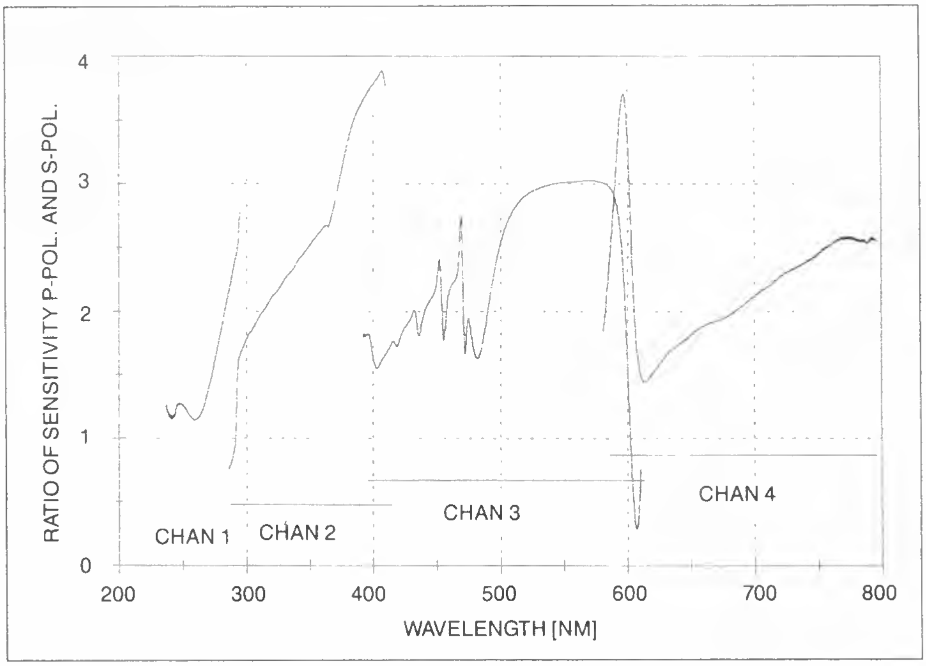

5. Results of the BBM calibration/characterisation

BSDF: The BSDF as measured on the flight diffuser is a smooth function of both the azimuth/elevation angles and the wavelength (see Fig. 6).

Polarisation response: As expected, the instrument shows a pronounced polarisation response. In particular, channel 3 shows some narrow structure in the polarisation ratio (*s* over *p*), which is believed to be due to the combined effects of the dichroic beam-splitter and grating (Fig. 9).

Radiance/irradiance measurements: For schedule reasons, the BSDF of the BBM calibration unit could not be measured prior to integration into the BBM, so that a proper consistency check was not possible.

Wavelength calibration: During instrument- and payload-level thermal-vacuum and thermal-balance tests, the spectral stability as a function of temperature was verified. Spectral shifts in all channels were less than 0.02 pixel/°C. With an orbital temperature swing of about ±1°C, an excellent spectral stability for a passive thermal design is achieved. Figure 10 shows the instrument mounted in the Galileo thermal-vacuum chamber.

Detector characterisation: Both the dark current and its noise proved to be very low (also due to the good stability of the detector cooling loop). Pixel-to-pixel sensitivity variations across the 1024-pixel arrays were, at less than 2%, much better than the detector manufacturer had envisaged. Some electronic noise was detected in certain

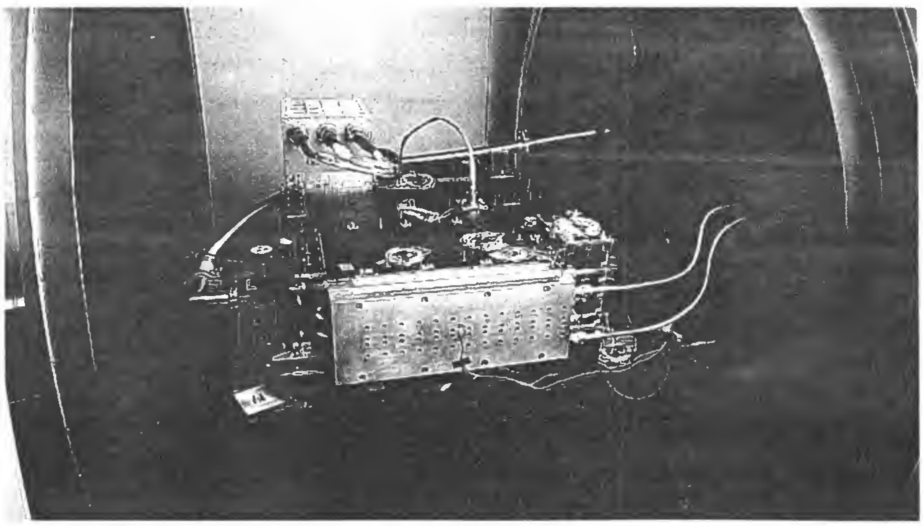

Figure 10. GOME breadboard model (BBM) during the TV test

readout situations. This was due to the ringing of the leading edge of the strobe pulse and to interference with the read-out of a temperature sensor. Both problems have been fed back into the instrument design and should be solved for the flight model.

Straylight characterisation: Quite detailed investigations were necessary to clarify the observed levels of straylight. A path for external straylight was identified and the problem solved via more and improved instrument internal baffling. Inter-channel straylight proved to be low and presented no problem.

More crucial was the intra-channel straylight, particularly that in channel 2, where at the short-wavelength end a roll-off of the signal level (by three orders of magnitude) presented a significant problem. Multiple reflections between the detector and the objective lenses and the gratings, respectively, were identified as the major cause. In channels 3 and 4 the problem could be resolved by the provision of improved anti-reflection coatings on the lenses and by slightly tilting the gratings. For channel 2, this would not have been sufficient and so, in consultation with the GOME scientists, it was decided to move the wavelength split between channels 1 and 2 to a higher value, thereby safeguarding the important channel 2, but sacrificing the performance of channel 1 slightly. The problem was alleviated by measuring straylight levels on some (so far unused) pixels, enabling some correction to be made for straylight in the ground processing.

Field-of-view characterisation

The design parameters for the GOME FOV are 0.14° x 2.8°. Under normal observational conditions, the entire slit and the entire GOME pupil are illuminated. However, when the Moon is observed, only a fraction of the slit is illuminated. For that reason, several scans have been made of the FOV by using collimated light as input for the GOME telescope. These measurements provide information on:

- actual dimensions of the FOV
- out-of-field scattered light
- influence on radiometric response and on wavelength scale when only a fraction of the FOV is illuminated.

Figure 11 shows the radiometric output of GOME for channel 3 when the FOV is scanned along the 2.8° axis of the FOV.

Slit function

This function represents the spectral line shape output for monchromatic input. It is a convolution of entrance slit width as imaged onto the spectral plane, detector pixel

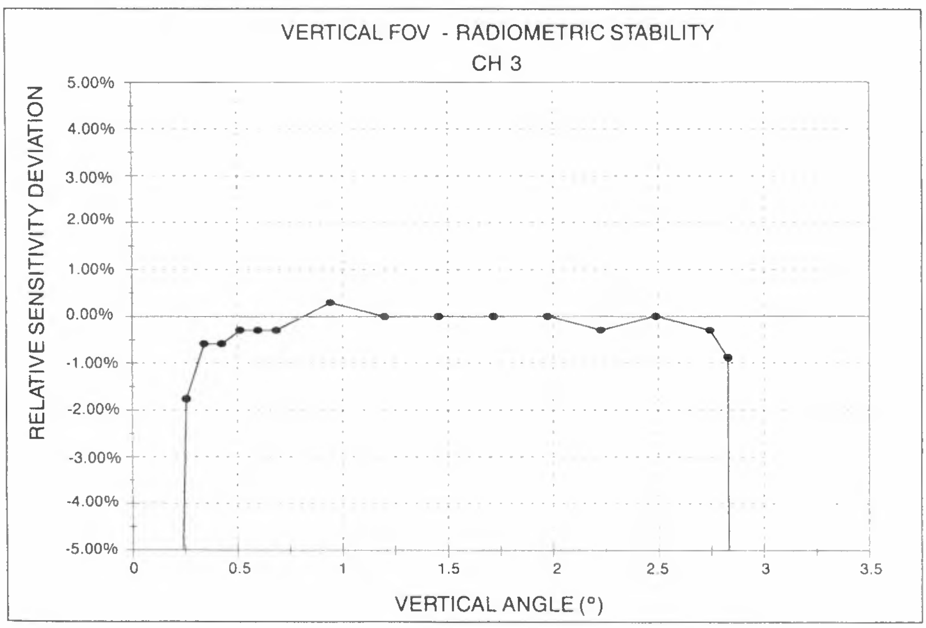

Figure 11. Radiometric response variation along the field of view

Figure 12. Slit function approximation in channel 4. The thin line is an approximation with a rectangular slit function.the thick line with a sixth-order polynomial

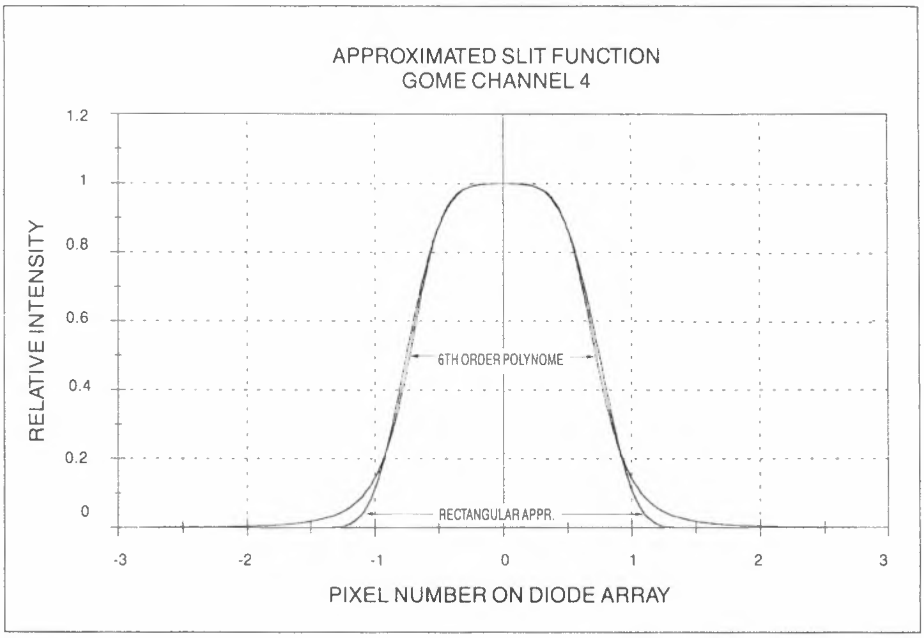

width, optical aberrations and residual effects, superimposed by straylight. Selected spectral lines from the on-board wavelength calibration lamp can be used as a test case for different mathematical approximations. In addition, observations have also been made using an external mercury lamp, providing spectral lines that are less crowded (and thus better isolated) than the lines of the on-board PtCr/Ne lamp. Two examples of approximated slit functions are shown in Figure 12.

6. Further programme

Scientists involved with the GOME instrument are presently using the breadboard model to measure the reference spectra of ozone, nitrogen dioxide and sulphur dioxide. These spectra will subsequently be used for the retrieval of ozone concentrations.

An irritating feature in atmospheric radiative transfer is the so-called 'ring effect', which fills in some of the strong Fraunhofer lines in the solar spectrum when it is viewed through the atmosphere. This will be measured as a quasi-absorption spectrum for use in the ground processing.

In consultation with the scientists, priorities have been agreed for the conduct of the flight-model calibration, which will be performed after GOME has undergone satellite-level vibration/acoustic testing, in June 1994. Evaluation and processing of the acquired data will then follow. These data will be made available to DLR (D), which is responsible for the ground processing and the installation and maintenance of the calibration database.

Reference

1. Hahne A. et al. 1993, GOME: A New Instrument for ERS-2, *ESA Bulletin No. 73*, pp. 22–29.

Manuscript received 18 January 1994

esa journal

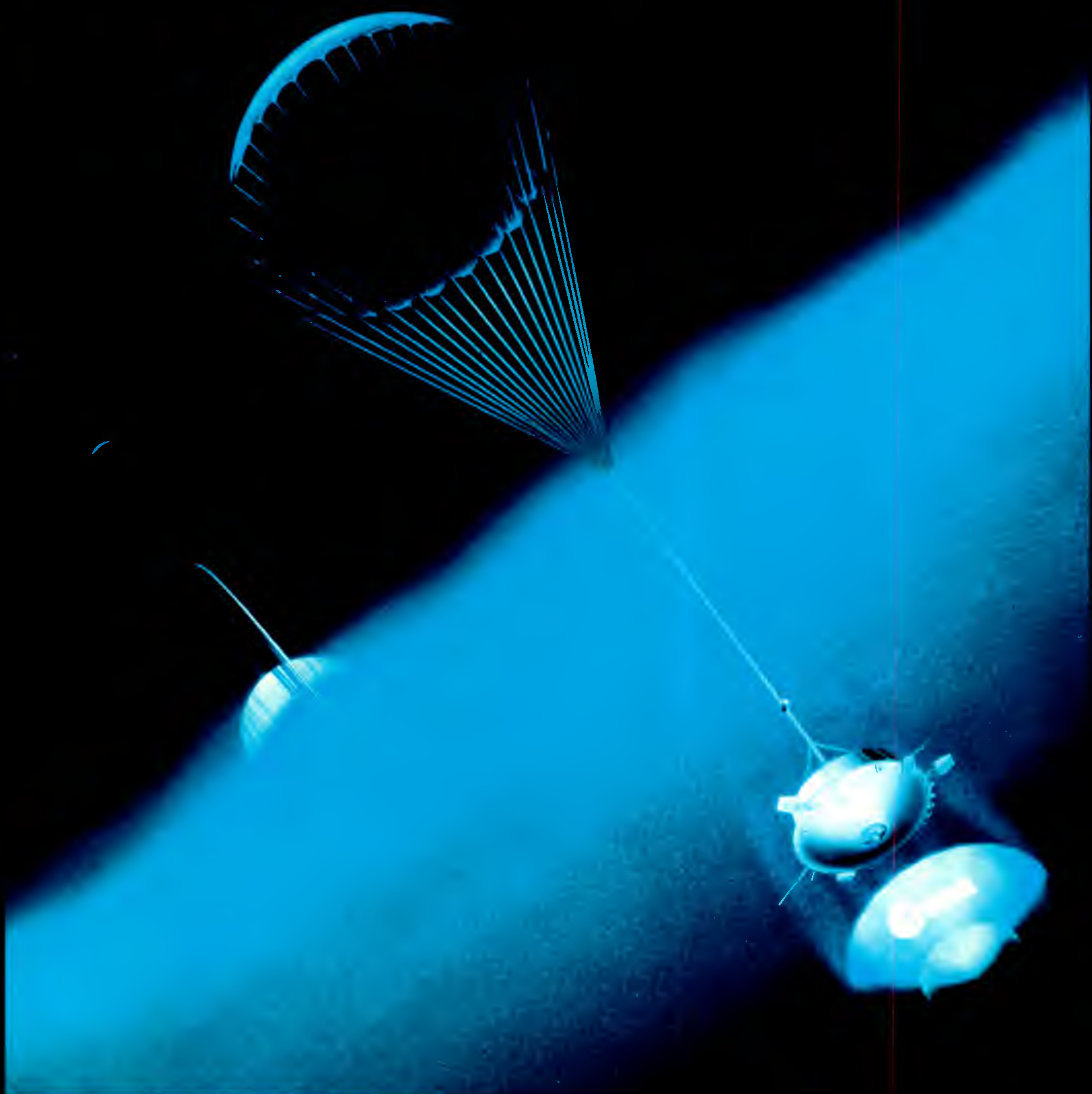

esa
european space agency

94/2

european space agency

The European Space Agency was formed out of, and took over the rights and obligations of, the two earlier European Space Organisations: the European Space Research Organisation (ESRO) and the European Organisation for the Development and Construction of Space Vehicle Launchers (ELDO). The Member States are Austria, Belgium, Denmark, France, Germany, Ireland, Italy, Netherlands, Norway, Spain, Sweden, Switzerland and the United Kingdom. Finland is an Associate Member of the Agency. Canada is a Cooperating State.

In the words of the Convention: The purpose of the Agency shall be to provide for and to promote, for exclusively peaceful purposes, co-operation among European States in space research and technology and their space applications, with a view to their being used for scientific purposes and for operational space applications systems.

(a) by elaborating and implementing a long-term European space policy, by recommending space objectives to the Member States, and by concerting the policies of the Member States with respect to other national and international organisations and institutions;
(b) by elaborating and implementing activities and programmes in the space field;
(c) by co-ordinating the European space programme and national programmes, and by integrating the latter progressively and as completely as possible into the European space programme, in particular as regards the development of applications satellites;
(d) by elaborating and implementing the industrial policy appropriate to its programme and by recommending a coherent industrial policy to the Member States.

The Agency is directed by a Council composed of representatives of Member States. The Director General is the chief executive of the Agency and its legal representative.

The Directorate of the Agency consists of the Director General; the Inspector General; the Director of Scientific Programmes; the Director of Observation of the Earth and its Environment; the Director of the Telecommunications Programme; the Director of Space Transportation Systems; the Director of the Space Station and Microgravity Programme; the Director of ESTEC; the Director of Operations and the Director of Administration.

The ESA HEADQUARTERS are in Paris.

The major establishments of ESA are:

THE EUROPEAN SPACE RESEARCH AND TECHNOLOGY CENTRE (ESTEC), Noordwijk, Netherlands.

THE EUROPEAN SPACE OPERATIONS CENTRE (ESOC), Darmstadt, Germany

ESRIN, Frascati, Italy.

Chairman of the Council: P.G. Winters

Director General: J.-M. Luton.

agence spatiale européenne

L'Agence Spatiale Européenne est issue des deux Organisations spatiales européennes qui l'ont précédée — l'Organisation européenne de recherches spatiales (CERS) et l'Organisation européenne pour la mise au point et la construction de lanceurs d'engins spatiaux (CECLES) — dont elle a repris les droits et obligations. Les Etats membres en sont: l'Allemagne, l'Autriche, la Belgique, le Danemark, l'Espagne, la France, l'Irlande, l'Italie, la Norvège, les Pays-Bas, le Royaume-Uni, la Suède et la Suisse. La Finlande est membre associé de l'Agence. Le Canada beneficie d'un statut d'Etat coopérant.

Selon les termes de la Convention: l'Agence a pour mission d'assurer et de développer, à des fins exclusivement pacifiques, la coopération entre Etats européens dans les domaines de la recherche et de la technologie spatiales et de leurs applications spatiales, en vue de leur utilisation à des fins scientifiques et pour des systèmes spatiaux opérationnels d'applications:

(a) en élaborant et en mettant en oeuvre une politique spatiale européenne à long terme, en recommandant aux Etats membres des objectifs en matière spatiale et en concertant les politiques des Etats membres à l'égard d'autres organisations et institutions nationales et internationales;
(b) en élaborant et en mettant en oeuvre des activités et des programmes dans le domaine spatial;
(c) en coordonnant le programme spatial européen et les programmes nationaux, et en intégrant ces derniers progressivement et aussi complètement que possible dans le programme spatial européen, notamment en ce qui concerne le développement de satellites d'applications.
(d) en élaborant et en mettant en oeuvre la politique industrielle appropriée à son programme et en recommandant aux Etats membres une politique industrielle cohérente.

L'Agence est dirigée par un Conseil, composé de représentants des Etats membres. Le Directeur général est le fonctionnaire exécutif supérieur de l'Agence et la représente dans tous ses actes.

Le Directoire de l'Agence est composé du Directeur général; de l'Inspecteur général; du Directeur des Programmes scientifiques; du Directeur des Programmes d'Observation de la Terre et de son Environnement; du Directeur du Programme de Télécommunications; du Directeur des Systèmes de Transport spatial; du Directeur du Programme Station spatiale et Microgravité; du Directeur de l'ESTEC, du Directeur des Opérations et du Directeur de l'Administration.

Le SIEGE de l'Agence est à Paris.

Les principaux Etablissements de l'Agence sont:

LE CENTRE EUROPEEN DE RECHERCHE ET DE TECHNOLOGIE SPATIALES (ESTEC), Noordwijk, Pays-Bas.

LE CENTRE EUROPEEN D'OPERATIONS SPATIALES (ESOC), Darmstadt, Allemagne.

ESRIN, Frascati, Italie

Président du Conseil: P.G. Winters

Directeur général: J.-M. Luton.

esa journal

Volume 18 Number 2

Cover: Artist's impression of the Huygens Probe

Editorial Office
ESA Publications Division
c/o ESTEC, PO Box 299
2200 AG Noordwijk
The Netherlands
Tel. (31) 1719-83400
Fax. (31) 1719-85433

Publication Manager
Bruce Battrick

Editors
Bruce Battrick
Clare Mattok

Layout
Carel Haakman
Keith Briddon

Advertising
Brigitte Kaldeich
Tel. (31)1719-83794

Printed in The Netherlands
ISSN 0379-2285

esa
european space agency
agence spatiale européenne

AMP TEK®

SPACEFLIGHT DATA RECORDER

FDR-8000

Product Spotlight

Model:	FDR-8500C
Capacity:	5 Gigabytes (uncompressed)
	10 Gigabytes (2:1 compression)
	250 Gigabytes (50:1 compression)
Date Rate:	10 Mbit/s per channel (burst)
	4 to 12 Mbit/s total (sustained)
Weight:	16 lbs (7.3 kg)
Power:	18 Watts @ 28VDC
Size:	11.8" x 9" x 6"
	(300mm x 229mm x 152mm)
Interface:	RS-422

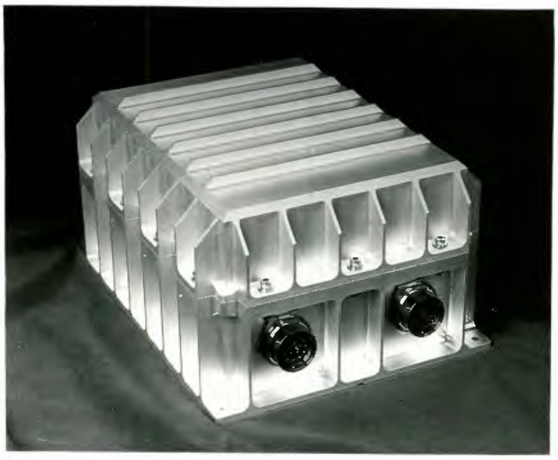

FDR-8000 series recorders are flight-proven, high performance data storage units built for operation within the Space Shuttle bay, on the aft flight deck, and aboard space platforms. Designed with 8mm helical scan technology, the FDR-8000 line provides economical mass data storage. These recorders' unique characteristics make them equally useful in avionics and satellite applications.

Capacity

The newest member of the FDR-8000 family is the FDR-8500C. The capacity of the FDR-8500C is 5 Gigabytes of uncompressed data. Hardware compression is typically 2:1, yielding 10 Gigabytes of storage space. Depending on data content, compression rates of 50:1 are attainable. Peak data rates are 10 Mbit/s per channel into a 4 Mbit buffer. Multiple input models are available. Total sustained data rates from combined channels are from 4 Mbit/s to 12 Mbit/s depending on compression efficiency. The error rate is less than one in 10^{13} bits read.

Mechanical

The FDR-8000 enclosure is a sealed box purged with nitrogen. The inert gas provides an air cushion around the recording head and protects the tape from common corrosive gases during long term storage. Internal heaters activate below +10°C. During initialization, recording is disabled until heaters can stabilize the internal environment above 0°C. Shock and vibration isolation allow the tape transport assembly to surpass Shuttle launch and landing requirements.

The recorder's footprint measures 11.8" x 9" (300mm x 229mm), with a height of 6" (152mm). The mounting hole pattern is on 70mm centers for easy interfacing with ESA cold plates and Hitchhiker pallets. Total weight is 16 lbs (7.3 kg).

Electrical

Power dissipation is 18 Watts at 28V. Each recorder contains its own DC/DC power converter. An internal controller supports serial data transfer, file structures, error recovery, and regulation of the recorder's operating environment.

Interface

Communication with the FDR-8000 is provided via RS-422 compatible channels. The command channel is asynchronous at 1200 baud. The data channel is synchronous from DC to 10 MHz.

Let Amptek provide the solution to your high-capacity data storage needs.

AMPTEK, INC. 6 DE ANGELO DRIVE, BEDFORD, MA 01730 U.S.A. TEL 617/275-2242 FAX 617/275-3470

R.D. Lorenz
Unit for Space Sciences, University of Kent, Canterbury, UK

Huygens Probe Impact Dynamics

Abstract

The ESA Huygens Probe is due for launch as part of the NASA/ESA Cassini mission in 1997, to arrive at Titan in late 2004, and will make a 2–2.5 h exploratory descent to the surface. However, the state of Titan's surface is largely unknown and it may be at least partially covered in liquid hydrocarbons. With such ignorance of the surface state, and the limited financial envelope of the project, it is not practicable to design the Probe to 'soft-land'. Survival may, nevertheless, be possible and this paper presents various impact-dynamics analysis methods and assesses the likely impact scenarios and their survivability.

It is concluded that the Probe has a good chance of surviving to continue its scientific mission from the surface. The scientific information about the surface that could be gathered from impact-dynamics measurements is also discussed.

1. Introduction

The Huygens Probe[1–5] will make a 2.25 h (nominal) descent to the surface of Saturn's enigmatic moon Titan (Fig. 1), which it will hit with a vertical velocity of about 5 m/s. Although for cost and complexity reasons post-impact survival has never been a design driver for the Probe, it has long been realised that survival is possible[6,7], and at the current stage in Probe development (early Phase-C/D; i.e. main development phase) prospects for a productive surface mission look relatively good, with a modest impact velocity and healthy energy and link margins. In the event of Probe survival, a surface mission lasting of the order of 30 min should be possible.

Thus a major factor in the surface mission becomes the load sustained by the Probe at impact. Both the energy and momentum of the descent must be dissipated: where they are dissipated depends largely on the relative hardnesses or strengths of the Probe and the surface. Ideally, dissipation would occur in the material on which the Probe must land, which will happen in the event of a soft surface material.

An earlier paper[8] has reviewed the likely surface types to be encountered on Titan. Here I examine the range of expected impact parameters and loads, and the likely effects on the Probe and its payload. The most up-to-date and comprehensive descriptions of the Probe and its payload are to be found in two recent articles in ESA Bulletin No. 77, February 1994 [9,10].

The aims of the present paper are to:

- summarise work on spacecraft impact dynamics, on which the literature is sparse and scattered
- investigate the impact dynamics of the Huygens Probe, in order to assess the likelihood of its survival on the surface of Titan
- examine the variation in impact deceleration with surface mechanical properties to see how acceleration measurements on the Probe can be used to measure these properties.

Figure 1. Huygens mission profile. The Probe makes measurements from an altitude of 170 km down to the surface, the descent taking between 2.0 and 2.5 h. Mission energy and link budgets are sized for a minimum of 3 min operation post-impact, although an extended surface mission of 30 additional minutes may be possible (Figure from Reference 2)

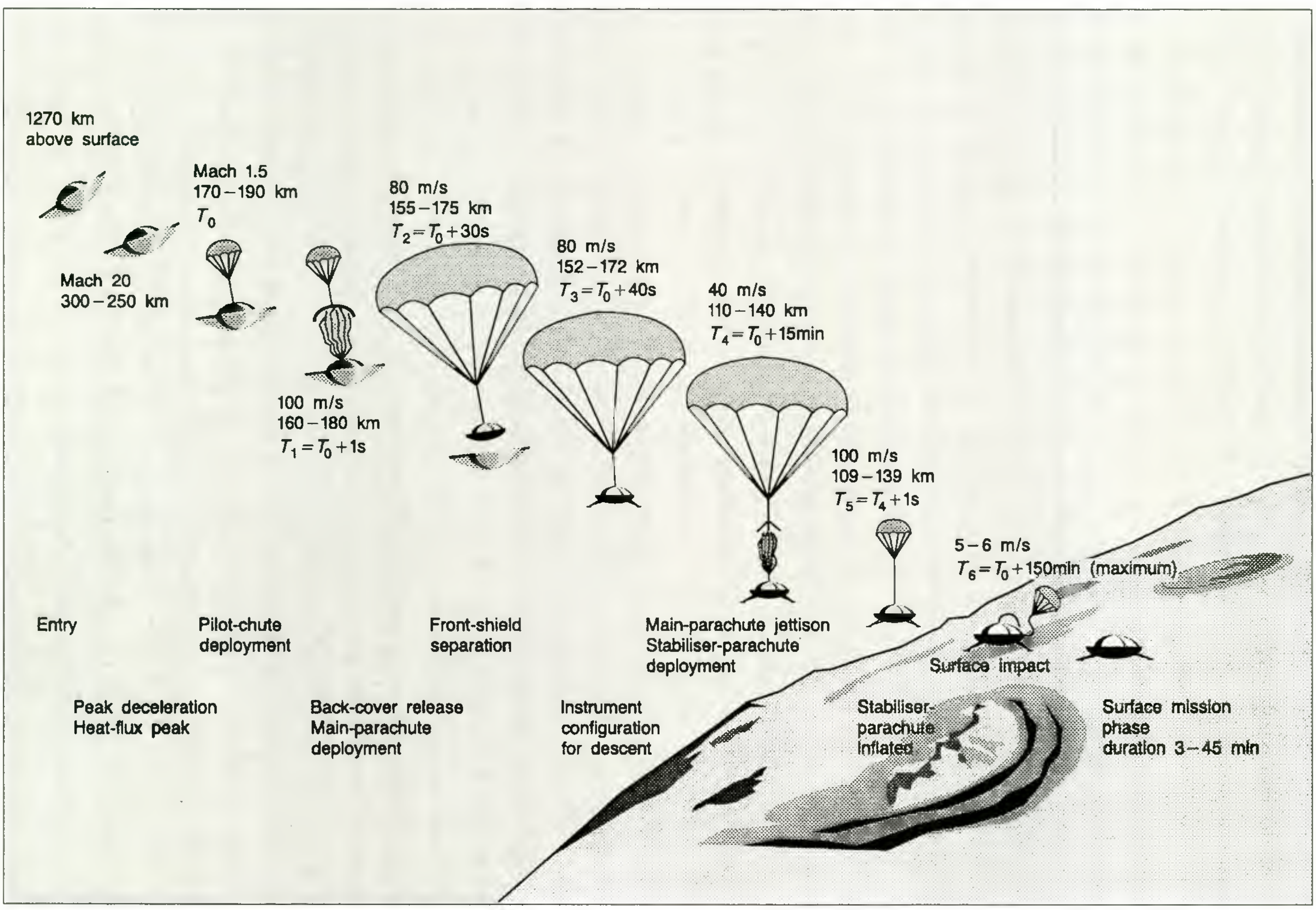

2. Comparisons with previous missions

Some useful comparisons may be drawn with previous planetary missions to put the Huygens landing scenario in context. A convenient summary of planetary missions is that by Wilson[11].

Luna 9, the first man-made object to have survived on the lunar surface, hit at approx. 6 ms^{-1}. Its internal equipment was 'protected by shock-absorbers'. It had a mass of about 100 kg. Luna 16 (an automatic sample return) and its successors were considerably larger, and soft-landed at about 2.5 ms^{-1}.

The Surveyor spacecraft had shock-absorbing legs and a propulsion system for soft-landing on the Moon; at touchdown they weighed just under 300 kg, and had vertical velocities of the order of 3 ms^{-1}. The main-structure loads were 8–20 g, although load-amplification effects on the spidery lander led to loads on the antenna and solar array (mounted on a mast) of the order of 90 g. The Viking landers on Mars (equipped with a throttlable hydrazine retro-rocket system, and shock-absorbing legs for soft-landing) touched down at about 2.5 ms^{-1}.

The Pioneer Venus (PV) probes have many similarities with the Huygens Probe, and a detailed comparison is given in a following section. They, and the Russian Venera probes, hit the surface of Venus at about 9 ms^{-1}, relying only on aerodynamic drag to brake their descent, and weighed between 93 kg (PV small probes) and 700 kg (Venera). The pictures sent back by the Veneras suggest they landed on rock slabs (possibly covered with some dust); these probes recorded landing loads[12] of up to 75 g.

Of the 30 or so missions described above, only Luna 18, Mars 2, and three of the four Pioneer Venus probes failed completely at impact (Table 1). Veneras 11 and 12 appear to have suffered extensive instrument failures on landing; Mars 3 sent back 20 s of (blank) TV signals before failing, and the sampler of Luna 23 was damaged by a rough landing. It is noteworthy that if spacecraft survived for a few seconds on the surface, they generally continued to function up to and often beyond their design life, with some missions being terminated either by command from Earth, or by relay spacecraft passing out of sight.

The impact velocity of the Huygens Probe is only slightly higher than that of 'true' soft-landers, and rather less than for several previous 'hard' or 'semi-hard' landers on the Moon and Venus. Thus, in relative terms, prospects for Huygens survival seem quite good, even though it has not been designed with impact survival in mind.

3. Comparions with Pioneer Venus

The NASA Pioneer Venus multi-probe mission is perhaps the most useful analogue for the Huygens impact: in part because the masses and velocities are comparable (Pioneer Venus, though robust, was not designed to survive impact), and because (unlike the Russian Mars and Venus missions) it is relatively well-documented in the open literature[13–15].

Four Pioneer Venus probes (three small and one large) were sent to Venus. The large probe was spherical (73 cm diameter) and had a mass of 310 kg (including its 1.4 m diameter heat shield, which it released after deploying a parachute). The small probes (50 cm diameter; 90 kg) descended without parachutes and kept their 76 cm-diameter, 45° half-angle entry protection shields attached throughout their descent.

The probes all transmitted directly to Earth using antennas with approximately hemispherical coverage[15]. The dispersion of the probes over the surface of Venus was such that the Earth (where the signals were received) was about 30° above the horizon over each landing site (except, significantly, for the day probe, where the Earth elevation was about 40°).

The probes impacted the surface at velocities of approximately 9–10 m/s, impact being indicated by a sudden change in the Doppler shift of the received radio frequency. Signals from two of them (the large probe and the north probe) were lost at impact. Signals were received from the night probe for 2 s after impact, but the day probe continued to transmit for 67 min, at which time its internal temperature reached 126° C. Telemetry suggests that the signal was lost at this point not due to battery exhaustion, but due to thermal failure of a power-amplifier component[14].

Table 1. Previous missions to planetary surfaces

Year	Mission	Nation	Target	Mass (kg)	Dimensions
1966	Luna 9	USSR	Moon	~ 100	Sphere 58 cm diam.
1966	Surveyor 1	US	Moon	293	Tripod, 3 m high, 4 m across Footpads 30 cm diam.
1966	Luna 13	USSR	Moon	116	As Luna 9
1967	Surveyor 3	US	Moon	293	As Surveyor 1
1967	Surveyor 4	US	Moon	293	As Surveyor 1
1967	Surveyor 5	US	Moon	305	As Surveyor 1
1967	Surveyor 6	US	Moon	300	As Surveyor 1
1968	Surveyor 7	US	Moon	306	As Surveyor 1
1969	Luna 15	USSR	Moon	As Luna 16?	
1970	Venera 7	USSR	Venus	~ 500	Sphere 1 m diam.?
1970	Luna 16	USSR	Moon	1880	4 m-square platform 4 footpads 30 cm diam.?
1970	Luna 17	USSR	Moon	As Luna 16?	
1971	Mars 2	USSR	Mars	450	1.2 m diam.
1971	Mars 3	USSR	Mars	450	1.2 m diam.
1971	Luna 18	USSR	Mon	As Luna 16	
1972	Luna 20	USSR	Moon	As Luna 16	
1972	Venera 8	USSR	Venus	495	As Venera 7
1973	Luna 21	USSR	Moon	As Luna 17	
1973	Mars 6	USSR	Mars		
1974	Luna 23	USSR	Moon	As Luna 16	
1975	Venera 9	USSR	Venus	660	2.1 m disc + 1 m sphere
1975	Venera 10	USSR	Venus	660	As Venera 9
1975	Viking 1	US	Mars	612	2.1 m tall, 3 m wide 3 footpads, 31 cm diam.
1975	Viking 2	US	Mars	612	As Viking 1
1976	Luna 24	USSR	Moon	As Luna 16	
1978	PV Large	US	Venus	316	Sphere 73 cm diam.
1978	PV Day	US	Venus	93	50 cm-diam. sphere, with 76 cm diam. conical nose
1978	PV Night	US	Venus	93	As PV Day Probe
1978	PV North	US	Venus	93	As PV Day Probe
1978	Venera 11	USSR	Venus	700?	As Venera 9?
1978	Venera 12	USSR	Venus	700?	As Venera 9?
1981	Venera 13	USSR	Venus	760	As Venera 9?
1981	Venera 14	USSR	Venus	760	As Venera 9?
1984	Vega 1	USSR	Venus	760	As Venera 9?
1984	Vega 2	USSR	Venus	760	As Venera 9?

On the one hand, the Pioneer Venus probes were more robustly built than Huygens, the small probes having to endure entry accelerations of the order of 560 g. Also, the probes were built as spherical pressure vessels (the shells were of titanium, several millimetres thick), able to withstand the 200 bar surface pressure at Venus. Huygens has much more modest entry loads (of order 20 g) and has a thin outer aluminium shell which is not sealed.

On the other hand, the Huygens impact velocity will be lower by a factor of almost 2. Secondly, pictures from the Soviet Venera spacecraft (which had broadly similar impact velocities but were equipped with impact-attenuation systems) indicate a very unpleasant surface on which to land, strewn with boulders and large slabs of volcanic rock (see Ref. 8, Fig. 12). Hopefully Titan's surface may be more forgiving!

The two failures that occurred at impact are probably a result either of impact damage directly, or the tipping-over of the probes at impact such that the Earth was no longer in the main antenna lobe. The failure of the night probe 2 s after impact may have been due to tipping over, or perhaps to thermal failure following inrush of the hot (600 K) atmosphere if the pressure vessel was ruptured by the impact.

Thus a major contributing factor to the loss-of-signal of the Pioneer Venus probes

Speed (m/s)	Comments
Less than 3	8 h of contact over 3 d
3	True soft-landing. Operated for 6 months
8.3	Impact accelerometry recorded soil structure to depth of 20–30 cm
Less than 2	Bounced 30 cm at landing (engines on): OK after engines turned off by ground command
Unknown	Contact lost 2.5 min before landing, although automatic landing may have been successful
4.2	Pressurant leak forced late retro sequence
3.8	
130	Crashed
10?	Telemetry multiplexer failure — only temperature data (23 min) from surface. Bad attitude caused 20 dB signal loss (rolled in wind?)
2.5	Sample-return mission
2.5?	Rover mission
?	Crashed (dust storm?)
21	Transmissions discontinued after 20 s: high winds, or failure of relay orbiter?
	Crashed 'due to rugged terrain'
10?	Operated for 50 min
2	
	Contact lost before landing
?	Rough landing damaged drill
8	First pictures from Venus: lasted 53 min
8	Operated for at least 65 min (relay passed out of sight)
2.4	Operated until 1982
2.5	Shut down 1980
9	Failed at impact
10	Operated for 67 min on surface: thermal failure?
10	Operated for 2 s
10	Failed at impact
8?	Instrument failures on landing: operated 95 min
8?	Instrument failures on landing: operated 110 min
8?	Operated for 127 min
8?	Operated for 57 min
8?	Drill sequence started prematurely: no surface science
8?	Operated for 57 min

may well have been the presence of the entry shields on the small probes causing antenna depointing at impact. Indeed, Venus surface data was recovered from what was originally thought [11] to be noise, when the Venera 7 lander's telemetry signal fell to 1% of its nominal value at impact. Because Huygens is a relatively flat and soft-bottomed spacecraft, we might expect that (except in the case of extremely steep or rocky surfaces) such antenna depointing is unlikely. Further, since the cold Titan atmosphere is much less harsh than the dense, scorching atmosphere on Venus, thermal failure should be at least slower, and perhaps less likely, to occur on Huygens.

4. Spacecraft impact dynamics

A substantial amount of work has been performed on impact dynamics for military applications. Most civil work is in connection with safety engineering, for aircraft[16,17] and automotive crashes[18–20], and the accidental dropping of flasks used to transport radioactive waste[21]. Comparatively little work is reported in the open literature in the West on the impact dynamics of spacecraft (Ref. 22 gives some general information; see references hereafter for particular cases).

The bulk of the available work was performed in connection with the US Mercury, Apollo and Surveyor programmmes, although some recent ESA-sponsored studies have been performed on Mars penetrator/landers[23]. For the Mercury and later Apollo programmes, the work was focussed on estimating impact loads to ensure crew survival, both for the nominal sea landing and for possible impact on land in the event of a launch abort.

As part of the Apollo Programme, models of the mechanical properties of the lunar surface had to be developed (there were initial fears that the surface might be so soft that a spacecraft, or astronauts not equipped with snowshoes, might sink into it[24]) and the Surveyor series of soft-lander missions was designed to assess the lunar surface in preparation for the manned Apollo landings. Some instrumentation (strain gauges on the landing legs and accelerometers on the main body) was devoted to measuring landing loads to assess the bearing strength of the surface[25]. Further indications of soil physical properties were obtained by photographing the 'feet' of the landing legs to measure foot penetration and ejecta throwout, and by measuring motor currents on the sampling arm.

Most of the Apollo and Mercury work was devoted to liquid landings (which were, of course, the nominal mode of ending their missions). Analytic simulation of such landings became well-developed and predictions for Huygens are made in a following section.

Simulation of landings on solid surfaces is rather more difficult and available data is more scarce. First, since the 'hardness' of the surface is comparable with that of the spacecraft, the partitioning of energy and momentum dissipation between the vehicle and the surface becomes complex, so analytical treatment is extremely difficult (although Ref. 26 provides an instructive analysis of a simple case). Secondly, the higher impact loads generally cause damage to the spacecraft, such that even for small-scale models, large series of tests are prohibitively expensive, so there is relatively little available experimental data. Modern finite-element techniques allow the detailed investigation of impact dynamics and structural response, but are also expensive.

In the following sections, relatively simple methods of estimating the loads and response of an impacting spacecraft are presented, with Huygens as the example. While relatively simple, these methods offer useful insight into what may occur at the climax of the Huygens mission.

5. Impact conditions

The Huygens Probe (Figs. 2–4), during most of its descent, is suspended beneath a stabilising drogue parachute (a polyester/kevlar disk-gap-band chute with a reference diameter of 2.45 m)[27]. The terminal velocity of the Probe with parachute at the surface of Titan, with a surface gravity of 1.35 ms^{-2} and an atmospheric density of 5.3 kgm^{-3}, is 5.2 ms^{-1} (approximately the velocity attained on Earth by an object dropped from a height of 130 cm, which is convenient for impact testing!). This is about half of the impact velocity of the Apollo capsules and the Pioneer Venus spacecraft.

There is some uncertainty in the radio-occultation data from the Voyager encounter, and a consequent uncertainty in the knowledge of the atmospheric density[28], which could be 4.57–6.01 kgm^{-3}. Similarly, there is a 10% uncertainty in the drag performance of the parachute, and so combining these uncertainties gives the terminal velocity of the Probe at the surface between 4.6 and 5.8 ms^{-1}.

The horizontal velocity of the Probe is unlikely to be exactly zero as parachutes tend to have a slight 'gliding' action, but certainly the sideways component will be small (say <1 ms^{-1}). The Probe will be moving along with any winds at the surface, but these (e.g. Ref. 29) are likely to be very small (again <1 ms^{-1}). The specification on the stabiliser requires it to have pendulum-type oscillations of less than 10° amplitude. Should a wind gust cause a swing greater than this, it should return to within 10° of vertical within about 10 s. Wind gusts near the surface are unlikely anyhow, so for the purposes of this study it is assumed that the impact attitude is vertical, and the corresponding horizontal velocity component is zero.

The Probe mass at impact is expected to be about 207 kg, and its transverse moment of inertia is about 20 kgm^2.

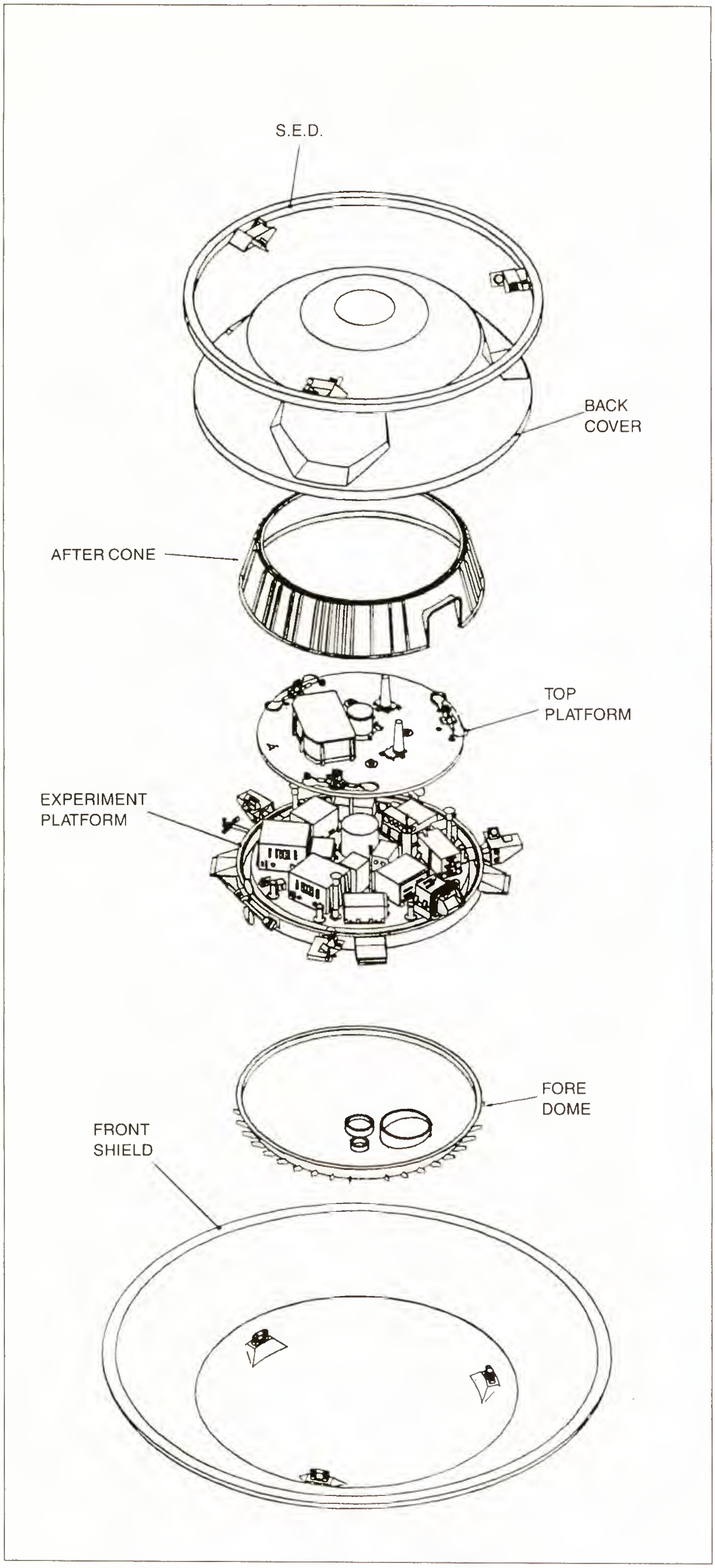

Figure 2. Exploded view of the Huygens Probe. The 2.7 m diameter front shield and an aft cover protect the Probe during entry. The Probe's descent module comprises a round fore-dome and a conical aft section: a top platform carries the two antennas and the parachute box, while the payload and subsystems are mounted on the experiment platform at the centre

Figure 3. Drop test of Probe in descent configuration, with drogue parachute (photo courtesy of Martin-Baker Aircraft Co.)

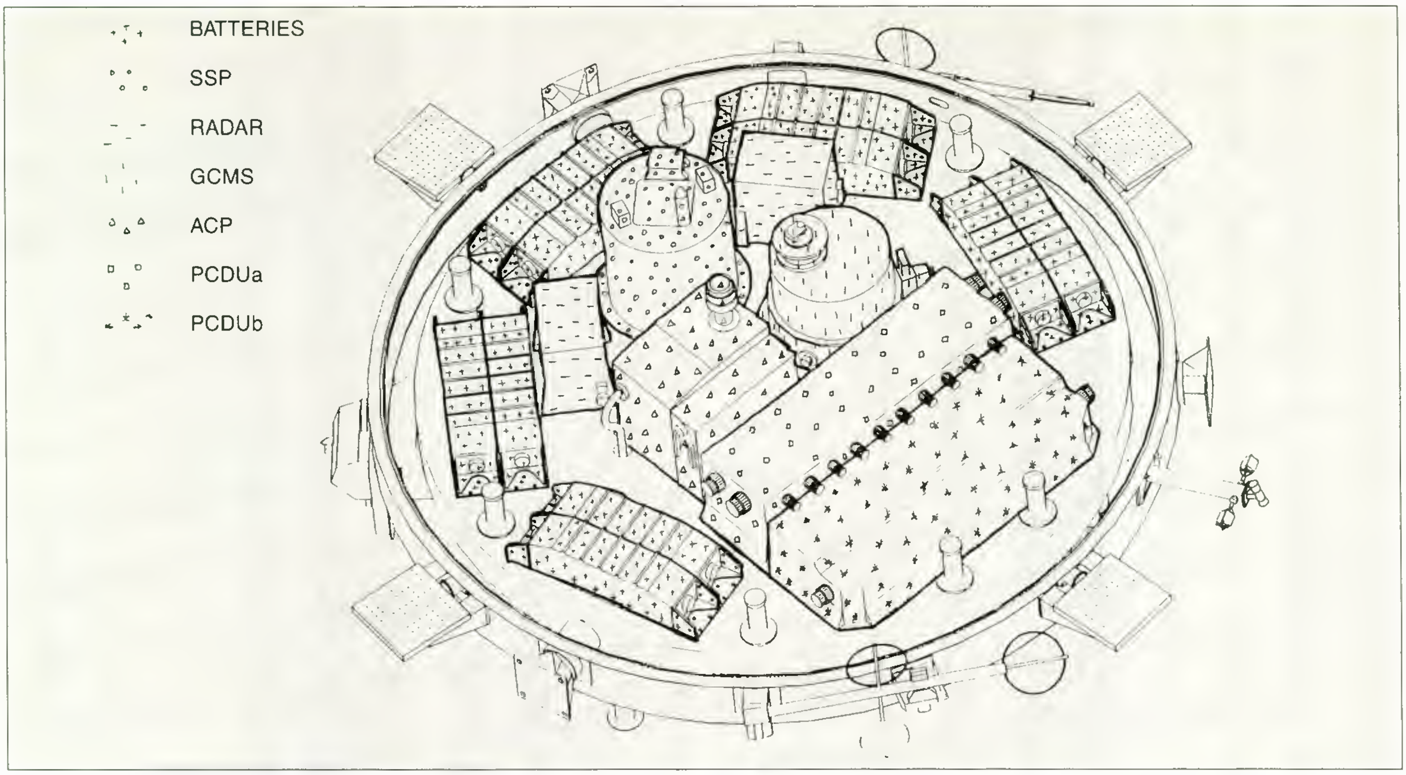

Figure 4. View of the experiment platform's underside, showing the individual units. Colour coding shows the breakdown of components used in the impact model. The aluminium fore-dome, and the insulating foam layer have been removed for clarity

6. Ocean impact

A landing of a space vehicle on an extraterrestrial hydrocarbon ocean is indeed an exotic and imaginative scenario, but is by no means improbable. While such an event would be a first in space exploration, the problem of landing on liquids is a fairly familiar one in a terrestrial context.

Vehicle splashdown loads were first considered theoretically in 1929 (although there was some experimental work in the UK in 1919) by Von Karman[30], for the purpose of estimating landing loads on seaplane floats, but received detailed examination for the Mercury and Apollo Programmes. Two theoretical approaches are possible to estimate loads: one is to model the impacting probe as a source sheet in potential-flow theory, and compute the resulting pressure and flow distribution in the liquid[31]; the other is to assume that the impacting probe becomes 'loaded' with a virtual mass of ocean, using more-or-less empirical factors.

The second method was found to give excellent agreement with results from scale-model and full-size impact experiments[32] and, being considerably simpler than the potential-flow method, is used here. The method was also used to evaluate splashdown loads on the crew compartment of the Space Shuttle 'Challenger'[33].

Let us assume a mass M_0 for the Probe, and vertical impact velocity V_0. As it penetrates, it becomes loaded with a virtual mass M_v of liquid, with the Probe/liquid ensemble moving at a velocity V. The virtual mass, which varies as a function of time, may be considered as the effective mass of liquid with which the Probe shares its momentum at a given instant.

Applying conservation of momentum and ignoring drag, weight and buoyancy forces (e.g. during the first 0.05 s of impact, weight would make only a 1% change in the Probe's momentum) gives

$$(M_o+M_v)V = M_oV_o \tag{1}$$

Differentiating,

$$(M_o+M_v)\frac{dV}{dt} + V\frac{dM_v}{dt} = 0 \tag{2}$$

The virtual mass M_v is usually taken as a fraction k (0.75 in Ref. 32 and $2/\pi$ (=0.64) in Ref. 34: here k=0.75 is used) of the mass of a hemisphere of liquid with a radius R equal to that of the (assumed axisymmetric) body at the plane of the undisturbed liquid surface (Fig. 5). Thus, for a liquid of density ρ, the virtual mass is

$$M_v = 2k\pi\rho R^3/3 \tag{3}$$

For a general axisymmetric shape $R=f(h)$, where h is the penetration distance, it is easy to show that

$$\frac{dM_v}{dh} = 2k\pi\rho\, R^2 \frac{dR}{dh} \tag{4}$$

noting that $\frac{dh}{dt} = V$ and $\frac{dV}{dt} = a$

we obtain

$$a = \frac{-V^2(2\pi k\rho R^2)}{(M_0+M_v)} \frac{dR}{dh} \tag{5}$$

These equations are easy to solve numerically (indeed in the early days[32] the numerical computation was performed manually). Terms for drag, weight and buoyancy could be added, but do not significantly affect the peak loads.

For a spherically-bottomed vehicle with a radius of curvature R_N and a penetration distance h (Fig. 5), this 'waterline' radius is given simply as

$$R = (2R_N h - h^2)^{1/2} \tag{6}$$

and the equations can be solved analytically to derive (for example) the peak loads (see, for example Ref. 34).

The above method can also be used to estimate the loads on a 75 kg human diving into a swimming pool. If the nose radius corresponds to the size of the head, the peak load is a little under 1 g: if, on the other hand, the nose radius is increased to, say, 30 cm (i.e. a 'bellyflop'), the loads increase to ~6 g. This order-of-magnitude change in load is painfully apparent to those unfortunate enough to verify the nose-radius dependence experimentally!

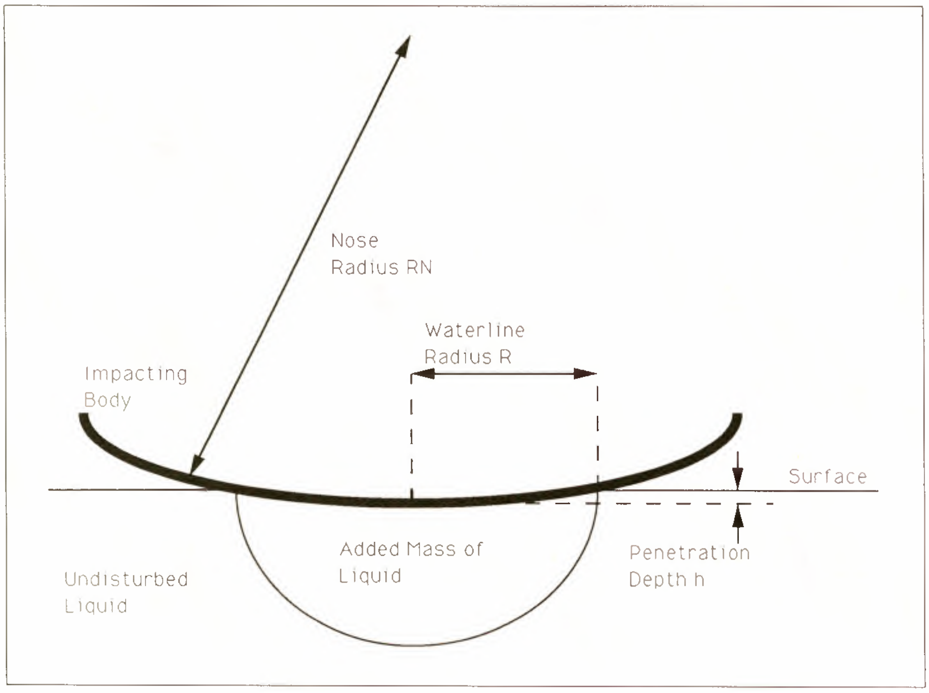

Figure 5. Idealised geometry for a vertical impact of a sphere-nosed body into a liquid

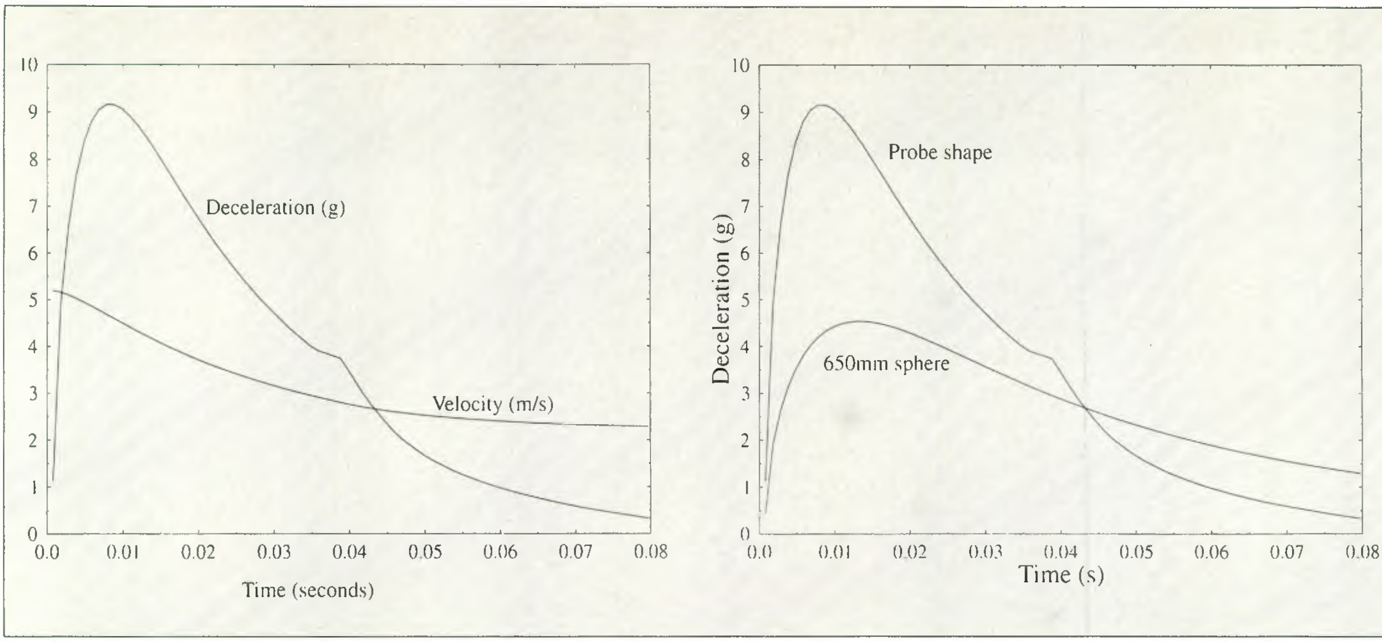

Figure 6a. Deceleration and velocity profile for the nominal impact case, assuming the Probe shape as described in the Appendix to be perfectly rigid (drag and buoyancy not modelled)

Figure 6b. Deceleration profile for the same impact case, but also showing the profile for a spherical nose radius of 650 mm for comparison (drag and buoyancy not modelled)

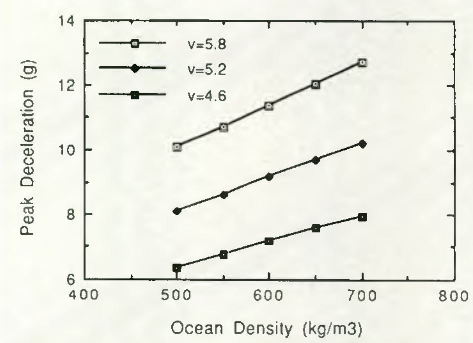

Figure 7. Peak impact decelerations for a 207 kg Probe (assuming rigid 'real' shape) in various ocean densities at various speeds

It is tempting to approximate the shape of the Probe with a sphere of 650 mm but, due to the sensitivity to nose radius, this might lead to underestimation of the peak loads. Figure 6 shows the acceleration versus time and speed versus time profiles for a 207 kg Probe splashing into liquid of density 600 kgm^{-3} for the actual Huygens Probe shape (see Appendix). A corresponding profile assuming a sphere of 650 mm radius is shown for comparison. It is apparent that the peak load is reached after about 0.01 s, after the Probe has penetrated to a depth of about 5 cm. After the peak, the loads decay away; after this, drag, buoyancy and weight begin to significantly modify the Probe's motion, but this is not evaluated here.

(Note that there should be a slight jump in the acceleration level at about t=0.1 s as the bulky attachment mechanisms used to hold the front shield during entry hit the liquid, but this has not been modelled here).

The peak impact loads are shown in Figure 7 for the actual Huygens Probe shape with mass 207 kg for various impact velocities and ocean densities (pure liquid methane has a density of about 450 kgm^{-3}, ethane about 600 kgm^{-3} and liquid nitrogen about 800 kgm^{-3}). The ocean compositions suggested in Reference 35 indicate the most likely density range as 600–650 kgm^{-3}.

A method similar to that above can be used to estimate the loads on appendages, such as the booms of the Huygens Atmospheric Structure Instrument (HASI). First estimates suggest that the splash loads should generate bending moments at the boom roots of the order of 10 Nm, and so, provided the boom hinge attachments do not act as stress concentrators, the booms should survive.

It was found during tests on a 1/4-scale model of the Apollo Capsule[36] that vertical landing loads are virtually independent of any impact-velocity component parallel to the surface. Additionally, impacts with the axis of the Capsule in a non-vertical orientation had lower accelerations (e.g. 60% of normal load for a 10° pitch at impact) than the nominal vertical case (intuitively we might expect this, as the interface of the spheroidal bottom of Apollo with the upper conical structure makes a 'sharp' corner which penetrates the ocean more easily than the 'blunt' bottom).

Thus, loads along the main axis of the Probe at impact are highest for vertical impact (the nominal case). The worst-case loads occur for a light Probe, high impact velocity, and dense ocean. These worst-case loads are about 13 g, assuming the Probe to be rigid; nominal loads are of the order of 9 g.

Tests on the Apollo Module[37] showed that vehicles with non-rigid bottoms (such as Huygens) may experience peak loads approximately 50% in excess of those encountered with a rigid bottom, so perhaps a margin should be added to the above figures (in Ref. 36, for example, accelerations of 38 g were measured when calculations indicated a rigid-body value of 22 g). An estimate of the impact pressure on the Probe can be made by dividing the impact force (equals Probe mass times instantaneous acceleration) by the wetted surface area of the Probe. Ignoring the singularity at the instant of impact, this pressure is of the order of $10-20\ N/cm^2$. Comparing this with the strengths of Probe elements (see Section 9 and the Appendix) indicates that the Probe will indeed deform, modifying the deceleration history given in Figure 6. No attempt is made here, however, to model the coupled flow/structural effects.

Since the Huygens Probe is designed for (axial) entry loads of the order of 20 g in any case, the axial loads for liquid impact should be perfectly survivable, even with a margin for non-rigid effects imposed on the splash load predictions. Note, however, that the entry loads are conducted to the experiment platform via a different load path, leading to compressive stress on underside units.

Should there be a sideways velocity component at impact, there will naturally be a sideways (radial) acceleration. This will be small, however, compared with the axial loads (in Ref. 36, for example, an impact with an 11° pitch angle, a $7\ ms^{-1}$ vertical velocity, and a $3\ ms^{-1}$ horizontal velocity had an axial load of 30 g, with a sideways load of only 2.9 g). The radial loads on the Probe are in effect in the same direction as the launch loads (the Probe is attached sideways to the Cassini Orbiter at launch), so that, given the anticipated impact conditions, sideways loads should not cause damage to the Probe. A sideways impact will also produce an angular acceleration pulse, but this is not considered further here.

After the initial acceleration pulse, the acceleration decays until the Probe's entire lower surface is immersed. There will be a slight pulse due to liquid inertia loads on the radar altimeter antennae and the appendages used to attach the Probe to its entry shield. After this, however, the inertia loads are minimal and the forces of hydrodynamic drag and buoyancy are the most important. For the nominal ($5.2\ ms^{-1}$) vertical impact with an ethane ocean ($600\ kgm^{-3}$), the Probe will have been decelerated to about $2.5\ ms^{-1}$ by the time its lower surface is completely immersed. Rough estimates suggest that the Probe will continue moving for another 1 s to a depth of about 1 m, with the top platform a few tens of centimetres below the depth of the ocean (the antennas should be submerged only momentarily, if at all). Buoyancy brings the Probe bobbing back up to the surface about 1.5 s after first contact. Note that the slightly lower impact loads and deeper penetration reported in Reference 7 were computed for a somewhat narrower Probe shape, before the current design had evolved.

7. Post-impact dynamics for liquid landing

In the event of a landing in a lake or sea, the subsequent dynamics and flotation characteristics of the Probe are of interest, since these will affect the post-impact scientific measurements.

A key question is naturally whether the Probe will float at all. Since the bulk density of the Probe is of the order of $200-300\ kgm^{-3}$, while that of the ocean (assuming it is free of bubbles) is about $600\ kgm^{-3}$, the answer is that it will. However, the level at which it floats is also of interest, to determine whether the Descent Imager and Spectral Radiometer (DISR) is above the 'waterline', and to verify that the measurement cavity of the Surface Science Package (SSP) is below it, so that its transducers are in contact with the liquid.

In order to determine the flotation level, a simple model (Fig. 8) has been set up to calculate the force and moment due to buoyancy for the Probe at any immersion depth and orientation. This is done simply by assuming that the Probe is axisymmetric, and breaking it down into small elements. Simple geometry determines whether each element is submerged or not; if submerged, it has a buoyant force equal to the weight of the displaced liquid. This force also has a moment arm associated with it. Summing these forces and moments allows the overall upthrust and torque to be determined. These quantities are given in Figures 9 and 10 for a nominal ocean density of $600\ kgm^{-3}$; the forces and moments scale directly with ocean density.

It is seen, by comparing the upthrusts with the Probe weight (Fig. 9), that the Probe should float with the 'waterline' almost at the level of the Probe centre-of-gravity. Thus, happily, the DISR is above the surface, and the SSP cavity is filled.

Figure 8. Geometry of floating Probe. Upthrust acts at centroid of the submerged portion of the Probe: weight acts at centre-of-gravity

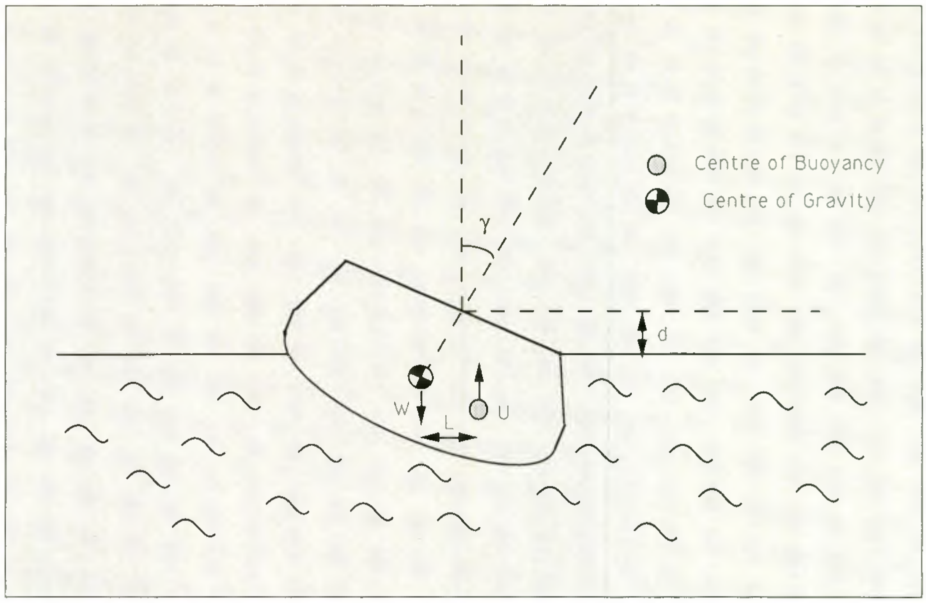

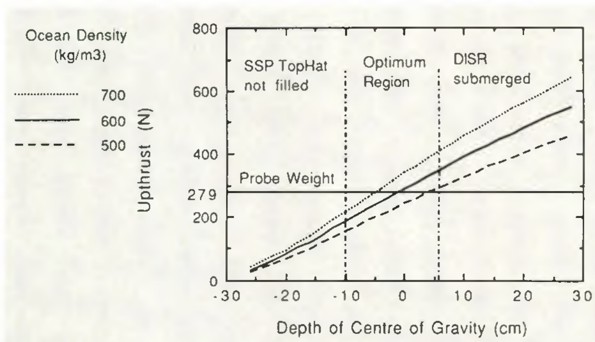

Figure 9. Upthrust as a function of depth of immersion for various ocean densities. The 'waterline' exists where the upthrust equals the weight. The waterline for the expected cases lies, reassuringly, in the most suitable region, around the 'equator' of the Probe

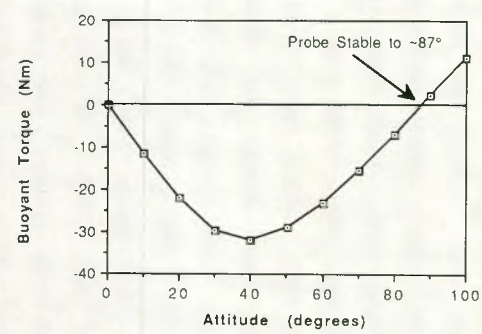

Figure 10. Buoyant torque (negative torque indicates a restoring, i.e. stable, moment). Note the linear dependence for small angles, and the onset of capsizing instability at large tilt

As all the moments are negative, the Probe is stable in its nominal vertical attitude (assuming that it is not significantly deformed during the impact). It would need to be tilted to about 87° before capsizing, which is presumably only possible in the event of improbably high (>impact speed) surface winds.

These negative moments are, for small angles, approximately proportional to the angle of the Probe (Fig. 10). A 'rocking' period can thus be determined by assuming that the rocking is a simple harmonic motion. If the buoyant torque $J = UD = k\gamma$, where γ is the angle of the Probe (Fig. 8), then the period of the motion is simply $2\pi\sqrt{(I/k)}$ where I is the Probe's transverse moment of inertia. Further, since the constant of proportionality (~ 68 Nm/rad for $P = 600$ kgm^{-3}) is itself proportional to the ocean density, and the Probe's orientation can be measured with tilt sensors (part of the SSP experiment), this leads to a crude method of determining ocean density. For a density of 600 kgm^{-3}, the rocking period is 3.4 s; for a 650 kgm^{-3} ocean, the period is 3.26 s. Bobbing periods for vertical oscillations (since the upthrust is proportional to displacement) can also be established, and can be measured with Probe accelerometers to derive another, albeit coarse, density measurement.

In the event of landing in a lake or sea, the payload will be able to measure currents and wave properties, ocean composition, physical properties (e.g. dielectric constant, useful in interpreting radar data), turbidity, and depth. The DISR camera will be above the 'waterline' and will be able to image the surface and lower atmosphere. The detailed science plans for the surface are still under discussion (see later).

8. Impact with solid surface

Impacts with solid surfaces are much harder to evaluate, due both to the paucity of experimental data and the difficult analytical treatment. A handful of drop tests onto sandy surfaces were performed in connection with the Mercury[38] and Apollo[36] programmes. In addition, a large series of experiments were conducted in connection with using penetrators to evaluate the lunar surface (before the Surveyor series of missions was performed). In these experiments[39], small dense ball-nosed vehicles were dropped or shot into a variety of materials including sand, earth, lead, balsa wood and concrete.

If the rock/ice at the landing site is finely-divided and non-cohesive (since it is so cold), we may perhaps treat it as sand (although it will have a lower density than sand, so predictions here will perhaps be slightly pessimistic). A formula developed in Reference 39 gives peak deceleration for nose diameter D (m), mass M (kg) and impact velocity V (ms^{-1}) as proportional to $D^{1.6}V^{1.6}M^{-1}$. However, this empirical formula does not appear to scale well to the Apollo and Mercury results (see Table 2).

Reférence 39 also gives some theoretical expressions for the impact of spheres into elastic ('The Hertz Law') and plastic ('The Meyer Law') materials which appear to scale with much more success to the other results. Since the Mercury and Apollo models are more similar in size to Huygens, and their speeds and masses are comparable, these results are the most pertinent to validating the estimation methods. Expressions (7) and (8) below predict peak decelerations (assuming Huygens has a diameter of 1.3 m, and mass and velocity as in the previous sections) of 32 g and 26 g, respectively, for landing on sand surfaces.

The expressions as given in Reference 39 depend explicitly on given material properties: in the expressions below, however, I have simply made an empirical fit to the data in Table 2. Thus the peak impact accelerations are given (in Earth g) as

$$a_{max} = 35\ D^{0.2}V^{1.2}M^{-0.4} \tag{7}$$

or

$$a_{max} = 60\ D^{0.5}V^{1.6}M^{-1} \tag{8}$$

Since the bearing stress in sand increases with depth (see later), Expression (7) is probably preferable on theoretical grounds. Additionally, it appears to give a marginally better fit to the (limited) dataset in Table 2.

Thus if Huygens can be considered as a rigid sphere of radius 650 mm, its peak impact deceleration on landing on sand (i.e. a moderately dense, non-cohesive fine particulate material, or regolith) should be in the range 26–32 g. The presence of larger lumps of material like boulders will, of course, modify this prediction (see, for example, Ref. 40).

This impact deceleration is rather larger than the entry deceleration, but perhaps is within engineering margins. Consider, for example, the power distribution relays (Deutsch EL415). Sudden deceleration at impact could cause these to 'chatter', causing momentary interruption to the power supply. The 'all axes' acceleration specification is 15 g, but the shock (6 ms) tolerance is 200 g. For the Probe to stop with 30 g from 5.2 ms^{-1} takes about 16 ms, and so one would cautiously expect that the specification should not be exceeded. However, the situation is marginal.

Table 2. Comparison of theoretical predictions of peak impact loads for sand impact with experimental data. Huygens model data are from unpublished work by A. Seiff of NASA Ames, using 1/3 and 1/9 scale models of the Phase-A Huygens Probe design

Model	Ref	Peak load measured	Hertz law $35D^{0.2}V^{1.2}M^{-0.4}$	Meyer law $60D^{0.5}V^{1.6}M^{-1}$	Empirical (Ref. 39) $80D^{1.6}V^{1.6}M^{-1}$
1/3-scale Phase-A Huygens	-	26	27.1	27.4	10.72
1/9-scale Phase-A Huygens	-	20	17.4	15.67	2.2
1/6-scale Mercury Capsule	38	74	102	103	106
1/4-scale Apollo Capsule	36	49	49.6	52	54.77
3-inch hemisphere	39	50	249	149	51.8
Huygens	-	??	31.6	24.7	8.2

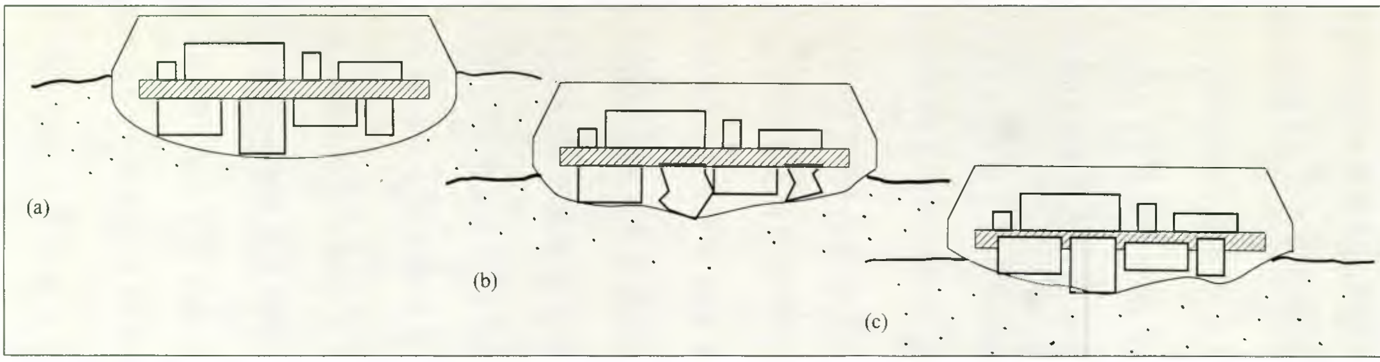

Figure 11. Consequences of impact depend on relative strengths of landing-site material, subsystems boxes and experiment platform:
(a) soft material: becomes compressed
(b) hard material: loads applied to boxes, causing failure
(c) hard material: loads applied to boxes, punching them into honeycomb of experiment platform

All the above considerations assume the Probe does not deform. However, since the impact process leads to the application of structural loads directly onto units on the Probe's underside, these units may be deformed, leading to failure. Figure 11 indicates how the impact energy may be dissipated in the soil, the units, or the experiment platform. To examine in detail the structural effects of the impact on the Probe, and the sensitivity of the Probe deceleration history to surface mechanical properties, a more detailed approach is required.

9. Impact-dynamics model

The model considers the Probe essentially as a point mass, mounted atop several (seven in the nominal model) 'stacks', each of four elements (Fig. 12). Each element is defined with an undistorted length, and a stress vs. compression characteristic described by linear interpolation between four given points (Fig. 13). Each stack is allocated a cross-sectional area.

For example, one 'stack' represents the spacecraft batteries, and comprises the following elements: the experiment platform (a honeycomb sandwich), the batteries themselves (modelled as essentially rigid boxes), an airgap, and a layer of thermal-insulation foam. Note that although there are actually five batteries on the Probe, they are modelled (for speed) as one stack with an area equal to that of the sum of the actual battery boxes. The 0.8 mm aluminium fore-dome is treated separately in these calculations (see Appendix). It is assumed that the dome does not interact (i.e. exchange loads) with the stacks.

The impact simulation works as follows: starting from a given height above the surface (assumed flat), the program steps down in height increments of 1 mm (the height is defined from the upper side of the experiment platform to the undisturbed surface). The penetration of a given stack into the surface material is computed by subtracting the sum of the lengths of its elements (each multiplied by its own compression factor) from the height. The penetration yields a certain bearing strength (see Section 10). The program considers each element in turn, to determine which element is the 'softest' (i.e. yields the lowest compressive stress for the next height decrement), whether one of the stack elements or the soil itself, and allows this selected element to deform.

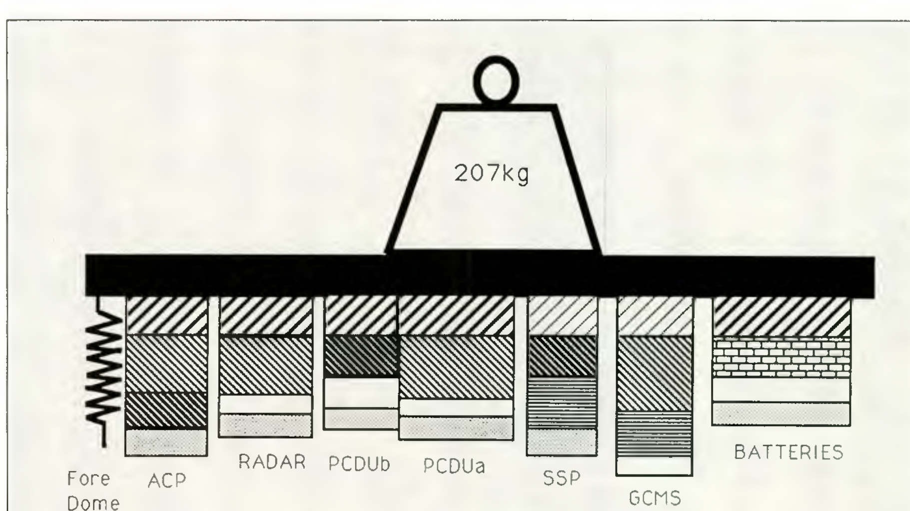

Figure 12. Schematic of crash model used in this study. Different box shadings indicate different element strengths

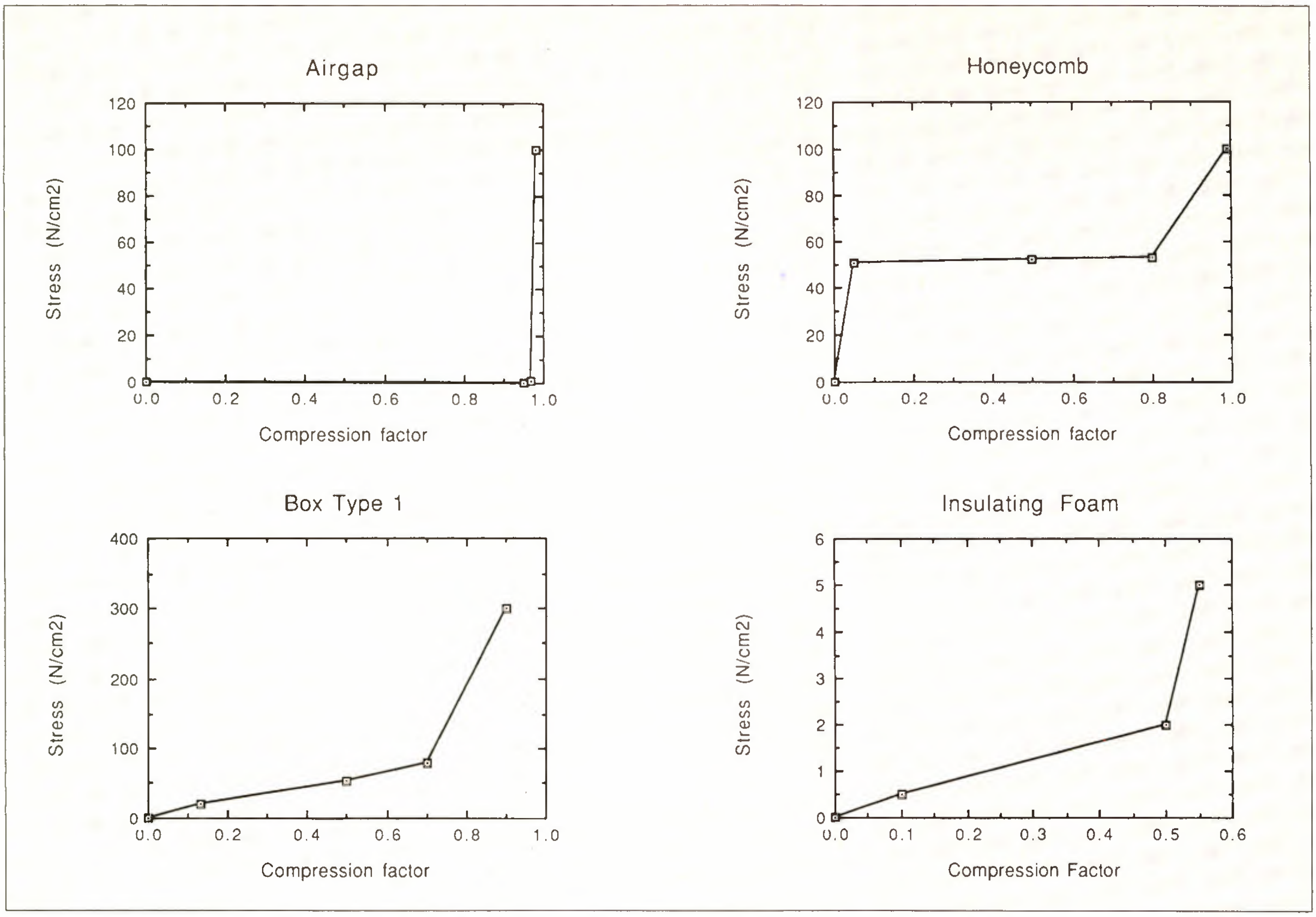

Figure 13. Stress-compression characteristics for four example elements from Table 4

As an element deforms, it resists more stress (typically), and thus is less likely to be deformed in the next iteration. Naturally soft elements (such as foam or airgaps) deform first, while stronger elements do not begin to deform until the loading on the stack becomes quite high (e.g. due to deeper soil penetration). The deceleration of the Probe platform is derived by summing the various loads and dividing by the Probe mass. Note that depth is the independent variable, not time. The simulation is stopped when the velocity falls to zero, giving the peak loads and depth of penetration.

The element lengths and stack areas are taken from Probe engineering drawings, and (for ACP, GCMS and SSP) from payload engineering drawings, and are summarised in Table 3. The methods used to estimate the stress-compression characteristics of the various elements, listed in Table 4, are described in the Appendix.

The program runs in a couple of minutes on a standard 386 PC: sample screen dumps are shown in Figure 14. The (quite primitive) numerical methods used in the program yield results accurate to about 10%. More accurate methods are not justified, given the overall simplicity of the model and the uncertainty of model parameters (such as buckling stresses, etc.). Thus, while the model's results are useful in gaining a qualitative idea of what is happening (i.e. discriminating between the cases in

Table 3. Elements of Probe impact model: lengths are in millimetres, while stress/compression characteristics are given in Table 4

Unit	Area (cm^2)	Element 1 length/type		Element 2 length/type		Element 3 length/type		Element 4 length/type	
SSP	250	80	4	50	9	150	8	30	2
ACP	506	80	3	165	11	40	12	50	2
GC-MS	302	80	4	150	7	50	6	50	2
BATTS	2625	80	3	80	5	40	1	50	2
PCDUa	1044	80	3	150	10	40	1	50	2
RADAR	295	80	3	150	11	40	1	50	2
PDCUb	1140	80	3	110	10	50	1	50	2

Table 4. Characteristics of element types used in the model. C denotes compression factor (i.e. strain), while S is the stress in N/cm^2

No	Type		1	2	3	4
1	Air gap	C	0.95	0.97	0.98	1.00
		S	0.01	1.00	100.00	1000.00
2	Basotect foam	C	0.10	0.50	0.55	0.90
		S	0.50	2.00	5.00	1000.00
3	100% honeycomb	C	0.05	0.50	0.80	0.99
		S	51.00	52.00	53.00	1000.00
4	50% honeycomb	C	0.05	0.50	0.80	0.99
		S	25.00	26.00	27.00	1000.00
5	Hard box	C	0.01	0.10	0.20	0.99
		S	10.00	100.00	1000.00	2000.00
6	GCMS top dome	C	0.25	0.50	0.70	0.90
		S	4.60	10.00	20.00	200.00
7	GCMS cylinder	C	0.10	0.20	0.30	0.90
		S	80.00	100.00	400.00	600.00
8	SSP top-hat body	C	0.10	0.20	0.50	0.90
		S	80.00	60.00	30.00	200.00
9	SSP top-hat cone	C	0.10	0.20	0.80	0.90
		S	200.00	400.00	500.00	600.00
10	Box type 1	C	0.13	0.50	0.70	0.90
		S	20.00	55.00	80.00	2000.00
11	Box type 2	C	0.13	0.55	0.90	0.95
		S	40.00	50.00	200.00	300.00
12	Box type 3	C	0.20	0.55	0.90	0.95
		S	13.00	50.00	200.00	300.00

Fig. 11) and estimating deceleration histories for the Probe, not too much attention should be paid to the deformation of individual units until the model has been refined with as-built structural parameters or validated with finite-element simulations.

10. Surface models

Having established the structural properties of the Probe, it remains to obtain plausible, but usable, surface models to interact with it. A review of current understanding of Titan's surface can be found in Reference 8. In principle, any surface type is possible, but only three principal types are examined, namely regolith, sludge, and hard ice/rock.

Since surface heat flow on Titan is sufficiently high that the crust may be convective, mountain-building and tectonics cannot be ruled out, and so the possibility of sloping terrain cannot be excluded. Similarly, aeolian transport[8,29] of surface particulates could form dunes[41]. However, for the purposes of this work, I assume that the impact occurs on flat, horizontal terrain.

Fresh, hard ice might exist where there has been recent cryo-volcanic activity, at the base of young impact craters, or where fluvial or aeolian activity has scoured the surface free of loose particulates. This may be modelled by setting the surface hardness to an arbitrarily large value.

Particulate material is likely to cover some, if not all, of Titan's surface. This material would include solid photochemical aerosols (acetylene and higher organics) and icy impact ejecta. However, the mechanical properties of these deposits are not well-constrained. Dry deposits of aerosol particles (which appear to have a fractal

```
HUYGENS IMPACT SIMULATION    R D Lorenz 93/94   a:\res\sl

Soil Parameters: k1= 1  k2= .1  k3= 0   Mprobe= 207 kg      Vimpact= 5.2 m/s
Shell Model   1000  N/m       GC-MS fails at 8000 N

Time : 50 ms        Height  150 mm        Speed 0.000m/s        Accel(g)23.383

                    .SSP.  .ACP.  GC-MS  BATTS  PCDUa  RADAR  PCDUb

crush( 1 )          0.03   0.01   0.01   0.00   0.00   0.00   0.00  Shell Load (N)
crush( 2 )          0.00   0.04   0.01   0.00   0.07   0.03   0.05      175.0
crush( 3 )          0.01   0.20   0.52   0.97   0.99   0.99   0.98
crush( 4 )          0.53   0.90   0.90   0.54   0.56   0.56   0.56

Stress:            15.00  13.40  11.60   4.40  10.24  10.74   6.90
Force (N)           3750   6780   3503  11550  10691   3168   7866
Pen (cm)           14.00  12.40  10.60   3.40   9.24   9.74   5.90

             AngleZ (deg) -1.3     AngleY (deg)   1.9   DISR clearance (mm) 211.6
maximum g 23.38315   at  48.09193  msecs
```

(a)

```
HUYGENS IMPACT SIMULATION    R D Lorenz 93/94   a:\res\sl

Soil Parameters: k1= 1  k2= .1  k3= 0   Mprobe= 207 kg      Vimpact= 5.2 m/s
Shell Model   1000  N/m       GC-MS fails at 8000 N

Time : 9 ms        Height  289 mm        Speed 5.102m/s        Accel(g) 2.244

                    .SSP.  .ACP.  GC-MS  BATTS  PCDUa  RADAR  PCDUb

crush( 1 )          0.00   0.00   0.00   0.00   0.00   0.00   0.00  Shell Load (N)
crush( 2 )          0.00   0.01   0.01   0.00   0.01   0.01   0.01      36.0
crush( 3 )          0.01   0.03   0.10   0.00   0.77   0.77   0.02
crush( 4 )          0.43   0.70   0.52   0.00   0.00   0.00   0.00

Stress:             1.70   2.00   2.00   0.00   1.00   1.00   1.00
Force (N)            425   1012    604      0   1044    295   1140
Pen (cm)            0.70   1.00   1.00   0.00   0.00   0.00   0.00

             AngleZ (deg) -0.0     AngleY (deg)   0.0   DISR clearance (mm) 329.1
```

(b)

Figure 14. Example screen dumps from the program. Rows of figures marked 'Crush(X)' denote the current compression of each element; X = 1 are topmost elements (honeycomb). Also shown are the stress, total force and penetration depth of each stack. Figure 14a shows status early in impact event, with large crushing of airgaps (PCDU, RADAR 3) and deformation of foam on SSP, GCMS, ACP 4. Figure 14b shows status at end of impact, with more extensive crushing

structure, judging from Pioneer 11 polarimetry and Voyager 1 infrared results, and theoretical modelling) could be very soft, like fluffy snow. On the other hand, rainfall or other processes could compact these deposits into much harder soils.

A comprehensive soil-mechanics[42] treatment would be impractical and so a simple soil model is given here. Following Sperling & Galba[25], I use a soil stress p of the form

$$p = k_1 + k_2 x + k_3 v^2 \tag{9}$$

where p is the force per unit area on the spacecraft, x is the penetration depth into the soil, and v is the instantaneous impact velocity of the spacecraft. For all the cases I examine here, k_3 is set to zero (as in Ref. 25). Note that in Reference 26, $k_1 = 0$, and k_2 is called the 'subgrade modulus'.

In order to obtain realistic figures for k_1 and k_2, data for a variety of terrestrial and planetary surfaces have been collected in Table 5. These values, and their corresponding soil stresses from Equation (9), are used to select appropriate values for use in the model. It is instructive to compare the soil stress at various depths with, for example, the pressure on the sole of a shoe (say $1-2$ Ncm^{-2})

From a review of the data in Table 5, the nominal 'regolith' model assumed in this work is essentially that of the lunar soil as measured by Surveyor, namely $k_1 = 1$ N/cm^2, $k_2 = 0.1$ N/cm^2/mm. A 'soft, fluffy aerosol' deposit would have parameters $k_1 \sim 0$, $k_2 \sim 0.01$ N/cm^2/mm.

As for wet mixes of aerosols/ejecta with liquid ethane/methane, i.e. 'sludge', a useful terrestrial analogue may be clay, at one extreme. The other extreme, naturally, is thin sludge, which should be treated similar to a 'pure' liquid impact. Penetration tests on clay typically yield a constant 'flow presure': i.e. $k_2 \sim 0$. Tests on sod (Ref. 39 found that a value of 37 psi, or $k_1 = 25$ N/cm^2 gave a good fit to data, so sludge models in this study have k_1 values around, or lower than, this.

Table 5. Soil parameters from field measurements, and data from planetary landers

Type	Density kg m^{-3}	'Bearing strength' N cm^{-2}	Modulus N cm^{-2} mm^{-1}	Conditions	References
Very soft snow	200	0.6		5 kg load on fist will penetrate	43
Soft snow		4		5 kg load on fingers will penetrate	43
Medium snow	400	16		5 kg load on one finger will penetrate	43
Hard snow	600	150		5 kg load on pencil will penetrate	43
Very hard snow		300		5 kg load on knife will penetrate	43
Compacted snow	500	10	0.5	Collins Glacier. 30 cm diam. load plate	44
	720	15	1.3	Collins Glacier. 30 cm diam. load plate	44
Lunar dust	300	0.16		For 1 m support, based on pre-Surveyor photographs of crater slopes	24
Lunar soil		1.3	0.08	Surveyor landing dynamics	25
	1100–1600	0	0.1	Surveyor footpad penetration, etc.	45
Compressed lunar soil	1800	100		Yield strength	46
Mars soil 'Sandy Flats'	1000–1600		.03	Viking 1 landing dynamics - footpad penetration	47
Mars soil 'Rocky Flats'	1800		0.6	Viking 1 landing dynamics - footpad penetration	47
Venus soil (Venera 13)	1400–1500	4–5		Shock absorber loads on landing	12
(Venera 13)		2.5–10		Penetrometer	48
(Venera 14)	1150–1200	2		Shock absorber loads on landing	12
Venus rock		65–250		Venera 14 penetrometer	48
White Sands Missile Range 'Coarse-grained sandy silt'			2.7–10		26
0.18 mm glass beads	2230	0.7	.11	Penetration by flat-ended 2 cm-diam. rod	49
0.36 mm resin beads	1050	0.7	.05	Penetration by flat-ended 2 cm-diam. rod	49

11. Model results

Some useful comparisons with the rough estimations in Section 8 can be made by setting the stiffness of all Probe elements to large values (i.e. forcing the Probe to act like a 'rigid body'). For the nominal regolith model (k_1=0.1 Ncm^{-2}, k_2=0.1 Ncm^{-2}mm^{-1}) the peak acceleration obtained is 28 g, reassuringly in the estimate range of Section 8.

With the Probe structural strengths set as in the Appendix, and Tables 3 and 4, the peak acceleration is 23.4 g. Varying the impact velocity from 4.6 to 5.8 ms^{-1} yields peak accelerations of 19.6–27.4 g.

The deceleration history for the nominal Probe strengths, but various soil properties, is given in Figure 15; Figure 16 shows the dependence of the peak load on soil hardness.

If the ground is made very stiff (i.e. generates extremely large bearing strength for minimal penetration, by setting k_2 to very large values), the peak load is determined by the stiffness of the Probe elements alone. It was found that loads were >100 g, and significant crushing of most of the Probe elements occurred. Thus, impact on an arbitrarily hard surface would lead to failure of the Probe.

Table 6. Peak accelerations, and loads on individual Probe units, for various soil strengths

Soil stiffness k_2 (N/cm^2/mm)	Peak deceleration (g)	Load on GCMS (kN)	Load on SSP (kN)	Load on ACP (kN)	Load on PCDU box (kN)	Load on radar boxes (kN)
0.01	11.6	.95	.83	1.6	5	0.8
0.1	25	3.6	3.6	7.0	19	3.4
1	35	7.6	6.5	21	28	8.6
10	40 (41)	7.6 (7.6)	8.3 (8.3)	23 (23)	31 (32)	13 (13)
100	79 (75)	8 (45)	32 (32)	75 (75)	42 (0.2)	12 (0.1)

Figures in parentheses refer to the case where the GCMS mounting is deformed 'normally', without the GCMS being removed from the model when its load exceeds 8 kN

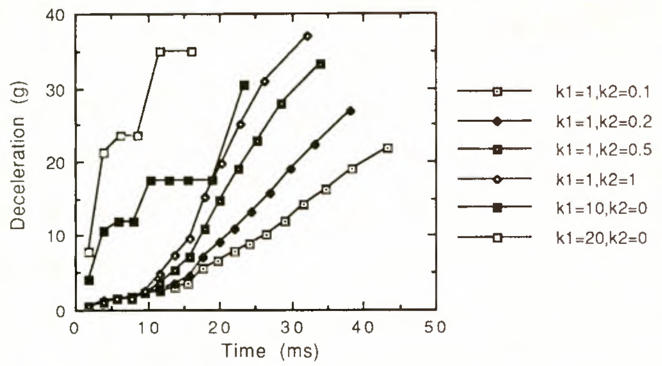

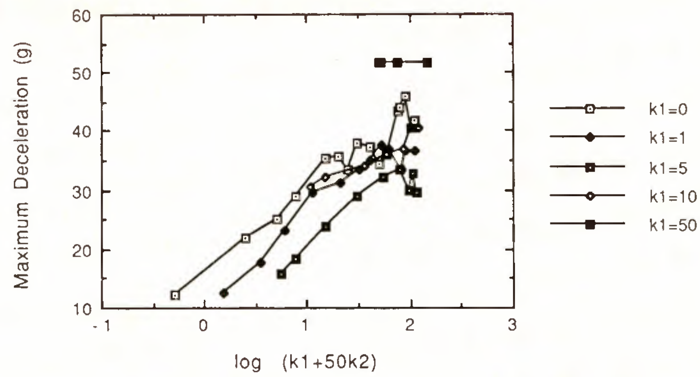

Figure 15. Deceleration profiles for various soil parameters

Figure 16. Correlation of peak g-load with average strength of top 10 cm of soil

For the nominal Probe model, landing onto regolith, the peak deceleration is marginally above the entry g-load. Some slight deformation of the GCMS and PCDU occurs, and the experiment platform above the SSP and GCMS is somewhat deformed. Nevertheless, at least partial Probe operation after such an impact seems likely.

For heavy sludge impact, the partitioning of loads is less effective than for regolith and so the GMCS and its attachment to the experiment platform would be damaged, with the ACP and SSP also receiving large loads. However, the Probe stops sufficiently quickly that loads are not applied to the PCDU box, so that survival of the Probe (and topside experiments such as the DISR) is still probable.

Landing on fluffy aerosols (k_1=0, k_2=0.01) leads to modest g-loads, and very little deformation of the Probe. However, the Probe does penetrate deep enough for the sensor head of the DISR to be buried, compromising post-impact imaging.

The caveat mentioned in Section 9 is repeated: while the depth of penetration and deceleration histories predicted by the model are probably representative, the structural results for individual units should be trusted only qualitatively.

12. Probe survival and post-impact science

For a scientific data return post-impact, one or more of the experiments must survive the impact, the power system must remain operational, and at least one of the redundant data-handling and transmission chains must function. An additional aspect is that the attitude of the Probe must be such as to keep the orbiter spacecraft within the antenna lobe to keep the radio link open. As the Huygens Probe is relatively flat-bottomed, this is quite probable. Furthermore, the link is guaranteed for Probe attitudes up to 10° from normal, so for shallow slopes at least (and surfaces with 'boulders' of the order of 20 cm) the attitude of the Probe should not be sufficiently perturbed to break the link: without knowledge of Titan's topography, it is impossible to assign probabilities to this (see Ref. 50 for an approach where topography is known). Should there be a significant horizontal velocity component at impact, the Probe could also roll[51].

Other aspects vital to Probe survival (e.g. thermal environment) are unlikely to be dramatically altered at impact (although the performance of the insulating foam will be degraded by crushing). The mission energy and link budgets are guaranteed for a minimum of 3 min after impact but, depending on the exact descent location (which affects the time-above-horizon and link margin of the radio link to the Cassini Saturn Orbiter) and spacecraft performance in terms of energy utilisation, could permit a somewhat longer surface mission, of perhaps 30 min or more. Thus impact damage is probably the main constraint on surface operation.

As for the experiment payload, the Ultra-Stable Oscillator for the Doppler Wind Experiment, the Huygens Atmospheric Structure Instrument, and the Descent

Imager/Spectral Radiometer are all on the upper side of the experiment platform, as are the electronics for the Surface Science Package. These elements (including the accelerometers which will measure the impact accelerations, and may subsequently search for seismic activity) should be safe from impact damage by crush loading.

The Aerosol Collector/Pyrolyser (ACP) is mounted on the lower surface, but has completed its mission well before impact. The 'TopHat' sensor accommodation structure of the Surface Science Package is made of glass-fibre panels and insulating foam. In the event of an impact with a hard surface, the TopHat will probably break, although the individual sensor subsystems may still function (in any case, most of these sensors are optimised for liquid surfaces, so the science loss in this scenario is small). The Gas Chromatograph/Mass Spectrometer is a long cylindrical instrument and projects from the base of the Probe through the experiment platform. A hard impact will probably crush the inlets of the instrument, although some instrument operation may still be possible (the inlets are heated to volatilise surface material for analysis); extreme loading would punch the GCMS through the experiment platform.

Thus a reasonable portion of the payload should remain operational after impact on a solid surface, in particular the Descent Imager/Spectral Radiometer, on the upper part of the spacecraft, which will be able to return images (using its side-looking imager) and spectra from the surface. Additionally, upward-looking photometric sensors on this instrument will be able to measure any impact-generated dust cloud (see later). A group has been set up within the Huygens Science Working Team (HSWT) to consider the measurements that are expected (or should be aimed for) post-impact.

13. Impact-dynamics measurements

The impact decelerations of Huygens will be recorded by the accelerometers of the HASI experiment (three-axis piezoresistive, with a force-balance ('servo') accelerometer along the vertical axis, all mounted near the Probe centre of gravity, and by a piezoelectric accelerometer in the SSP electronics box, about 20 cm from the Probe axis. Since both the SSP and HASI are on the upper side of the experiment platform, they should measure accelerations similar to those predicted by the model (i.e. they are in the same location as the 207 kg mass in Figure 12). Combining the data from both sensors should allow the elimination of structural oscillations generated by the impact.

As seen from Figure 7, the peak deceleration is a possible way of measuring ocean density. However, given the uncertainty in Probe structural effects and the presence of various appendages, etc., on the fore-dome, it should probably not be relied upon. The bobbing/rocking periods described in Section 7 may be better in this respect. In any case, ocean composition will be measured directly by the GCMS, and by inference from physical-properties measurements (refractive index, speed of sound, density, etc.) on the SSP.

The impact deceleration for landing on solid surfaces is strongly dependent on soil hardness. From the peak load alone it is not possible to discriminate between high-k_1 and high-k_2 materials, although the combination of the two (e.g. $k_1+50\ k_2$ is a measure of the average bearing strength in the top 10 cm of soil) does show a broad correlation with peak load (Fig. 16) for weaker soils. However, examining the acceleration-time profiles (Fig. 15) shows that high-k_1 materials (sludge) have a much faster rise-time than high-k_2 materials. It is possible to discriminate sludge from liquids because, although their rise times are similar, the peak load for sludge is higher. Further investigations with the model will explore the sensitivity of acceleration profiles to surface properties, and variation of the stiffness of Probe structural elements.

It is probably impossible to discriminate from accelerometry between coarse and fine-grained soil deposits and, for that matter, determine soil stiffness for hard soils. However, there is a small impact sensor or 'penetrometer'[52] that forms part of the University of Kent's Surface Science Package (SSP), comprising a small (14 mm diameter) force transducer mounted on a short mast projecting from the bottom of the Probe. The force profile measured by this instrument (over a much shorter time scale, and thus corresponding to a much smaller spatial scale) should give an indication of particle size in the range 4 – 25 mm, discriminate between cohesive and non-cohesive surface materials, and give a better indication of soil stiffness for regolith and harder soils.

Identification of particle size would provide an indication as to whether the surface materials at the landing site had been sorted by aeolian or fluvial processes. For example, pyroclastic fall deposits (tephra) from terrestrial volcanoes often display a strong central peak in a grain-size histogram[53] due to 'winnowing' by wind as the erupted material falls back to Earth.

14. Impact-induced dust clouds

Following the landing of spacecraft on Venus and Mars, optical measurements have indicated the generation of dust clouds. These have been thrown up owing to the interaction of the aerodynamic wakes of the Venera and Pioneer Venus probes and the retro-rockets on the Viking spacecraft[54]. Calculations of the mass and momentum in the aerodynamic wake of Huygens, and a comparison of the terminal descent velocity of dust particles on Mars, Venus and Titan[61], suggests that a similar phenomenon may occur at the Huygens impact.

Generation of a dust cloud implies that material at the landing site is fine and non-cohesive. Efforts[56,57] to measure the particle size on the basis of the opacity history (i.e. decay time) of the dust cloud have been relatively unsatisfactory, as the interaction of the wake with the ground is complex. However, recent theoretical and experimental investigations[58,59] of the associated fluid-dynamics processes (e.g. the wake of a decelerating disk is of interest for the sometimes catastrophic 'wake recontact' problem in parachute dynamics where the wake catches up with a decelerating parachute and causes it to deflate) show promise that, by the time Huygens reaches Titan, interpretation of dust-cloud data should yield better results.

A significant complication for Huygens is the fact that the parachute is still attached: it may be difficult to discriminate a drop in ambient light due to a dust cloud from that due to the parachute[60].

15. Conclusions

Simple analytical expressions have been presented for estimating the impact decelerations when landing space probes onto liquid and solid (particulate) surfaces. While necessarily limited in utility, these expressions are convenient 'rules of thumb'.

A modest numerical model has been presented to make more accurate predictions of the Huygens impact-deceleration history for impacts onto solid surfaces. This model has enabled the investigation of the sensitivity of impact deceleration to surface mechanical properties, and the estimation of the Probe's deformation during the impact.

These studies, and analogy with the Pioneer Venus and other missions, lead us to be cautiously optimistic about the prospects for a productive scientific return from the surface of Titan. Additionally, measurements of the impact deceleration and any impact-induced dust cloud will make modest, but useful, contributions to our knowledge of the physical state of Titan's surface.

Acknowledgements

The author acknowledges the support of the ESA Huygens Project, and a postgraduate research grant from the UK SERC/PPARC. Some early parts of the work reported here were conducted while the author was a Young Graduate Trainee in the Huygens Project Team (PYP) at ESTEC in 1990/91.

Useful insights into crash-dynamics analysis techniques for aerospace vehicles were gained by a visit to the Cranfield Impact Centre Ltd., and fruitful discussions there with Dr Sadeghi and his colleagues. B. Steckemetz, of OHB System (Germany) helpfully provided details of the ESA Mars Lander study.

A. Seiff of San Jose State University (USA) is thanked for providing unpublished model impact data. J. Underwood of Martin Baker Aircraft (UK) is thanked for providing Figure 3.

The review of an early version of the paper by J-P. Lebreton of ESA Space Science Department is gratefully acknowledged, as are useful discussions with members of the Huygens Science Working Team, in particular T. Owen and J. Lunine.

The author thanks the following individuals for their cooperation in providing information on the Huygens Probe, payload and components: D. Wyn-Roberts (ESTEC, NL), M. Bannister (RAL, UK), J-F. Brun and M. Tintignac (CNRS, France), A. Nairn (ETCA, Belgium), C. Lewis and S. Way (GSFC, USA) and J. Underwood (Martin Baker, UK).

References

1. Kohhase C. 1993, Meeting with a Majestic Giant: The Cassini Mission to Saturn, *The Planetary Report*, Vol. 13, No. 4, pp. 5–10.
2. Lebreton J-P. & Matson D. 1992, An Overview of the Cassini Mission, *Il Nuovo Cimento*, Vol. 15C, pp. 1137–1147.
3. Lebreton J-P. & Matson D. 1990, Cassini – A Mission to Saturn and Titan, Proc. 24th ESLAB Symposium on the Formation of Stars and Planets and the Evolution of the Solar System, Freidrichshafen, September 1990, ESA SP-315, November 1990, pp. 7–12.
4. Lebreton J-P. 1992, The Huygens Probe, Proc. Symposium on Titan, Toulouse, 9–12 September 1991, ESA SP-338, April 1992, pp. 287–292.
5. Mooij E. 1992, De Cassini-missie, *Ruimtevaart*, June 1992, pp. 2–8.
6. NASA/ESA Cassini Phase-A Study, ESA/SCI 88(5).
7. Lorenz R. 1992, Huygens Probe – The Surface Mission, Proc. Symposium on Titan, Toulouse, 9–12 September 1991, ESA SP-338, April 1992, pp. 359–364.
8. Lorenz R. 1993, The Surface of Titan in the Context of ESA's Huygens Probe, *ESA Journal*, Vol. 17, pp. 275–292.
9. Lebreton J-P., Verdant M. & Wills R. 1994, Huygens: The Science, Payload and Mission Profile, *ESA Bulletin No. 77*, February 1994, pp. 31–41.
10. Hassan H., McCarthy C. & Wyn-Roberts D., Huygens – A Technical and Programmatic Overview, *ESA Bulletin No. 77*, February 1994, pp. 21–30.
11. Wilson A. 1987, Solar System Log, Janes Publishing Company 1987.
12. Arduevsky V.S. et al. 1983, Physico-Mechanical Characteristics of the Venusian Surface by Measuring Shock-Worker at Landing of Automatic Stations Venera 13 and Venera 14 (in Russian), *Kosmicheski Issledovania*, Vol. 21, pp. 331–339.
13. Fimmel R.O., Colin L. & Burgess E. 1983, Pioneer Venus, NASA SP-461.
14. Brodsky R.F. (Ed.) 1985, Pioneer Venus Case Study in Spacecraft Design, AIAA Professional Study Series.
15. Hanson A.H. 1978, Antenna Design for Pioneer Venus Probes, IEEE International Symposium Digest — Antennas and Propagation, 15–19 May 1978, Washington DC.
16. Melosh R.J. & Karat M.F. 1977, Computer Simulation of Light-Aircraft Crash, *J. Aircraft*, Vol. 14, No. 10, pp. 1009–1014.
17. Fasanella E.L., Widmeyer E. & Robinson M.P. 1986, Structural Analysis of the Controlled Impact Demonstration of a Jet Transport Plane, AIAA-86-0939, 27th Structures, Structural Dynamics and Materials Conference, San Antonio, Texas, May 1986.
18. Argyris J., Balmer H.A., Doltsinis I.S. & Kurz A. 1986, Computer Simulations of Crash Phenomena, *Int. J. Numerical Methods in Engineering*, Vol. 22, pp. 497–519.
19. Argyris J., Balmer H. & Doltsinis I.S. 1988, Some Thoughts on Shell Modelling for Crash Analysis, *Computer Methods in Applied Mechanics and Engineering*, Vol. 71, pp. 341–365.
20. Hagiwara I., Satoh Y. & Tsuda M. 1990, Study of an analytical technique and system for conducting vehicle crash simulations, *Int. J. Vehicle Design*, Vol. 11, pp. 564–577.
21. Miller G.K. 1993, Calculation of Impact Loads for High-Energy Drops of Cylindrical Containers, *Int. J. Impact Engineering*, Vol. 13, pp. 511–526.

22. Thomson R.P. 1966, The Practical Problem of Landing on Mars, *Aeronautics & Astronautics*, July 1966, pp. 66–73.
23. Steckemetz B., Wienss W., Bradbury B., Pickett A., Natenbruck P. & Roumeas R. 1993, Flight and Impact Dynamics of Landers for Mars Exploration, IAF-93-Q.1.379, Presented at the 44th International Astronautical Federation, Graz, Austria, October 1993.
24. Jaffe L.D. 1965, Strength of the Lunar Dust, *J. Geophys. Res.*, Vol. 70, pp. 6139–6146.
25. Sperling F. & Garba J. 1967, Treatise on the Surveyor Lunar Landing Dynamics and an Evaluation of Pertinent Telemetry Data Returned by Surveyor 1, Technical Report 32-1035, Jet Propulsion Laboratory, Pasadena, USA.
26. Mironet A., Urquhart R. & Walters R. 1983, Limiting Payload Deceleration during Ground Impact, *J. Spacecraft & Rockets*, Vol. 20, pp. 193–194.
27. Neal M.F. & Wellings P.J. 1993, Descent Control System for the Huygens Probe, AIAA 93-1221 RAeS/AIAA 12th Aerodynamic Decelerator Systems Technology Conference, London, 10–13 May 1993.
28. Lellouch E. & Hunten D.M. 1989, Titan Atmosphere Engineering Model, ESLAB 87/199 (see also Lellouch et al. 1989, Titan's Atmosphere and Ocean: A re-analysis of the Voyager 1 IRIS 7.7 micron data, *Icarus*, Vol. 79, pp. 328–349).
29. Allison M. 1992, An Assessment of Titan's Boundary Layer, Symposium on Titan, Toulouse, September 1991, ESA SP-338, pp. 113–118.
30. Von Karman T. 1929, The Impact of Seaplane Floats during Landing, NACA TN-321, October 1929.
31. Parr W.E. 1966, Water Entry, Proc. Seminar on Theoretical Inviscid Fluid Mechanics NOLTR 66-191, US Naval Ordnance Laboratory, September 1966.
32. McGehee R., Hathaway M.E. & Vaughan V.L. Jr. 1959, Water-Landing Characteristics of a Reentry Capsule, NASA Memorandum 5-23-59L.
33. Wierzbicki T. & Yue D.Y. 1986, Impact Damage of the Challenger Crew Compartment, *J. Spacecraft & Rockets*, Vol. 32, pp. 646–654.
34. Hirano Y. & Miura K. 1970, Water Impact Accelerations of Axially Symmetric Bodies, *J. Spacecraft & Rockets*, Vol. 7, pp. 762–764.
35. Dubouloz N., Raulin F., Lellouch E. & Gautier D. 1989, Titan's Hypothesized Ocean Properties: The influence of Surface Temperature and Atmospheric Composition Uncertainties, *Icarus* , Vol. 82, pp. 81–96.
36. Stubbs S.M. 1967, Dynamic Model Investigation of Water Pressures and Accelerations Encountered during Landings of the Apollo Spacecraft, NASA TN D-3980.
37. Stubbs S.M. & Hathaway M.E. 1967, Effects of Bottom-Structure Flexibility on Water Landing Loads of Apollo Spacecraft Models, NASA TN D-5108.
38. Vaughan V.L. 1961, Landing Characteristics and Flotation Properties of a Reentry Capsule, NASA TN D-655.
39. McCarty J.L. & Carden H.D. 1962, Impact Characteristics of Various Materials Obtained by an Acceleration-Time-History Technique Applicable to Evaluating Remote Targets, NASA TN D-1269.
40. McCarty J.L. & Howlett J.T. 1969, Protuberance Effects on Limiter-Equipped Hard Landing Payloads, *Shock & Vibration Bulletin 40*, pp. 183–191.
41. Grier J.A. & Lunine J.I. 1993, Speculation into Possible Aeolian and Fluvial Dune Deposits on Titan, *Bull. Amer. Astron. Soc.*, Vol. 25, p. 1105.
42. Scott R.F. 1963, Principles of Soil Mechanics, Addison-Wesley, Reading, Massachusetts.
43. Perla R.I. & Martinelli M. 1976, Avalanche Handbook, Agriculture Handbook 489, US Department of Agriculture, Forestry Service.
44. Retamal E. 1983, Some Experimental Results on Snow Compaction, Proc. 5th International Conference on Permafrost, Fairbanks, Alaska, pp. 1054–1059.
45. Jaffe L.D. 1969, Lunar Surface Material: Spacecraft Measurements of Density and Strength, *Science*, Vol. 164, pp. 1514–1516.
46. Jaffe L.D. 1971, Bearing Strength of Lunar Soil, *The Moon*, Vol. 3, pp. 337–345.

47. Shorthill R.W., Moore H.J., Scott R.F., Hutton R.E., Liebes S. & Spitzer C.R. 1976, The 'Soil' of Mars (Viking 1) *Science*, Vol. 194, pp. 91–97.
48. Kemurdzan A.L. et al. 1983, Preliminary Results of the Determination of Physico-Mechanical Properties of Venusian Ground by Soviet Automatic Stations Venera-13 and Venera-14 (in Russian), *Kosmicheski Issledovania*, Vol. 21, pp. 323–330.
49. Yamashiro M. & Yuasa M. 1983, A Penetration Test for Granular Materials using Various Tip Angles and Penetrometer Shapes, *Powder Technology*, Vol. 34, pp. 99–103.
50. Chenoweth H.B. 1971, Monte Carlo Simulation of the Apollo Command Module Land Landing, *J. Spacecraft & Rockets*, Vol. 8, pp. 1074–1078.
51. Perminov V.G. 1990, Dynamics of Soft Landing of Spherically-Shaped Probes, *Cosmic Research*, Vol. 28, pp. 960–965 (translated from *Kosmicheskie Issledovaniya*, Vol. 28, pp. 539–544, 1990).
52. Lorenz R. et al. 1994, An Impact Penetrometer for a Landing Spacecraft, to be published in *Measurement Science & Technology*.
53. Francis P. 1993, Volcanoes: A Planetary Perspective, Oxford University Press.
54. Garvin J.B. 1981, Landing Induced Dust Clouds on Venus and Mars, Proc. Lunar and Planetary Science Conference 12B, pp. 1493–1505.
55. Lorenz R. 1993, Wake-Induced Dust Cloud Formation following Impact of Planetary Landers, *Icarus*, Vol. 101, pp. 165–167.
56. Moshkin B.E., Ekonomov A.P. & Golovin Yu.M. 1979, Dust on the Surface of Venus, *Cosmic Research*, Vol. 17, pp. 232–237 (translated from *Kosmicheskii Issiedovania*, Vol. 17, pp. 280–285, 1979).
57. Ragent B. & Blamont J. 1979, Preliminary Results of the Pioneer Venus Nephelometer Experiment, *Science*, Vol. 203, pp. 790–792.
58. Balligand H. A. & Higuchi H. 1993, Wake of a Decelerating Disk, AIAA-93-1218, Proc. 12th RAeS/AIAA Aerodynamic Decelerator Systems Technology Conference, London, May 1993.
59. Walker J.D.A., Smith C.R., Cerra A.W. & Doligalski T.L. 1987, The Impact of a Vortex Ring on a Wall, *J. Fluid Mechanics*, Vol. 181, pp. 99–140.
60. Lorenz R.D. 1993, Scientific Implications of the Huygens Parachute System, AIAA-93-1215, Proc. 12th RAeS/AIAA Aerodynamic Decelerator Systems Technology Conference, London, May 1993.
61. Timoshenko S. 1940, Theory of Plates and Shells, McGraw-Hill, New York.
62. Weber H. & Krueckau F. 1985, New Melamine-based Elastic Foam, translated from *Kunstoffe*, Vol. 75, pp. 843–848.

Appendix

Shape and Strength of Probe Shell

The Probe shape used in this study for the liquid-impact and post-impact dynamics is that of the outer aluminium shell, and is taken from Aerospatiale drawings. Essentially it is a dome with radius of curvature 1.25 m, until 15 cm along the Probe's central axis, when it becomes 15 cm, to meet a short cylindrical section (height ~7 cm, diameter 1.3 m) which corresponds to the location of the experiment platform. For about 30 cm above this, the shell is conical, meeting the flat top platform of 1.1 m diameter.

The various appendages (attach mechanisms, HASI booms, radar-altimeter antennae and the DISR) are not considered.

For the impacts with a solid surface, the contact area with the soil is computed by assuming the fore dome is an ellipsoid of revolution, with major and minor axes equal to the diameter and height of the actual shell.

Calculation of the force/deformation characteristics of even a simple shell is difficult (see, for example, Ref. 61) and so it has been assumed here that the shell obeys a linear force/deformation law. Thus, the force on the shell is directly proportional to the distance between the surface and where the shell's apex would be had it not been deformed, except where this force is more than the surface bearing strength multiplied by the contact area, in which case the shell force is set to be the latter.

In the nominal model, a shell force constant of 1000 N/m has been used. Investigation of various impact cases suggests that the impact deceleration history is relatively insensitive to variations of one order of magnitude in this parameter. In this case, the work done in deforming the shell is only about 2% of the impact kinetic energy.

Estimation of Structural Characteristics of Probe Underside Units

Detailed study of each individual unit could yield accurate stress/compression relations. However, this would be impractably labour-intensive, and difficult to justify given the uncertainties elsewhere (e.g. in the soil models, impact orientation, etc.). Thus what follows is a set of engineering estimates, using rules-of-thumb, to derive first-order guesses for the response of individual elements. The loads and accelerations calculated by the model are only modestly sensitive to variations in individual element properties; the aggregate validity of the 28 elements should be adequate. Consequently, it is hoped that the results of the model are believable.

Only the aluminium fore-dome, parts of the insulating foam, and exposed experiment components will be chilled to ambient temperature (94 K), and so the engineering properties assumed here are the room-temperature values, obtained from standard data books, except where indicated otherwise.

Air gaps have essentially zero bearing strength until their compression exceeds 95%, when the strength is increased to transfer loads to other elements.

Foam layers have a modest initial stiffness, readily deforming to about 50% compression, and then bearing strength rises sharply. The points used to define the stress-compression characteristic (Fig. 13) were taken from Figure 8 in Reference 62.

The honeycomb sandwich of the experiment platform takes a fairly large loading, until the 'punch-through' threshold of 51 N/cm^2 is exceeded. This value was supplied by CASA, contractor for the Probe's inner structure susbsystem, via Aerospatiale and the ESA Project Team. The overall response shape (Fig. 13) was set to resemble that of the aluminium footpads of the Surveyor spacecraft[25].

Note that for some units (SSP and GCMS) the platform area that supports the unit is smaller than the area used to compute the soil loads: e.g. the GCMS is a 9-inch diameter cylinder, with an effective soil penetration area of 300 cm^2 (its end is domed and has a circular inlet flange), but is only held by a support ring of area ~ 160 cm^2 bolted to inserts in the platform. Consequently, the failure stress used in the model for the honeycomb element in these stacks is modified by the ratio of the two areas.

Unit boxes are assumed to be relatively rigid, with a slight deformation due to the inward bending of the loaded face (using relations from Ref. 61), until a fail stress is reached, estimated by multiplying the yield stress of the box material (assumed glass-fibre-reinforced plastic for SSP, magnesium alloy for the PCDU box, and aluminium elsewhere) by the cross-sectional area of the box walls (and any reinforcement pillars). Note that all the box units are sufficiently squat that yield failure occurs before an Euler buckling stress is reached. Additional justification for this approach is the equivalence of experimental loads measured during the collisional crushing of a box-beam section, finite-element analysis of the same case[20], and the yield load computed as above. Since the boxes are not empty, however, a change of stress is assumed to occur as compression continues and the internal components are crushed together.

Some elements (e.g. the batteries) are considered rigid (i.e. their stiffness is considerably larger than that of the other elements).

Manuscript received 22 April 1994

A. Hahne, J. Callies, A. Lefebvre & B. Christensen
ERS Project Division, ESTEC, Noordwijk, The Netherlands

R. Hoekstra, L. Fontijn, C. Olij, E. Zoutman & G. Nützel
TPD-TNO, Delft, The Netherlands

Calibration of the GOME Instrument for ERS-2

Abstract

The Global Ozone Monitoring Experiment (GOME) is an optical spectrometer to be flown on the second European Remote-Sensing Satellite, ERS-2 [1]. Its main task will be to measure the ozone content of the atmosphere and to monitor its long-term variation. Ozone is a trace gas of vital importance to mankind, as it absorbs the harmful ultraviolet radiation emitted by the Sun and prevents it from reaching the Earth's surface. This absorption occurs in an ozone layer concentrated in the stratosphere, at altitudes of between 18 and 40 km, which is threatened by human activities, in particular by the release of Chloro-Fluoro-Carbons (CFCs) used in spray cans, refrigerators and foams, and as a cleaning agent. Ozone depletion is believed to be taking place at a rate of about 0.3% per year.

The reliable measurement of such a small global trend against the background of normal spatial and temporal variability, places high demands on the instrument's accuracy and stability. To meet with these requirements, the instrument needs thorough calibration and characterisation, both on the ground and in orbit.

The breadboard model of the GOME instrument – which is functionally fully representative including the on-board means of calibration – has been subjected to a dry calibration run on the ground, and the test results are reported here.

1. Calibration requirements and the on-board calibration concept

The conventional approach for measuring ozone, which is the underlying principle of the American SBUV and TOMS instruments, is the monitoring of upwelling backscattered radiance at a number of discrete wavelengths. To yield meaningful results, the radiometric response of an instrument used in this mode must be known to better than 1%. Because the space environment is known to change the radiometric response of the instrument (e.g. by radiation-induced darkening of transmissive optics), the means for carrying out on-board calibration with the necessary stability have to be provided to enable re-calibration at regular intervals.

This is normally done by looking at the Sun, which is a rather stable light source for the wavelength range in question. However, because the solar irradiance is several orders of magnitude higher than the radiance coming from the Earth, the Sun cannot be used directly, but only via a diffuser. This diffuser attenuates the light to a level that falls within the dynamic range of the detection system, and also makes the measurement path insensitive to the variations in the line-of-sight to the Sun as function of the seasonal change in the Earth–Sun distance.

As GOME is intended to achieve continuity with the long-term records of ozone concentrations already accrued by the SBUV and TOMS instruments, this concept has been adopted for GOME also. There is, however, an alternative measurement principle known as 'Differential Optical Absorption Spectroscopy', which is made possible by the availability of multi-pixel array detectors capable of recording a continuous spectrum over a large wavelength range. With this technique, a recorded atmospheric spectrum is divided by a solar spectrum, thereby compensating for the Sun's variability (which, of course, also appears in the backscattered light), as well as for the variations in the optical throughput. To the divided spectrum obtained in this way, the absorption spectra of ozone and possibly other trace gases are then fitted, thus providing the means to retrieve the amounts of the target (absorbing) species.

For this technique to work, the wavelength observations (for both the solar spectrum and the backscattered spectrum from the atmosphere) have to be very accurate*. However, launch effects and temperature variations around the orbit prevent this stability from being achieved. Thus with GOME it is proposed to measure the wavelength shifts with the aid of a calibration lamp, which provides a sufficient number of sharp atomic emission lines in each channel to map wavelength shifts around the orbit and correct for them in the ground processing (Fig. 1).

* Ideally, the wavelength stability between recordings should be 1/100 th of a pixel.

Figure 1. The spectrometer optics of the GOME instrument

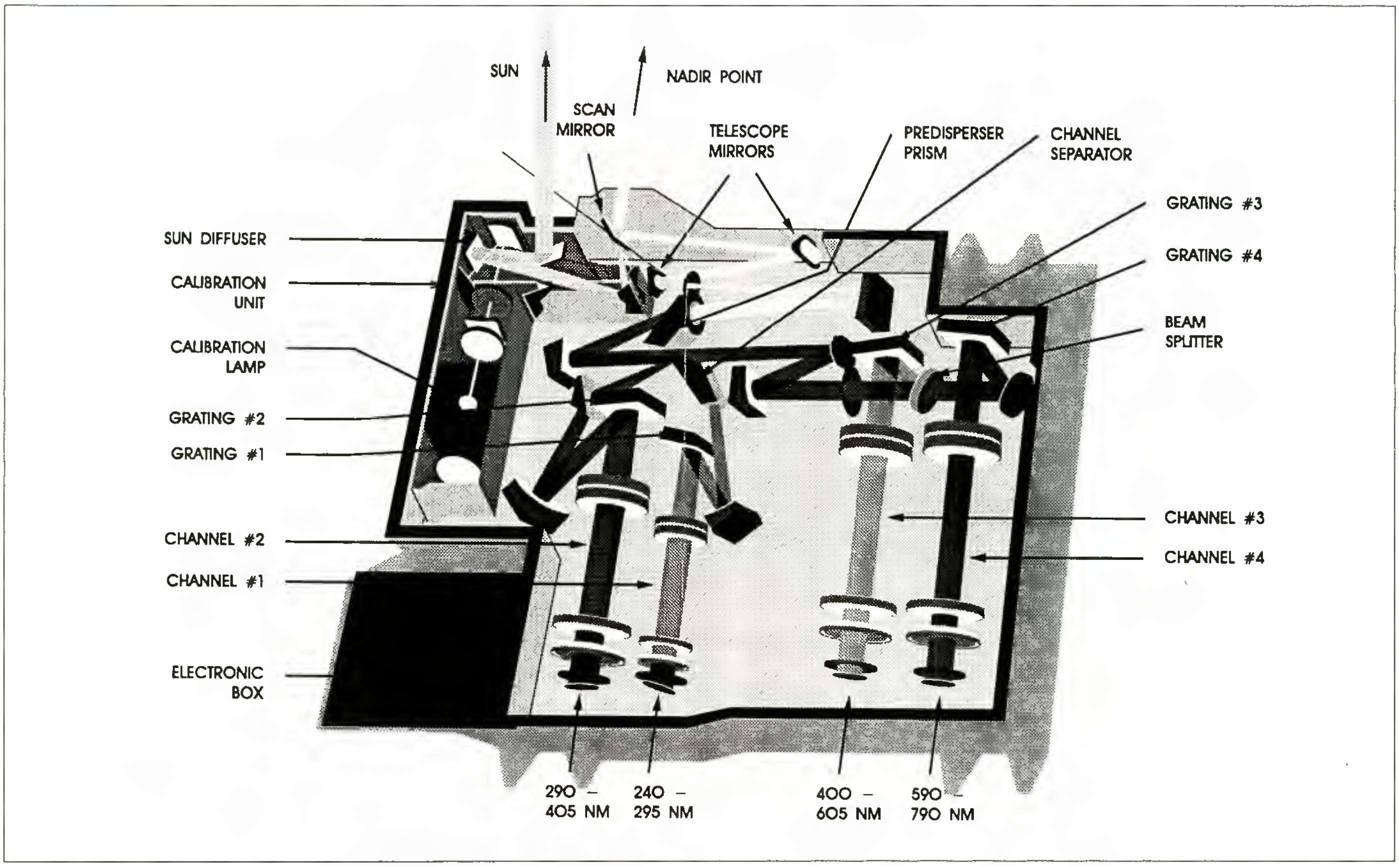

In addition to this basic calibration facility, there are in-flight provisions for:
- measuring the dark current and fixed pattern noise of the detectors and the readout chain
- calibrating the Analogue-to-Digital Converters (ADCs)
- monitoring pixel-to-pixel variability by illuminating the detectors with Light-Emitting Diodes (LEDs) built into the optical objectives of the four channels
- monitoring the reflectance of the Sun diffuser, by channelling the light from the wavelength calibration lamp via the diffuser and ratioing the measurements with the corresponding ones made when the lamp is observed directly
- finally, by tilting the scan mirror to an angle between 70° and 85° with respect to nadir, it is possible to use the Moon as a calibration target.

2. The on-board calibration unit

Almost all on-board calibration facilities (except the LEDs mentioned in the previous section) are grouped in the Calibration Unit, which is shown in Figure 2. Its two key elements are:
- the calibration lamp, and
- the Sun diffuser.

2.1. The calibration lamp

Key requirements for the calibration lamp are:
- a number of sharp spectral lines spanning the entire wavelength range observed by GOME
- a lifetime compatible with the mission (500 h, with at least 1000 on/off cycles)
- low power consumption: less than 5 W, including DC/DC conversion losses
- a rugged design, as the lamp must be able to withstand both the launch and in-orbit environments.

The lamp selected is a hollow-cathode type, which has already been flown in a similar configuration on several NASA missions. The fill-gas is neon, with a platinum cathode with 10% chromium in order to provide some additional lines needed to span the GOME wavelength range.

A small life-test programme has been conducted, operating one lamp continuously for 1500 h and another intermittently, with 5 min on and 5 min off, for 6000 cycles. The lamp current was regulated to 10 mA. The test showed very satisfactory results, as did the environmental (vibration and thermal vacuum) test programme.

Figure 3a shows the 'naked' lamp, and Figure 3b the lamp in the suspension used in the calibration unit. Figure 4 shows the spectrum of the lamp used in the GOME Breadboard Model (BBM).

Figure 2. The on-board calibration unit

Figure 3a. The 'naked' wavelength calibration lamp

Figure 3b. The calibration lamp in its calibration-unit mount

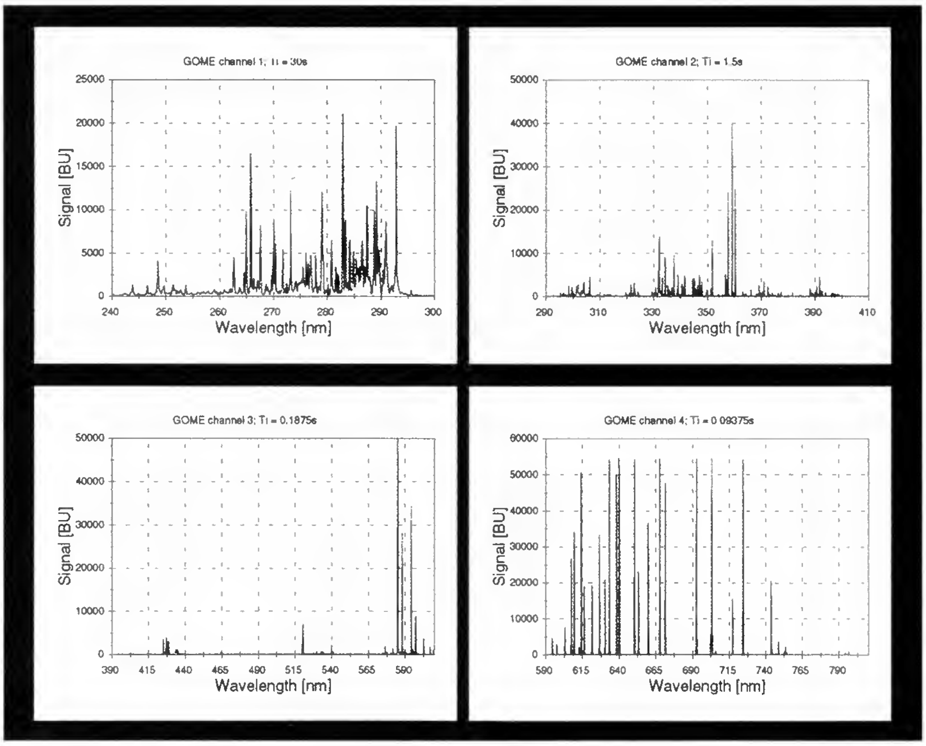

Figure 4. Spectrum of the calibration lamp, as measured for the GOME breadboard model (BBM)

2.2. The diffuser

The purpose of the Sun diffuser is to enable a calibration to be carried out with the standard system without the need for an accurate Sun acquisition and tracking mechanism. In order to obtain a reliable Sun calibration, the diffuser must have:

- a well-known Bi-Directional Scattering Function (BSDF)
- good uniformity over the illuminated surface
- a smooth and well-known wavelength response for the wavelength range of interest
- excellent in-orbit stability.

A short technology-development programme has been conducted at TPD/TNO Delft (NL) to select the most suitable material/process for the diffuser. Materials that have been investigated include aluminium oxide, quartz, magnesium oxide, titanium dioxide, barium sulphate, and aluminium with various surface treatments and coatings. Mainly for in-orbit stability reasons, a wet-blasted Aluminium 6082 with a 5 nm chromium and a 100 nm aluminium vacuum-deposited coating have been selected.

Figure 5 shows the diffuser produced with this technology, and Figure 6 the measured BSDF with the angular range of interest indicated.

2.3. The calibration unit

Aside from the lamp (with its housing) and the Sun diffuser, the Calibration Unit comprises:

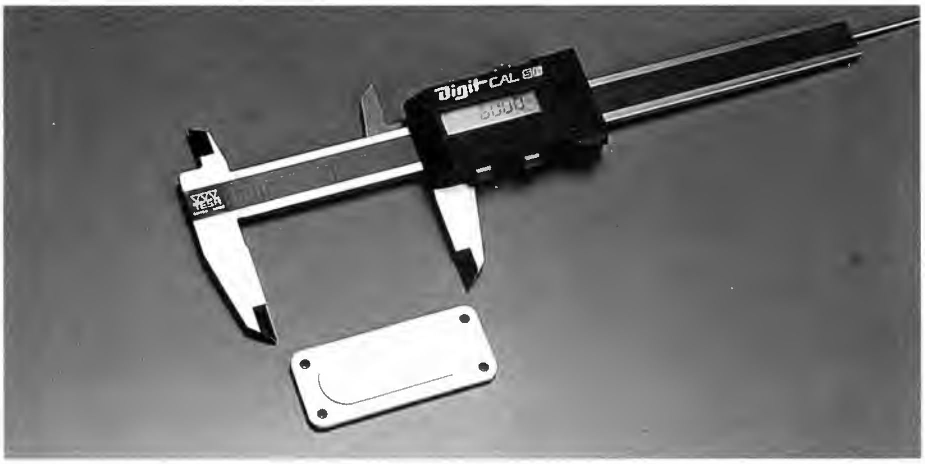

Figure 5. Wet-blasted aluminium diffuser

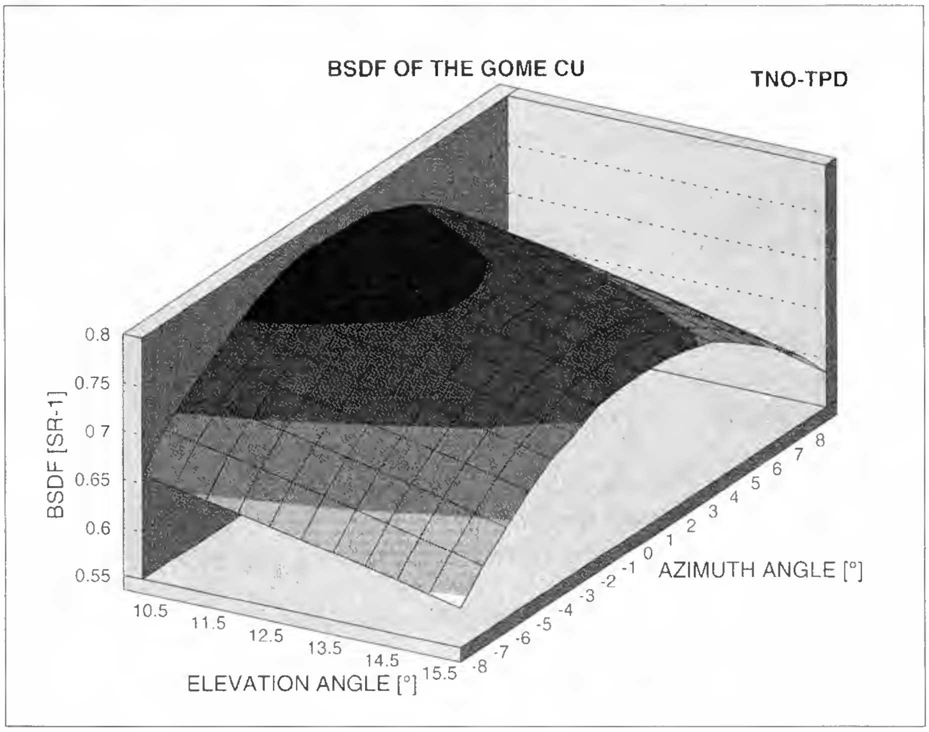

Figure 6. BSDF for the angular range of interest

- the power supply for the lamp, providing a voltage ramp to supply the ignition voltage of about 300 V and a stabilised current across the lamp of 10 mA
- the optical elements needed to ensure that the spectrometer slit and pupil are fully illuminated for both the lamp-calibration and Sun-calibration modes
- a shutter, which protects the diffuser when it is not being used for Sun calibration
- a mesh between shutter and diffuser, providing further protection to the diffuser and an additional attenuation of the light level received from the Sun.

The latter two items have been implemented based on NASA experiences which have shown that diffuser degradation is directly correlated with the time of exposure to sunlight (probably due to polymerisation of deposited contaminants caused by hard ultraviolet light).

3. The ground-calibration programme

Although a number of means for on-board calibration are included in GOME, they do not provide access to all the necessary parameters. These parameters are measured during the on-ground calibration programme and are not anticipated to change from ground to orbit.

The most important measurements to be conducted on the ground are:

- the measurement of the diffuser BSDF over the GOME wavelength range

- the characterisation of the polarisation response of the instrument as a function of the optical path (normal observation path and Sun observation path), scan mirror position (the scan mirror reflectivity for *s*- and *p*-polarisation is a function of the mirror angle), and wavelength.

On top of this, there are a number of additional measurements used for various purposes: more comprehensive instrument characterisation, consistency cross-checking, backup measurement for the case of lamp failure, and generation of test data for processing-algorithm checking.

In particular, the programme comprises:

Radiance/irradiance measurements: By illuminating the normal observation path and the Sun observation path with known radiance/irradiance, the radiometric calibration concept can be checked.

Wavelength calibration: During instrument-level thermal-vacuum testing, spectra of the calibration lamp have been recorded at different temperatures to measure wavelength shifts as a function of the temperature and the air/vacuum difference.

Detector characterisation: Dark current, readout noise, pixel-to-pixel sensitivity variations, and electronic chain performances including response linearity have been measured.

Straylight characterisation: This includes intra-channel (from high-intensity end to low-intensity end), inter-channel (from one channel to the other), and out-of-field and out-of-band straylight measurements.

Field-of-view characterisation: The variability, if any, in the radiometric response and spectral shift in the along-slit direction is measured. This is of particular interest for the lunar calibration, as the Moon only partially fills the spectrometer slit.

Measurement of the slit function: The slit function (i.e. the modulation transfer function of the entire optical system from the slit up to and including the detector) is determined. This is used to convolute high-resolution reference spectra of atmospheric species to the resolution of GOME.

4. The breadboard-model calibration programme

Recognising that this is quite a demanding programme, preparations for the calibration started as early as 1991. After agreement in principle on the scope of the programme with the scientists involved in GOME, TPD in Delft (NL) proceeded with the design, manufacturing, procurement and testing of all the necessary elements:

- turntable and fixtures to accommodate the instrument during the measurements
- calibrated lamps, diffusers and reference detectors procured from the National Institute of Standards
- monochromator and polariser covering the entire GOME wavelength range
- a temperature-controlled room to host the whole setup, clean room class 10.000, all black-painted (even including storage cabinet and water sink and tap) to suppress external straylight
- computer and software to control all the settings and provide them to the GOME Electrical Ground-Support Equipment (EGSE), to enable correlation between the GOME measurement data and the settings of the calibration setup
- algorithms and software to analyse the data, e.g. for noise correction, wavelength shift detection, BSDF computation, etc.
- procedures for setting up, aligning and performing the measurements
- calibration error budgets to establish the expected accuracy and precision of the measurements.

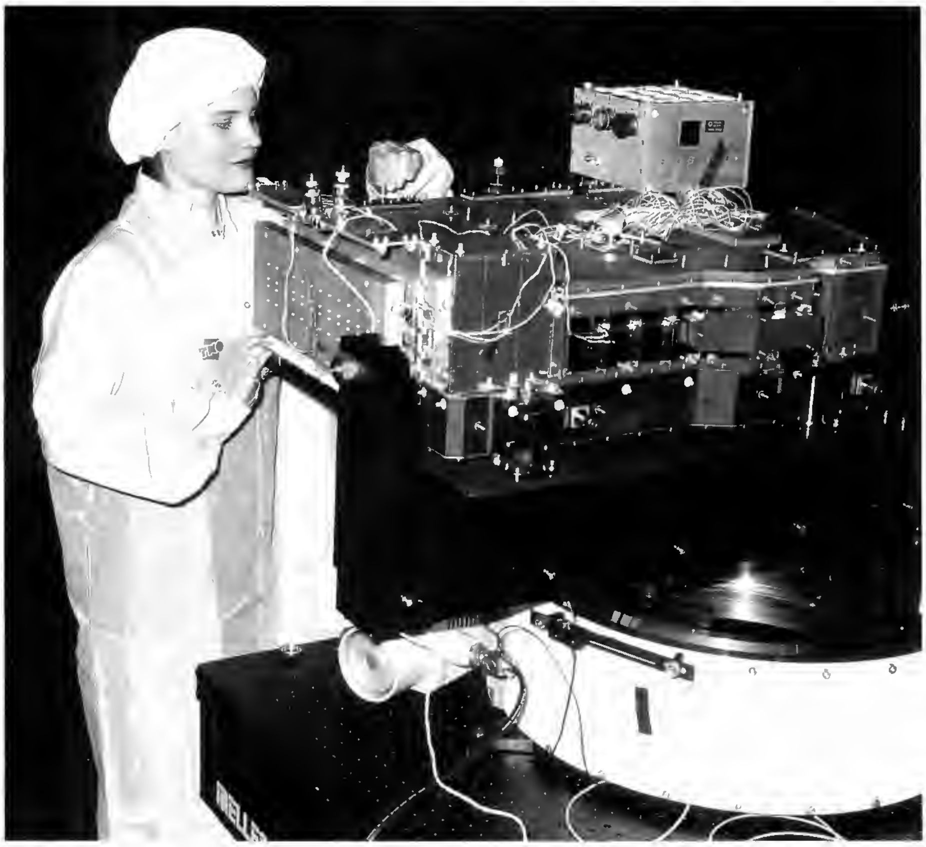

Figure 7. GOME on the turntable in the calibration facility

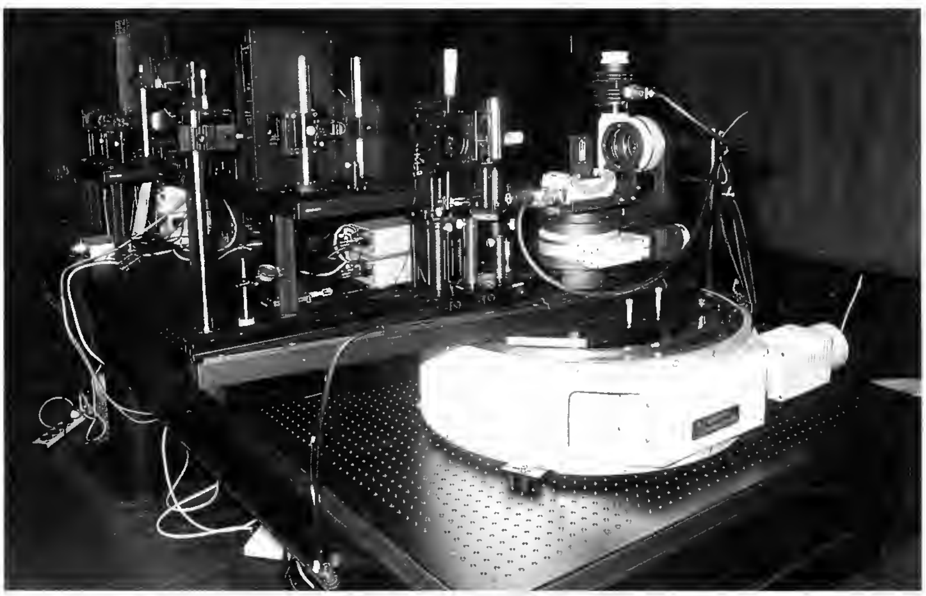

Figure 8. Part of the GOME calibration setup. Note the black environment for reducing external straylight

It was realised that to perform this exercise on only the flight model would be very risky and schedule-critical. A dry run involving all the steps and procedures has therefore been carried out on the GOME breadboard model which, since the negotiation of the main GOME development contract (Phase-C/D), has evolved into a fully-fledged de-facto engineering model, being very representative of the final flight-model configuration.

Figure 7 shows the GOME BBM mounted on the turntable in the TPD facility, while Figure 8 shows part of the optical instrumentation for performing the calibration.

First, wavelength characterisation and radiometric stability checking were carried out during the thermal-vacuum test at instrument level in the vacuum chamber of the instrument's prime contractor, Officine Galileo (I). This was then followed by two calibration periods, April–August 1993 and November–December 1993, with an intermediate review to scrutinise the results. A final review in March 1994 then concluded the BBM calibration, and the modifications necessary for the flight-model programme were agreed.

Figure 9. Polarisation response of the breadboard model (BBM)

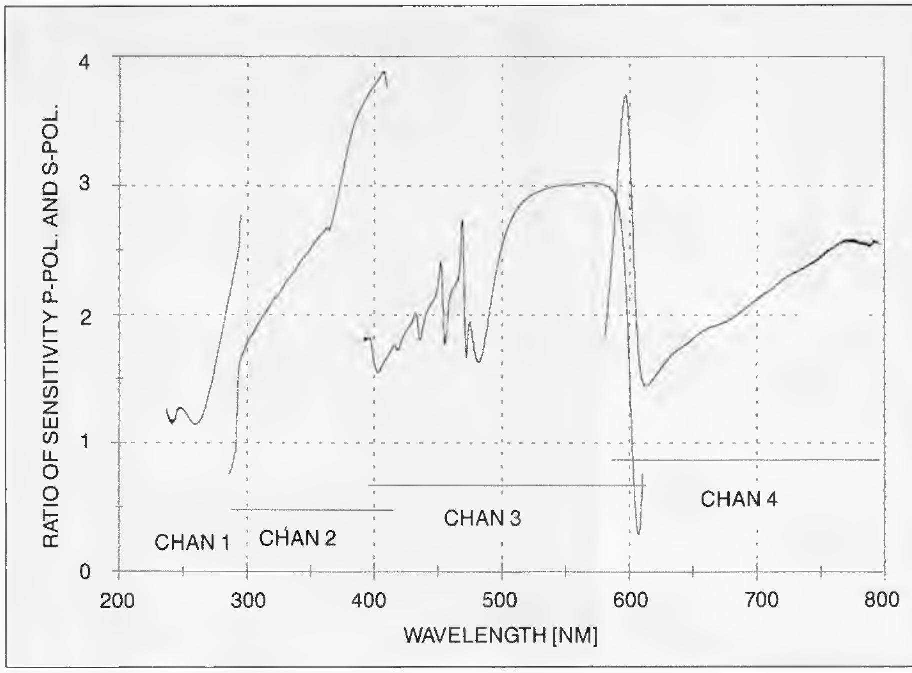

5. Results of the BBM calibration/characterisation

BSDF: The BSDF as measured on the flight diffuser is a smooth function of both the azimuth/elevation angles and the wavelength (see Fig. 6).

Polarisation response: As expected, the instrument shows a pronounced polarisation response. In particular, channel 3 shows some narrow structure in the polarisation ratio (*s* over *p*), which is believed to be due to the combined effects of the dichroic beam-splitter and grating (Fig. 9).

Radiance/irradiance measurements: For schedule reasons, the BSDF of the BBM calibration unit could not be measured prior to integration into the BBM, so that a proper consistency check was not possible.

Wavelength calibration: During instrument- and payload-level thermal-vacuum and thermal-balance tests, the spectral stability as a function of temperature was verified. Spectral shifts in all channels were less than 0.02 pixel/°C. With an orbital temperature swing of about ±1°C, an excellent spectral stability for a passive thermal design is achieved. Figure 10 shows the instrument mounted in the Galileo thermal-vacuum chamber.

Detector characterisation: Both the dark current and its noise proved to be very low (also due to the good stability of the detector cooling loop). Pixel-to-pixel sensitivity variations across the 1024-pixel arrays were, at less than 2%, much better than the detector manufacturer had envisaged. Some electronic noise was detected in certain

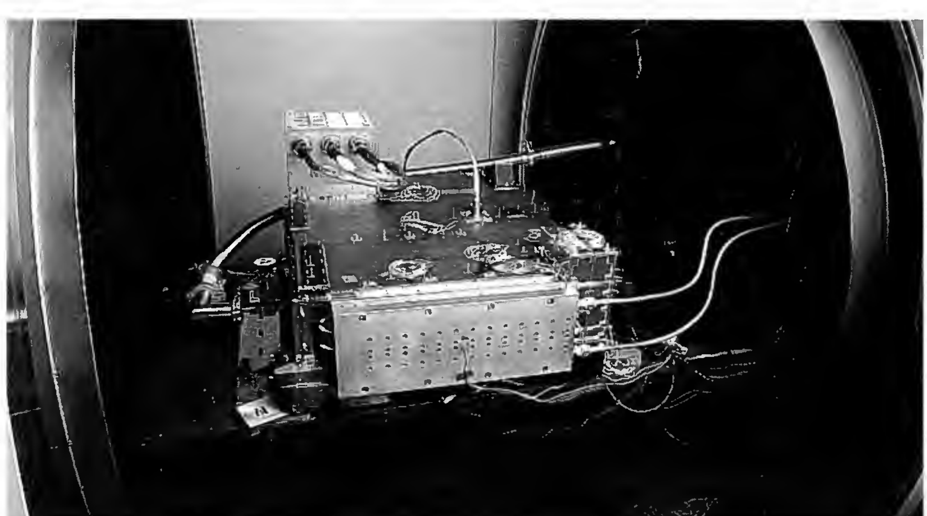

Figure 10. GOME breadboard model (BBM) during the TV test

readout situations. This was due to the ringing of the leading edge of the strobe pulse and to interference with the read-out of a temperature sensor. Both problems have been fed back into the instrument design and should be solved for the flight model.

Straylight characterisation: Quite detailed investigations were necessary to clarify the observed levels of straylight. A path for external straylight was identified and the problem solved via more and improved instrument internal baffling. Inter-channel straylight proved to be low and presented no problem.

More crucial was the intra-channel straylight, particularly that in channel 2, where at the short-wavelength end a roll-off of the signal level (by three orders of magnitude) presented a significant problem. Multiple reflections between the detector and the objective lenses and the gratings, respectively, were identified as the major cause. In channels 3 and 4 the problem could be resolved by the provision of improved anti-reflection coatings on the lenses and by slightly tilting the gratings. For channel 2, this would not have been sufficient and so, in consultation with the GOME scientists, it was decided to move the wavelength split between channels 1 and 2 to a higher value, thereby safeguarding the important channel 2, but sacrificing the performance of channel 1 slightly. The problem was alleviated by measuring straylight levels on some (so far unused) pixels, enabling some correction to be made for straylight in the ground processing.

Field-of-view characterisation

The design parameters for the GOME FOV are 0.14° x 2.8°. Under normal observational conditions, the entire slit and the entire GOME pupil are illuminated. However, when the Moon is observed, only a fraction of the slit is illuminated. For that reason, several scans have been made of the FOV by using collimated light as input for the GOME telescope. These measurements provide information on:
- actual dimensions of the FOV
- out-of-field scattered light
- influence on radiometric response and on wavelength scale when only a fraction of the FOV is illuminated.

Figure 11 shows the radiometric output of GOME for channel 3 when the FOV is scanned along the 2.8° axis of the FOV.

Slit function

This function represents the spectral line shape output for monchromatic input. It is a convolution of entrance slit width as imaged onto the spectral plane, detector pixel

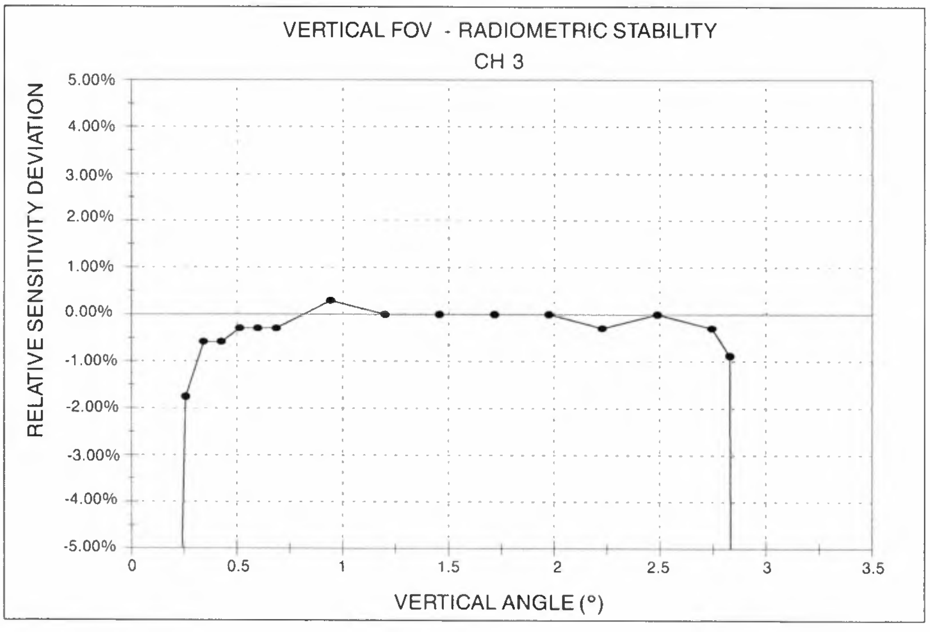

Figure 11. Radiometric response variation along the field of view

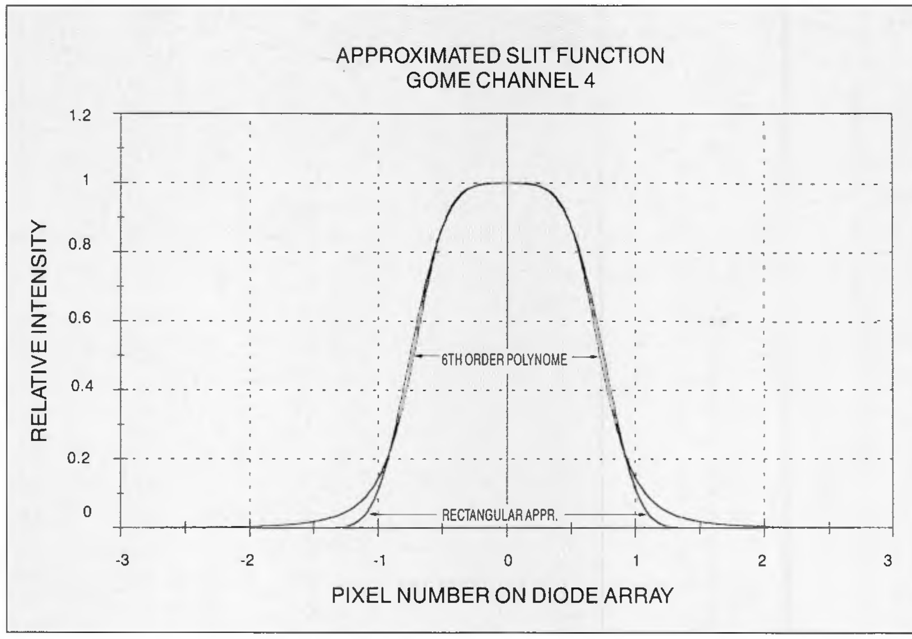

Figure 12. Slit function approximation in channel 4. The thin line is an approximation with a rectangular slit function,the thick line with a sixth-order polynomial

width, optical aberrations and residual effects, superimposed by straylight. Selected spectral lines from the on-board wavelength calibration lamp can be used as a test case for different mathematical approximations. In addition, observations have also been made using an external mercury lamp, providing spectral lines that are less crowded (and thus better isolated) than the lines of the on-board PtCr/Ne lamp. Two examples of approximated slit functions are shown in Figure 12.

6. Further programme

Scientists involved with the GOME instrument are presently using the breadboard model to measure the reference spectra of ozone, nitrogen dioxide and sulphur dioxide. These spectra will subsequently be used for the retrieval of ozone concentrations.

An irritating feature in atmospheric radiative transfer is the so-called 'ring effect', which fills in some of the strong Fraunhofer lines in the solar spectrum when it is viewed through the atmosphere. This will be measured as a quasi-absorption spectrum for use in the ground processing.

In consultation with the scientists, priorities have been agreed for the conduct of the flight-model calibration, which will be performed after GOME has undergone satellite-level vibration/acoustic testing, in June 1994. Evaluation and processing of the acquired data will then follow. These data will be made available to DLR (D), which is responsible for the ground processing and the installation and maintenance of the calibration database.

Reference

1. Hahne A. et al. 1993, GOME: A New Instrument for ERS-2, *ESA Bulletin No. 73*, pp. 22–29.

Manuscript received 18 January 1994

M. Schautz & G. Dudley
Energy Storage Section, European Space Research & Technology Centre (ESTEC), Noordwijk, The Netherlands

F. Baron
Manned Spaceflight and Microgravity Directorate, ESA, Toulouse, France

V. Popov & B. Pospelov
Uralskii Elektrochimtscheskii Kombinat (UEIP), Ekaterinburg, Russia

Testing of a Buran Flight-Model Fuel Cell

Abstract A demonstration test programme has been performed at ESTEC on a flight-model Russian 'Photon' fuel cell. The tests, conducted at various power levels up to 23 kW, included current/voltage characteristics, transient behaviour, autothermal startup, and impedance measurements. In addition, the product water and the purge gas were analysed. All test goals were met and no electrochemical limitations were apparent.

1. Introduction

In the context of closer cooperation with Russia in future space activities, a number of key Russian space technologies have been made available to ESA for detailed evaluation, including the 'Photon' fuel cell. Therefore, in parallel with the European fuel-cell development programme, with Dornier and Siemens as main industrial contributors, the state of the art of Russian space fuel-cell technology has also been evaluated, and its suitability as a backup to the existing European (alkaline) fuel-cell development investigated.

A flight-model fuel-cell power plant already qualified for the Russian spaceplane 'Buran' was obtained on loan and subjected to an intensive two-week continuous test campaign in ESTEC's Fuel-Cell Test Facility (FCTF). This paper provides a summary of the main results obtained.

2. Fuel-cell technology

Fuel cells, in general, convert the chemical energy stored in the reactants directly, and without any form of combustion, into electrical energy. The fuel-cell technology chosen for spaceplanes uses hydrogen as the 'fuel' and oxygen as the oxidant. The electrochemical process runs at around 100°C and at high efficiency. In the process, hydrogen and oxygen are not allowed to mix, but react on dedicated electrodes, which are separated by electrolyte. In simple terms, the hydrogen is oxidised – and consumed – on the anode, producing two protons (H^+), and oxygen is reduced on the cathode, 'borrowing' a molecule of water from the electrolyte and forming two hydroxyl ions (OH^-). The latter combine in the electrolyte with the protons from the hydrogen side to form the reaction product, water (H_2O), which has to be removed from the cells to prevent them from flooding. The two electrons released in the oxidation of hydrogen to protons move through the anode to the negative fuel-cell terminal and from there to the electricity consumer, where they perform electrical work. To complete the electrical circuit, the electrons move back via the positive terminal into the fuel cell to the cathode, where they are needed for the reduction of oxygen to hydroxyl ions. This electrochemical process is illustrated in Figure 1.

Each cell theoretically delivers about 1.23 V and consumes, if its efficiency would be 100%, just 2 gm of hydrogen and 16 gm of oxygen to produce 53.6 Ah of electricity and 18 gm of pure water. In practice, the voltage is lower and the energy conversion efficiency is nearer to 60%. This is still well above the efficiency that could be obtained by burning the reactants in a typical heat engine, the efficiency of which is limited by the thermodynamics of the Carnot cycle.

To obtain a 'useful' output voltage, a number of cells have to be stacked in series, and to increase the output current several such stacks can be connected electrically in parallel.

Figure 1. Fuel-cell schematic

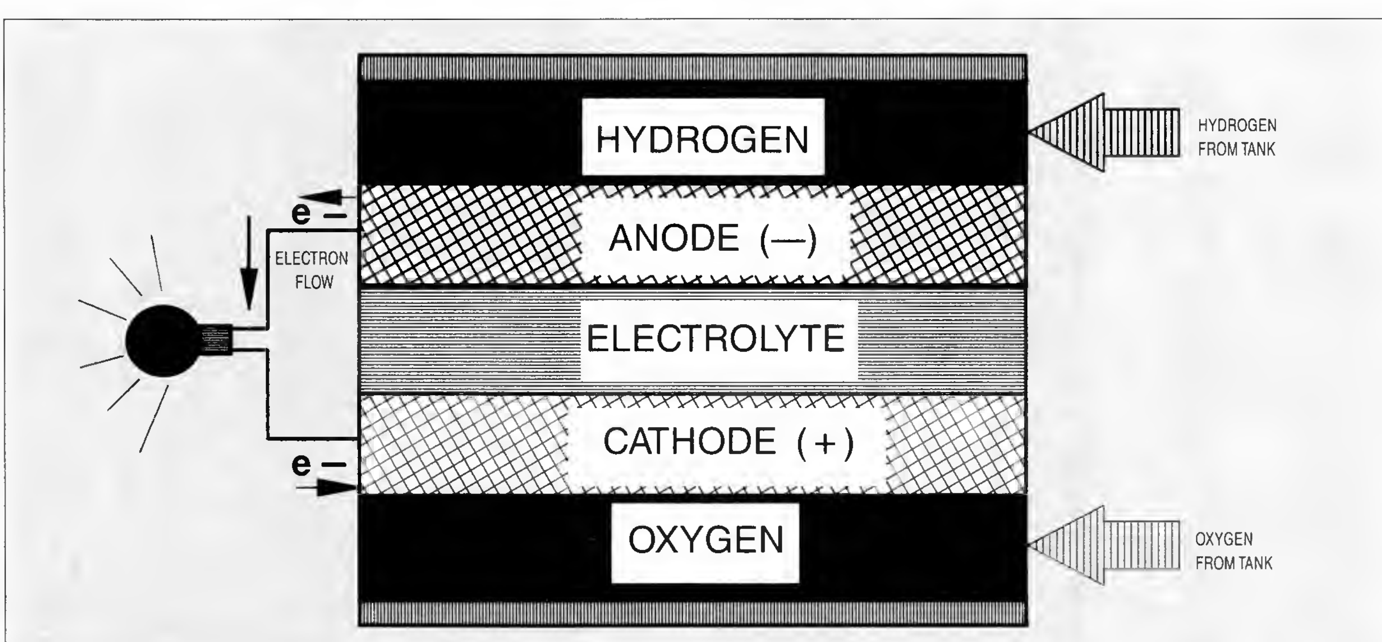

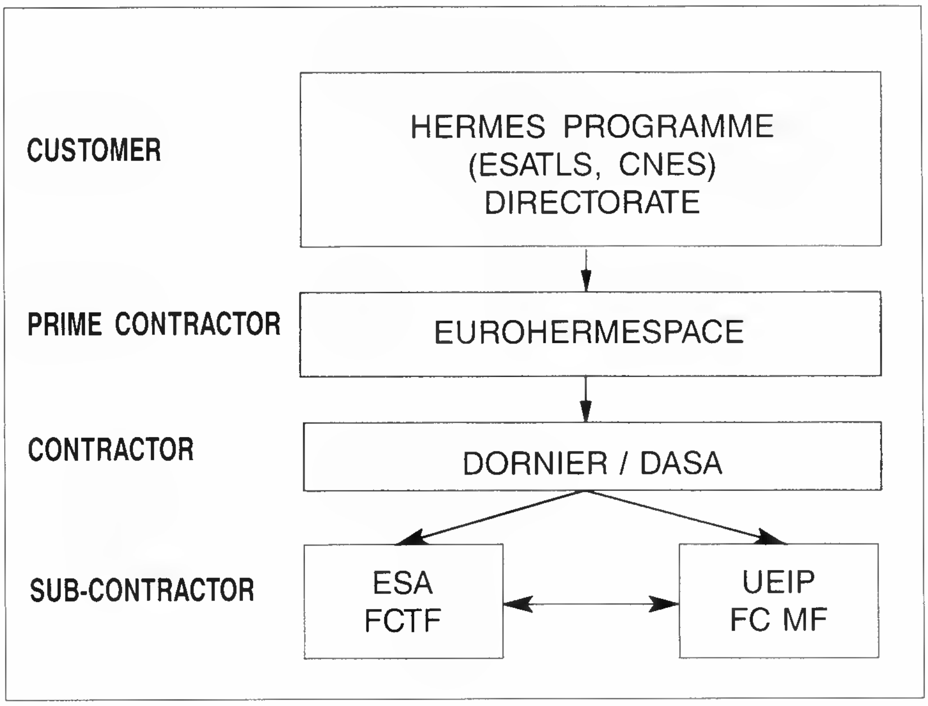

Figure 2. Organigram for the demonstration testing

3. The testing

3.1. The 'Photon' fuel cell

The 'Photon' power generator was developed by UEIP (the 'Ural Electrochemical Integrated Plant') in Ekaterinburg, in the Sverdlovsk Region of Russia in the seventies and eighties. More than 120 complete power units were assembled and tested to achieve flight-model quality qualification.

The particular flight-model unit used for testing at ESTEC was manufactured in December 1991 and was subjected by the manufacturer to flight acceptance tests including leak tests, insulation resistance, vibration tests and electrochemical performance. It was certified in accordance with Russian standards for application in manned space transportation.

The 'Photon' power unit consists of the electrochemical generator containing eight fuel-cell stacks, which are connected in parallel, and a number of peripherals which are necessary for the process control. Each cell stack contains 32 cells in series. The active cell area is 176 cm^2. The electrolyte is potassium-hydroxide solution in an asbestos matrix. The product water is removed by means of excess hydrogen flow, whereby the hydrogen is saturated with water vapour when flowing alongside the hot and wet electrode surface. Further down the 'hydrogen loop', water is condensed and then removed in a so-called 'hydrophilic membrane separator'.

Figure 3 shows a substack assembly, and Figure 4 the complete fuel-cell generator with its housing removed.

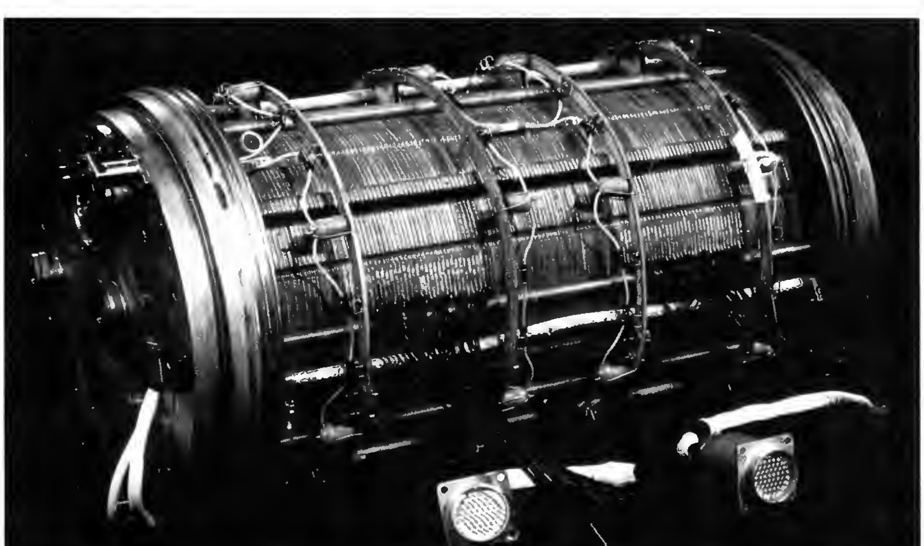

Figure 3. 'Photon' substack assembly

Figure 4. The 'Photon' fuel-cell unit

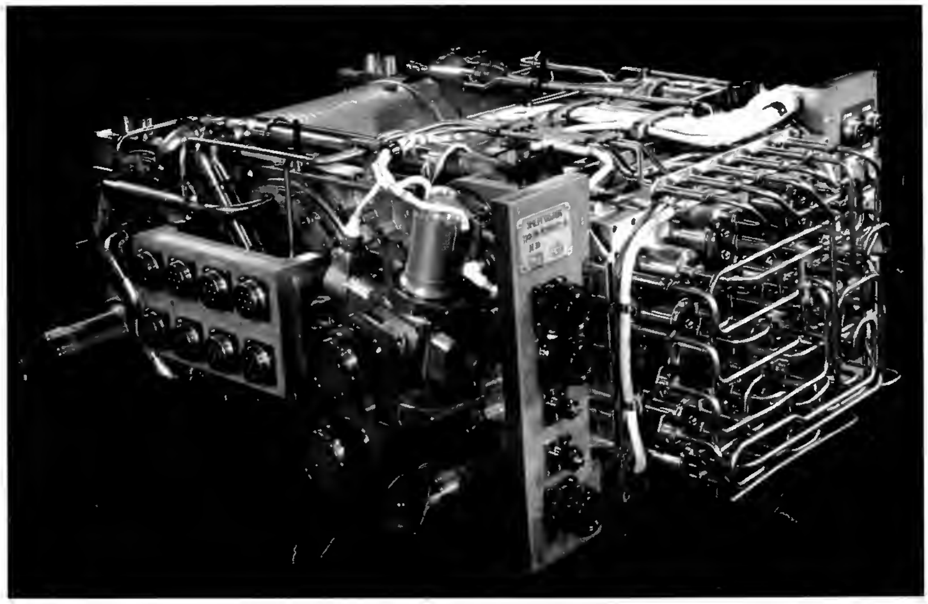

3.2. The test facility

The ESTEC Fuel-Cell Test Facility (FCTF), an annex to the Battery Test Centre, was originally designed to perform endurance tests on hardware produced throughout the development and qualification phases of the baseline fuel cell for Europe's Hermes spaceplane. The three existing test benches have been designed to accommodate both small and large cell stacks, which do not include peripheral equipment like pumps, regulators, valves and sensors. For this test of a complete power plant, it was only necessary to provide laboratory-level interfaces, which included:

- The safety-system monitoring for excess gas flow, hydrogen leakage, gas pressures, cooling-water supply, ventilation and electricity supply.
- The high-purity gas storage, consisting of 4 million litres of hydrogen in pressurised cylinders on a trailer, 2 million litres of oxygen in a 3 ton liquid-oxygen (LOX) tank, and 160 000 litres of nitrogen as inert gas for emergency shutdown.
- A closed-circuit cooling-water loop for the removal of waste heat.
- Electronic loads, and data acquisition and archiving systems.

3.3. Integration and test setup

Following several months of interface document exchange and the elaboration of a test plan acceptable to all parties, the fuel-cell generator was delivered, along with most of its associated ground-support equipment, to ESTEC by UEIP. It was filled with inert gas and organic coolant medium. It had accumulated only 150 h of operation before being delivered and installed at ESTEC.

The fuel-cell generator is housed in an isolation box for thermal insulation and internal leakage checks. The additional ground-support equipment consisted of:

- The *electromechanical control rack*, which contained all process-control units to maintain coolant temperatures and temperature gradients, as well as the fuel-cell internal pressure and pressure differentials between the reactants and the electrolyte, within pre-defined ranges. The right balance between temperature and water removal has to be maintained to prevent the fuel cell from drying out or flooding with product water.

  Alarm handling and out-of-range emergency corrections of, for example, temperatures were performed by the electronic control unit, which was attached directly to the fuel-cell unit. Whereas the electromechanical control rack has means for operator intervention, the electronic control is a completely automatic unit with no such possibility.
- The *gas-supply panel with purge control* enables the operator to pre-set the reactant gas pressures, the inert-gas supply and the purge-gas release. In the case of an emergency, manual pressure reduction is possible if needed.
- The *electronic loads* are computer-controlled and are a combination of several 2 kW loads connected electrically in parallel.

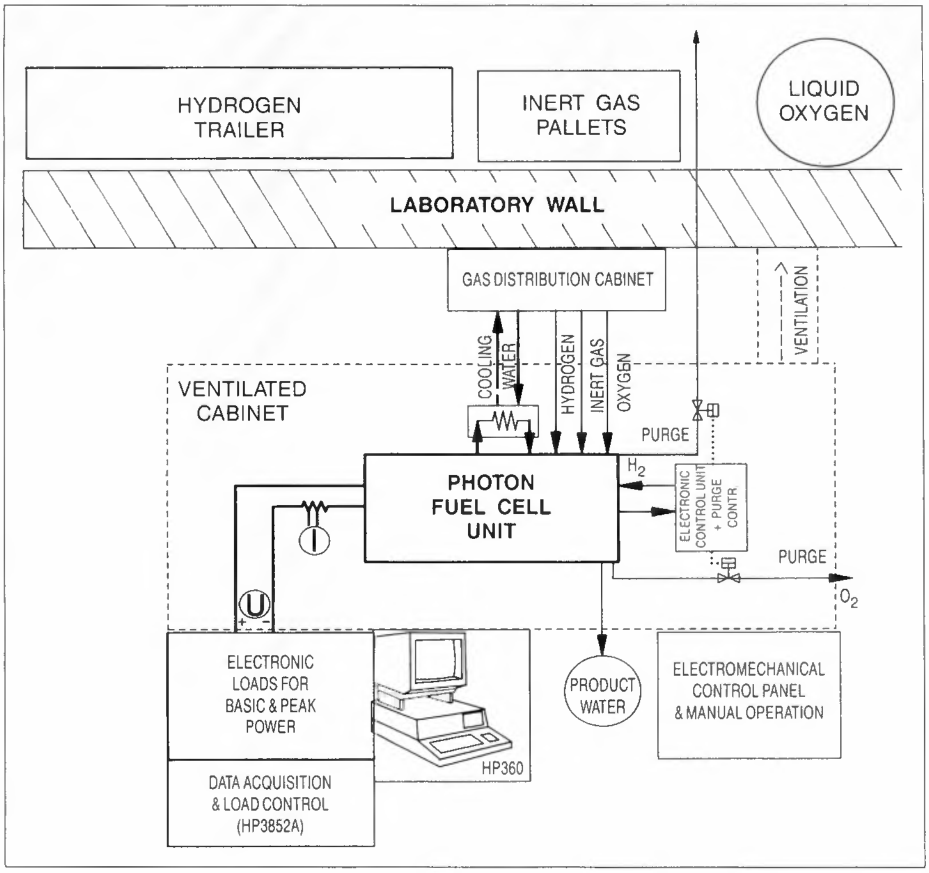

Figure 5. Layout of the test setup

- The main *cooling-water supply* was taken from the existing FCTF closed circuit and connected to the 'Photon' power plant's cooling loop.
- For *data acquisition*, a standard test station was used, which is based on a Hewlett Packard 300 series microcomputer and a Hewlett Packard 3852 data-acquisition and control unit. It has been configured for 25 analogue channels. A scanning frequency of 60 s was sufficient for this test. The much faster sampling rate required for transient response measurements (see later) was obtained using a digital storage oscilloscope.

As for all fuel-cell tests in the FCTF, the laboratory safety system monitored fire and hydrogen detectors, electrical supplies and the thermal laboratory controls (air-conditioning and closed cooling-water loop). Reactant gas supplies and electrical power are shut off automatically in the event of an emergency.

The fuel-cell power plant was installed in a temporary, ventilated cabinet, together with its electronic control unit and the gas-supply panel.

3.4. Execution of the tests

The test conditions were as follows:

Reactant inlet pressure	11 – 12.5 bar
Electrolyte	40% (w) avg.
Stack temperature	102°C avg.
System pressure in stack	4.7 bar
Gas purge frequency	< 12 h
Hydrogen purity	99.99%
Oxygen purity	99.9995%
Nitrogen purity	99.999%
Load profile	See Figure 6.

After warming up with external heating, taking 1.5 h to reach 100°C, the system was fully operational and the hydrogen and oxygen were connected and the load switched on. Whereas on the Buran spaceplane a fully automatic control unit takes care of safe fuel-cell operation, the design of the ground-support equipment does not allow automatic (unattended) tests. Hence, during this campaign, the test was attended round the clock by UEIP and ESTEC operators.

The load profile, shown in Figure 6, combined a sequence of different test steps in order to provide as much information as possible from this relatively short test. The selected test steps included:

- Current/voltage characteristics
- Constant load
- Transient response
- Underload and overload
- Autothermal startup
- Impedance study.

The analogue signals recorded online by the data-acquisition unit included fuel-cell voltage, fuel-cell current, mass flows of hydrogen, oxygen and product-water hydrogen, oxygen and nitrogen supply pressure, stack and membrane separator temperature, heat-exchanger inlet and outlet temperature, and product-water conductivity.

The 'purge' lines and associated valves shown in the diagram allowed periodic expulsion of small quantities of reactant gases, which are necessary to avoid the accumulation of impurities such as inert gases which would otherwise reduce the efficiency of the electrochemical reaction.

Four offline measurements were performed to evaluate the quality of the product water, since this could be used by the spaceplane crew. The pH of the water was always within the acceptable range of 6.5 to 8.5. Noble metal content (from the electrode catalyst) was not detectable, and the number of crysotile (asbestos) fibres longer than 10 microns per litre averaged 600, which is more than four orders of magnitude lower than the the upper limit foreseen for the Hermes spaceplane (7000 per cc).

4. The test results

4.1. Current/voltage characteristics

The *V/I* characteristics were obtained by measuring the fuel-cell voltage at ten different steps of constant current. Each current value was maintained for 1 h. During the test programme, three such curves were recorded and showed excellent reproducibility. The resulting current–voltage–power curve is shown in Figure 7. The ohmic drop in the power plant was calculated as 5 mΩ, which has been confirmed by the impedance study performed by ETCA (B).

4.2. Duty cycles at constant load

During the day shift, the fuel cell was loaded at two-hourly intervals with a varying sequence of 30, 310 and 400 A constant currents to investigate the basic performance of the unit. At night, the load was kept constant for 12 h at either 100, 200, 300 or 400 A. The corresponding voltage showed very good stability and reproducibility. The thermal control and water management was stable under all conditions. Figure 8 shows the typical relation between fuel cell current and voltage during one of the 24 h standard duty cycles.

4.3. Overload, underload and transient response

In fuel cells, underload and overload disturb the thermal equilibrium, and therefore the water balance, in the cell. In the 'Photon' cell, the underload starts at a current lower than 30 A in flight configuration. At that point, additional heating has to be switched on to prevent flooding of the cells. The tests included 2 h of underload at zero load, and 4 h at 5 A.

A current higher than 400 A is considered as overload. We encountered no problems, however, when operating for 1 h at 600 A, or with 5 s peaks of up to 800 A, which was the limit of the electronic loads.

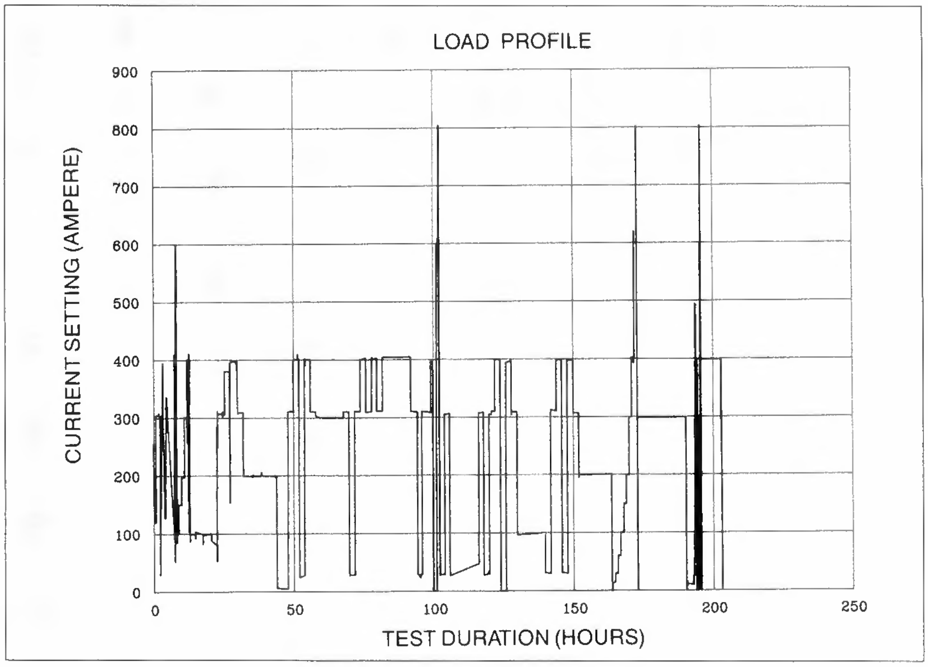

Figure 6. Load profile

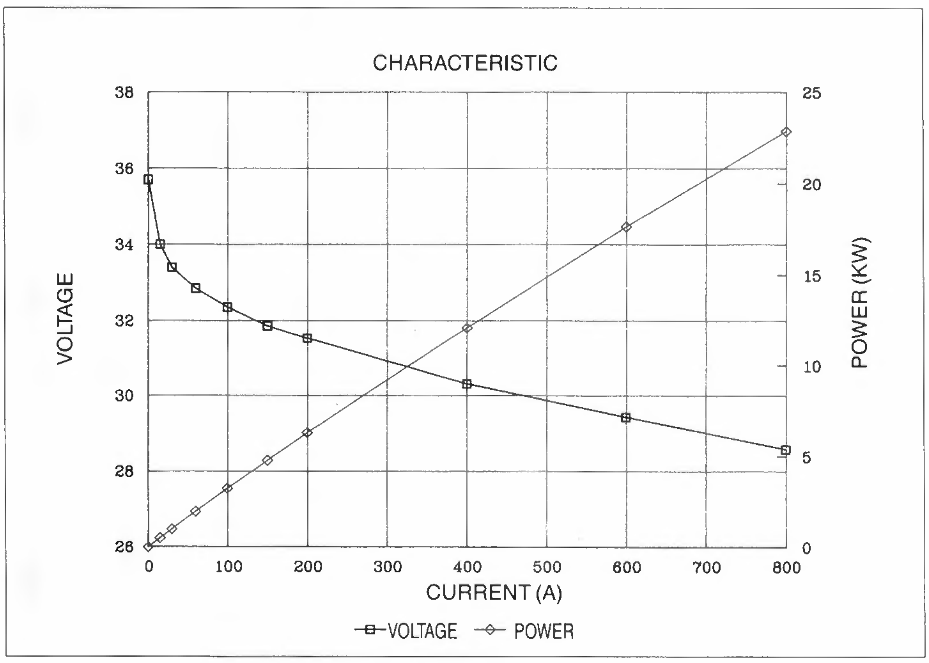

Figure 7. Current – voltage – power characteristic

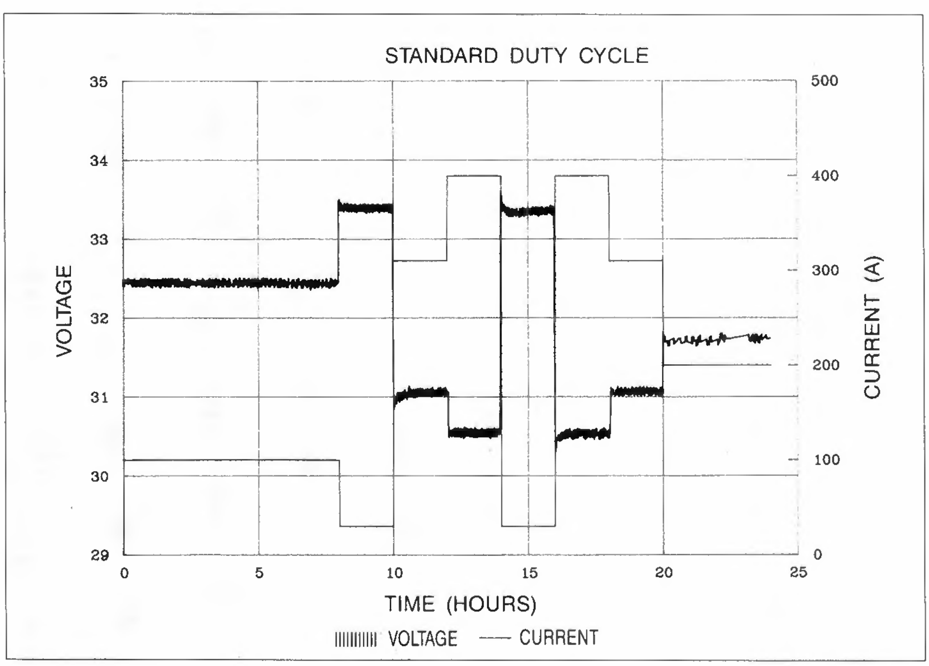

Figure 8. Standard duty cycle

The time taken by the energy source to get back to equilibrium conditions after a big load step is important in the design of a spacecraft power system. To measure relatively fast changes, a digital storage oscilloscope was used to record the voltage transient when the load was switched from 800 A to 100 A. The resulting transient curve (Fig. 9) shows that the fuel cell reacts very quickly to load changes and does not show any significant delays in voltage recovery.

4.4. Autothermal startup

On a spaceplane, it is desirable that a fuel cell that has shut down and cooled can be restarted without needing to apply external power to bring the cell back up to working temperature ('autothermal startup'). Such a startup was simulated by the application of a load of 310 A to the 'cold' fuel cell. At low temperatures, the efficiency is lower and the resulting waste heat causes the temperature to rise. Because of time constraints, the starting point was 43°C (reached after overnight cooling). As shown in Figure 10, autothermal startup from this temperature presented no difficulties.

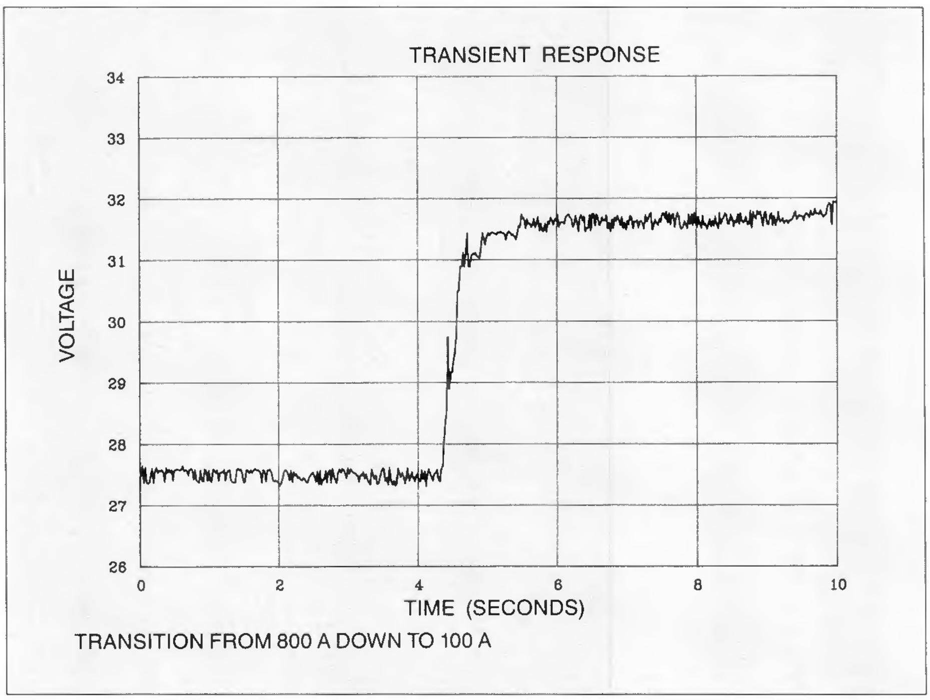

Figure 9. Voltage transient at a load change from 800 to 100 A

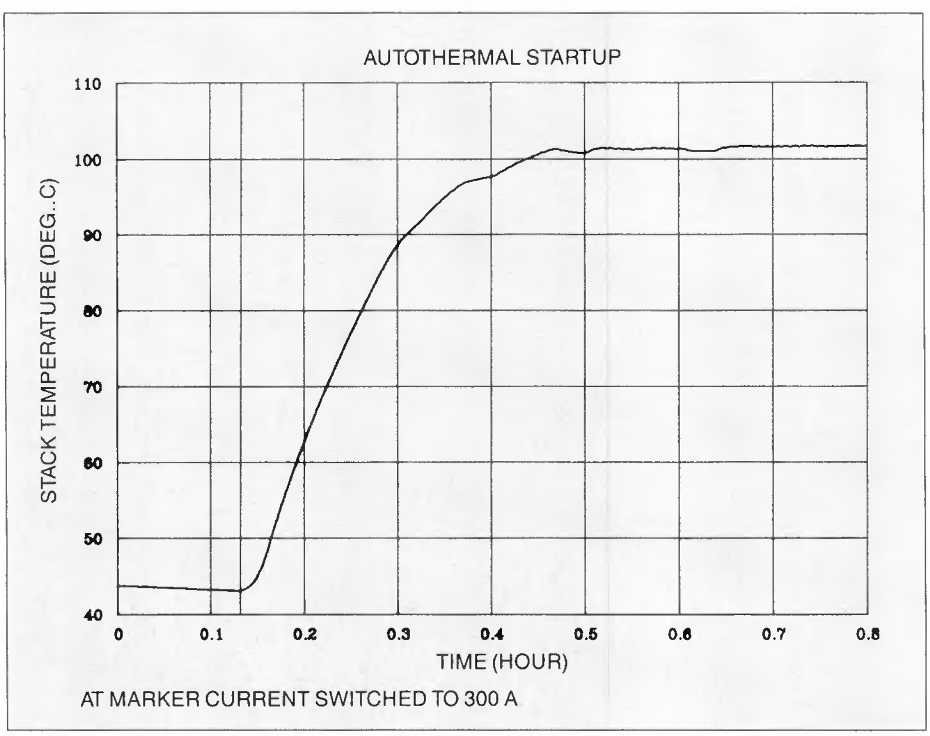

Figure 10. Autothermal startup

5. Conclusions

This test campaign demonstrated not only the excellent performance of the fuel-cell stacks, but also the maturity of the complete 'Photon' power plant. In so far as sensors could be attached to or integrated into this sealed system, it showed better performance than was called for in the Hermes specification. The temperature control was stable and reliable over the whole operating range and, coupled with that, the water removal system functioned well. The product water is of higher purity than required in the World Health Organisation's drinking-water standards. Although it was not strictly a life test, there was no measurable electrochemical performance degradation, even at high loads, during the programme.

The results clearly indicate that the 'Photon' fuel-cell technology, and in particular the cell stack, would be likely to meet the requirements of future ESA manned (or unmanned) space vehicles if an alternative or backup to a dedicated European fuel-cell development effort is sought.

Acknowledgement

A notable feature of the novel test campaign that has been described was the harmonious and enthusiastic manner in which the UEIP and ESTEC (SERCO) teams worked together. This spirit of international cooperation was much appreciated by the test organisers.

Manuscript received 27 May 1994

O. Baetz
Deutsche Aerospace, Ottobrunn, Germany

E.M. Soop
European Space Operations Centre (ESOC), Darmstadt, Germany

U. Soppa
ERNO Raumfahrttechnik, Bremen, Germany

Inter-Satellite Tracking for Co-Location

Abstract The design and performance of systems for inter-satellite tracking between co-located satellites in geostationary orbit have been studied. The goal is to improve the accuracy of the relative satellite-position determination that is necessary to allow denser packing of satellites within the same latitude and longitude control box.

This paper summarises the results of a 'Study on Inter-Satellite Tracking for Co-Location' performed by ERNO and DASA under ESA Contract 10035/92/D/CS. It was a logical continuation of the 'Study on Station-Keeping Strategies for Co-Located Satellites' carried out by ERNO in 1991 and 1992 under ESA Contract 9297/91/NL/PM.

1. Introduction

Preparations for the co-location of spacecraft in geostationary orbit became necessary after the World Administrative Radio Conference 1977 (WARC77) allocated the same longitudinal positions to several geostationary satellites. At that time, the risk of collision was estimated to be small, because the shared control boxes were typically more than 100 km wide in longitude and latitude and 50 km deep. However, several studies since then have shown that the potential risk of collisions needs to be minimised by the coordination of station-keeping manoeuvres. Without a separation strategy, co-located satellites of similar size, mass and shape would fly in closely similar orbits and be operated according to the same optimal methods, resulting in a non-negligible risk of collisions.

It was soon found that an important limiting factor in the application of a successful co-location strategy are the errors in the knowledge of the positions of the satellites relative to each other. The most common ground tracking system for geostationary missions relies upon ranging and antenna angles from one station only. Ranging measures the satellite position with an accuracy of the order of 10 m in the direction to the ground station, but the two orthogonal directions are known only to an accuracy of several kilometres via the ground antenna angles[1]. Better accuracy can be achieved by ranging from two or more stations or by employing a land-based transponder, but this is often deemed to be too expensive and still not accurate enough. An alternative method of increasing the position-determination accuracy is therefore highly desirable.

2. Study guidelines

The purpose of the present study was to investigate how the accuracy of the measurement of the satellite's position orthogonal to the direction to the station can be improved by adding inter-satellite tracking as a complement to the ground system. It was specified in the statement of work that the on-board hardware should be designed in parallel with mission-analysis studies of the corresponding accuracy, in order to provide the most efficient trade-off between performance and cost.

Assuming that traditional ground tracking will continue to be used for some years to come, efforts were concentrated on finding a minimal additional type of measurement capable of improving the inter-satellite determination accuracy. Particular efforts were made to identify simple, inexpensive tracking methods that would be serious candidates for flight on future geostationary satellite missions.

The ideal inter-satellite tracking system, in addition to being low-cost, must also involve only lightweight on-board equipment and be simple to operate. It should also make use of technology that already exists or will soon become available. From the start, therefore, it was decided to rule out designs with antenna-pointing mechanisms or any other moving mechanical parts. Because the tracking system will be used for close co-location, one can design it for inter-satellite distances of between 1 km and 100 km.

At an early stage in the study, it became clear that two-way range and range-rate techniques were the only methods of interest. One-way measurements or signal loops involving ground stations do not offer any advantage. A relatively low radio frequency was selected for providing a nearly omni-directional set of on-board antennas for transmission and reception. The time-tagged measurements can be included in the normal housekeeping telemetry for transmission to ground.

The first co-location configuration to be studied was a pair of typical three-axis-stabilised communications spacecraft operated by the same control centre. This was later extended to include larger groups of satellites of different designs, operated by different control centres. The latter case also involved important logistics considerations on how to organise the data flow and decision making.

3. On-board hardware

In addition to the design constraints mentioned in the study guidelines, a preliminary analysis was performed in order to establish accuracy requirements for the inter-satellite measurements. This analysis took into account the relative drifting of two satellites due to an initial position or velocity error, which corresponds to the evolution of the residual state estimation uncertainty due to orbital dynamics. Allowing a maximum admissible drift of about 1 km in 24 h, and assuming the typical manoeuvre errors observed during geostationary orbit control, a measurement resolution of about 10 m for range measurements and 1 mm/s for range-rate measurements (3σ) was derived.

Apart from the measurement performance to be achieved, the major problems to be resolved during the hardware design were the signal interference protection, the satellite discrimination, and the allocation of a suitable frequency band to the inter-satellite tracking (ISTRA) service. Three different interference scenarios were considered:

- Interference of the inter-satellite tracking link with any ground-to-satellite signal, and vice versa (e.g. telemetry/telecommand). This scenario becomes relevant because the ISTRA and the telecommand receiver on-board the satellite have approximately the same sensitivity, which implies that the received field strengths of the ground-station telecommand uplink signal and of the ISTRA signal are approximately equal. The required damping ratio for separation of the competing signals is significant (> 64 dB) because of the 40 dB dynamic range to be covered by ISTRA (1 – 100 km), and due to the antenna gain variation as a function of RF incidence angle.
- Interference of inter-satellite tracking signals originating from different satellites within the satellite cluster. This interference scenario will be present for all clusters involving more than two satellites and is closely related to the discrimination of satellites discussed below.
- Coupling of the ISTRA signal into the ISTRA receiver on-board the same satellite, which becomes possible due to the application of low-gain antennas with a large coverage area. The required damping of 190 dB can be achieved by a frequency turnaround ratio of at least 1.1, low-level out-of-band spurious signals (<50 dBc), and the application of a transmit filter.

For satellite discrimination, the analysis yielded a preference for time discrimination, i.e. the allocation of time slots for the individual inter-satellite links to be scanned. Compared to the alternatives – namely discrimination either by frequency separation or code – this design option showed the smallest demands in terms of hardware and frequency resources. Moreover, modification of the cluster constellation (insertion or removal of satellites) can be achieved simply by telecommand.

The only drawback of a limited duty cycle, i.e. the fraction of a given reference period that is assigned to a particular inter-satellite link, must be seen in relation to the orbital period of 1 day. Tracking data should be equally spaced over this time in order to be able to track the satellite librations caused by the residual eccentricity or inclination. Considering that an inter-satellite link between two arbitrary satellites yields the same tracking information as the reverse link, the duty cycle for each link within a cluster of eight satellites is still about 3.5%, i.e. about 50 min/day which is available for tracking. This will be sufficient, taking into account that – as discussed below – only about 15 s of integration time are needed to obtain a set of one range and one range-rate measurement.

For the selection of a suitable frequency band for the ISTRA service, available frequencies allocated to the 'Space Operation Service' (SOS) have been evaluated with respect to such trade-off criteria as the complexity of the interference protection methods required, the required RF power level, the available bandwidth, the availability of (largely space-qualified) hardware, and the achievable measurement accuracy. The study has resulted in a recommendation to use the VHF band, which supplies sufficient bandwidth for a two-way measurement system with the necessary turnaround ratio, and has the significant advantage of requiring a very low transmit power (only 8 mW) in order to meet the receiver acquisition threshold. The inter-satellite range information is obtained on the basis of a sine-wave range tone of 80 kHz, which is used for phase-modulation of the selected RF carrier. After demodulation, the noise impact has to be reduced by a narrow-band phase-lock loop and an adequate integration time. For the ranging-tone frequency assumed above, this yields a random error of 10 m (1σ).

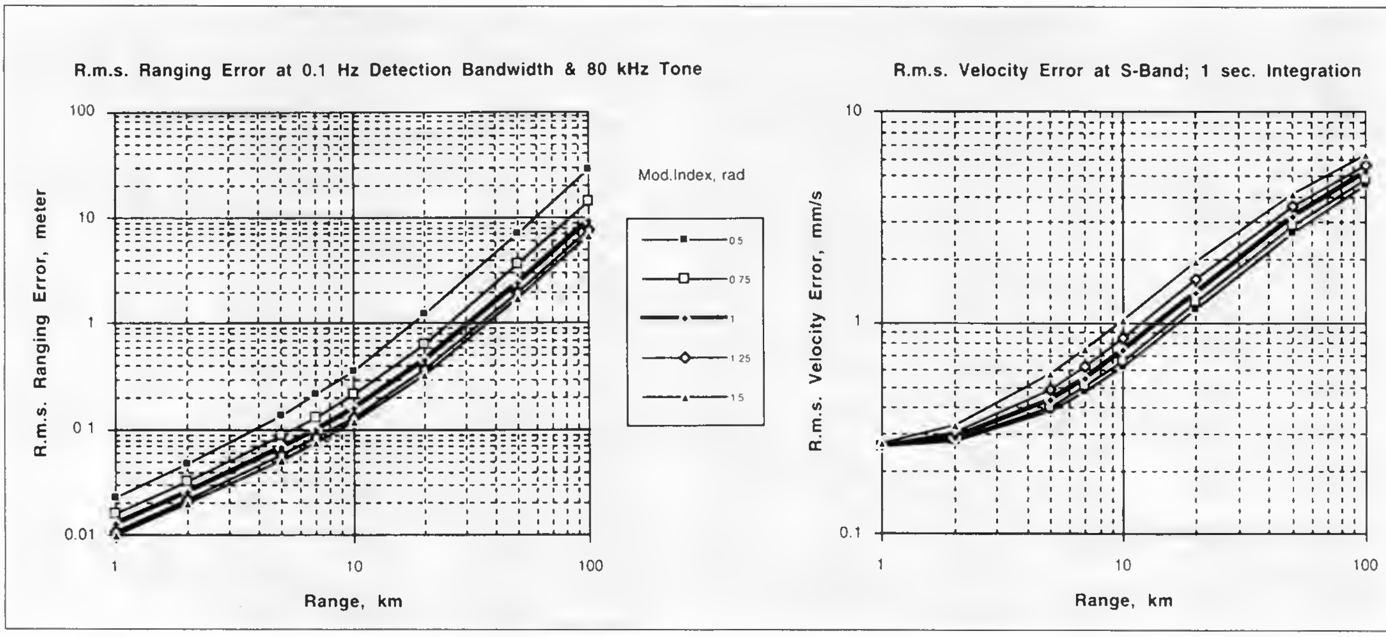

Figure 1. RMS ranging and Doppler error as a function of range (VHF band, two-way system)

The value of the ranging-error dispersion follows almost a quadratic relationship to the inter-satellite distance. Figure 1 shows the analysis results for the case of a VHF signal with 8 mW transmit power and an integration time of about 1 s. Using a 100 mW transmitter, there is even a margin of at least 10 dB, which allows a further reduction in the error or a shortening of the integration time.

The error characteristics for range-rate measurements shown in Figure 1 were obtained for an integration time of 1 s. The desired value of a 3σ-dispersion of 1 mm/s can be obtained after approx. 15 s. The slope of the curve is less than 2dB/dB, due to the counteracting effects of decreasing RF power and decreasing PLL noise bandwidth, if no AGC (Automatic Gain Control) is implemented.

The analyses described above have resulted in the specification of a feasible on-board hardware design satisfying the constraints of the study and meeting the performance objectives. The measurement technique will be according to ESA ranging and range-rate standards, except for the choice of RF frequency. The overall weight for a non-redundant on-board device has been assessed to be about 4.2 kg, and the DC power consumption will be less than 15 W.

Figure 2 shows the signal flow for a master–slave measurement link operating at 137 MHz (forward link) and 148 MHz (return link). All frequencies used by the

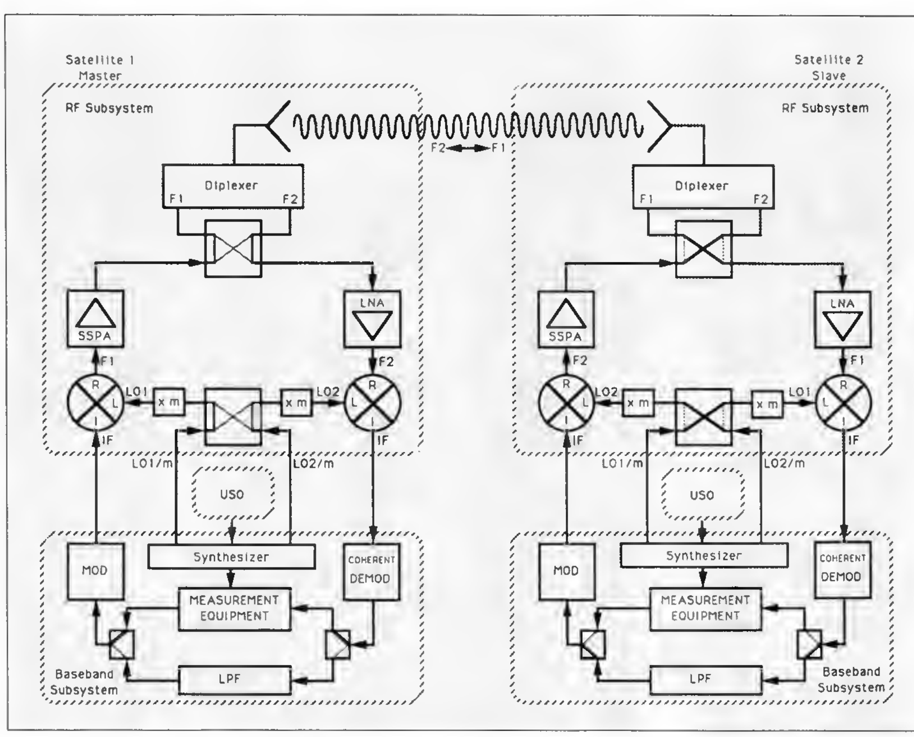

Figure 2. On-board hardware and signal flow for two-way inter-satellite range and range-rate measurements

on-board equipment are derived from the output signal of an ultra-stable oscillator with a stability of $\leq$ 0.004 ppm in any 50 s interval. The two-way measurement principle distinguishes a master (transmitting the forward signal) and a slave satellite (transmitting the return signal). The operating mode (master or slave) can be selected via two transfer switches connecting the diplexer and the local oscillator frequency to either the transmitter or the receiver. Solid-state switches can be used for selecting between the multiplier input signals LO1/m and LO2/m, while switching of the RF signals to the proper diplexer ports must be carried out by low-loss, highly isolating co-axial switches.

4. Orbit accuracy

For an assessment of the orbit-determination accuracy that can be obtained by means of a combined processing of conventional (ground-based) and inter-satellite tracking data, a numerical performance analysis has been conducted. This analysis has been based on the method of weighted least-squares used for most of today's orbit-determination applications. The covariance analysis was chosen because of the need for a considerable amount of parameter variations accounting for uncertainties of measurement error parameters (bias uncertainties, noise dispersions), different scenarios (separation strategy, manoeuvres, tracking schedule), and orbit perturbations (uncertainty regarding solar radiation pressure, manoeuvre errors). For a given parameter set, the analysis provided an estimate of the uncertainty of an orbit-determination run, which is due to the uncertainty in the system parameters considered and the tracking conditions, e.g. the geometrical observability of the state-vector components.

Free-flight orbit determination

The analysis was carried out first without any system-dynamics biases, i.e. assuming an error-free state prediction. In this way, the calculated estimation uncertainty was due only to the geometrical measurement conditions and to measurement errors. The residual estimation uncertainties obtained were rather insensitive to the separation strategy and small with respect to the errors induced by orbit-prediction uncertainties. A closer co-location enhanced the orbit-determination performance due to the smaller measurement noise at smaller distances.

Secondly, the effect of system-dynamics biases was taken into account in the state error prediction, but not solved for. The results revealed that these effects dominate the error budget of the orbit determination, overruling the smaller effects of the inter-satellite measurement types and the separation strategy.

As an example, Figure 3 shows the residual position error after the orbit determination as a function of the tracking period and the uncertainty in the area-to-mass ratios of the individual satellites (as a percentage of the nominal value of 0.03 m^2/kg). The curves have been obtained for an eccentricity/inclination separation within a 0.1° window, using two-way ranging measurements. One can observe that the secular growth of the prediction error for the in plane-state components cannot be removed completely by the estimation. On the contrary, the error in the out-of-plane component, which is only slightly affected by the perturbation, decreases due to the larger tracking-data sample size.

Figure 3. Effect of system dynamics biases on the orbit-determination accuracy

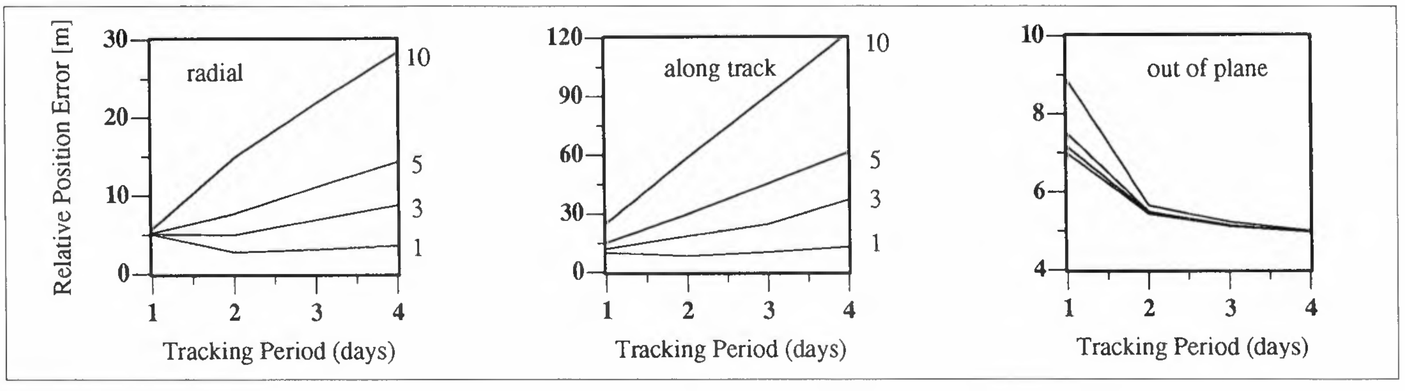

Autonomous spacecraft operations may also induce significant perturbations into the relative motion, reaction wheels carried on-board geostationary satellites being one such example. Unfortunately, these actions are mostly unpredictable and can therefore not be taken into account properly in the orbit-determination process. Considering that future co-location scenarios may require inter-satellite distances of just a few kilometres, a drift of about 800 m/day introduced by a velocity increment of only 5 mm/s along-track is not acceptable. The numerical analysis of this aspect has shown that inter-satellite measurements can significantly reduce this estimation uncertainty to less than 100 m, which however is still much worse than the accuracies given in Table 1.

If the manoeuvre epoch is made available to the orbit-determination process, the thrust can be solved for by the orbit-determination program. The minimum residual estimation uncertainty, however, is limited if the perturbation occurs once a day or even more often. Assuming a daily off-loading manoeuvre, the analysis has shown that the induced ΔV can be estimated to an accuracy of about 10% of the expected effect.

Table 1

Separation		Relative position error [m]			Relative velocity error [mm/s]			
strategy	window	X	Y	Z	X	Y	Z	Measurement type
λ—i	0.1	0.4	5.0	4.0...8.0	0.02	0.04	0.2...0.8	Two-way range
λ—i	0.01	<0.1	5.0	0.4...2.0	<0.01	<0.01	0.01...0.6	Two-way range
e	0.1	0.5	0.5...5.0	10...20	0.01...0.1	0.01...0.5	0.5...1.0	Integrated Doppler
e	0.01	<0.4	0.1	—	0.01...0.07	0.01...0.06	—	Integrated Doppler
e—i	0.1	0.1	0.5...2.5	0.1...1.0	0.01...0.08	0.04	0.2...0.8	Integrated Doppler
e—i	0.01	<0.1	5.0	0.4...2.0	<0.01	<0.01	0.01...0.6	Integrated Doppler

Manoeuvre error determination

Another major point for the numerical tracking-system analysis was to investigate the benefit of inter-satellite measurements for the estimation of station-keeping manoeuvres, and their performance errors. The deviation from the nominal relative effect needs to be compensated quickly in order to avoid a relative drift between the two satellites. An offset of the absolute manoeuvre vector from its nominal value may be tolerable if no station-keeping window violation occurs. In particular, the size of the (unwanted) in-plane components of the manoeuvre needs to be estimated in order to counteract a potential relative drifting of the cluster members.

It has been assumed that the two satellites execute their manoeuvres simultaneously, which is challenging from the orbit-determination point of view because the performance errors are statistically independent. On the other hand, one can take advantage of the possibility to solve for the relative effect of the manoeuvre, which may even vanish if the satellites have a purely longitudinal separation.

The study analysed impulsive and ion-propulsion manoeuvres for inclination and eccentricity/drift control. Different tracking schedules and separation strategies have also been tried and the best results have been obtained for the following scenario:

1. Tracking of a free-flight period up to the epoch of the manoeuvre.
2. Orbit determination at the manoeuvre epoch, solving for position and velocity only.
3. Tracking for N hours after the manoeuvre.
4. Orbit determination, solving for the manoeuvre and taking into account the result of the previous estimation as an a priori estimate.

This method reduces the amount of solving for variables for every part of the estimation, and consequently reduces the amount of tracking data that has to be acquired. An example is given in Table 2, which shows that the objective of obtaining information about the manoeuvre (error) within a tolerance of less than 1 mm/s can indeed be already achieved just a few hours after the manoeuvre. As expected, the direct velocity measurements yield slightly better results for the time immediately after the manoeuvre.

Table 2a. Intersatellite range measurements

Component [mm/s]	Tracking after manoeuvre [h] 3	6	12
Radial	0.79	0.74	0.11
Along-track	0.37	0.41	0.05
Out-of-plane	3.05	1.56	0.59

Table 2b. Intersatellite Doppler measurements

Component [mm/s]	Tracking after manoeuvre [h] 3	6	12
Radial	0.52	0.50	0.15
Along-track	0.33	0.29	0.05
Out-of-plane	1.80	1.63	0.67

The improved accuracy in the measurements of the inter-satellite distances will allow the use of smaller margins for the proximity operations, thereby enabling a denser packing of satellites in a cluster. In particular, the along-track relative positions, which are difficult to control by ground tracking alone, can now be directly determined and corrected. These along-track positions are easily disturbed by the cumulative effect of small differences in the longitude drift-rates.

An important consequence is that use of a pure in-plane separation strategy by means of different eccentricity vectors now becomes possible. Without inter-satellite tracking, one would need to apply the combined inclination/eccentricity separation, which is independent of along-track position differences. The latter is its only advantage, whereas the drawback is that inclination manoeuvres may be difficult to coordinate when many manoeuvre constraints have to be accommodated. For both separation strategies, the number of co-located satellites is the same[1].

5. Operations concept

When looking at the impact of inter-satellite tracking on satellite operations, it is necessary to distinguish the consequences of the application of the new tracking method and those of the co-location of satellites. The study has included the development of possible scenarios for the operation of a cluster of up to 7−8 satellites, applying the results of the preceding analyses. It became obvious that, once routine-operation status is achieved, the majority of the additional work will be related to satellite control rather than orbit determination, i.e. the coordination of absolute (conventional geostationary station-keeping) manoeuvres and relative manoeuvres required to maintain a certain relative motion pattern for the cluster members.

The study has emphasised the re-use of existing technology and infrastructure for the new system, which means that the effort that needs to be devoted to the implementation of the orbit-determination system using inter-satellite tracking as described above is quite low. Again, manpower and infrastructure must be seen in the context of the resources required if the satellites are operated independently.

The orbit-determination software needs only minor upgrades in order to account for the new measurement types and the relative motion state vectors being used. Assuming that there will still be one operator assigned to each member of the cluster, the additional work load due to the measurement links to be considered increases linearly with the cluster size. This work will be in the acquisition, archiving and configuration of the tracking data to be entered into the orbit-determination system. Since inter-satellite tracking data must be treated like regular telemetry, this task can be well supported by the computer system available to the operator.

The coordination of operator activities is more difficult if the satellites within a cluster belong to different organisations. The study recommends exchanging pre-processed tracking data rather than raw data, which reduces the amount of data and also only requires agreement on a common standard for the interface to the orbit-determination tool, as opposed to unifying different telemetry standards. For the limited amount of tracking data to be expected (the analyses considered a minimum sampling rate of 10 min for post-manoeuvre tracking phases), exchange via electronic mail would even be feasible.

Concerning the layout of a routine operations scheme for a satellite cluster using inter-satellite tracking data, the study particularly investigated the possibilities for determining the relative orbits and manoeuvre errors such that relative motion control manoeuvres can be planned and scheduled within less than 12 h after a conventional station-keeping manoeuvre. Obviously, the time available for tracking between manoeuvres is constrained by the station-keeping manoeuvre strategy. Different scenarios have been studied using the performance data obtained from the numerical analyses. Due to the improved accuracy of the orbit determination, especially in the along-track direction, the appropriate scheduling of relative motion control manoeuvres would be possible within the available time, even for the challenging case in which the inclination correction is done with ion propulsion, which results in frequent manoeuvres and consequently short tracking periods.

6. Conclusions

The proposed system for performing inter-satellite range or range-rate measurements in the VHF band has been found to be a promising candidate for providing the improved inter-satellite determination accuracy that is necessary for closer co-location of the large clusters of geostationary satellites foreseen for the future. An important further advantage is that the system enables the implementation of purely in-plane eccentricity separation strategies. This removes the need for coordinating inclination manoeuvres, which is often difficult in view of the many constraints that have to be considered.

References

1. Soop E.M. 1994, Handbook of Geostationary Orbits, Space Technology Library, Kluwer Academic Publishers, Dordrecht.
2. Soppa U. et al. 1994, Study on Inter-Satellite Tracking for Co-location, Final Report, ESA Contract 10035/92/D/CS.

Manuscript received 26 April 1994

M.N. De Parolis
Thermal Control and Heat Rejection Section, ESTEC, Noordwijk, The Netherlands

A Controlled Pump Assembly for Spacecraft Cooling Loops

Abstract The role of thermal-control systems is to maintain the temperature of every item onboard a spacecraft within pre-defined temperature limits, throughout all phases of a space mission, with a minimum resource allocation. This includes, in particular, efficient management of the power dissipated onboard. The trend with both applications spacecraft and space vehicles is one of a continuous increase in the services offered to the users. This implies both an increase in the power produced and dissipated onboard, and the provision of a high degree of operational flexibility, including the possibility to change the power load distribution on the spacecraft quickly and safely. Furthermore, many payloads require a high degree of uniformity and stability in terms of their temperature, or the temperature of the environment in which they operate. All of these requirements point to the use of cooling loops, based on either single- or two-phase fluid operation, as the optimum thermal-management system.

1. Cooling loops

1.1. Single-phase loops

In single-phase cooling loops, the refrigerating liquid absorbs the heat from the power-dissipating items, increasing its temperature, and transports it to the heat-rejecting devices. There, the heat is released to the heat sink and the fluid is brought back to a low temperature so as to be ready to begin another cycle. A pump is essential to provide the fluid with the hydraulic energy needed to perform this task (Fig. 1a).

The advantage of these systems is the relative simplicity of regulation and control and the lack of sensitivity as regards spatial orientation and the mechanical environment.

1.2. Two-phase loops

Two-phase cooling loops can be of three kinds:
- mechanically pumped loops (MPL, in Fig. 1b)
- capillary pumped loops (CPL in Fig. 1c), or
- hybrid loops (Fig. 1d).

The first type are similar to single-phase loops, except that the fluid changes its state (evaporating while absorbing the heat and condensing in the heat-rejecting devices) instead of just changing its temperature. Consequently, a pump is essential for these loops also. The advantage that they have compared with the single-phase loops is the large reduction in the fluid flow rate needed to manage the same quantity of power, and the accompanying decrease in the level of resources needed for the thermal-control system.

For the capillary systems, the driving force is provided by the capillary action of the material constituting the wick of the evaporators. Hence, a separate pump is not needed. There are, however, particular operations or mission phases for which the capillary actions might reach their limits (e.g. loop start-up, peak power loads, high mechanical loads or ground testing).

For these reasons, hybrid loops have been proposed in which the nominal driving force is provided by the capillary actions with a pump acting during particular mission phases (e.g. launch) and/or operational phases (e.g. peak loads or during ground testing).

To date, only single-phase loops have been flown onboard spacecraft and space vehicles (e.g. the Apollo missions and the Space Shuttle in the USA; Soyuz capsules and the Mir Station in the CIS). European spacecraft also have profitted from single-phase loops, including Spacelab and Eureca. In both cases, however, the pump technology was based on US components. ESA therefore initiated two technological studies, the first in the framework of the Columbus Preparatory Support Technology Programme (PSTP, 1986), and the second in the framework of the Basic Technology Research Program (TRP). The first study programme was subsequently transformed into a development programme under the direct responsibility of the Columbus Project. This paper reports the results of the second study programme within the TRP, which was the subject of a contract (ESTEC/9039/FG/NL) awarded in October 1990. The Prime Contractor was Reusser AG, which was responsible for the assembly and the hydro-mechanical parts, with Etel SA as a subcontractor responsible for the development of the electrical and electronic components.

2. Objectives and requirements

The scope of the technology study was the design, development and qualification-level testing of a pump unit having the following general features:
- the ability to maintain or to assist the circulation of the fluid along the loop at the required flow rate(s) during all mission phases, including launch and re-entry
- the facility to be multi-fluid, i.e. to be compatible with a wide range of fluids, including de-mineralised water, ammonia and fluoro-carbons (freon)
- the ability to be reliable and provide operational flexibility
- have an efficiency as high as possible, to avoid unnecessary power consumption (single-phase loops) or a high heat loads on the fluid (two-phase loops).

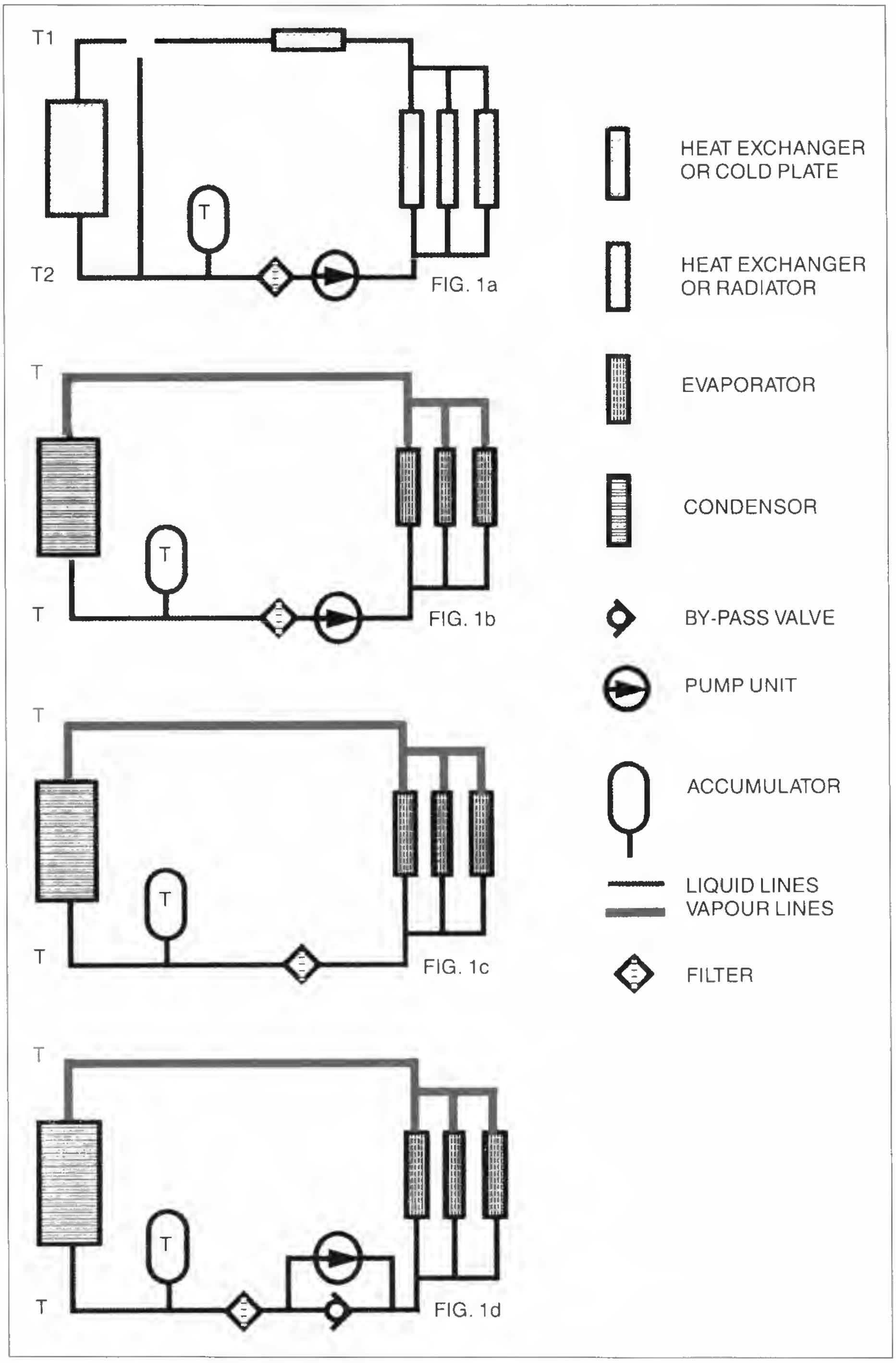

Figures 1a—d

Table 1. Main requirements

Requirement	Nominal value	Range/note
Flow rate (kg/h)	315	150 to 380
Δp (Pa 10^{-5})	1.4	0.35 to 2.15
Fluid	Freon 114	Water—ammonia
Temperature (°C)	20	0 to 30
Efficiency (%)	>30	—
Power (W)	<80	—
Proof pressure (Pa 10^{-5})	22.5	—
Burst (Pa 10^{-5})	30	
Microgravity disturbance (N)	0.01	0.1 to 500 Hz
Environmental temperature (°C)	20	−30 to 40
Environmental pressure (Pa 10^{-5})	1	Vacuum to 1.15
Lifetime	50 000 h or 15 yr from delivery	

The main requirements on the Controlled Pump Assembly (CPA) are shown in Table 1. The functional requirements were established taking into account the results and objectives of a previous technology programme[1] involving a freon-operated two-phase mechanical loop. For this reason, freon-114 was chosen as the reference operating fluid.

The environmental requirements, and in particular the mechanical loads, were defined as a worst-case envelope of the requirements available at the time for Hermes and Columbus Man-Tended Free-Flyer (MTFF) hardware.

3. The CPA

Three identical units have been built by the contractors, known as CPA-1, CPA-2 and CPA-3. This has allowed the same manufacturing standards to be maintained, despite the challenges of the design to be verified, and in particular:
- the greatly reduced dimensions and tolerances of the impeller-rotor assembly
- the need to balance the pump with the greatest possible accuracy to allow stringent in-orbit microgravity requirements to be respected.

Figures 2 and 3 show CPA-1 and its mechanical interfaces. The overall dimensions (including two 3/4-inch connectors) are $240 \times 240 \times 140$ mm^3 and its mass is 3.1 kg. It is interesting to note that the Electronics Control Unit (ECU) shown, which is not optimised for space applications, takes up about two thirds of the overall length of the assembly and about half its mass. There is therefore considerable scope for further mass and volume reductions.

Figures 4 and 5 show two cross-sections of the pump-motor assembly. The fluid enters the assembly through the connector and the pump body inlet, from which it is routed into the impeller, the volute and the diffuser. It finally exits the CPA through the outlet connector.

At the outlet of the impeller, a small quantity of fluid is diverted into the tiny lubrication and cooling passages: first through the gap between the motor stator and the sleeve and then into the clearance of the radial bearings, from where it is pushed into a capillary tube inserted into the shaft, which drives it back to the impeller eye. The impeller has five backward curved blades and five splitters, to allow better fluid distribution and guidance without imposing excessive resistance on the flow.

Two platinum-resistance (PT100) temperature sensors are fitted into the inlet and outlet sections to monitor any functional anomaly. The pressure rise can be monitored via the differential pressure transducer mounted on top of the unit.

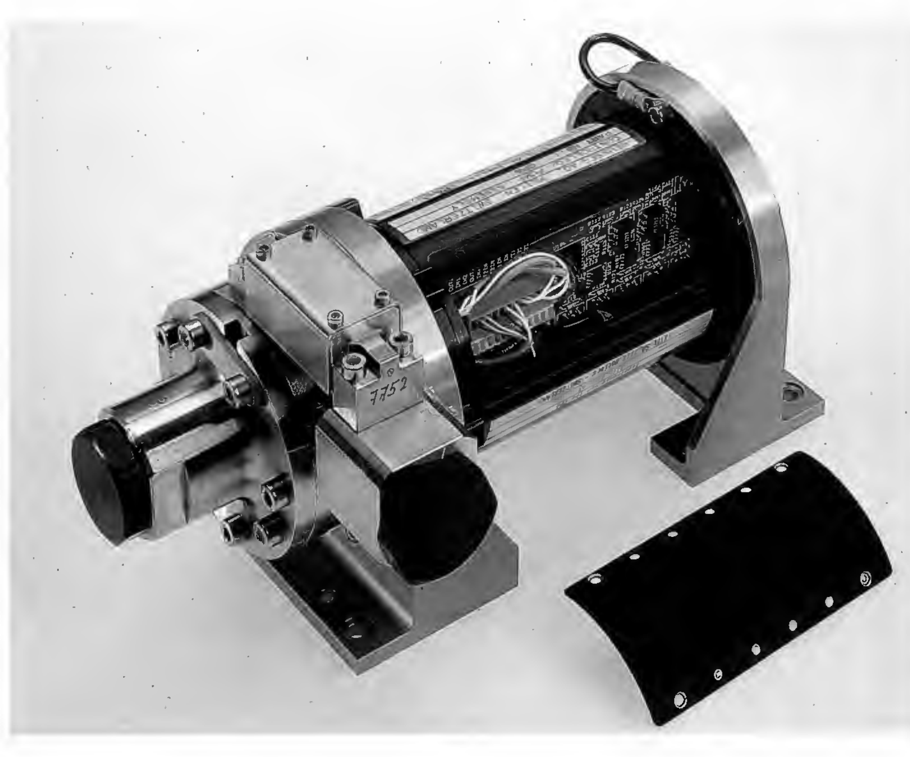

Figure 2

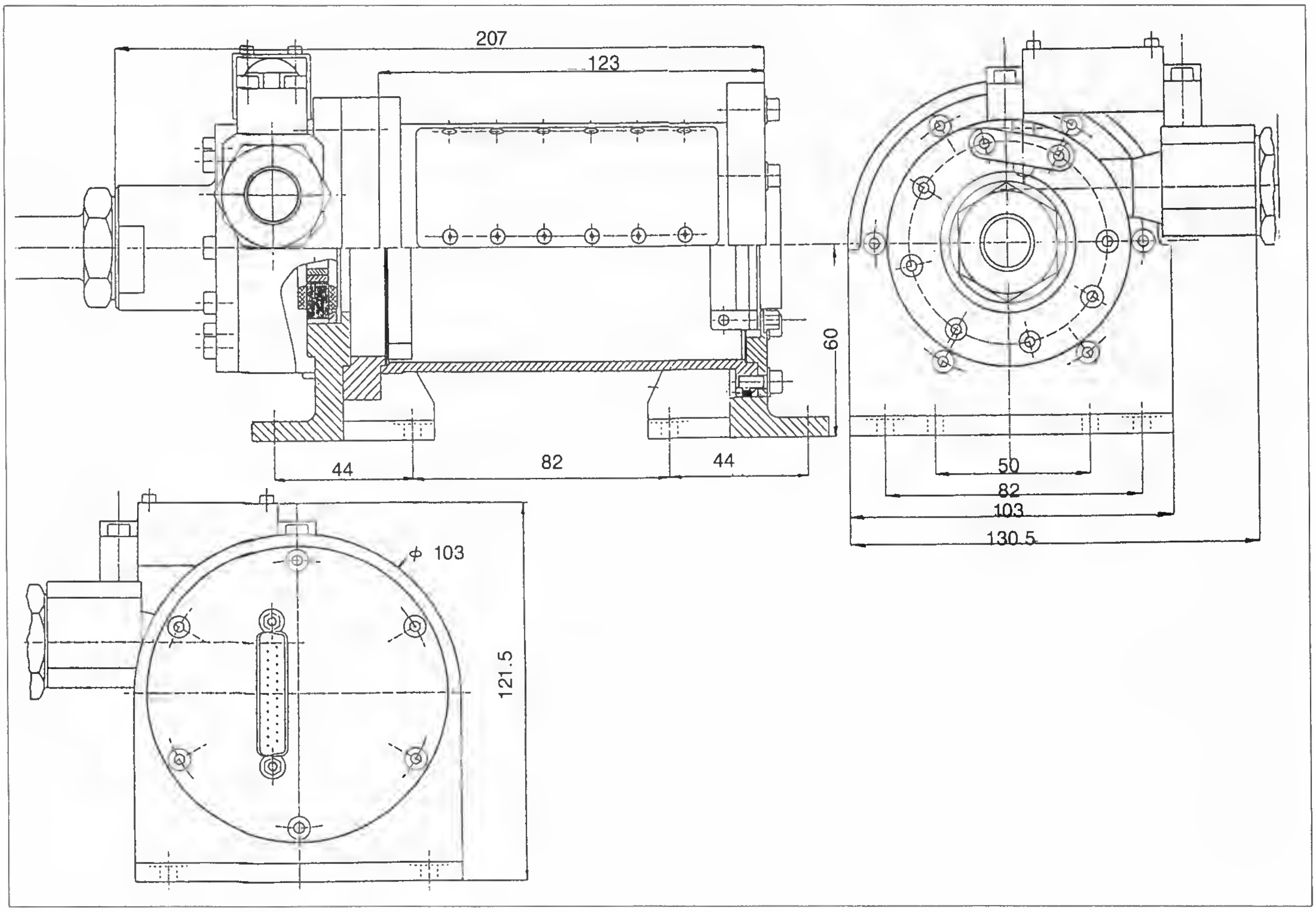

Figure 3

The motor is a miniature brushless DC motor with an eight-pole samarium–cobalt magnet rotor. The motor is sensorless as the measurements of rotor speed and position, needed for its control, are performed via the back electromotive force (EMF) zero-crossing detection, as explained below.

A schematic of the motor driver (ECU) is shown in Figure 6. The external system controller (spacecraft data-handling manager or a thermal-control unit) can enable/disable the ECU. When enabled, the ECU receives a speed signal which is fed into a Phase Lock Loop (PLL), where it is 'locked' with the actual speed calculated via the back-EMF directly available from the motor's three phases and processed in the dedicated board. The error is used to drive the current loop, which supplies the motor via a three-phase power bridge.

The DC/DC converter supplies the power bridge with 120 V DC and the sensors and transistors with their required voltages.

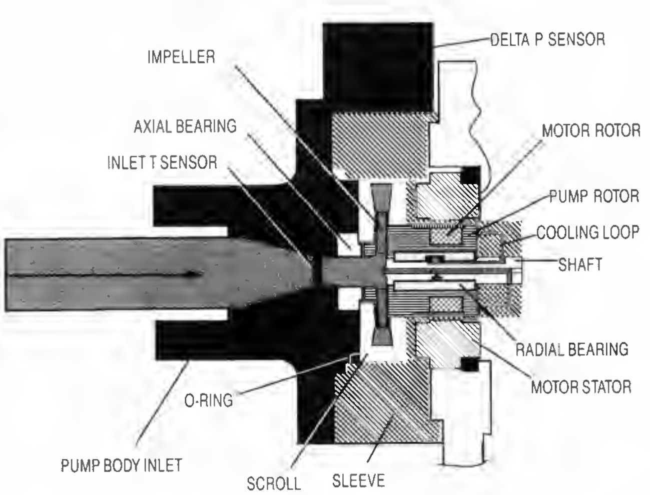

Figure 4

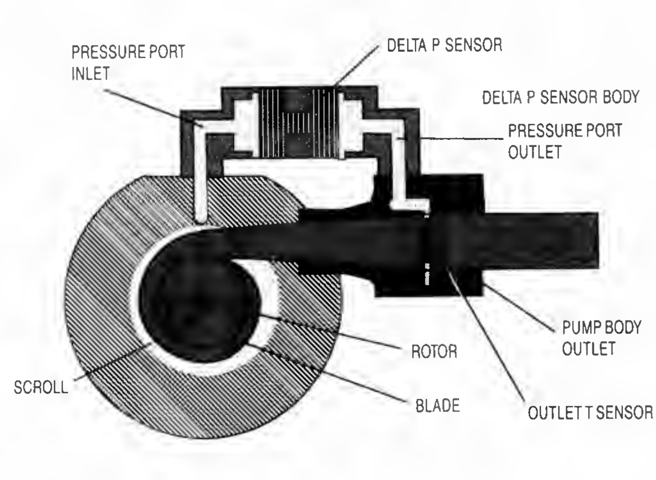

Figure 5

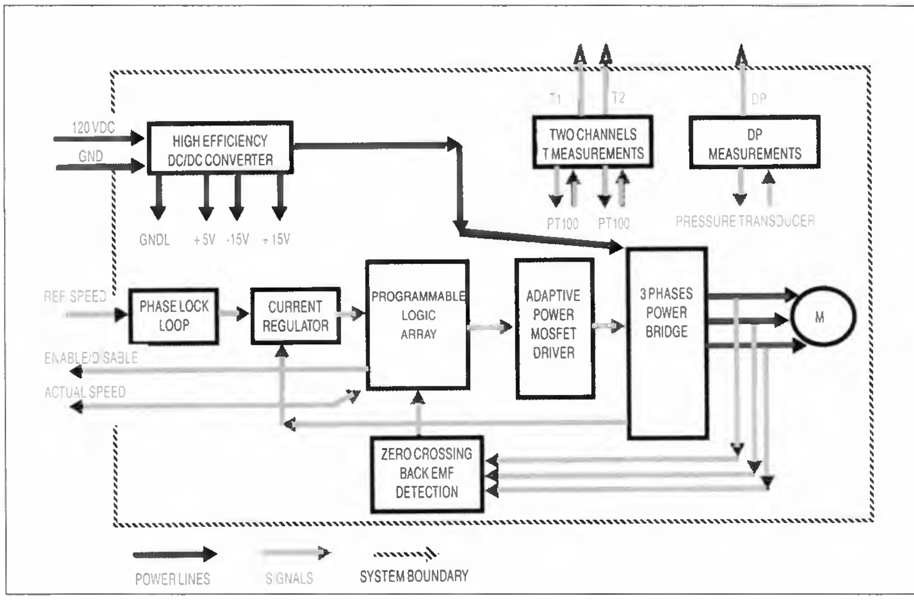

Figure 6

Reliability

All the materials used for parts in contact with the fluid are compatible with all the specified fluids and are widely accepted for space use. For reliability, the design has been implemented with the minimum number of critical parts. In particular:

- No dynamic seals are included in the design. This was in fact a configuration driver, pushing towards the use of a canned-type pump-motor assembly. Only one static seal is employed in the pump-unit body, to separate the pressurised part from the external world (interface between the sleeve and the housing).
  Two other seals are used for the differential pressure transducer inlet and outlet ports. Every O-ring is made of 'Chemraz', a Teflon-based material widely used in propulsion engines and compatible with the operating fluids specified.
- As explained above, no sensors are used to control the motor's speed and thus the pump-delivered flow rate and pressure rise. This feature not only reduces the number of parts, but it also avoids the use of less reliable, non-space-qualified components (e.g. Hall-effect sensors).

The calculated reliability figure for the CPA is about 3.5×10^{-6} failures per hour, or a lifetime in excess of 280 000 h. This does not include the possibility of failures due to external causes, such as contaminated fluid.

Partly to confirm these results, a one-year life test was begun in September 1993 with two CPAs (Fig. 7):

- CPA-1, following a daily speed cycle to examine the effect of changing speed regimes on the lifetimes of rotating parts
- CPA-3 running at constant speed.

Performance

Given the lack of literature or product data on this kind of miniature pump, the whole development programme involved a trial-and-error approach based on prototype model testing. These tests allowed fine tuning of the relative dimensions of

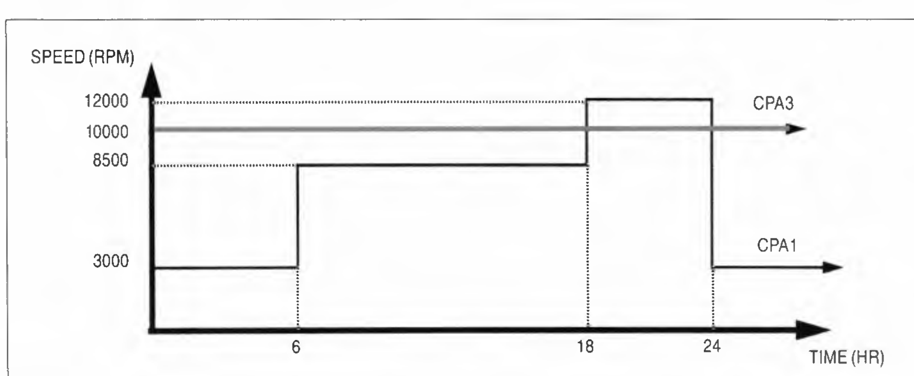

Figure 7

the impeller, the volute and the diffuser of the pump to achieve the desired performance. Following assembly of the engineering model, an intensive test plan was defined, which was performed using CPA-1 (Fig. 8). It is worth mentioning that CPA-2 and CPA-3 underwent the first seven tests at the same level as CPA-1.

Ten of the boxes in Figure 8 represent performance tests, run either at the contractor's site under normal room conditions, or at ESTEC in the thermal-vacuum chamber of the Mechanical Systems Laboratory, both in vacuum and in air. Freon 114 was used for the official qualification tests according to the ESA Statement of Work requirements.

The main performance parameters are the pressure rise, the electrical power absorbed, and the efficiency. The latter is defined as the ratio between the output hydraulic power (i.e. the product of the flow rate and the pressure rise) and the electrical power absorbed. In other words, it represents a global value for the CPA system, including all the losses (electrical, mechanical, hydraulic, etc.).

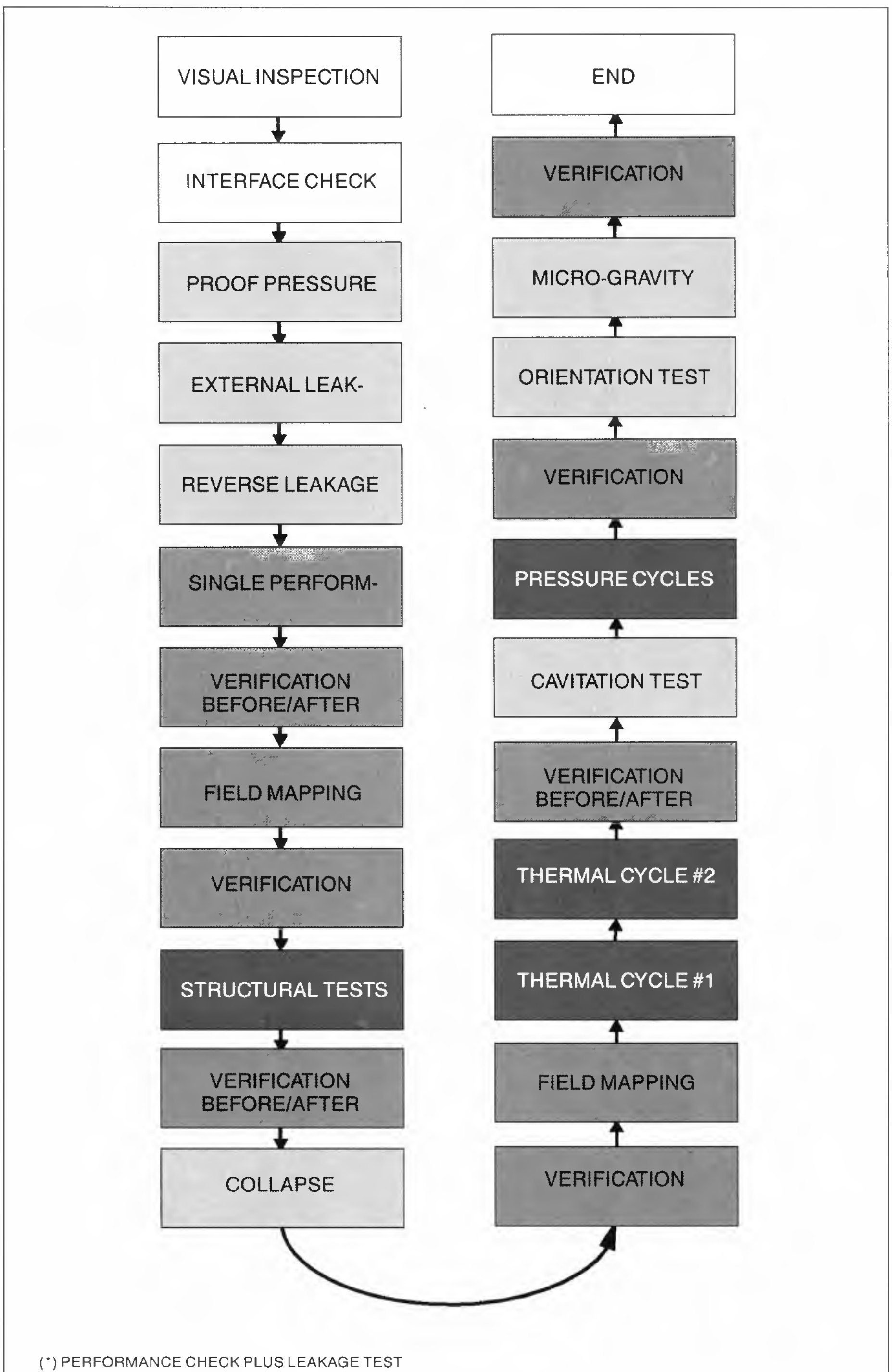

Figure 8

The conclusions from the test campaign were as follows:

- The CPA's performance range is much wider than required. The flow-rate range extends up to 800 kg/h and the maximum achievable pressure rise, at that flow rate, is 2.25 bar.
- The absorbed electrical power, at the design point, turned out to be less than required (about one third). Even under the worst specified operating (reduced voltage, maximum speed) and environmental (freon temperature −30°C) conditions, the absorbed power was about 65% of the maximum specified value.
- The efficiency at the design point is 33%, going up to 45% for the highest flow rates (800 kg/h). In the low-flow-rate range (100 to 150 kg/h), the efficiency is always higher than 10%.

Figures 9a−c summarise those results, showing the pressure rise, the efficiency and the absorbed electrical power as a function of flow rate for five selected speeds. These plots refer to the field mapping test performed after all of the environmental testing. Comparisons between the test data gathered before and after the environmental tests never showed performance differences greater than ±5%.

Cavitation behaviour

A special performance test was conducted to verify the cavitation resistance of the pump. Cavitation is a very disturbing phenomenon that can dramatically affect the performance of pumps, valves and any fluid component in general. When the local fluid pressure falls below the fluid vapour pressure, vapour bubbles can be generated. These bubbles, transported by the fluid stream, can flow to locations where the pressure is higher than the fluid vapour pressure, where they collapse back into the liquid. The process of bubble generation and subsequent collapse is highly dangerous because:

- it reduces the hydraulic power imparted to the fluid and thus the pump efficiency
- it causes vibration and acoustic noise, which would disturb the microgravity environment
- it can accelerate corrosion and erosion processes in the equipment.

The phenomenon's occurrence is particularly critical for two-phase loops, where the fluid is under saturation conditions all around the loop. Thus, in order to avoid cavitation, the fluid temperature must be reduced just before the pump (sub-cooling) so that the local vapour pressure is lower than the loop pressure. The sub-cooling reduces the efficiency of the two-phase loop action and thus should be kept to a minimum. This value is determined by the pump characteristics (speed, geometrical dimensions of the impeller, shape and number of blades, etc.) and can only be defined via proper testing.

The test consisted of reducing the pump inlet pressure in small steps until the onset of cavitation, which was signalled by a sudden decrease in the pump pressure rise and flow rate, as well as by the direct observation of small bubbles in the flowmeter window. The test was performed at five different operating points and at two different temperatures (0° and 28°C).

Under the worst operating and temperature conditions (i.e. highest speed and lowest temperature), the freon-114-operated CPA required a minimum pressure differential, between the inlet pressure and the saturation pressure, of about 0.22 bar. This corresponds to a freon sub-cooling of about 6°C, well within the actual 10°C normally adopted in two-phase loops in order to have correct evaporator operation.

Pressure and leakage tests

As noted above, the specification called for full compatibility of the CPA with a wide range of fluids, including ammonia. The proof pressure was therefore defined by the worst-case Maximum Operating Pressure (MOP), i.e. the ammonia vapour pressure at 40°C (15 bar). The allowed leak rates were also fixed based on the safety rules connected with the use of ammonia.

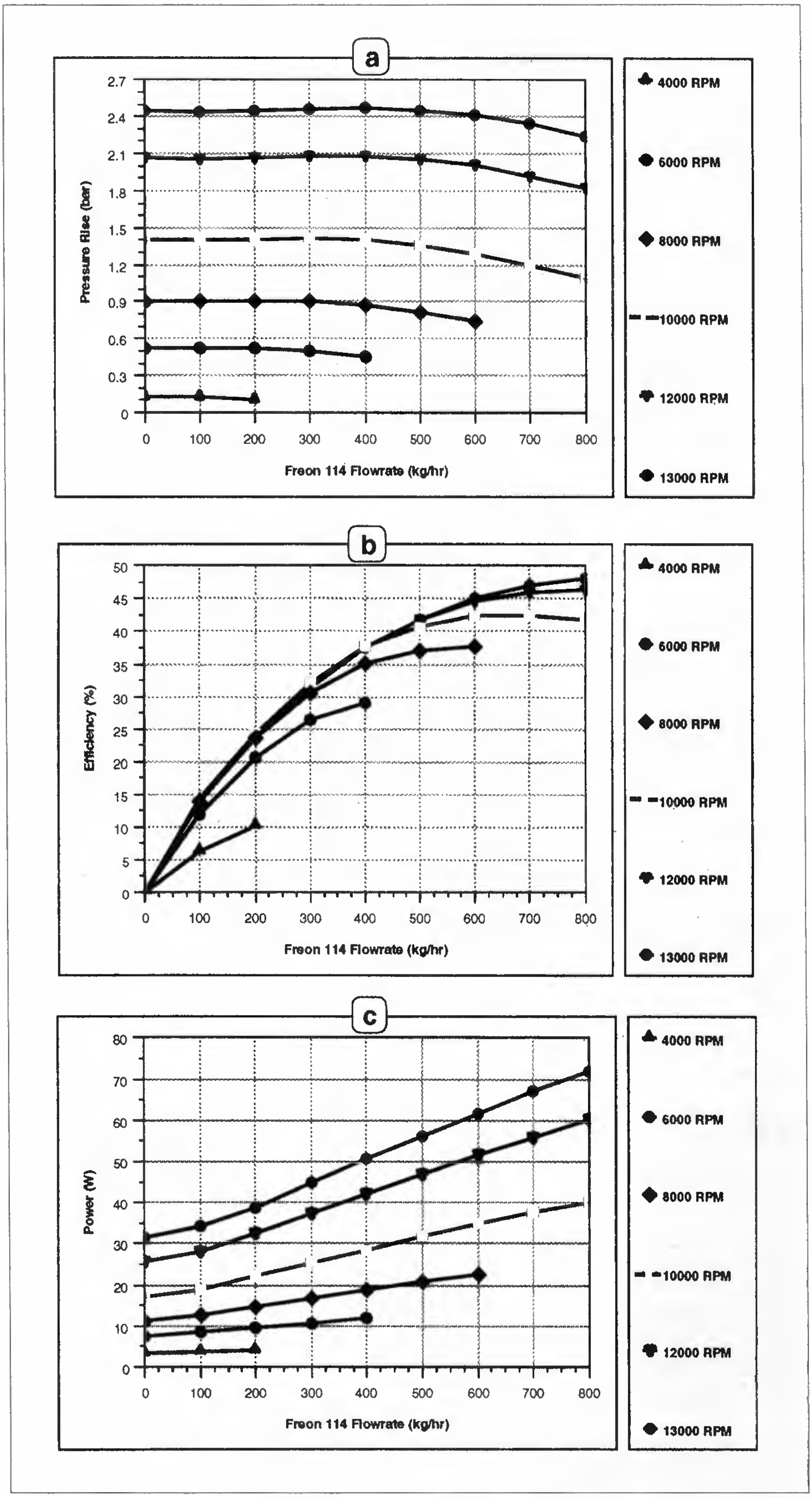

Figures 9a—c

The proof pressure test and the leakage-rate tests, both from the fluid side and from the air side (reverse), were successfully completed at BOA, a Swiss firm producing advanced-technology pressurised components.

A development model of the CPA rotor assembly also underwent a burst test. The measured burst pressure was 142 bar. As the required burst pressure, including the safety factor, was 30 bar, an interesting design possibility might be to reduce the thickness of the pressure container, i.e. the sleeve separating the fluid from the motor stator.

As the eddy-current losses induced in the sleeve by the magnetic field are one of the major contributors to the overall losses, a reduction in the sleeve thickness can increase the pump unit's efficiency. A test on a development model has demonstrated that reducing the thickness from 0.145 to 0.10 mm can provide a gain in efficiency of about 60% at 100 kg/h, and about 35% at 500 kg/h.

This result should be taken into consideration when specifying the MOP of a fluid loop. Unnecessarily high values in fact not only increase the system mass (the thickness of a fluid component depends linearly on the pressure), but can definitely reduce system performance.

Microgravity disturbances test

One of the worst problems for rotating machinery, and hence for the equipment used in fluid loops, lies in the disturbance forces induced at structural interfaces. For the CPA, the maximum allowable disturbance was 0.01 N in the frequency range 0–500 Hz.

An extensive series of tests was performed at DASA-ERNO[2] to verify the dynamic behaviour of CPA-1 (Fig. 10). Those tests included:

- complete field mapping at ambient conditions
- steady-state runs, i.e. CPA running at a specific speed and delivering a fixed flow rate
- transient runs, including switch-on/off, abrupt speed changes, or fixed-rate transitions between two different speeds.

During the steady-state runs, the broadband disturbance level was always below the requirement. The latter was, however, exceeded at specific frequencies directly related to the rotation speed and its higher-order harmonics. Those peaks are due to the residual imbalance of the rotor assembly and it will be very difficult to eliminate them since the best possible balancing grade (G 0.4) was used to balance the CPA rotor assembly. It is worth mentioning that the problematic peaks (examples in Fig. 11) occur at frequencies higher than 100 Hz, which means that active damping can be used to reduce the disturbance force to the required levels.

The dynamic runs demonstrated that abrupt changes – switching on/off or sudden changes from a low speed to a high speed – will cause disturbances much higher than the specified value (up to 1 N for a duration of about 2 s). The disturbances are negligible, however, if the speed rate-of-change can be maintained at levels lower than 500 rpm/s. Thus, during gravity-sensitive operating phases, switching the pump

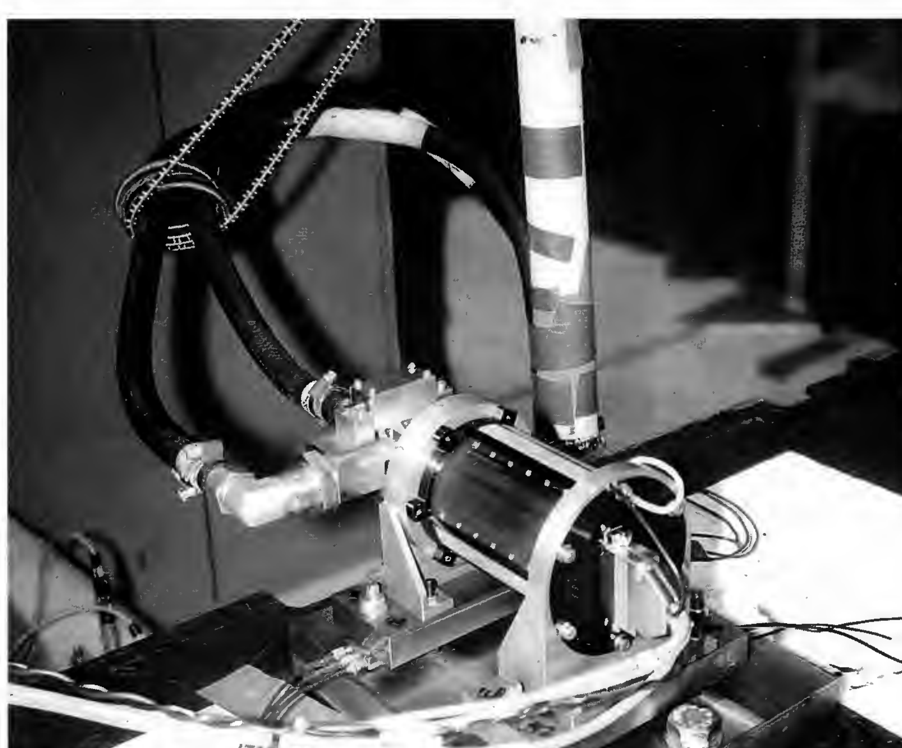

Figure 10

Figure 11

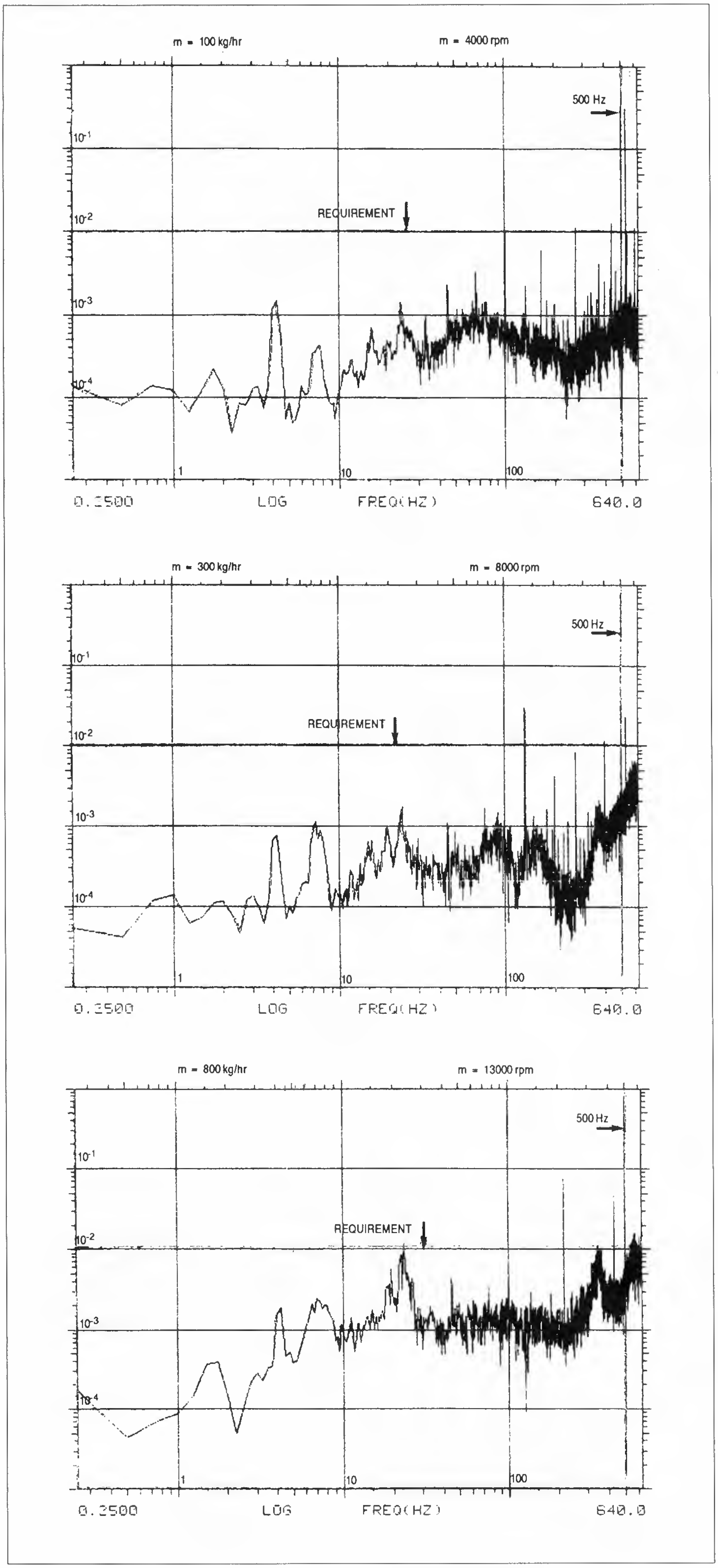
m = 100 kg/hr
m = 4000 rpm
500 Hz
REQUIREMENT
0.2500
LOG
FREQ(HZ)
640.0
m = 300 kg/hr
m = 8000 rpm
500 Hz
REQUIREMENT
0.2500
LOG
FREQ(HZ)
640.0
m = 800 kg/hr
m = 13000 rpm
500 Hz
REQUIREMENT
0.2500
LOG
FREQ(HZ)
640.0

on and off should be avoided and any speed variations needed must be performed by applying well-defined control laws.

Environmental tests (boxes with white text in Fig. 8)

These were the most critical tests as:

- the test levels were defined taking the worst envelope of the conditions met on various spacecraft
- the specification called for CPA operation during every test, including vibration tests.

Vibrations

The structural verification was performed on the 7-ton shaker of ESTEC's Test Services Division (NL). The test specification called for quasi-static, sinusoidal and random tests, at the levels shown in Table 2. The values used during the actual tests are also shown in the same table. The test item included the hydro-mechanical parts of the CPA, but not the ECU (replaced by a suitable mass dummy), placed a short distance away to be able to drive the pump. The CPA was operating at the nominal design point during every vibration test.

The actual test conditions deviated slightly from the requirements in that:

- The quasi-static level on the x- and y-axes was lower than required, as the facility used did not allow 35 g's to be applied in these directions.
- The sine tests were not performed. This decision was taken after conducting resonance searches for every axis. In fact, it was found that the CPA's first resonance frequency was well above 100 Hz, and thus the quasi-static test was adequate to characterise the assembly's dynamic behaviour in the low frequency range of interest.

During the load application, the power needed to achieve the defined performance was slightly higher (less than 10%) than the 'normal' value. This was due to the fact that the vibration caused a displacement of the motor's magnetic field, to which the control system reacts by increasing the current, and thus the absorbed power. Moreover, given the very close tolerances in the rotor assembly, it is possible that the contact area between the bearing and the shaft increases, thereby increasing the friction losses. This effect is fully reversible, i.e. as soon as the load is removed all the parameters return to their 'normal' values. In fact, performance verification tests run before and after every run did not show any significant variations.

Thermal tests

The thermal-vacuum/thermal-cycling tests were all performed in the vacuum chamber of ESTEC's Mechanical Systems Laboratory. They included many verifications, as shown in Table 3. Of particular interest were the no-flow and the freon temperature-cycling tests.

During the no-flow test, the CPA was run for 5 min in vacuum at the design point, without any flow passing through it. The performance parameter during the test did not change and the temperatures at various locations were monitored with dedicated thermocouples and with the two CPA internal sensors. The maximum temperature increase was measured at the inlet of the pump, at a point in thermal contact with the rotor assembly, and was less than 7°C.

Eight freon temperature-cycling tests were run between −30 and +30°C, with the environment at 20°C, in vacuum. No hysteresis was noted. In other words, at every cycle, once the temperatures had been stabilised, the performance characteristics were the same as in the previous cycle.

The objectives of every test were successfully achieved. In particular:

- The Electronic Control Unit (ECU) was subjected to all the tests without showing any failure or degradation in performance, even though it was not required to be compliant with these conditions.
- No particular signs of outgassing or, worse, leakage under the extreme pressures and/or temperatures were detected.
- All the performance tests run before and after each individual phase gave results that were consistent to within a few percent.

Table 2. Vibration-test synopsis

Type of test	Axis	Frequency (Hz)	Required level	Sweep rate (oct/min)	Test level	Notes	Duration
Resonance search	All	5–2000	0.5 g (0-peak)	2	0.5 g (0-peak)		n.a.
Sinus:	All						
Intermediate		5–19.3	±5 mm				
		19.3–60	±7 g		Not	See text	
		60–100	±3 g	2	performed		n.a.
Full level		5–19.3	±10 mm				
		19.3–60	±15 g				
		60–100	±6 g				
Quasi-static:							
Intermediate	x, y	40	16 g		16 g		
	z	40	16 g	n.a.	16 g		15 s
Full level	x, y	40	35 g		24 g	See text	per axis
	z	40	35 g		35 g		
Random	All	20–100	3 dB/oct		3 dB/oct		2 min
		100–400	0.22 g^2/Hz	n.a.	0.22 g^2/Hz	14.79 grms	per axis
		400–2000	−3 dB/oct		−3 dB/oct		

Table 3. Thermal test synopsis

Test	Runs	Pressure	Test level	Number of cycles	Duration
	(a) Field Mapping		T_{fluid}=0, 14, 28°C	n.a.	n.a.
	(b) Environment		−30 to 40°C	1	n.a.
Thermal Cycling #1		Vacuum			
	(c) No-Flow Run		at 40°C, design point	n.a.	5 min
	(d) Start-up		T_{env}=−30 and +40°C T_{fluid}=0 and 30°C	n.a.	n.a.
	(a) Running at various design point		T_{fluid}=0°C T_{fluid}=28°C	n.a.	12+12 h 12+12 h
Thermal Cycling #2	(b) Fluid temperature cycles	Vacuum	T=−30 to +30°C	8	n.a.
	(c) Performance under worst power input conditions		T_{fluid}=−30 and +30°C Voltage = 120 ±3% VDC	n.a.	n.a.
Pressure Cycling	Environmental pressure cycles	Vacuum to ambient	P_{env} = 10^{-2} mbar to ambient	8	n.a.

Performance with other fluids

After the 'official' test programme described above, some performance tests were run using water instead of freon in order to check the applicability of the similarity theory for scaling the CPA's performance from one fluid to another and to have an experimental confirmation of the design procedures.

The physical properties that have the greatest influence on the pump's performance are the fluid's density and viscosity. At 20°C, the ratio between the densities of water and freon is about 2/3, and the ratio of their viscosities is about 3. Fixing the operating conditions, i.e. the pump speed, the flow rate and the inlet pressure, the lower density should induce a reduction in the outlet pressure (i.e. in the hydraulic power), while the higher viscosity should produce an increase in the fluid friction losses. The two factors together should therefore cause a decrease in efficiency.

Two test series were performed, the first running CPA-2 and the second running a system consisting of CPA-2 and CPA-3, connected in series. Figures 12a–c and 13a–c show the pressure rise, the global efficiency and the absorbed power as a function of the water flow rate for the two series of tests. Comparison of these plots with those for the freon tests (Figs. 9a–c) shows that the scaling theory is indeed applicable. In fact, at a particular speed and flow rate, both the pressure rise and the efficiency measured on the water-operated CPA-2 are lower than the corresponding values measured on the freon-operated CPA-1. Still, the efficiency of CPA-2 is quite good, being between 10% and 35% in the range 100–600 kg/h, despite the fact that this impeller was not optimised for water.

Figure 12a–c

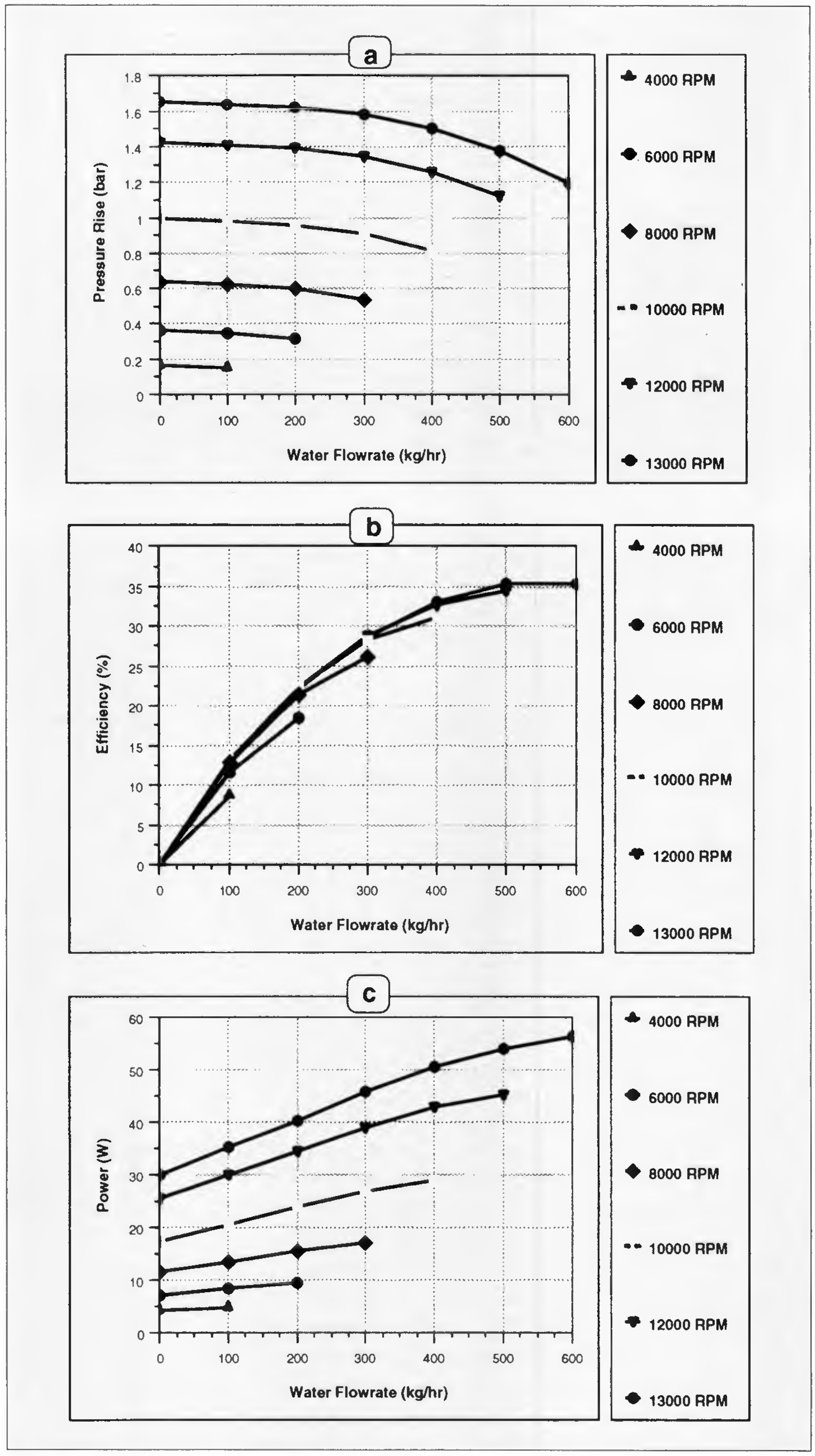

An important lesson learned during this programme was that the critical element in the design of low-flow-rate (50 – 1500 kg/h), low-pressure-rise (under 4×10^5 Pa) pump units is not the dimensioning of the impeller, which can be done with the usual procedures, but the choice of configuration for the overall pump assembly. Thus, adapting the actual design to other operating conditions, or to the other fluids normally used in thermal-control-system loops, will merely require a different dimensioning of

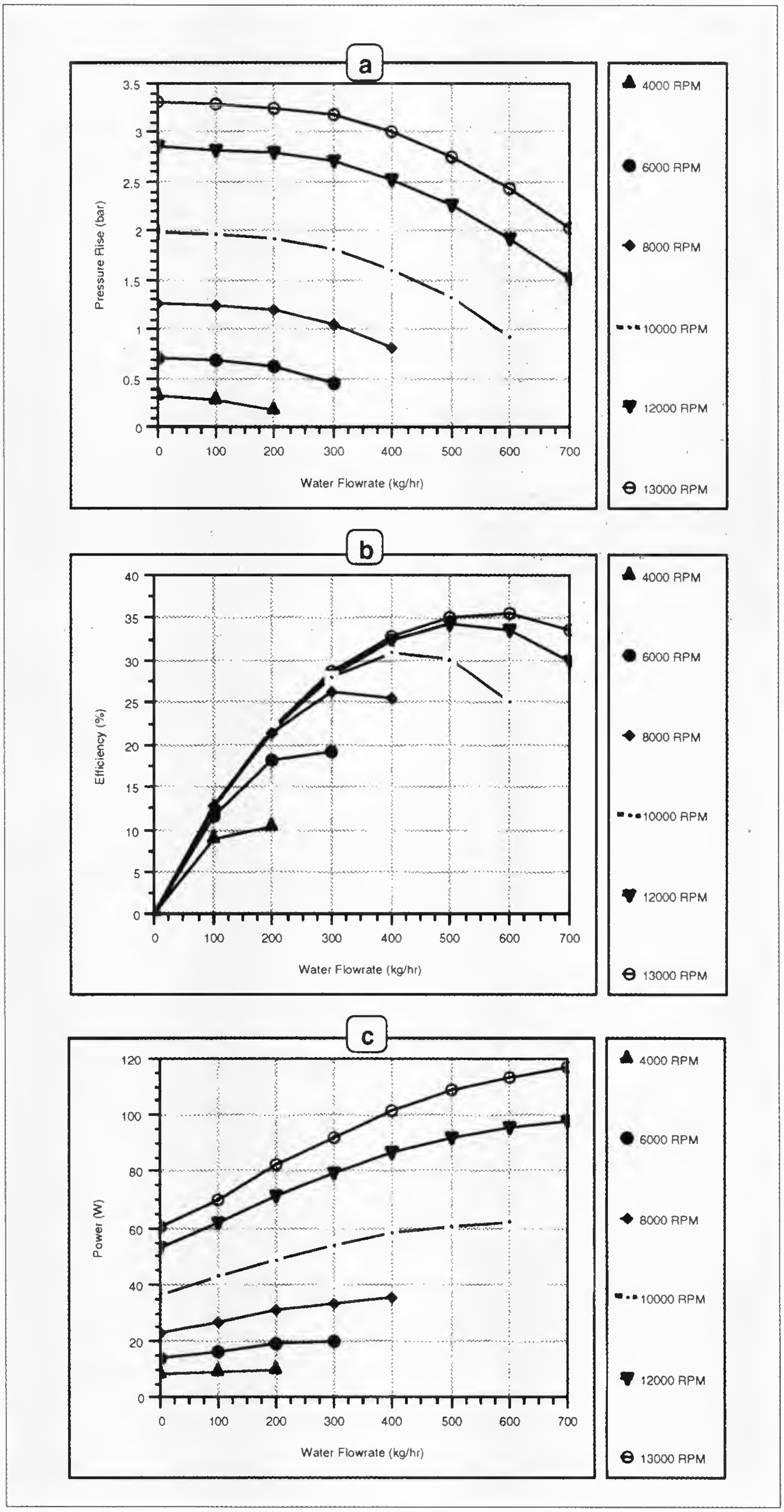

Figure 13a—c

the impeller. Therefore, unless the specified requirements are very far away from the existing ones, similar performances can be expected.

The series configuration including identical pump assemblies and bypass valves (Fig. 14) could be attractive in terms of system reliability and/or operational flexibility. In fact, during normal operations, the pressure rise can be adapted to the load, using a single pump for low loads and the two pumps together for higher loads. In the event of a pump failing, that pump can be isolated and the system can still function, albeit in a degraded mode.

Figure 14

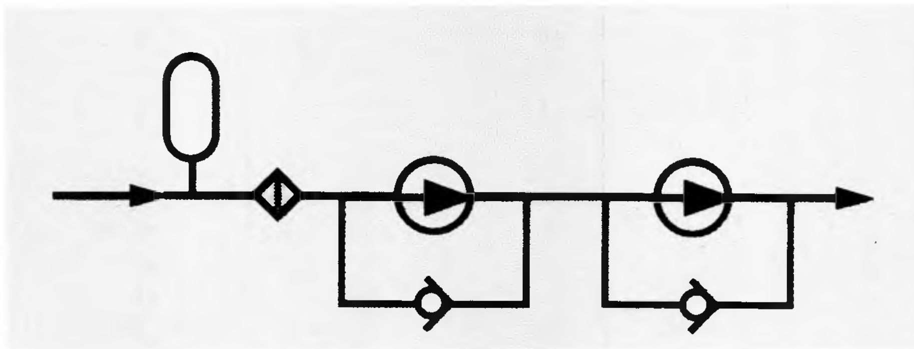

Conclusions

The main features of the Controlled Pump Assembly (CPA) that has been developed under an ESA/ESTEC Technology Research Programme contract[3] are its compactness, lightness and high efficiency, together with its compatibility with different operating fluids, including water, freons and ammonia. The development model has been optimised for use with freon in the low pressure-rise (up to 2.4×10^5 Pa) and flow-rate (less than 800 kg/h) range. An extensive test campaign has verified the performance and flight-worthiness of the design.

The successful completion of this programme led to the definition of further development efforts, and more specifically to:

- the development of a even smaller pump unit for application in ammonia two-phase loops (ACPA)
- the life-testing of two further CPA models, which are showing no sign of degradation after six months of operation
- the upgrading of the ECU design to engineering-model level.

At the completion of this coordinated programme, a range of pump units will be available for use in both single- and two-phase cooling loops onboard the demanding spacecraft of the future.

Acknowledgements

The hardware described in this article and the article itself have benefitted from the work performed by Reusser AG and Etel SA during the course of the Technology Research Programme contract. Special thanks are due to the personnel of ESTEC's Mechanical Systems Laboratory and Testing Division and of DASA-ERNO's Microgravity Test Section, for their valuable contributions during the test campaign.

References

1. Two-Phase Heat Transport Systems Critical Components, ESTEC Contract 6592/86/NL/FG.
2. DASA-ERNO, Micro-gravity Compatibility Test Report on the CPA, TN-ROT213-25/9.
3. Reusser AG, CPA Final Report, ESA Contractor Report CR(P)-3728.

Manuscript received 25 January 1994

ESA Publications and Publications by ESA Staff in the External Literature

The following publications have been recorded by ESA Publications Division since the last issue of the Journal.

Entries are grouped according to Subject Categories: where a publication could be listed under several categories, only the principal category is used.

Where an entry relates to a publication by ESA, the ESA reference of the document is given at item 3 and for those ESA publications available on sale, item 4 shows either the price code for a printed copy or 'AVAIL MF' if only microfiche (or photocopy) versions have been made available. Information on the procurement and costs of these publications can be found inside the back cover of this Journal. Only complete ESA publications can be supplied (not reprints of individual papers). External publications cannot be supplied by ESA but in these cases item 3 gives sufficient information for retrieval via libraries or bookshops.

The entries presented here are archived for use in the annual ESA Catalogue of Publications (available free from ESA Publications Division). If an author/editor considers that an entry requires amendment, he should notify ESA Publications Division, quoting the accession number of the entry, i.e. the first five digits in the heading of the entry.

Astronautics

Astronautics (General) 12

* 940306E CRP 3764 12
1 EURECA - MICROMETEOROID AND DEBRIS POST FLIGHT INVESTIGATION FINAL REPORT (APRIL 1994)
2 UNISPACE, U.K. (CONTR NO. 10335/93/NL/JG)
3 ESA CR(P)-3764 // 15 PP
4 AVAIL MF AND HARD COPY (ESA PRICE CODE E0)

Astrodynamics 13

* 940063E CRP 3742 13
1 STUDY OF POINCARE MAPS FOR ORBITS NEAR LAGRANGIAN POINTS - FINAL REPORT (NOVEMBER 1993)
2 FUNDACIO BOSCH I GIMPERA, SPAIN (CONTR NO. 9711/91/D/IM(SC))
3 ESA CR(P)-3742 // 276 PP
4 AVAILABLE MF & HARD COPY (ESA PRICE CODE E3)

* 940319E E B 0078 13
1 ESA'S PRECISE ORBIT DETERMINATION FACILITY (MAY 1994)
2 DOW J.M. ET AL.
3 ESA BULLETIN NO. 78 // PP 40-49
4 SEE ESA BULLETIN NO. 78, INDEXED UNDER 99
5 -

Ground Support Systems and Facilities (Space) 14

* 940069E CRP 3744 14
1 IGS-TB MANAGEMENT FACILITY - FINAL REPORT AND EXECUTIVE SUMMARY (JANUARY 1994)
2 ALCATEL, FRANCE (CONTR NO. 10038/92/D/DK)
3 ESA CR(P)-3744 // 38 PP AND 11 PP
4 AVAIL MF & HARD COPY (ESA PRICE CODE E0, E0)

Launch Vehicles and Space Vehicles 15

* 940071E CRP 3747 15
1 STAMP - STUDY ON TECHNOLOGY OF AEROBRAKING FOR MARS PENETRATORS FINAL REPORT AND EXECUTIVE SUMMARY (SEPTEMBER 1993)
2 DASSAULT AVIATION, FRANCE (CONTR NO. 9519/91/NL/FG(SC))
3 ESA CR(P)-3747 // 59 PP AND 8 PP
4 AVAIL MF & HARD COPY (ESA PRICE CODE E1, E0)

* 940300E CRP 3757 15
1 STUDY ON THERMAL PROTECTION FOR ADVANCED LAUNCHERS - FINAL REPORT (DECEMBER 1993)
2 DEUTSCHE AEROSPACE, GERMANY (CONTR NO. 9650/91/NL/FG)
3 ESA CR(P)-3757 // 91 PP
4 AVAIL MF AND HARD COPY (ESA PRICE CODE E1)

* 940308E CRP 3767 15
1 A PRELIMINARY FEASIBILITY STUDY OF THE SPACECAB LOW-COST SPACE PLANE AND OF THE SPACECAB DEMONSTRATOR - FINAL REPORT (APRIL 1994)
2 BSL, U.K. (CONTR NO. 10411/93/F/TB)
3 ESA CR(P)-3767 // 44 PP
4 AVAIL MF AND HARD COPY (ESA PRICE CODE E0)

* 940318E E B 0078 15
1 SATELLITE SERVICING IN GEO BY A ROBOTIC SERVICE VEHICLE (MAY 1994)
2 DE PEUTER W. ET AL.
3 ESA BULLETIN NO. 78 // PP 33-39
4 SEE ESA BULLETIN NO. 78, INDEXED UNDER 99
5 -

Spacecraft Communications, Command and Tracking 17

* 940062E CRP 3743 17
1 SOFTWARE TOOL FOR INTERPLANETARY NAVIGATION - FINAL REPORT (DECEMBER 1993)
2 GMV, SPAIN (CONTR NO. 9715/91/D/IM)
3 ESA CR(P)-3743 // 114 PP
4 AVAILABLE MF & HARD COPY (ESA PRICE CODE E2)

* 940065E CRP 3740 17
1 DRAG-FREE SATELLITE CONTROL STUDY - FINAL REPORT AND EXECUTIVE SUMMARY (DECEMBER 1993)
2 MATRA MARCONI SPACE, FRANCE (CONTR NO. 9558/91/NL/JG(SC))
3 ESA CR(P)-3740 // 89 PP AND 12 PP
4 AVAILABLE MF & HARD COPY (ESA PRICE CODE E1, E0)

* 940067E CRP 3738 17
1 AUTONOMOUS AND ADVANCED NAVIGATION TECHNIQUES - FINAL REPORT AND EXECUTIVE SUMMARY (APRIL 1993)
2 MATRA MARCONI SPACE, FRANCE (CONTR NO. 8808/90/NL/PM(SC))
3 ESA CR(P)-3738 // 367 PP AND 67 PP
4 AVAILABLE MF & HARD COPY (ESA PRICE CODE E3, E1)

* 940298E CRP 3755 17
1 AUTONOMOUS AND ADVANCED NAVIGATION TECHNIQUES: "PROBE CONCEPT ANALYSIS" - FINAL REPORT AND EXECUTIVE SUMMARY (OCTOBER 1993)
2 MMS, FRANCE (CONTR NO. 8808/90/NL/PM(SC))
3 ESA CR(P)-3755 // 58 PP AND 16 PP
4 AVAIL MF AND HARD COPY (ESA PRICE CODE E1, E0)

* 940320E E B 0078 17
1 USING ADVANCED GRAPHIC MMI TECHNIQUES FOR TELEMETRY MONITORING (MAY 1994)
2 DI GIROLAMO G. & PECCIA N.
3 ESA BULLETIN NO. 78 // PP 51-59
4 SEE ESA BULLETIN NO. 78, INDEXED UNDER 99
5 -

* 940331E X J 1801 17
1 CCSDS PROTOCOL FOR ADVANCED ORBITING SYSTEMS, NETWORK AND DATA LINKS: ANALYSIS OF ASYNCHRONOUS TRAFFIC SERVICES (MARCH 1994)
2 VANGHI V.
3 ESA JOURNAL VOL. 18, NO. 1 // PP 73-86
4 SEE ESA JOURNAL, INDEXED UNDER 99
5 THE CONSULTATIVE COMMITTEE FOR SPACE DATA SYSTEMS (CCSDS) HAS RECENTLY DEVELOPED A NUMBER OF STANDARDS FOR DATA HANDLING AND TRANSMISSION TO BE APPLIED IN FORTHCOMING GENERATIONS OF SPACE DATA NETWORKS. IN THIS CONTEXT, THE CCSDS HAS WORKED TOWARD THE DEFINITION OF A DIGITAL SATELLITE NETWORK OFFERING A WIDE VARIETY OF SERVICES. THIS PAPER ANALYSES THE PERFORMANCE OF THE ASYNCHRONOUS SERVICES ACROSS THE SPACE LINK SUBNETWORK. A MODEL FOR THE ASYNCHRONOUS TRAFFIC IS DEVELOPED, GENERATING THE SOLUTION FOR PACKET AVERAGE DELAY, FRAME-OCCUPANCY DISTRIBUTION AND FRAME-LOSS PROBABILITY AT THE TRANSMITTER SITE. THE RESULTS ARE ALSO USEFUL IN PROVIDING AN UPPER AND LOWER BOUND TO THE SYSTEM PERFORMANCE ATTAINABLE UNDER A VARIETY OF TRAFFIC CONFIGURATIONS. MOREOVER, A SETTING OF IMPLEMENTATION-DEPENDANT PARAMETERS, SUCH AS FRAME COMPLETION TIMEOUT PERIOD AND FRAME SIZE, IS DISCUSSED IN TERMS OF ITS INFLUENCE ON SYSTEM PERFORMANCES.

Spacecraft Design, Testing and Performance 18

* 940048E STM 248 18
1 THE EXOSAT OPERATIONAL EXPERIENCE (JUNE 1993)
2 PARKES A.G. ET AL. KALDEICH B. (ED.)
3 ESA STM-248 // 88 PAGES
4 ESA PRICE CODE: E1
5 EXOSAT, A 'FIRST' FOR ESA IN MANY WAYS, WAS LAUNCHED ON 26 MAY 1983 AND RE-ENTERED THE EARTH'S ATMOSPHERE ON 6TH MAY 1986, EXCEEDING ITS PLANNED LIFETIME OF TWO YEARS. THIS REPORT REVIEWS CRITICALLY THE EXOSAT SYSTEM AND HIGHLIGHTS NOT ONLY THE SUCCESS OF THE MISSION, BUT ALSO THOSE AREAS WHICH GAVE RISE TO OPERATIONAL PROBLEMS, AND THE LESSONS TO BE LEARNED.

* 940053E CRP 3730 18
1 DESIGN RULES FOR RADIATION TOLERANCE - FINAL REPORT (JULY 1993)
2 MATRA MARCONI, FRANCE (CONTR NO. 9291/90)
3 ESA CR(P)-3730 // 163 PP
4 AVAILABLE MF & HARD COPY (ESA PRICE CODE E2)

* 940072E CRX 3748 18
1 STUDY OF EXPERT TOOLS FOR FLIGHT OPERATIONS PLANS: FOPSET FINAL REPORT (DECEMBER 1993)
2 VEGA SPACE SYSTEMS, UK (CONTR NO. 9534/91/D/IM)
3 ESA CR(X)-3748 // 40 PP
4 AVAIL MF & HARD COPY (ESA PRICE CODE E0)

* 940304E CRP 3762 18
1 MATING/DEMATING MECHANISM STUDY - EXECUTIVE SUMMARY (NOVEMBER 1993)
2 SENER, SPAIN (CONTR NO. 10155/92/NL/JG(SC))
3 ESA CR(P)-3762 // 74 PP
4 AVAIL MF AND HARD COPY (ESA PRICE CODE E1)

* 940312E CRP 3766 18
1 ADAPTIVE CONTROL FOR AOCS/GNC - FINAL REPORT AND EXECUTIVE SUMMARY (JANUARY 1994)
2 BAE, U.K. (CONTR NO. 9936/92/NL/FM(SC))
3 ESA CR(P)-3766 // 628 PP AND 103 PP
4 AVAIL MF AND HARD COPY (ESA PRICE CODE E4, E2)

Spacecraft Instrumentation 19

* 940295E CRX 3752 19
1 DEVELOPMENT OF HW AND SW FOR A RAD HARD MICROCOMPUTER - FINAL REPORT (OCTOBER 1992)
2 LABEN, ITALY (CONTR NO. 8044/88/NL/SF)
3 ESA CR(X)-3752 // 55 PP
4 AVAIL MF AND HARD COPY (ESA PRICE CODE E1)

* 940310E CRP 3751 19
1 FTOBC CARD CRATE - FINAL REPORT (JANUARY 1993)
2 SAAB ERICSSON SPACE, SWEDEN (CONTR NO. 7150/87/NL/PP)
3 ESA CR(P)-3751 // 78 PP
4 AVAIL MF AND HARD COPY (ESA PRICE CODE E1)

Spacecraft Propulsion and Power 20

* 940051E CRP 3728 20
1 CPA - CONTROLLED PUMP ASSEMBLY - FINAL REPORT (JULY 1993)
2 REUSSER, GERMANY (CONTR NO. 9039/90/NL/FG)
3 ESA CR(P)-3728 // 77 PP
4 AVAILABLE MF & HARD COPY (ESA PRICE CODE E1)

* 940326E E J 1801 20
1 SPACE POWER ELECTRONICS - DESIGN DRIVERS (MARCH 1994)
2 O'SULLIVAN D.
3 ESA JOURNAL VOL. 18, NO. 1 // PP 1-23
4 SEE ESA JOURNAL, INDEXED UNDER 99
5 THIS PAPER ADDRESSES THE WIDE RANGING CONSTRAINTS AND REQUIREMENTS THAT ARE PART OF THE OVERALL DESIGN CRITERIA FOR THE OPTIMAL DESIGN OF SPACECRAFT POWER SYSTEMS AND EQUIPMENT. TOPICS COVERED INCLUDE OPERATIONAL RELIABILITY, MODULARITY, SPACE ENVIRONMENT, PAYLOAD AND ORBIT REQUIREMENTS, SYSTEM AND EQUIPMENT TOPOLOGIES AND SPECIAL DESIGN TECHNIQUES EMPLOYED IN SPACECRAFT POWER-SYSTEM DESIGNS. IN ORDER TO UNDERSTAND THE KEY DIFFERENCES BETWEEN SPACE AND INDUSTRIAL POWER ELECTRONICS, IT IS ESSENTIAL THAT THOSE FEATURES THAT ARE UNIQUE TO THE SPACE ENVIRONMENT BE CLEARLY IDENTIFIED. IN THE FIRST PART OF THIS PAPER THOSE KEY DRIVERS THAT AFFECT THE CHOICE OF DESIGN APPROACH ARE DESCRIBED AND THE REMAINDER OF THE PAPER ILLUSTRATES HOW THESE DRIVERS AFFECT THE CHOICE OF REGULATOR TOPOLOGIES AND THE OVERALL APPROACH TO POWER-SYSTEM DESIGN.

Material Sciences (General) 21

* 940327E X J 1801 21
1 BACTERIORHODOPSIN CRYSTAL GROWTH UNDER MICROGRAVITY - RESULTS OF IML-1 AND SPACEHAB-1 EXPERIMENTS (MARCH 1994)
2 WAGNER G.
3 ESA JOURNAL VOL. 18, NO. 1 // PP 25-32
4 SEE ESA JOURNAL, INDEXED UNDER 99
5 THE RESULTS OF TWO CRYSTAL-GROWTH EXPERIMENTS IN MICROGRAVITY WITH THE MEMBRANE PROTEIN BACTERIORHODOPSIN ARE REPORTED, NAMELY THE IML-1 EXPERIMENT IN THE ADVANCED CRYOSTAT WHICH RESULTED IN A SIGNIFICANT IMPROVEMENT IN THE COMPACT CRYSTAL MORPHOLOGY OF THE NEEDLES, AND THE SPACEHAB-1 EXPERIMENT IN THE ADVANCED PROTEIN CRYSTALLISATION FACILITY WHICH EXTENDED THE IML-1 RESULTS WITH IMPROVED MORPHOLOGY OF THE TRICLINIC NEEDLES. THE ENHANCED DIFFRACTIONAL POWER OF THESE BACTERIORHODOPSIN CRYSTALS GROWN IN MICROGRAVITY HAS EXTENDED THE HITHERTO 8 ANGSTROM RESOLUTION LIMIT BY 2 ANGSTROM.

Chemistry and Materials

Nonmetallic Materials 27

* 940296E CRX 3753 27
1 FINAL REPORT ON THE RADIATION HARDENING STUDY OF DISPLACEMENT DAMAGE IN SILICON - FINAL REPORT AND EXECUTIVE SUMMARY (FEBRUARY 1994)
2 IMEC, BELGIUM (CONTR NO. 8615/90/NL/PM(SC))
3 ESA CR(X)-3753 // 120 PP AND 11 PP
4 AVAIL MF AND HARD COPY (ESA PRICE CODE E2, E0)

Propellants and Fuels 28

* 940329E X J 1801 28
1 LIQUID GAUGING IN SPACE: THE G-22 EXPERIMENT (MARCH 1994)
2 MONTI R. & BERRY W.
3 ESA JOURNAL VOL. 18, NO. 1 // PP 51-61
4 SEE ESA JOURNAL, INDEXED UNDER 99
5 AS THE LIFE OF A SATELLITE IS TERMINATED WHEN ITS ONBOARD PROPELLANTS ARE DEPLETED, ACCURATE KNOWLEDGE OF THOSE REMAINING PROPELLANTS THROUGHOUT A MISSION IS ESSENTIAL. WHEREAS THE MEASUREMENT OF PROPELLANT CONTENTS ("LIQUID GAUGING") IS A TRIVIAL MATTER ON THE GROUND, IT IS A MOST DIFFICULT TASK IN SPACE BECAUSE OF THE MICROGRAVITY CONDITIONS THAT PREVAIL. MOTIVATED BY THE NEED TO DEVELOP AN ACCURATE METHOD OF LIQUID GAUGING IN SPACE, ESA SPONSORED THE DEVELOPMENT AT TECHNOSYSTEM (ITALY) OF TWO THERMODYNAMIC METHODS OF LIQUID GAUGING: THE PERIODIC VOLUME STIMULUS METHOD (PVSM) AND THE FOREIGN MASS INJECTION METHOD (FMIM). THESE METHODS WERE SUBSEQUENTLY TESTED IN SPACE AS THE G-22 GET-AWAY-SPECIAL (GAS) EXPERIMENT ABOARD SHUTTLE FLIGHT STS-57 IN JUNE 1993. THE SPACE TEST WAS COMPLETELY SUCCESSFUL AND SHOWED GOOD CORRELATION WITH THE RESULTS OF GROUND EXPERIMENTS.THE PVSM PROVED TO BE A PRECISE METHOD WITH GOOD REPEATABILITY; THE FILL-FACTOR ERROR (DIFFERENCE BETWEEN ACTUAL AND MEASURED CONTENTS) WAS LESS THAN 0.6%. THE FMIM PROVED TO BE LESS ACCURATE, DUE TO TEMPERATURE EFFECTS AND PRESSURE-TRANSDUCER INACCURACIES. IMPROVEMENTS TO THE FMIM HAVE SINCE BEEN EVALUATED THEORETICALLY.

Materials Processing 29

* 940058E CRP 3735 29
1 AUTOMATED HIGH TEMPERATURE MATERIALS PROCESSING LABORATORY (HTMPL) FOR COLUMBUS - FINAL REPORT (MARCH 1994)
2 DORNIER GMBH, GERMANY (CONTR NO. 9950/92/NL/JSC)
3 ESA CR(P)-3735 // 15 PP
4 AVAILABLE MF & HARD COPY (ESA PRICE CODE E0)

* 940301E CRP 3758 29
1 INTEGRATED PAYLOAD AUTOMATION - IPA - EXECUTIVE SUMMARY (FEBRUARY 1993)
2 TECNOSPAZIO, SPAIN (CONTR NO. 9829/92/NL/JC(SC))
3 ESA CR(P)-3758 // 58 PP
4 AVAIL MF AND HARD COPY (ESA PRICE CODE E1)

* 940302E CRP 3759 29
1 INTEGRATED PAYLOAD AUTOMATION - IPA - FINAL REPORT (SEPTEMBER 1993)
2 DORNIER, GERMANY (CONTR NO. 9830/92/NL/JG(SC))
3 ESA CR(P)-3759 // 50 PP
4 AVAIL MF AND HARD COPY (ESA PRICE CODE E0)

Engineering

Communications 32

* 940297E CRP 3754 32
1 KU-BAND DUAL POLARISED ARRAY ELEMENT - EXECUTIVE SUMMARY (OCTOBER 1992)
2 ERSA TECHNOLOGY, U.K. (CONTR NO. 8715/90/NL/GM(SC))
3 ESA CR(P)-3754 // 24 PP
4 AVAIL MF AND HARD COPY (ESA PRICE CODE E0)

* 940309E CRP 3768 32
1 STATUS OF EUROPEAN R&D PROGRAMMES IN SATELLITE COMMUNICATIONS EARTH SEGMENT - FINAL REPORT (DECEMBER 1993)
2 EUROCONSULT, FRANCE (CONTR NO. 9952/92)
3 ESA CR(P)-3768 // 219 PP
4 AVAIL MF AND HARD COPY (ESA PRICE CODE E3)

Electronics and Electrical Engineering 33

* 940054E CRP 3731 33
1 ADVANCED CONVERTER TOPOLOGY ASSESSMENT - FINAL REPORT AND EXCUTIVE SUMMARY (DECEMBER 1993)
2 DEUTSCHE AEROSPACE, GERMANY (CONTR NO. 9513/91/NL/US(SC))
3 ESA CR(P)-3731 // 114 PP AND 10 PP
4 AVAILABLE MF & HARD COPY (ESA PRICE CODE E2, E0)

* 940056E CRP 3733 33
1 HYBRID CONNECTOR - FINAL REPORT (OCTOBER 1993)
2 FRAMATOME CONNECTORS, FRANCE (CONTR NO. 9838/92/NL/PP)
3 ESA CR(P)-3733 // 82 PP
4 AVAILABLE MF & HARD COPY (ESA PRICE CODE E1)

* 940057E CRP 3734 33
1 ARC - TRACKING TEST OF WIRES - FINAL REPORT (JANUARY 1994)
2 DEUTSCHE AEROSPACE, GERMANY (CONTR NO. 9891/92)
3 ESA CR(P)-3734 // 114 PP
4 AVAILABLE MF & HARD COPY (ESA PRICE CODE E2)

* 940073E CRP 3749 33
1 TEST STRUCTURES FOR ASIC TECHNOLOGY ASSESSMENT - FINAL REPORT (OCTOBER 1993)
2 CSEM, SWITZERLAND (CONTR NO. 9207/90/NL/PB(SC))
3 ESA CR(P)-3749 // 45 PP
4 AVAIL MF & HARD COPY (ESA PRICE CODE E0)

* 940074E CRP 3750 33
1 APPLICATION DE NOUVELLES TECHNOLOGIES D'ELECTRODES POUR DES ACCUMULATEURS NICKEL CADMIUM A HAUTE ENERGIE MASSIQUE - TRAVAUX HEM PHASE 2 - FINAL REPORT (DECEMBER 1993)
2 CNES, FRANCE (CONTR NO. 9601/91/NL/US(SC))
3 ESA CR(P)-3750 // 25 PP
4 AVAIL MF & HARD COPY (ESA PRICE CODE E0)

* 940307E CRX 3765 33
1 DEVELOPMENT OF A HIGH FREQUENCY DC/DC AUXILIARY CONVERTER - FINAL REPORT AND EXECUTIVE SUMMARY (MAY 1994)
2 UNIVERSITY OF SURREY, U.K. (CONTR NO. 8560/89/NL/JG)
3 ESA CR(X)-3765 // 199 PP AND 8 PP
4 AVAIL MF AND HARD COPY (ESA PRICE CODE E2, E0)

Fluid Mechanics and Heat Transfer 34

* 940061E CRP 3746 34
1 THERMAL CONTROL IN EXTRATERRESTRIAL PLANETARY ENVIRONMENT - FINAL REPORT (DECEMBER 1993)
2 DORNIER, GERMANY (CONTR NO. 9512/91/NL/FG)
3 ESA CR(P)-3746 // 458 PP
4 AVAILABLE MF & HARD COPY (ESA PRICE CODE E4)

Mechanical Engineering 37

* 940047E BR 92 37
1 ESTL - KEEPING SPACE MOVING
2 ROWNTREE R., ANDREWS J., LONGDON N.
3 ESA BR-92 // 16 PP
4 -
5 THE BROCHURE DESCRIBES THE TYPE OF WORK DONE AT THE EUROPEAN SPACE TRIBOLOGY LABORATORY, AND THE DIFFERENT FACILITIES AVAILABLE TO SPACE AND NON-SPACE INDUSTRY.

* 940293E PSS 03-203 37
1 STRUCTURAL MATERIALS HANDBOOK (FEBRUARY 1994)
- VOL 1: POLYMERCOMPOSITES
- VOL 2: NEW ADVANCED MATERIALS
2 STRUCTURAL AND MECHANISMS DEVISION, ESTEC
3 ESA PSS-03-203 // 514 PP AND 492 PP
4 ESA PRICE CODE: E4, E4
5 THE STRUCTURAL MATERIALS HANDBOOK SERVES TO COMBINE THE ESTABLISHED

MATERIALS AND DESIGN INFORMATION ON THE CARBON, GLASS AND ARAMID FIBRE-REINFORCED POLYMER COMPOSITES HAVING EITHER (A) THERMOSETTING RESIN MATRICES OR (B) THERMOPLASTIC MATRICES WITH PROVISIONAL INFORMATION ON THE EMERGING GROUPS OF NEW ADVANCED MATERIALS AND THEIR COMPOSITES. SIGNIFICANT EFFORT HAS BEEN EXPENDED ON THE DEVELOPMENT OF MATERIALS WITH, OR SEEKING, HIGH-STRENGTH, HIGH-STIFFNESS AND/OR DIMESIONAL STABILITY FOR APPLICATIONS IN EUROPEAN SPACE PROJECTS. NEW ADVANCED MATERIALS ALSO OFFER HIGHER TEMPERATURE CAPABILITIES. THE USE OF SUCH MATERIALS AIMS TO CAPITALISE ON THEIR MASS-SAVING PROPERTIES OR THEIR IMPROVED PERFORMANCE WITH RESPECT TO MORE CONVENTIONAL MATERIALS. THIS HANDBOOK REPRESENTS AN EXPANDED VERSION OF ESA PSS-03-1101, WHICH IT SUPERSEDES.

Quality Assurance and Reliability 38

* 940049E PSS 01-746 38
1 GENERAL REQUIREMENTS FOR THREADED FASTENERS (JUNE 1993)
2 PRODUCT ASSURANCE & SAFETY DEPARTMENT, ESTEC
3 ESA PSS-01-746 ISSUE 1 // VIII + 97 PP
4 ESA PRICE CODE: E2
5 THIS DOCUMENT SETS FORTH THE ESSENTIAL REQUIREMENTS THAT MUST BE MET IN THE MANUFACTURE AND CONTROL OF FASTENERS INTENDED FOR USE IN THE FABRICATION OF ESA SPACE SYSTEMS.

* 940064E CRP 3741 38
1 QUALITY ASSURANCE LEVEL 3 STANDARDS - FINAL REPORT (DECEMBER 1993)
2 DEUTSCHE AEROSPACE, GERMANY (CONTR NO. 9696/91/NL/LC(SC))
3 ESA CR(P)-3741 // 862 PP
4 AVAILABLE MF (ESA PRICE CODE E4)

* 940066E CRP 3739 38
1 IMPLEMENTATION OF SA CAPABILITY IN EUROPE - FINAL REPORT AND EXECUTIVE SUMMARY (NOVEMBER 1993)
2 AEROSPATIALE, FRANCE (CONTR NO. 9414/91/NL/LC)
3 ESA CR(P)-3739 // 85 PP AND 12 PP
4 AVAILABLE MF & HARD COPY (ESA PRICE CODE E1, E0)

* 940294E PSS 01-70 38
1 MATERIAL, MECHANICAL PART AND PROCESS SELECTION AND QUALITY CONTROL FOR ESA SPACE SYSTEMS AND ASSOCIATED EQUIPMENT (JANUARY 1994)
2 PRODUCT ASSURANCE & SAFETY DEPARTMENT, ESTEC
3 ESA PSS-01-70 ISSUE 4 // VI + 27 PP
4 ESA PRICE CODE: E0
5 THIS SPECIFICATION ESTABLISHES THE REQUIREMENTS FOR A MATERIAL, MECHANICAL-PART AND PROCESS SELECTION AND CONTROL PROGRAMME FOR SPACE SYSTEMS AND ASSOCIATED EQUIPMENT IN WHICH THE USE OF CONTROLLED MATERIALS, MECHANICAL PARTS AND PROCESSES IS MANDATORY.

* 940305E CRP 3763 38
1 EVALUATION AND INTEGRATION OF ISO 9001 IN ESA PSS SYSTEM FINAL REPORT (DECEMBER 1993)
2 BUREAU VERITAS, FRANCE (PO 123689)
3 ESA CR(P)-3763 // 191 PP
4 AVAIL MF AND HARD COPY (ESA PRICE CODE E2)

Geosciences

Earth Resources 43

* 940052E CRP 3729 43
1 STUDY ON ADVANCED SIGNAL RECONSTRUCTION TECHNIQUES - FINAL REPORT (APRIL 1993)
2 CSL, BELGIUM (CONTR NO. 9249/90/NL/SF(SC))
3 ESA CR(P)-3729 // 50 PP
4 AVAILABLE MF & HARD COPY (ESA PRICE CODE E0)

* 940060E CRP 3737 43
1 STUDY OF THE GEOPHYSICAL IMPACT OF HIGH RESOLUTION EARTH POTENTIAL FIELDS INFORMATION - FINAL REPORT (FEBRUARY 1994)
2 UNIV. OF CALIFORNIA, USA (P.O. 112540(1991))
3 ESA CR(P)-3737 // 282 PP
4 AVAILABLE MF (ESA PRICE CODE E3)

* 940075E SP 361 43
1 SECOND ERS-1 SYMPOSIUM: SPACE AT THE SERVICE OF OUR ENVIRONMENT (JANUARY 1994)
2 KALDEICH B.H. (ED.)
3 ESA SP-361 // 1360 PAGES (2 VOLS.)
4 PRICE DFL 200.00
5 THE TWO VOLUMES CONTAIN THE PROCEEDINGS OF THE 'SECOND ERS-1 SYMPOSIUM: SPACE AT THE SERVICE OF OUR ENVIRONMENT, HELD IN HAMBURG, GERMANY, 11-14 OCTOBER 1993.
THE SYMPOSIUM WAS ORGANISED IN 24 SESSIONS DEVOTED TO: ERS-1 DATA ASSIMILATION INTO SEA STATE MODELS; AGRICULTURE; GLACIOLOGY; ERS-1 DATA ASSIMILATION INTO ATMOSPHERIC CIRCULATION MODELS; WAVE IMAGING; SEA ICE; LARGE SCALE LAND SURFACE STUDIES; APPLICATIONS OF SAR IMAGERY AT SEA; FOREST MONITORING; OCEAN CIRCULATION; LAND USE, MAPPING AND TOPOGRAPHY; ICE OPERATIONAL APPLICATIONS; INTERFEROMETRY: METHODOLOGY AND TOOLS; ORBIT DETERMINATION AND GEOPHYSICAL MODELS; ATMOSHERIC PARAMETERS AND PROCESSES AS SEEN FROM ERS-1; SOIL MOISTURE; GEOLOGY; SHALLOW WATER AND COASTAL ZONE PROCESSES; SNOW; WIND FIELD RETRIEVAL; MARINE GEOID AND GEODYNAMICS; WATER SURFACE TEMPERATURE; WIND FIELD APPLICATIONS STUDIES; HYDROLOGY, RIVERS AND LAKES.

* 940076E X SP 361 43
1 APPLICATION OF ERS-1 SAR DATA IN WAVE MODELS - AN OVERVIEW (JANUARY 1994)
2 HASSELMANN K.
3 ESA SP-361 // P 15 VOL. 1
4 -
5 PAPER IN PROC. OF THE 'SECOND ERS-1 SYMPOSIUM: SPACE AT THE SERVICE OF OUR ENVIRONMENT', PROCEEDINGS OF A SYMPOSIUM HELD IN HAMBURG, GERMANY, 11-14 OCTOBER 1993 (INDEXED UNDER 43)

* 940077E X SP 361 43
1 OPERATIONAL USE OF ERS-1 OBSERVATIONS IN OCEAN WAVE FORECASTING AT ECMWF (JANUARY 1994)
2 GUILLAUME A & HANSSEN B.
3 ESA SP-361 // P 17 VOL. 1
4 -
5 PAPER IN PROC. OF THE 'SECOND ERS-1 SYMPOSIUM: SPACE AT THE SERVICE OF OUR ENVIRONMENT', PROCEEDINGS OF A SYMPOSIUM HELD IN HAMBURG, GERMANY, 11-14 OCTOBER 1993 (INDEXED UNDER 43)

* 940078E X SP 361 43
1 TOWARDS A GENERALIZED OPTIMAL INTERPOLATION METHOD FOR THE ASSIMILATION OF ERS-1 SAR RETRIEVED WAVE SPECTRA IN A WAVE MODEL (JANUARY 1994)
2 HASSELMANN S., BRUENING C & LIONELLO P.
3 ESA SP-361 // P 21 VOL. 1
4 -
5 PAPER IN PROC. OF THE 'SECOND ERS-1 SYMPOSIUM: SPACE AT THE SERVICE OF OUR ENVIRONMENT', PROCEEDINGS OF A SYMPOSIUM HELD IN HAMBURG, GERMANY, 11-14 OCTOBER 1993 (INDEXED UNDER 43)

* 940079E X SP 361 43
1 ASSIMILATION OF OCEAN WAVE SPECTRA RETRIEVED FROM ERS-1 SAR INTO THE WAVE MODEL WAM (JANUARY 1994)
2 BAUER E.
3 ESA SP-361 // P 27 VOL. 1
4 -
5 PAPER IN PROC. OF THE 'SECOND ERS-1 SYMPOSIUM: SPACE AT THE SERVICE OF OUR ENVIRONMENT', PROCEEDINGS OF A SYMPOSIUM HELD IN HAMBURG, GERMANY, 11-14 OCTOBER 1993 (INDEXED UNDER 43)

* 940080E X SP 361 43
1 GLOBAL COMPARISON OF SIGNIFICANT WAVE HEIGHTS DERIVED FROM ERS-1 SAR WAVE MODE, ERS-1 ALTIMETER AND TOPEX ALTIMETER DATA (JANUARY 1994)
2 HANSEN B., BRUENING C. & STAABS C.
3 ESA SP-361 // P 33 VOL. 1
4 -
5 PAPER IN PROC. OF THE 'SECOND ERS-1 SYMPOSIUM: SPACE AT THE SERVICE OF OUR ENVIRONMENT', PROCEEDINGS OF A SYMPOSIUM HELD IN HAMBURG, GERMANY, 11-14 OCTOBER 1993 (INDEXED UNDER 43)

* 940081E X SP 361 43
1 DEVELOPMENT OF AN OPERATIONAL DATA ASSIMILATION SYSTEM FOR ERS-1 WAVE SPECTRA (JANUARY 1994)
2 DUNLAP E., WILSON L.J. & OLSEN R.
3 ESA SP-361 // P 37 VOL. 1
4 -
5 PAPER IN PROC. OF THE 'SECOND ERS-1 SYMPOSIUM: SPACE AT THE SERVICE OF OUR ENVIRONMENT', PROCEEDINGS OF A SYMPOSIUM HELD IN HAMBURG, GERMANY, 11-14 OCTOBER 1993 (INDEXED UNDER 43)

* 940082E X SP 361 43
1 USE OF SAR-WAVE MODE ALTIMETER AND WIND SCATTEROMETER DATA IN OPERATIONAL WAVE FORECASTING SYSTEM (JANUARY 1994)
2 LASNIER P. ET AL.
3 ESA SP-361 // P 43 VOL. 1
4 -
5 PAPER IN PROC. OF THE 'SECOND ERS-1 SYMPOSIUM: SPACE AT THE SERVICE OF OUR ENVIRONMENT', PROCEEDINGS OF A SYMPOSIUM HELD IN HAMBURG, GERMANY, 11-14 OCTOBER 1993 (INDEXED UNDER 43)

* 940083E X SP 361 43
1 CROP DISCRIMINATION USING MULTI-TEMPORAL ERS-1 SAR DATA (JANUARY 1994)
2 WOODING M.G., ZMUDA A.D. & GRIFFITHS G.H.
3 ESA SP-361 // P 41 VOL. 1
4 -
5 PAPER IN PROC. OF THE 'SECOND ERS-1 SYMPOSIUM: SPACE AT THE SERVICE OF OUR ENVIRONMENT', PROCEEDINGS OF A SYMPOSIUM HELD IN HAMBURG, GERMANY, 11-14 OCTOBER 1993 (INDEXED UNDER 43)

* 940084E X SP 361 43
1 MULTI-TEMPORAL ERS-1 FOR CROP DISCRIMINATION (JANUARY 1994)
2 BROWN R.J. ET AL.
3 ESA SP-361 // P 57 VOL. 1
4 -
5 PAPER IN PROC. OF THE 'SECOND ERS-1 SYMPOSIUM: SPACE AT THE SERVICE OF OUR ENVIRONMENT', PROCEEDINGS OF A SYMPOSIUM HELD IN HAMBURG, GERMANY, 11-14 OCTOBER 1993 (INDEXED UNDER 43)

* 940085E X SP 361 43
1 AGRICULTURAL APPLICATIONS OF ERS-1 SAR DATA: PRELIMINARY RESULTS OF THE PASTA PROJECT (JANUARY 1994)
2 HARTL PH. ET AL
3 ESA SP-361 // P 63 VOL. 1
4 -
5 PAPER IN PROC. OF THE 'SECOND ERS-1 SYMPOSIUM: SPACE AT THE SERVICE OF OUR ENVIRONMENT', PROCEEDINGS OF A SYMPOSIUM HELD IN HAMBURG, GERMANY, 11-14 OCTOBER 1993 (INDEXED UNDER 43)

* 940086E X SP 361 43
1 SUITABILITY OF ERS-1 SAR PRI-DATA FOR MULTITEMPORAL AND AGRICULTURAL LAND-USE MAPPING (JANUARY 1994)
2 MUELLER U. ET AL.
3 ESA SP-361 // P 69 VOL. 1
4 -
5 PAPER IN PROC. OF THE 'SECOND ERS-1 SYMPOSIUM: SPACE AT THE SERVICE OF OUR ENVIRONMENT', PROCEEDINGS OF A SYMPOSIUM HELD IN HAMBURG, GERMANY, 11-14 OCTOBER 1993 (INDEXED UNDER 43)

* 940087E X SP 361 43
1 COMPARISON OF ERS-1 SLC AND LANDSAT THEMATIC MAPPER DATA FOR MONITORING GRASSLAND AND DETECTING CHANGES IN AGRICULTURAL USE (JANUARY 1994)
2 SCHADT R., KELLNDORFER J. & MAUSER W.
3 ESA SP-361 // P 75 VOL. 1
4 -
5 PAPER IN PROC. OF THE 'SECOND ERS-1 SYMPOSIUM: SPACE AT THE SERVICE OF OUR ENVIRONMENT', PROCEEDINGS OF A SYMPOSIUM HELD IN HAMBURG, GERMANY, 11-14 OCTOBER 1993 (INDEXED UNDER 43)

* 940088E X SP 361 43
1 COMPARISON OF MULTITEMPORAL ERS-1 AND AIRBORNE DLR E-SAR IMAGE DATA FOR CROP MONITORING (JANUARY 1994)
2 SCHMULLIUS C., NITHACK J. & KERN M.
3 ESA SP-361 // P 79 VOL. 1
4 -
5 PAPER IN PROC. OF THE 'SECOND ERS-1 SYMPOSIUM: SPACE AT THE SERVICE OF OUR ENVIRONMENT', PROCEEDINGS OF A SYMPOSIUM HELD IN HAMBURG, GERMANY, 11-14 OCTOBER 1993 (INDEXED UNDER 43)

* 940089E X SP 361 43
1 INTEGRATION OF ERS-1 DATA INTO THE EUROPEAN PROJECT OF AGRICULTURAL STATISTICS (JANUARY 1994)
2 HARMS J. ET AL.
3 ESA SP-361 // P 85 VOL. 1
4 -
5 PAPER IN PROC. OF THE 'SECOND ERS-1 SYMPOSIUM: SPACE AT THE SERVICE OF OUR ENVIRONMENT', PROCEEDINGS OF A SYMPOSIUM HELD IN HAMBURG, GERMANY, 11-14 OCTOBER 1993 (INDEXED UNDER 43)

* 940090E X SP 361 43
1 AGRICULTURAL STATISTICS: COMPARISON OF ERS-1 AND SPOT FOR THE CROP ACREAGE ESTIMATION OF THE MARS PROJECT (JANUARY 1994)
2 KOHL H.-G., KING C., & GROOF H. DE
3 ESA SP-361 // P 87 VOL. 1
4 -
5 PAPER IN PROC. OF THE 'SECOND ERS-1 SYMPOSIUM: SPACE AT THE SERVICE OF OUR ENVIRONMENT', PROCEEDINGS OF A SYMPOSIUM HELD IN HAMBURG, GERMANY, 11-14 OCTOBER 1993 (INDEXED UNDER 43)

* 940091E X SP 361 43
1 AGRICULTURAL POTENTIALS OF ERS-1 DATA (JANUARY 1994)
2 KOLAR J. & FERANEC J.
3 ESA SP-361 // P 93 VOL. 1
4 -
5 PAPER IN PROC. OF THE 'SECOND ERS-1 SYMPOSIUM: SPACE AT THE SERVICE OF OUR ENVIRONMENT', PROCEEDINGS OF A SYMPOSIUM HELD IN HAMBURG, GERMANY, 11-14 OCTOBER 1993 (INDEXED UNDER 43)

* 940092E X SP 361 43
1 RICE CROP MONITORING WITH ERS-1 SAR: A FIRST YEAR RESULT (JANUARY 1994)
2 KUROSU T. ET AL.
3 ESA SP-361 // P 97 VOL. 1
4 -
5 PAPER IN PROC. OF THE 'SECOND ERS-1 SYMPOSIUM: SPACE AT THE SERVICE OF OUR ENVIRONMENT', PROCEEDINGS OF A SYMPOSIUM HELD IN HAMBURG, GERMANY, 11-14 OCTOBER 1993 (INDEXED UNDER 43)

* 940093E X SP 361 43
1 CROP MONITORING WITH ERS-1 SAR IN EAST ANGLIA, UK (JANUARY 1994)
2 WRIGHT P., SAICH P. & CORDEY R.
3 ESA SP-361 // P 103 VOL. 1
4 -
5 PAPER IN PROC. OF THE 'SECOND ERS-1 SYMPOSIUM: SPACE AT THE SERVICE OF OUR ENVIRONMENT', PROCEEDINGS OF A SYMPOSIUM HELD IN HAMBURG, GERMANY, 11-14 OCTOBER 1993 (INDEXED UNDER 43)

* 940094E X SP 361 43
1 ANTARCTIC TOPOGRAPHY DERIVED FROM ERS-1 ALTIMETRY (JANUARY 1994)
2 BAMBER J.L. ET AL.
3 ESA SP-361 // P 113 VOL. 1
4 -
5 PAPER IN PROC. OF THE 'SECOND ERS-1 SYMPOSIUM: SPACE AT THE SERVICE OF OUR ENVIRONMENT', PROCEEDINGS OF A SYMPOSIUM HELD IN HAMBURG, GERMANY, 11-14 OCTOBER 1993 (INDEXED UNDER 43)

* 940095E X SP 361 43
1 ANALYSIS OF ERS-1 RADAR ALTIMETER DATA OVER ANTARCTICA (JANUARY 1994)
2 IHDE J. ET AL.
3 ESA SP-361 // P 119 VOL. 1
4 -
5 PAPER IN PROC. OF THE 'SECOND ERS-1 SYMPOSIUM: SPACE AT THE SERVICE OF OUR ENVIRONMENT', PROCEEDINGS OF A SYMPOSIUM HELD IN HAMBURG, GERMANY, 11-14 OCTOBER 1993 (INDEXED UNDER 43)

* 940096E X SP 361 43
1 MEASURING ICE SHEET CHANGES WITH THE ERS-1 ALTIMETER (JANUARY 1994)
2 WINGHAM D.J. ET AL.
3 ESA SP-361 // P 127 VOL. 1
4 -
5 PAPER IN PROC. OF THE 'SECOND ERS-1 SYMPOSIUM: SPACE AT THE SERVICE OF OUR ENVIRONMENT', PROCEEDINGS OF A SYMPOSIUM HELD IN HAMBURG, GERMANY, 11-14 OCTOBER 1993 (INDEXED UNDER 43)

* 940097E X SP 361 43
1 APPLICATIONS OF ERS-1 SAR AND SCATTEROMETER DATA FOR STUDIES OF THE ANTARCTIC ICE SHEET (JANUARY 1994)
2 ROTT H. ET AL.
3 ESA SP-361 // P 133 VOL. 1
4 -
5 PAPER IN PROC. OF THE 'SECOND ERS-1 SYMPOSIUM: SPACE AT THE SERVICE OF OUR ENVIRONMENT', PROCEEDINGS OF A SYMPOSIUM HELD IN HAMBURG, GERMANY, 11-14 OCTOBER 1993 (INDEXED UNDER 43)

* 940098E X SP 361 43
1 EXTRACTION OF ANTARCTIC TOPOGRAPHIC-GLACIOLOGICAL FEATURES FROM ERS-1 SAR DATA (JANUARY 1994)
2 BENNAT H., HEIDRICH B. & SIEVERS J.
3 ESA SP-361 // P 141 VOL. 1
4 -
5 PAPER IN PROC. OF THE 'SECOND ERS-1 SYMPOSIUM: SPACE AT THE SERVICE OF OUR ENVIRONMENT', PROCEEDINGS OF A SYMPOSIUM HELD IN HAMBURG, GERMANY, 11-14 OCTOBER 1993 (INDEXED UNDER 43)

* 940099E X SP 361 43
1 VELOCITIES AND MASS BALANCE OF PINE ISLAND GLACIER, WEST ANTARCTICA, DERIVED FROM ERS-1 SAR IMAGES (JANUARY 1994)
2 LUCCHITTA B.K. ET AL.
3 ESA SP-361 // P 147 VOL. 1
4 -
5 PAPER IN PROC. OF THE 'SECOND ERS-1 SYMPOSIUM: SPACE AT THE SERVICE OF OUR ENVIRONMENT', PROCEEDINGS OF A SYMPOSIUM HELD IN HAMBURG, GERMANY, 11-14 OCTOBER 1993 (INDEXED UNDER 43)

* 940100E X SP 361 43
1 ERS-1 DATA FOR MAPPING OF THE ANTARCTIC PENINSULA BY SHAPE-FROM-SHADING TECHNIQUE (JANUARY 1994)
2 FISKEL T., HARTMANN R. & WINZER W.
3 ESA SP-361 // P 153 VOL. 1
4 -
5 PAPER IN PROC. OF THE 'SECOND ERS-1 SYMPOSIUM: SPACE AT THE SERVICE OF OUR ENVIRONMENT', PROCEEDINGS OF A SYMPOSIUM HELD IN HAMBURG, GERMANY, 11-14 OCTOBER 1993 (INDEXED UNDER 43)

* 940101E X SP 361 43
1 ICE SHEET TOPOGRAPHY FROM RETRACKED ERS-1 ALTIMETRY (JANUARY 1994)
2 ZWALLY H.J. ET AL.
3 ESA SP-361 // P 159 VOL. 1
4 -
5 PAPER IN PROC. OF THE 'SECOND ERS-1 SYMPOSIUM: SPACE AT THE SERVICE OF OUR ENVIRONMENT', PROCEEDINGS OF A SYMPOSIUM HELD IN HAMBURG, GERMANY, 11-14 OCTOBER 1993 (INDEXED UNDER 43)

* 940102E X SP 361 43
1 COMPARISON OF RADAR-ALTIMETRY DATA OVER GREENLAND WITH SURFACE TOPOGRAPHY DERIVED FROM AIRBORNE LASER ALTIMETRY (JANUARY 1994)
2 THOMAS R.H. ET AL.
3 ESA SP-361 // P 165 VOL. 1
4 -
5 PAPER IN PROC. OF THE 'SECOND ERS-1 SYMPOSIUM: SPACE AT THE SERVICE OF OUR ENVIRONMENT', PROCEEDINGS OF A SYMPOSIUM HELD IN HAMBURG, GERMANY, 11-14 OCTOBER 1993 (INDEXED UNDER 43)

* 940103E X SP 361 43
1 VALIDATION OF SAR DATA FROM ERS-1 ON SPITSBERGEN, SVALBARD: PRELIMINARY GLACIOLOGICAL AND GEOMORPHOLOGICAL INTERPRETATION (JANUARY 1994)
2 LEFAUCONNIER B. ET AL.
3 ESA SP-361 // P 171 VOL. 1
4 -
5 PAPER IN PROC. OF THE 'SECOND ERS-1 SYMPOSIUM: SPACE AT THE SERVICE OF OUR ENVIRONMENT', PROCEEDINGS OF A SYMPOSIUM HELD IN HAMBURG, GERMANY, 11-14 OCTOBER 1993 (INDEXED UNDER 43)

* 940104E X SP 361 43
1 RESULTS FROM ERS-1 RADAR ALTIMETRY GROUND TRUTHING ON THE FILCHNER-RONNE-SCHELFEIS (JANUARY 1994)
2 SCHENKE H.W. ET AL.
3 ESA SP-361 // P 177 VOL. 1
4 -
5 PAPER IN PROC. OF THE 'SECOND ERS-1 SYMPOSIUM: SPACE AT THE SERVICE OF OUR ENVIRONMENT', PROCEEDINGS OF A SYMPOSIUM HELD IN HAMBURG, GERMANY, 11-14 OCTOBER 1993 (INDEXED UNDER 43)

* 940105E X SP 361 43
1 ERS-1 SAR: STRESS INDICATOR FOR ANTARCTIC ICE STREAMS (JANUARY 1994)
2 VAUGHAN D.G., FROLICH R.M. & DOAKE C.S.M.
3 ESA SP-361 // P 183 VOL. 1
4 -
5 PAPER IN PROC. OF THE 'SECOND ERS-1 SYMPOSIUM: SPACE AT THE SERVICE OF OUR ENVIRONMENT', PROCEEDINGS OF A SYMPOSIUM HELD IN HAMBURG, GERMANY, 11-14 OCTOBER 1993 (INDEXED UNDER 43)

* 940106E X SP 361 43
1 ERS-1 SCATTEROMETER DATA ASSIMILATION (JANUARY 1994)
2 STOFFELEN A., GAFFARD, C. & ANDERSON D.
3 ESA SP-361 // P 191 VOL. 1
4 -
5 PAPER IN PROC. OF THE 'SECOND ERS-1 SYMPOSIUM: SPACE AT THE SERVICE OF OUR ENVIRONMENT', PROCEEDINGS OF A SYMPOSIUM HELD IN HAMBURG, GERMANY, 11-14 OCTOBER 1993 (INDEXED UNDER 43)

* 940107E X SP 361 43
1 OPERATIONAL USE OF ERS-1 PRODUCTS IN THE METEOROLOGICAL OFFICE (JANUARY 1994)
2 BELL R.S.
3 ESA SP-361 // P 195 VOL. 1
4 -
5 PAPER IN PROC. OF THE 'SECOND ERS-1 SYMPOSIUM: SPACE AT THE SERVICE OF OUR ENVIRONMENT', PROCEEDINGS OF A SYMPOSIUM HELD IN HAMBURG, GERMANY, 11-14 OCTOBER 1993 (INDEXED UNDER 43)

* 940108E X SP 361 43
1 RESULTS FROM ASSIMILATION OF ERS-1 SCATTEROMETER WIND INFORMATION IN AN OPERATIONAL LIMITED AREA WEATHER FORECAST MODEL (JANUARY 1994)
2 BREIVIK L.A., HAUGSE B. & HOMLEID M.
3 ESA SP-361 // P 201 VOL. 1
4 -
5 PAPER IN PROC. OF THE 'SECOND ERS-1 SYMPOSIUM: SPACE AT THE SERVICE OF OUR ENVIRONMENT', PROCEEDINGS OF A SYMPOSIUM HELD IN HAMBURG, GERMANY, 11-14 OCTOBER 1993 (INDEXED UNDER 43)

* 940109E X SP 361 43
1 AN ASSESSMENT OF THE USE OF ERS-1 SCATTEROMETER WINDS IN CANADIAN WEATHER FORECASTING CENTRES (JANUARY 1994)
2 KING P.
3 ESA SP-361 // P 201 VOL. 1
4 -
5 PAPER IN PROC. OF THE 'SECOND ERS-1 SYMPOSIUM: SPACE AT THE SERVICE OF OUR ENVIRONMENT', PROCEEDINGS OF A SYMPOSIUM HELD IN HAMBURG, GERMANY, 11-14 OCTOBER 1993 (INDEXED UNDER 43)

* 940110E X SP 361 43
1 THE IMPACT OF SCATTEROMETER DATA ON MEAN SEA LEVEL ANALYSES (JANUARY 1994)
2 POLAVARAPU S.
3 ESA SP-361 // P 211 VOL. 1
4 -
5 PAPER IN PROC. OF THE 'SECOND ERS-1 SYMPOSIUM: SPACE AT THE SERVICE OF OUR ENVIRONMENT', PROCEEDINGS OF A SYMPOSIUM HELD IN HAMBURG, GERMANY, 11-14 OCTOBER 1993 (INDEXED UNDER 43)

* 940111E X SP 361 43
1 A GENERALISED NONLINEAR OCEAN WAVE-SAR SPECTRAL INTEGRAL TRANSFORM AND ITS APPLICATION TO ERS-1 SAR OCEAN WAVE IMAGING (JANUARY 1994)
2 BAO M., BRUENING C. & ALPERS W.
3 ESA SP-361 // P 219 VOL. 1
4 -
5 PAPER IN PROC. OF THE 'SECOND ERS-1 SYMPOSIUM: SPACE AT THE SERVICE OF OUR ENVIRONMENT', PROCEEDINGS OF A SYMPOSIUM HELD IN HAMBURG, GERMANY, 11-14 OCTOBER 1993 (INDEXED UNDER 43)

* 940112E X SP 361 43
1 VALIDATION OF A NUMERICAL MODEL DESCRIBING THE GENERATION AND PROPAGATION OF INTERNAL WAVES IN THE STRAIT OF GIBRALTAR BY USING ERS-1 SAR DATA (JANUARY 1994)
2 BRANDT P. & ALPERS W.
3 ESA SP-361 // P 225 VOL. 1
4 -
5 PAPER IN PROC. OF THE 'SECOND ERS-1 SYMPOSIUM: SPACE AT THE SERVICE OF OUR ENVIRONMENT', PROCEEDINGS OF A SYMPOSIUM HELD IN HAMBURG, GERMANY, 11-14 OCTOBER 1993 (INDEXED UNDER 43)

* 940113E X SP 361 43
1 ON THE RELATIVE IMPORTANCE OF THE OCEAN-WAVE RADAR MODULATION TRANSFER FUNCTION FOR INVERTING ERS-1 SAR IMAGE SPECTRA INTO OCEAN WAVE SPECTRA (JANUARY 1994)
2 BRUENING C.
3 ESA SP-361 // P 233 VOL. 1
4 -
5 PAPER IN PROC. OF THE 'SECOND ERS-1 SYMPOSIUM: SPACE AT THE SERVICE OF OUR ENVIRONMENT', PROCEEDINGS OF A SYMPOSIUM HELD IN HAMBURG, GERMANY, 11-14 OCTOBER 1993 (INDEXED UNDER 43)

* 940114E X SP 361 43
1 COMPARISON OF OCEAN WAVE IMAGING BY ERS-1 AND ALMAZ-1 SYNTHETIC APERTURE RADAR (JANUARY 1994)
2 WILDE A., BRUENING C. & ALPERS W.
3 ESA SP-361 // P 239 VOL. 1
4 -
5 PAPER IN PROC. OF THE 'SECOND ERS-1 SYMPOSIUM: SPACE AT THE SERVICE OF OUR ENVIRONMENT', PROCEEDINGS OF A SYMPOSIUM HELD IN HAMBURG, GERMANY, 11-14 OCTOBER 1993 (INDEXED UNDER 43)

* 940115E X SP 361 43
1 NONLINEAR THEORY OF OCEAN-SAR TRANSFORMATION AND STATISTICAL ANALYSIS OF ERS 1 SAR WAVE MODE IMAGETTES (JANUARY 1994)
2 CHAPRON B. ET AL.
3 ESA SP-361 // P 247 VOL. 1
4 -
5 PAPER IN PROC. OF THE 'SECOND ERS-1 SYMPOSIUM: SPACE AT THE SERVICE OF OUR ENVIRONMENT', PROCEEDINGS OF A SYMPOSIUM HELD IN HAMBURG, GERMANY, 11-14 OCTOBER 1993 (INDEXED UNDER 43)

esa SP - 361
Volume I

Proceedings of the Second ERS-1 Symposium

SPACE AT THE SERVICE OF OUR ENVIRONMENT

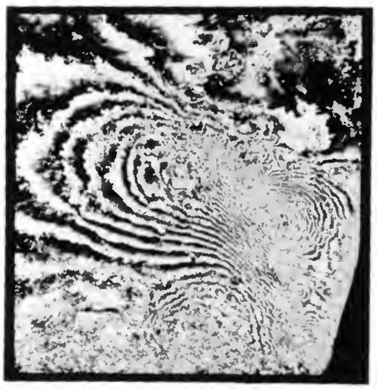

11-14 October 1993
Hamburg, Germany

esa
european space agency

* 940116E X SP 361 43
1 VALIDATION OF ERS-1 SAR FOR ARCTIC ICE PROPERTIES FROM ARCTIC-91 (JANUARY 1994)
2 ASKNE J. ET AL.
3 ESA SP-361 // P 257 VOL. 1
4 -
5 PAPER IN PROC. OF THE 'SECOND ERS-1 SYMPOSIUM: SPACE AT THE SERVICE OF OUR ENVIRONMENT', PROCEEDINGS OF A SYMPOSIUM HELD IN HAMBURG, GERMANY, 11-14 OCTOBER 1993 (INDEXED UNDER 43)

* 940117E X SP 361 43
1 THE TRANSPOLAR ICE DRIFT NORTH OF FRAM STRAIT STUDIED FROM ERS-1 SAR IMAGERY (JANUARY 1994)
2 KERGOMARD C. ET AL.
3 ESA SP-361 // P 263 VOL. 1
4 -
5 PAPER IN PROC. OF THE 'SECOND ERS-1 SYMPOSIUM: SPACE AT THE SERVICE OF OUR ENVIRONMENT', PROCEEDINGS OF A SYMPOSIUM HELD IN HAMBURG, GERMANY, 11-14 OCTOBER 1993 (INDEXED UNDER 43)

* 940118E X SP 361 43
1 SEA ICE LEAD DYNAMICS FROM ERS-1 SAR (JANUARY 1994)
2 STERN H.L., ROTHROCK D.A. & KWOK R.
3 ESA SP-361 // P 269 VOL. 1
4 -
5 PAPER IN PROC. OF THE 'SECOND ERS-1 SYMPOSIUM: SPACE AT THE SERVICE OF OUR ENVIRONMENT', PROCEEDINGS OF A SYMPOSIUM HELD IN HAMBURG, GERMANY, 11-14 OCTOBER 1993 (INDEXED UNDER 43)

* 940119E X SP 361 43
1 THE USE OF ERS-1 SAR DATA FOR SEA ICE MAPPING AND ICEBREAKER OPERATIONS IN THE GULF OF BOTHNIA (JANUARY 1994)
2 THOMPSON TH. ET AL.
3 ESA SP-361 // P 271 VOL. 1
4 -
5 PAPER IN PROC. OF THE 'SECOND ERS-1 SYMPOSIUM: SPACE AT THE SERVICE OF OUR ENVIRONMENT', PROCEEDINGS OF A SYMPOSIUM HELD IN HAMBURG, GERMANY, 11-14 OCTOBER 1993 (INDEXED UNDER 43)

* 940120E X SP 361 43
1 MONITORING SEA ICE FLUX THROUGH FRAM STRAIT (JANUARY 1994)
2 SCHWEIGER A.J. & ROTHROCK D.A.
3 ESA SP-361 // P 277 VOL. 1
4 -
5 PAPER IN PROC. OF THE 'SECOND ERS-1 SYMPOSIUM: SPACE AT THE SERVICE OF OUR ENVIRONMENT', PROCEEDINGS OF A SYMPOSIUM HELD IN HAMBURG, GERMANY, 11-14 OCTOBER 1993 (INDEXED UNDER 43)

* 940121E X SP 361 43
1 THE GEOPHYSICAL PROCESSOR SYSTEM - AUTOMATED ANALYSIS OF ERS-1 SAR IMAGERY (JANUARY 1994)
2 STERN H.L. ET AL.
3 ESA SP-361 // P 281 VOL. 1
4 -
5 PAPER IN PROC. OF THE 'SECOND ERS-1 SYMPOSIUM: SPACE AT THE SERVICE OF OUR ENVIRONMENT', PROCEEDINGS OF A SYMPOSIUM HELD IN HAMBURG, GERMANY, 11-14 OCTOBER 1993 (INDEXED UNDER 43)

* 940122E X SP 361 43
1 MULTI-SENSOR AND GROUND-TRUTH INVESTIGATION OF WEDDELL SEA ICE CONDITIONS (JANUARY 1994)
2 VIEHOFF T. & LI A.
3 ESA SP-361 // P 287 VOL. 1
4 -
5 PAPER IN PROC. OF THE 'SECOND ERS-1 SYMPOSIUM: SPACE AT THE SERVICE OF OUR ENVIRONMENT', PROCEEDINGS OF A SYMPOSIUM HELD IN HAMBURG, GERMANY, 11-14 OCTOBER 1993 (INDEXED UNDER 43)

* 940123E X SP 361 43
1 THE ODDEN ICE TONGUE IN THE GREENLAND SEA: SAR IMAGERY AND FIELD OBSERVATIONS OF ITS DEVELOPMENT IN 1993 (JANUARY 1994)
2 WADHAMS P. & VIEHOFF T.
3 ESA SP-361 // P 291 VOL. 1
4 -
5 PAPER IN PROC. OF THE 'SECOND ERS-1 SYMPOSIUM: SPACE AT THE SERVICE OF OUR ENVIRONMENT', PROCEEDINGS OF A SYMPOSIUM HELD IN HAMBURG, GERMANY, 11-14 OCTOBER 1993 (INDEXED UNDER 43)

* 940124E X SP 361 43
1 TEXTURE ANALYSIS AS AN AID FOR THE EVALUATION OF ERS-1 SAR DATA FROM A PART OF THE ANTARCTIC PENINSULA (JANUARY 1994)
2 SAURER H. & TRIEBFUERST B.
3 ESA SP-361 // P 297 VOL. 1
4 -
5 PAPER IN PROC. OF THE 'SECOND ERS-1 SYMPOSIUM: SPACE AT THE SERVICE OF OUR ENVIRONMENT', PROCEEDINGS OF A SYMPOSIUM HELD IN HAMBURG, GERMANY, 11-14 OCTOBER 1993 (INDEXED UNDER 43)

* 940125E X SP 361 43
1 SEA ICE MOTION IN THE WEDDELL SEA, ANTARCTICA FROM PAIRS OF ERS-1 SAR IMAGES (JANUARY 1994)
2 TURNER J. ET AL.
3 ESA SP-361 // P 303 VOL. 1
4 -
5 PAPER IN PROC. OF THE 'SECOND ERS-1 SYMPOSIUM: SPACE AT THE SERVICE OF OUR ENVIRONMENT', PROCEEDINGS OF A SYMPOSIUM HELD IN HAMBURG, GERMANY, 11-14 OCTOBER 1993 (INDEXED UNDER 43)

* 940126E X SP 361 43
1 INTERCOMPARISON OF ERS-1 SAR, AIRBORNE SLAR AND ELECTRO-MAGNETIC ICE-THICKNESS DATA (JANUARY 1994)
2 IKEDA M. & PRINSENBERG S.
3 ESA SP-361 // P 309 VOL. 1
4 -
5 PAPER IN PROC. OF THE 'SECOND ERS-1 SYMPOSIUM: SPACE AT THE SERVICE OF OUR ENVIRONMENT', PROCEEDINGS OF A SYMPOSIUM HELD IN HAMBURG, GERMANY, 11-14 OCTOBER 1993 (INDEXED UNDER 43)

* 940127E X SP 361 43
1 ERS-1 SAR OBSERVATION OF SWELL TRAVELLING INTO THE ICE (JANUARY 1994)
2 LEHNER S. & HASSELMANN K.
3 ESA SP-361 // P 311 VOL. 1
4 -
5 PAPER IN PROC. OF THE 'SECOND ERS-1 SYMPOSIUM: SPACE AT THE SERVICE OF OUR ENVIRONMENT', PROCEEDINGS OF A SYMPOSIUM HELD IN HAMBURG, GERMANY, 11-14 OCTOBER 1993 (INDEXED UNDER 43)

* 940128E X SP 361 43
1 OCEAN-ICE INTERACTION IN THE MARGINAL ICE ZONE (JANUARY 1994)
2 LIU A.K. & PENG C.Y.
3 ESA SP-361 // P 317 VOL. 1
4 -
5 PAPER IN PROC. OF THE 'SECOND ERS-1 SYMPOSIUM: SPACE AT THE SERVICE OF OUR ENVIRONMENT', PROCEEDINGS OF A SYMPOSIUM HELD IN HAMBURG, GERMANY, 11-14 OCTOBER 1993 (INDEXED UNDER 43)

* 940129E X SP 361 43
1 SEA ICE AND CLIMATE - AN APPROACH USING SAR DATA (JANUARY 1994)
2 ROTH R. ET AL.
3 ESA SP-361 // P 323 VOL. 1
4 -
5 PAPER IN PROC. OF THE 'SECOND ERS-1 SYMPOSIUM: SPACE AT THE SERVICE OF OUR ENVIRONMENT', PROCEEDINGS OF A SYMPOSIUM HELD IN HAMBURG, GERMANY, 11-14 OCTOBER 1993 (INDEXED UNDER 43)

* 940130E X SP 361 43
1 THE SEGMENTATION OF ERS-1 SEA-ICE IMAGERY FOR POLAR OPERATIONS (JANUARY 1994)
2 WALKER N.P. & RYE A.J.
3 ESA SP-361 // P 329 VOL. 1
4 -
5 PAPER IN PROC. OF THE 'SECOND ERS-1 SYMPOSIUM: SPACE AT THE SERVICE OF OUR ENVIRONMENT', PROCEEDINGS OF A SYMPOSIUM HELD IN HAMBURG, GERMANY, 11-14 OCTOBER 1993 (INDEXED UNDER 43)

* 940131E X SP 361 43
1 RADAR OBSERVATION OF AN ARCTIC POLYNA UNDER SUMMER CONDITIONS (JANUARY 1994)
2 GUDMANDSEN P. ET AL.
3 ESA SP-361 // P 335 VOL. 1
4 -
5 PAPER IN PROC. OF THE 'SECOND ERS-1 SYMPOSIUM: SPACE AT THE SERVICE OF OUR ENVIRONMENT', PROCEEDINGS OF A SYMPOSIUM HELD IN HAMBURG, GERMANY, 11-14 OCTOBER 1993 (INDEXED UNDER 43)

* 940132E X SP 361 43
1 SEA-ICE DETECTION IN THE BOHAI SEA USING THE ATSR/M AND AVHRR (JANUARY 1994)
2 EZRATY R., HUANG R. & LIU J.
3 ESA SP-361 // P 341 VOL. 1
4 -
5 PAPER IN PROC. OF THE 'SECOND ERS-1 SYMPOSIUM: SPACE AT THE SERVICE OF OUR ENVIRONMENT', PROCEEDINGS OF A SYMPOSIUM HELD IN HAMBURG, GERMANY, 11-14 OCTOBER 1993 (INDEXED UNDER 43)

* 940133E X SP 361 43
1 SURFACE PROCESSES IN GREENLAND SEA CONVECTION (JANUARY 1994)
2 CARSEY F. D.
3 ESA SP-361 // P 347 VOL. 1
4 -
5 PAPER IN PROC. OF THE 'SECOND ERS-1 SYMPOSIUM: SPACE AT THE SERVICE OF OUR ENVIRONMENT', PROCEEDINGS OF A SYMPOSIUM HELD IN HAMBURG, GERMANY, 11-14 OCTOBER 1993 (INDEXED UNDER 43)

* 940134E X SP 361 43
1 SIZEX'92 ERS-1 SAR ICE VALIDATION EXPERIMENT (JANUARY 1994)
2 SANDVEN S. ET AL.
3 ESA SP-361 // P 353 VOL. 1
4 -
5 PAPER IN PROC. OF THE 'SECOND ERS-1 SYMPOSIUM: SPACE AT THE SERVICE OF OUR ENVIRONMENT', PROCEEDINGS OF A SYMPOSIUM HELD IN HAMBURG, GERMANY, 11-14 OCTOBER 1993 (INDEXED UNDER 43)

* 940135E X SP 361 43
1 ERS-1 SEA ICE APPLICATIONS DEVELOPMENT ACTIVITIES AT THE CANADA CENTRE FOR REMOTE SENSING (JANUARY 1994)
2 MANORE M.J.
3 ESA SP-361 // P 359 VOL. 1
4 -
5 PAPER IN PROC. OF THE 'SECOND ERS-1 SYMPOSIUM: SPACE AT THE SERVICE OF OUR ENVIRONMENT', PROCEEDINGS OF A SYMPOSIUM HELD IN HAMBURG, GERMANY, 11-14 OCTOBER 1993 (INDEXED UNDER 43)

* 940136E X SP 361 43
1 FUSION OF ERS-1 SAR AND SSMI/I ICE DATA (JANUARY 1994)
2 RAMSEIER R. ET AL.
3 ESA SP-361 // P 361 VOL. 1
4 -
5 PAPER IN PROC. OF THE 'SECOND ERS-1 SYMPOSIUM: SPACE AT THE SERVICE OF OUR ENVIRONMENT', PROCEEDINGS OF A SYMPOSIUM HELD IN HAMBURG, GERMANY, 11-14 OCTOBER 1993 (INDEXED UNDER 43)

* 940137E X SP 361 43
1 THE OPERATIONAL MAPPING OF ICE CONDITIONS USING ERS-1 IMAGES IN THE BALTIC SEA (JANUARY 1994)
2 SEINA A. & GRONVALL H.
3 ESA SP-361 // P 369 VOL. 1
4 -
5 PAPER IN PROC. OF THE 'SECOND ERS-1 SYMPOSIUM: SPACE AT THE SERVICE OF OUR ENVIRONMENT', PROCEEDINGS OF A SYMPOSIUM HELD IN HAMBURG, GERMANY, 11-14 OCTOBER 1993 (INDEXED UNDER 43)

* 940138E X SP 361 43
1 ICE-ATMOSPHERE INTERACTIONS IN THE CENTRAL ARCTIC: REMOTELY-SENSED AND SIMULATED ICE CONCENTRATIONS AND MOTION (JANUARY 1994)
2 MASLANIK J.A. ET AL.
3 ESA SP-361 // P 373 VOL. 1
4 -
5 PAPER IN PROC. OF THE 'SECOND ERS-1 SYMPOSIUM: SPACE AT THE SERVICE OF OUR ENVIRONMENT', PROCEEDINGS OF A SYMPOSIUM HELD IN HAMBURG, GERMANY, 11-14 OCTOBER 1993 (INDEXED UNDER 43)

* 940139E X SP 361 43
1 USE OF ERS-1 WIND SCATTEROMETER DATA OVER LAND SURFACES: ARID AND SEMI-ARID LANDS (F1) (JANUARY 1994)
2 KERR Y.H. & MAGAGI R.D.
3 ESA SP-361 // P 383 VOL. 1
4 -
5 PAPER IN PROC. OF THE 'SECOND ERS-1 SYMPOSIUM: SPACE AT THE SERVICE OF OUR ENVIRONMENT', PROCEEDINGS OF A SYMPOSIUM HELD IN HAMBURG, GERMANY, 11-14 OCTOBER 1993 (INDEXED UNDER 43)

* 940140E X SP 361 43
1 LAND SURFACE TEMPERATURE RETRIEVAL FROM ATSR DATA OVER THE NIAMEY (NIGER) AREA (JANUARY 1994)
2 LABED J., LI Z.L. & STOLL M.P.
3 ESA SP-361 // P 389 VOL. 1
4 -
5 PAPER IN PROC. OF THE 'SECOND ERS-1 SYMPOSIUM: SPACE AT THE SERVICE OF OUR ENVIRONMENT', PROCEEDINGS OF A SYMPOSIUM HELD IN HAMBURG, GERMANY, 11-14 OCTOBER 1993 (INDEXED UNDER 43)

* 940141E X SP 361 43
1 ANALYSIS OF ERS-1 SCATTEROMETER DATA OVER LAND SURFACES. PRELIMINARY RESULTS (JANUARY 1994)
2 MOUGIN E. ET AL.
3 ESA SP-361 // P 393 VOL. 1
4 -
5 PAPER IN PROC. OF THE 'SECOND ERS-1 SYMPOSIUM: SPACE AT THE SERVICE OF OUR ENVIRONMENT', PROCEEDINGS OF A SYMPOSIUM HELD IN HAMBURG, GERMANY, 11-14 OCTOBER 1993 (INDEXED UNDER 43)

* 940142E X SP 361 43
1 MONITORING THE TEMPORAL BEHAVIOUR OF LAND SURFACES WITH ERS-1 WIND SCATTEROMETER DATA (JANUARY 1994)
2 WIESMANN A. & MAETZLER C.
3 ESA SP-361 // P 399 VOL. 1
4 -
5 PAPER IN PROC. OF THE 'SECOND ERS-1 SYMPOSIUM: SPACE AT THE SERVICE OF OUR ENVIRONMENT', PROCEEDINGS OF A SYMPOSIUM HELD IN HAMBURG, GERMANY, 11-14 OCTOBER 1993 (INDEXED UNDER 43)

esa SP - 361
Volume II

Proceedings of the Second ERS-1 Symposium

SPACE AT THE SERVICE OF OUR ENVIRONMENT

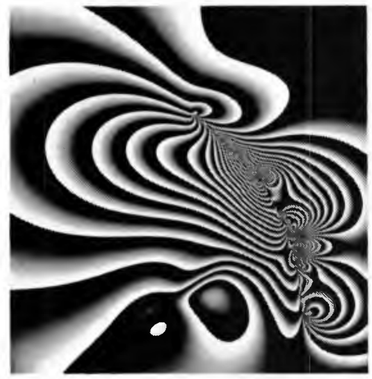

11-14 October 1993
Hamburg, Germany

esa
european space agency

* 940143E X SP 361 43
1 RADAR SIGNATURES OF LAND SURFACES MEASURED BY THE ERS-1 SCATTEROMETER (JANUARY 1994)
2 WISMANN V., BOEHNKE K. & SCHMULLIUS C.
3 ESA SP-361 // P 405 VOL. 1
4 -
5 PAPER IN PROC. OF THE 'SECOND ERS-1 SYMPOSIUM: SPACE AT THE SERVICE OF OUR ENVIRONMENT', PROCEEDINGS OF A SYMPOSIUM HELD IN HAMBURG, GERMANY, 11-14 OCTOBER 1993 (INDEXED UNDER 43)

* 940144E X SP 361 43
1 MAPPING COASTAL CURRENTS WITH SAR USING NATURALLY-OCCURRING SURFACE SLICK PATTERNS (JANUARY 1994)
2 GOWER J.F.R.
3 ESA SP-361 // P 415 VOL. 1
4 -
5 PAPER IN PROC. OF THE 'SECOND ERS-1 SYMPOSIUM: SPACE AT THE SERVICE OF OUR ENVIRONMENT', PROCEEDINGS OF A SYMPOSIUM HELD IN HAMBURG, GERMANY, 11-14 OCTOBER 1993 (INDEXED UNDER 43)

* 940145E X SP 361 43
1 TWO YEAR RESULTS OF ARTIFICIAL OIL POLLUTION DETECTION EXPERIMENTS IN THE SEA ADJACENT TO JAPAN BY ERS-1 SAR (JANUARY 1994)
2 OKAMOTO K. ET AL.
3 ESA SP-361 // P 419 VOL. 1
4 -
5 PAPER IN PROC. OF THE 'SECOND ERS-1 SYMPOSIUM: SPACE AT THE SERVICE OF OUR ENVIRONMENT', PROCEEDINGS OF A SYMPOSIUM HELD IN HAMBURG, GERMANY, 11-14 OCTOBER 1993 (INDEXED UNDER 43)

* 940146E X SP 361 43
1 OPERATIONAL USE OF 'REAL-TIME' ERS-1 SAR DATA FOR OIL SPILL DETECTION ON THE NORTH SEA. FIRST RESULTS (JANUARY 1994)
2 PELLEMANS A.H.J.M. ET AL.
3 ESA SP-361 // P 425 VOL. 1
4 -
5 PAPER IN PROC. OF THE 'SECOND ERS-1 SYMPOSIUM: SPACE AT THE SERVICE OF OUR ENVIRONMENT', PROCEEDINGS OF A SYMPOSIUM HELD IN HAMBURG, GERMANY, 11-14 OCTOBER 1993 (INDEXED UNDER 43)

* 940147E X SP 361 43
1 OIL SPILL DETECTION AND MONITORING WITH THE ERS-1 SAR (JANUARY 1994)
2 WISMANN V.
3 ESA SP-361 // P 431 VOL. 1
4 -
5 PAPER IN PROC. OF THE 'SECOND ERS-1 SYMPOSIUM: SPACE AT THE SERVICE OF OUR ENVIRONMENT', PROCEEDINGS OF A SYMPOSIUM HELD IN HAMBURG, GERMANY, 11-14 OCTOBER 1993 (INDEXED UNDER 43)

* 940148E X SP 361 43
1 EVALUATING MULTI-TEMPORAL ERS-1 SAR DATA FOR TROPICAL FOREST MAPPING: DATA SELECTION, PROCESSING AND TARGET IDENTIFICATION (JANUARY 1994)
2 CONWAY J,A,, LEYSEN M. & SIEBER A.J.
3 ESA SP-361 // P 441 VOL. 1
4 -
5 PAPER IN PROC. OF THE 'SECOND ERS-1 SYMPOSIUM: SPACE AT THE SERVICE OF OUR ENVIRONMENT', PROCEEDINGS OF A SYMPOSIUM HELD IN HAMBURG, GERMANY, 11-14 OCTOBER 1993 (INDEXED UNDER 43)

* 940149E X SP 361 43
1 EVALUATING MULTI-TEMPORAL ERS-1 SAR DATA FOR TROPICAL FOREST MAPPING: REGIONAL MAPPING AND CHANGE DETECTION APPLICATIONS (JANUARY 1994)
2 LEYSEN M., CONWAY J.A. & SIEBER A.J.
3 ESA SP-361 // P 447 VOL. 1
4 -
5 PAPER IN PROC. OF THE 'SECOND ERS-1 SYMPOSIUM: SPACE AT THE SERVICE OF OUR ENVIRONMENT', PROCEEDINGS OF A SYMPOSIUM HELD IN HAMBURG, GERMANY, 11-14 OCTOBER 1993 (INDEXED UNDER 43)

* 940150E X SP 361 43
1 AN APPLICATION OF ERS-1 IMAGES FOR FORSET DAMAGE ASSESSMENT (JANUARY 1994)
2 CIOLKOSZ A., ZAWILA-NIEDZWIECKI T. & BOCHENEK Z.
3 ESA SP-361 // P 453 VOL. 1
4 -
5 PAPER IN PROC. OF THE 'SECOND ERS-1 SYMPOSIUM: SPACE AT THE SERVICE OF OUR ENVIRONMENT', PROCEEDINGS OF A SYMPOSIUM HELD IN HAMBURG, GERMANY, 11-14 OCTOBER 1993 (INDEXED UNDER 43)

* 940151E X SP 361 43
1 CHARACTERISATION OF AUSTRALIAN VEGETATION TYPES USING ERS-1 SAR (JANUARY 1994)
2 MILNE A.K.
3 ESA SP-361 // P 459 VOL. 1
4 -
5 PAPER IN PROC. OF THE 'SECOND ERS-1 SYMPOSIUM: SPACE AT THE SERVICE OF OUR ENVIRONMENT', PROCEEDINGS OF A SYMPOSIUM HELD IN HAMBURG, GERMANY, 11-14 OCTOBER 1993 (INDEXED UNDER 43)

* 940152E X SP 361 43
1 SAR OBSERVATIONS AND BACKSCATTER MODELLING OF AUSTRALIAN NATIVE FORESTS (JANUARY 1994)
2 RICHARDS J.A., DONG Y. & CASHMAN J.D.
3 ESA SP-361 // P 463 VOL. 1
4 -
5 PAPER IN PROC. OF THE 'SECOND ERS-1 SYMPOSIUM: SPACE AT THE SERVICE OF OUR ENVIRONMENT', PROCEEDINGS OF A SYMPOSIUM HELD IN HAMBURG, GERMANY, 11-14 OCTOBER 1993 (INDEXED UNDER 43)

* 940153E X SP 361 43
1 SCOPE AND FIRST RESULTS OF ERS-1 PILOT PROJECT TRULI: TROPICAL RAIN FOREST AND USE OF LAND INVESTIGATION (JANUARY 1994)
2 SIEGERT F., WANNINGER A. & FUCHS U.
3 ESA SP-361 // P 469 VOL. 1
4 -
5 PAPER IN PROC. OF THE 'SECOND ERS-1 SYMPOSIUM: SPACE AT THE SERVICE OF OUR ENVIRONMENT', PROCEEDINGS OF A SYMPOSIUM HELD IN HAMBURG, GERMANY, 11-14 OCTOBER 1993 (INDEXED UNDER 43)

* 940154E X SP 361 43
1 ERS-1 SAR INTERFEROMETRY OVER FORESTED TERRAIN (JANUARY 1994)
2 ULANDER L.M.H., HAGBERG J.O. & J. ASKNE
3 ESA SP-361 // P 475 VOL. 1
4 -
5 PAPER IN PROC. OF THE 'SECOND ERS-1 SYMPOSIUM: SPACE AT THE SERVICE OF OUR ENVIRONMENT', PROCEEDINGS OF A SYMPOSIUM HELD IN HAMBURG, GERMANY, 11-14 OCTOBER 1993 (INDEXED UNDER 43)

* 940155E X SP 361 43
1 TROPICAL RAINFOREST INVESTIGATION IN BRAZIL USING ERS-1 SAR DATA (JANUARY 1994)
2 KEIL M., WINTER R. & HONSCH H.
3 ESA SP-361 // P 481 VOL. 1
4 -
5 PAPER IN PROC. OF THE 'SECOND ERS-1 SYMPOSIUM: SPACE AT THE SERVICE OF OUR ENVIRONMENT', PROCEEDINGS OF A SYMPOSIUM HELD IN HAMBURG, GERMANY, 11-14 OCTOBER 1993 (INDEXED UNDER 43)

* 940156E X SP 361 43
1 OCEANOGRAPHIC RESULTS FROM ANALYSIS OF ERS-1 ALTIMETRY (JANUARY 1994)
2 TAPLEY B.D ET AL.
3 ESA SP-361 // P 489 VOL. 1
4 -
5 PAPER IN PROC. OF THE 'SECOND ERS-1 SYMPOSIUM: SPACE AT THE SERVICE OF OUR ENVIRONMENT', PROCEEDINGS OF A SYMPOSIUM HELD IN HAMBURG, GERMANY, 11-14 OCTOBER 1993 (INDEXED UNDER 43)

* 940157E X SP 361 43
1 THE 1991-93 LOS NINOS FROM ERS-1 ALTIMETRY (JANUARY 1994)
2 LILLIBRIDGE J., CHENEY B & DOYLE N.
3 ESA SP-361 // P 495 VOL. 1
4 -
5 PAPER IN PROC. OF THE 'SECOND ERS-1 SYMPOSIUM: SPACE AT THE SERVICE OF OUR ENVIRONMENT', PROCEEDINGS OF A SYMPOSIUM HELD IN HAMBURG, GERMANY, 11-14 OCTOBER 1993 (INDEXED UNDER 43)

* 940158E X SP 361 43
1 OCEAN DYNAMICS FROM THE ERS-1 35-DAY REPEAT MISSION (JANUARY 1994)
2 NAEIJE M.C. ET AL.
3 ESA SP-361 // P 501 VOL. 1
4 -
5 PAPER IN PROC. OF THE 'SECOND ERS-1 SYMPOSIUM: SPACE AT THE SERVICE OF OUR ENVIRONMENT', PROCEEDINGS OF A SYMPOSIUM HELD IN HAMBURG, GERMANY, 11-14 OCTOBER 1993 (INDEXED UNDER 43)

* 940159E X SP 361 43
1 RADAR SIGNATURES OF EQUATORIAL UPWELLING REGIONS MEASURED BY THE ERS-1 SCATTEROMETER (JANUARY 1994)
2 BOEHNKE K. & WISMANN V.
3 ESA SP-361 // P 507 VOL. 1
4 -
5 PAPER IN PROC. OF THE 'SECOND ERS-1 SYMPOSIUM: SPACE AT THE SERVICE OF OUR ENVIRONMENT', PROCEEDINGS OF A SYMPOSIUM HELD IN HAMBURG, GERMANY, 11-14 OCTOBER 1993 (INDEXED UNDER 43)

* 940160E X SP 361 43
1 SEA SURFACE HEIGHT AND ITS VARIATION FROM ERS-1 ALTIMETER DATA (JANUARY 1994)
2 GANEKO Y. ET AL.
3 ESA SP-361 // P 513 VOL. 1
4 -
5 PAPER IN PROC. OF THE 'SECOND ERS-1 SYMPOSIUM: SPACE AT THE SERVICE OF OUR ENVIRONMENT', PROCEEDINGS OF A SYMPOSIUM HELD IN HAMBURG, GERMANY, 11-14 OCTOBER 1993 (INDEXED UNDER 43)

* 940161E X SP 361 43
1 SEA LEVEL VARIATIONS IN THE TROPICAL PACIFIC DURING 1992-1993 DERIVED FROM ERS-1 ALTIMETRY (JANUARY 1994)
2 ZOU J. & BURKERT R.
3 ESA SP-361 // P 519 VOL. 1
4 -
5 PAPER IN PROC. OF THE 'SECOND ERS-1 SYMPOSIUM: SPACE AT THE SERVICE OF OUR ENVIRONMENT', PROCEEDINGS OF A SYMPOSIUM HELD IN HAMBURG, GERMANY, 11-14 OCTOBER 1993 (INDEXED UNDER 43)

* 940162E X SP 361 43
1 TROPICAL PACIFIC SEA-SURFACE TEMPERATURE IN AN OCEAN GENERAL CIRCULATION MODEL AND AS MEASURED BY THE ATSR (JANUARY 1994)
2 MURRAY J. ET AL
3 ESA SP-361 // P 523 VOL. 1
4 -
5 PAPER IN PROC. OF THE 'SECOND ERS-1 SYMPOSIUM: SPACE AT THE SERVICE OF OUR ENVIRONMENT', PROCEEDINGS OF A SYMPOSIUM HELD IN HAMBURG, GERMANY, 11-14 OCTOBER 1993 (INDEXED UNDER 43)

* 940163E X SP 361 43
1 AN INVESTIGATION OF INTRASEASONAL VARIABILITY IN SEA-SURFACE TEMPERATURE IN THE TROPICAL PACIFIC USING DATA FROM THE ATSR (JANUARY 1994)
2 MURRAY J. ET AL.
3 ESA SP-361 // P 529 VOL. 1
4 -
5 PAPER IN PROC. OF THE 'SECOND ERS-1 SYMPOSIUM: SPACE AT THE SERVICE OF OUR ENVIRONMENT', PROCEEDINGS OF A SYMPOSIUM HELD IN HAMBURG, GERMANY, 11-14 OCTOBER 1993 (INDEXED UNDER 43)

* 940164E X SP 361 43
1 HIGH FREQUENCY SPACE-TIME VARIABILITY OF THE GULF STREAM AND KUROSHIO USING ERS-1 ALTIMETER DATA (JANUARY 1994)
2 MINSTER J-F. & GENNERO M-C.
3 ESA SP-361 // P 535 VOL. 1
4 -
5 PAPER IN PROC. OF THE 'SECOND ERS-1 SYMPOSIUM: SPACE AT THE SERVICE OF OUR ENVIRONMENT', PROCEEDINGS OF A SYMPOSIUM HELD IN HAMBURG, GERMANY, 11-14 OCTOBER 1993 (INDEXED UNDER 43)

* 940165E X SP 361 43
1 A STUDY ON THE INFLOW OF ATLANTIC WATER TO THE GIN SEA USING ALTIMETER DATA (JANUARY 1994)
2 SAMUEL P., JOHANNESSEN J.A. & JOHANNESSEN O.M.
3 ESA SP-361 // P 541 VOL. 1
4 -
5 PAPER IN PROC. OF THE 'SECOND ERS-1 SYMPOSIUM: SPACE AT THE SERVICE OF OUR ENVIRONMENT', PROCEEDINGS OF A SYMPOSIUM HELD IN HAMBURG, GERMANY, 11-14 OCTOBER 1993 (INDEXED UNDER 43)

* 940166E X SP 361 43
1 LARGE AND SMALL SCALE CIRCULATION SIGNATURES OF THE ERS-1 SAR OVER THE GULF STREAM (JANUARY 1994)
2 BEAL R.C. ET AL.
3 ESA SP-361 // P 547 VOL. 1
4 -
5 PAPER IN PROC. OF THE 'SECOND ERS-1 SYMPOSIUM: SPACE AT THE SERVICE OF OUR ENVIRONMENT', PROCEEDINGS OF A SYMPOSIUM HELD IN HAMBURG, GERMANY, 11-14 OCTOBER 1993 (INDEXED UNDER 43)

* 940167E X SP 361 43
1 DYNAMICAL OCEANOGRAPHY OF THE BRANSFIELD STRAIT (ANTARCTICA) DURING AUSTRAL SUMMER 1992/93: AN APPLICATION OF ERS-1 PRODUCTS (JANUARY 1994)
2 GARCIA M.A. ET AL
3 ESA SP-361 // P 553 VOL. 1
4 -
5 PAPER IN PROC. OF THE 'SECOND ERS-1 SYMPOSIUM: SPACE AT THE SERVICE OF OUR ENVIRONMENT', PROCEEDINGS OF A SYMPOSIUM HELD IN HAMBURG, GERMANY, 11-14 OCTOBER 1993 (INDEXED UNDER 43)

* 940168E X SP 361 43
1 DETECTION OF ARABIAN SEA EDDY USING ERS-1 ALTIMETER DATA (JANUARY 1994)
2 ALI M.M. & SHARMA R.
3 ESA SP-361 // P 557 VOL. 1
4 -
5 PAPER IN PROC. OF THE 'SECOND ERS-1 SYMPOSIUM: SPACE AT THE SERVICE OF OUR ENVIRONMENT', PROCEEDINGS OF A SYMPOSIUM HELD IN HAMBURG, GERMANY, 11-14 OCTOBER 1993 (INDEXED UNDER 43)

* 940169E X SP 361 43
1 DETECTION OF SURFACE CURRENT FEATURES WITH ERS-1 SAR (JANUARY 1994)
2 JOHANNESSEN J.A. ET AL.
3 ESA SP-361 // P 565 VOL. 1
4 -
5 PAPER IN PROC. OF THE 'SECOND ERS-1 SYMPOSIUM: SPACE AT THE SERVICE OF OUR ENVIRONMENT', PROCEEDINGS OF A SYMPOSIUM HELD IN HAMBURG, GERMANY, 11-14 OCTOBER 1993 (INDEXED UNDER 43)

* 940170E X SP 361 43
1 USE OF ERS-1 SCATTEROMETER DATA IN NUMERICAL MODELS (JANUARY 1994)
2 BORZELLI G. ET AL.
3 ESA SP-361 // P 571 VOL. 1
4 -
5 PAPER IN PROC. OF THE 'SECOND ERS-1 SYMPOSIUM: SPACE AT THE SERVICE OF OUR ENVIRONMENT', PROCEEDINGS OF A SYMPOSIUM HELD IN HAMBURG, GERMANY, 11-14 OCTOBER 1993 (INDEXED UNDER 43)

* 940171E X SP 361 43
1 MESOSCALE VARIABILITY REVEALED BY ERS-1 ALTIMETER FDC AND OPR AND ITS ASSIMILATION INTO A NUMERICAL OCEAN MODEL (JANUARY 1994)
2 IKEDA M.
3 ESA SP-361 // P 577 VOL. 1
4 -
5 PAPER IN PROC. OF THE 'SECOND ERS-1 SYMPOSIUM: SPACE AT THE SERVICE OF OUR ENVIRONMENT', PROCEEDINGS OF A SYMPOSIUM HELD IN HAMBURG, GERMANY, 11-14 OCTOBER 1993 (INDEXED UNDER 43)

* 940172E X SP 361 43
1 MESOSCALE CIRCULATION IN THE SOUTHERN OCEAN AS OBSERVED BY SATELLITE ALTIMETRY (JANUARY 1994)
2 SNAITH H.M.
3 ESA SP-361 // P 581 VOL. 1
4 -
5 PAPER IN PROC. OF THE 'SECOND ERS-1 SYMPOSIUM: SPACE AT THE SERVICE OF OUR ENVIRONMENT', PROCEEDINGS OF A SYMPOSIUM HELD IN HAMBURG, GERMANY, 11-14 OCTOBER 1993 (INDEXED UNDER 43)

* 940173E X SP 361 43
1 A SIGNAL FROM THE SOUTHERN OCEAN, DETECTABLE BY ALTIMETRY (JANUARY 1994)
2 HUGHES C.W., VASSIE J.M. & SMITHSON M.J.
3 ESA SP-361 // P 587 VOL. 1
4 -
5 PAPER IN PROC. OF THE 'SECOND ERS-1 SYMPOSIUM: SPACE AT THE SERVICE OF OUR ENVIRONMENT', PROCEEDINGS OF A SYMPOSIUM HELD IN HAMBURG, GERMANY, 11-14 OCTOBER 1993 (INDEXED UNDER 43)

* 940174E X SP 361 43
1 THE SUITABILITY OF ERS-1 RADAR-ALTIMETER DATA FOR OCEANOGRAPHIC AND GEODETIC APPLICATIONS FOR THE BALTIC SEA (JANUARY 1994)
2 METZNER M., GRAFAREND E.W. & DICK S.
3 ESA SP-361 // P 591 VOL. 1
4 -
5 PAPER IN PROC. OF THE 'SECOND ERS-1 SYMPOSIUM: SPACE AT THE SERVICE OF OUR ENVIRONMENT', PROCEEDINGS OF A SYMPOSIUM HELD IN HAMBURG, GERMANY, 11-14 OCTOBER 1993 (INDEXED UNDER 43)

* 940175E X SP 361 43
1 DETERMINATION OF ERS-1'S SEA-STATE BIAS FROM INSTANCES OF RAPID CHANGE IN WAVE HEIGHT (JANUARY 1994)
2 SROKOSZ M.A. & QUARTLY G.D.
3 ESA SP-361 // P 597 VOL. 1
4 -
5 PAPER IN PROC. OF THE 'SECOND ERS-1 SYMPOSIUM: SPACE AT THE SERVICE OF OUR ENVIRONMENT', PROCEEDINGS OF A SYMPOSIUM HELD IN HAMBURG, GERMANY, 11-14 OCTOBER 1993 (INDEXED UNDER 43)

* 940176E X SP 361 43
1 HEIGHTING FROM STEREOSCOPIC ERS-1 DATA (JANUARY 1994)
2 DOWMAN, I.J. ET AL.
3 ESA SP-361 // P 609 VOL. 1
4 -
5 PAPER IN PROC. OF THE 'SECOND ERS-1 SYMPOSIUM: SPACE AT THE SERVICE OF OUR ENVIRONMENT', PROCEEDINGS OF A SYMPOSIUM HELD IN HAMBURG, GERMANY, 11-14 OCTOBER 1993 (INDEXED UNDER 43)

* 940177E X SP 361 43
1 LAND COVER CHANGE DETECTION WITH ERS-1 DATA AND DATA FROM OTHER REMOTE SENSING SATELLITES. EXAMPLE: THE DELTA OF THE RIVER EBRO (SPAIN) (JANUARY 1994)
2 HARMS J. & ARIZZA F.
3 ESA SP-361 // P 615 VOL. 1
4 -
5 PAPER IN PROC. OF THE 'SECOND ERS-1 SYMPOSIUM: SPACE AT THE SERVICE OF OUR ENVIRONMENT', PROCEEDINGS OF A SYMPOSIUM HELD IN HAMBURG, GERMANY, 11-14 OCTOBER 1993 (INDEXED UNDER 43)

* 940178E X SP 361 43
1 ERS-1 SAR AND OPTICAL DATA FOR LAND USE/LAND COVER MAPPING: A CASE STUDY IN A SAVANNAH ZONE OF GUINEA (JANUARY 1994)
2 DALLEMAND J.F. ET AL.
3 ESA SP-361 // P 617 VOL. 1
4 -
5 PAPER IN PROC. OF THE 'SECOND ERS-1 SYMPOSIUM: SPACE AT THE SERVICE OF OUR ENVIRONMENT', PROCEEDINGS OF A SYMPOSIUM HELD IN HAMBURG, GERMANY, 11-14 OCTOBER 1993 (INDEXED UNDER 43)

* 940179E X SP 361 43
1 THE STRUCTURAL CONTENT OF ERS-1 IMAGES AND ITS IMPLICATIONS (JANUARY 1994)
2 QUEGAN S., CAVES R.G. & WHITE R.G.
3 ESA SP-361 // P 623 VOL. 1
4 -
5 PAPER IN PROC. OF THE 'SECOND ERS-1 SYMPOSIUM: SPACE AT THE SERVICE OF OUR ENVIRONMENT', PROCEEDINGS OF A SYMPOSIUM HELD IN HAMBURG, GERMANY, 11-14 OCTOBER 1993 (INDEXED UNDER 43)

* 940180E X SP 361 43
1 MOSAICING AND CLASSIFICATION FOR THE RADARMAP GERMANY (JANUARY 1994)
2 KOSMANN D. ET AL.
3 ESA SP-361 // P 629 VOL. 1
4 -
5 PAPER IN PROC. OF THE 'SECOND ERS-1 SYMPOSIUM: SPACE AT THE SERVICE OF OUR ENVIRONMENT', PROCEEDINGS OF A SYMPOSIUM HELD IN HAMBURG, GERMANY, 11-14 OCTOBER 1993 (INDEXED UNDER 43)

* 940181E X SP 361 43
1 HIGH RESOLUTION DETECTION AND MONITORING OF CHANGES USING ERS-1 TIME SERIES (JANUARY 1994)
2 KATTENBORN G. ET AL.
3 ESA SP-361 // P 635 VOL. 1
4 -
5 PAPER IN PROC. OF THE 'SECOND ERS-1 SYMPOSIUM: SPACE AT THE SERVICE OF OUR ENVIRONMENT', PROCEEDINGS OF A SYMPOSIUM HELD IN HAMBURG, GERMANY, 11-14 OCTOBER 1993 (INDEXED UNDER 43)

* 940182E X SP 361 43
1 THE OEEPE/GEOSAR TEST OF GEOCODING ERS-1 DATA BACKGROUND AND STATUS (JANUARY 1994)
2 DOWMAN I.
3 ESA SP-361 // P 643 VOL. 1
4 -
5 PAPER IN PROC. OF THE 'SECOND ERS-1 SYMPOSIUM: SPACE AT THE SERVICE OF OUR ENVIRONMENT', PROCEEDINGS OF A SYMPOSIUM HELD IN HAMBURG, GERMANY, 11-14 OCTOBER 1993 (INDEXED UNDER 43)

* 940183E X SP 361 43
1 FOREST AND CROP MONITORING: EXPERIENCES WITH ERS-1 IN BELGIUM (JANUARY 1994)
2 DE ROOVER B.P.E., DE MULDER S.C. & GOOSSENS R.E.
3 ESA SP-361 // P 647 VOL. 1
4 -
5 PAPER IN PROC. OF THE 'SECOND ERS-1 SYMPOSIUM: SPACE AT THE SERVICE OF OUR ENVIRONMENT', PROCEEDINGS OF A SYMPOSIUM HELD IN HAMBURG, GERMANY, 11-14 OCTOBER 1993 (INDEXED UNDER 43)

* 940184E X SP 361 43
1 GEOCODING SPOT PRODUCTS WITH ERS-1 SAR GEOMETRY (JANUARY 1994)
2 RENOUARD L. & PERLANT F.
3 ESA SP-361 // P 653 VOL. 1
4 -
5 PAPER IN PROC. OF THE 'SECOND ERS-1 SYMPOSIUM: SPACE AT THE SERVICE OF OUR ENVIRONMENT', PROCEEDINGS OF A SYMPOSIUM HELD IN HAMBURG, GERMANY, 11-14 OCTOBER 1993 (INDEXED UNDER 43)

* 940185E X SP 361 43
1 OPERATIONAL USE OF ERS-1 SAR DATA TO MONITOR SEA ICE CONDITIONS IN THE GULF OF ST LAWRENCE (JANUARY 1994)
2 SHOKR M., RAMSAY B. & FALKINGHAM J.C.
3 ESA SP-361 // P 663 VOL. 1
4 -
5 PAPER IN PROC. OF THE 'SECOND ERS-1 SYMPOSIUM: SPACE AT THE SERVICE OF OUR ENVIRONMENT', PROCEEDINGS OF A SYMPOSIUM HELD IN HAMBURG, GERMANY, 11-14 OCTOBER 1993 (INDEXED UNDER 43)

* 940186E X SP 361 43
1 COASTWATCH SAR APPLICATIONS DEMONSTRATION - DEVELOPMENT PHASE (JANUARY 1994)
2 PICHEL W. ET AL.
3 ESA SP-361 // P 669 VOL. 1
4 -
5 PAPER IN PROC. OF THE 'SECOND ERS-1 SYMPOSIUM: SPACE AT THE SERVICE OF OUR ENVIRONMENT', PROCEEDINGS OF A SYMPOSIUM HELD IN HAMBURG, GERMANY, 11-14 OCTOBER 1993 (INDEXED UNDER 43)

* 940187E X SP 361 43
1 GREAT LAKES SAR ICE RESEARCH APPLICATIONS DEMONSTRATION (JANUARY 1994)
2 LESHKEVICH G., PICHEL W. & CLEMENTE-COLON P.
3 ESA SP-361 // P 675 VOL. 1
4 -
5 PAPER IN PROC. OF THE 'SECOND ERS-1 SYMPOSIUM: SPACE AT THE SERVICE OF OUR ENVIRONMENT', PROCEEDINGS OF A SYMPOSIUM HELD IN HAMBURG, GERMANY, 11-14 OCTOBER 1993 (INDEXED UNDER 43)

* 940188E X SP 361 43
1 REAL TIME ICE MONITORING IN THE BALTIC SEA (JANUARY 1994)
2 HERLAND E.A.
3 ESA SP-361 // P 681 VOL. 1
4 -
5 PAPER IN PROC. OF THE 'SECOND ERS-1 SYMPOSIUM: SPACE AT THE SERVICE OF OUR ENVIRONMENT', PROCEEDINGS OF A SYMPOSIUM HELD IN HAMBURG, GERMANY, 11-14 OCTOBER 1993 (INDEXED UNDER 43)

* 940189E X SP 361 43
1 USE OF THE SPECTRAL SHIFT IN SAR INTERFEROMETRY (JANUARY 1994)
2 PRATI C. & ROCCA F.
3 ESA SP-361 // P 691 VOL. 2
4 -
5 PAPER IN PROC. OF THE 'SECOND ERS-1 SYMPOSIUM: SPACE AT THE SERVICE OF OUR ENVIRONMENT', PROCEEDINGS OF A SYMPOSIUM HELD IN HAMBURG, GERMANY, 11-14 OCTOBER 1993 (INDEXED UNDER 43)

* 940190E X SP 361 43
1 INFORMATION EXTRACTION FROM ERS-1 SAR DATA BY MEANS OF INSAR AND D-INSAR TECHNIQUES IN ANTARCTIC RESEARCH (JANUARY 1994)
2 HARTL PH., THIEL K-H. & WU X.
3 ESA SP-361 // P 697 VOL. 2
4 -
5 PAPER IN PROC. OF THE 'SECOND ERS-1 SYMPOSIUM: SPACE AT THE SERVICE OF OUR ENVIRONMENT', PROCEEDINGS OF A SYMPOSIUM HELD IN HAMBURG, GERMANY, 11-14 OCTOBER 1993 (INDEXED UNDER 43)

* 940191E X SP 361 43
1 VALIDATION OF ERS-1 INTERFEROMETRY AT CNES (JANUARY 1994)
2 MASSONET D.
3 ESA SP-361 // P 703 VOL. 2
4 -
5 PAPER IN PROC. OF THE 'SECOND ERS-1 SYMPOSIUM: SPACE AT THE SERVICE OF OUR ENVIRONMENT', PROCEEDINGS OF A SYMPOSIUM HELD IN HAMBURG, GERMANY, 11-14 OCTOBER 1993 (INDEXED UNDER 43)

* 940192E X SP 361 43
1 DERIVATION OF TERRAIN SLOPE FROM SAR INTERFEROMETRIC PHASE GRADIENT (JANUARY 1994)
2 WEGMULLER U., WERNER C.;. & ROSEN P.A.
3 ESA SP-361 // P 711 VOL. 2
4 -
5 PAPER IN PROC. OF THE 'SECOND ERS-1 SYMPOSIUM: SPACE AT THE SERVICE OF OUR ENVIRONMENT', PROCEEDINGS OF A SYMPOSIUM HELD IN HAMBURG, GERMANY, 11-14 OCTOBER 1993 (INDEXED UNDER 43)

* 940193E X SP 361 43
1 PRACTICAL APPLICATION OF SAR INTERFEROMETRY: EXPERIENCES MADE BY THE INSTITUTE OF NAVIGATION (JANUARY 1994)
2 HARTL PH. ET AL.
3 ESA SP-361 // P 717 VOL. 2
4 -
5 PAPER IN PROC. OF THE 'SECOND ERS-1 SYMPOSIUM: SPACE AT THE SERVICE OF OUR ENVIRONMENT', PROCEEDINGS OF A SYMPOSIUM HELD IN HAMBURG, GERMANY, 11-14 OCTOBER 1993 (INDEXED UNDER 43)

* 940194E X SP 361 43
1 APPLICATIONS OF INTERFEROMETRICALLY DERIVED TERRAIN SLOPES: NORMALIZATION OF SAR BACKSCATTER AND THE INTERFEROMETRIC CORRELATION COEFFICIENT (JANUARY 1994)
2 WERNER C.L. WEGMULLER U. & SMALL D.L.
3 ESA SP-361 // P 723 VOL. 2
4 -
5 PAPER IN PROC. OF THE 'SECOND ERS-1 SYMPOSIUM: SPACE AT THE SERVICE OF OUR ENVIRONMENT', PROCEEDINGS OF A SYMPOSIUM HELD IN HAMBURG, GERMANY, 11-14 OCTOBER 1993 (INDEXED UNDER 43)

* 940195E X SP 361 43
1 SAR INTERFEROMETRY: EXPERIENCES WITH VARIOUS PHASE UNWRAPPING METHODS (JANUARY 1994)
2 HARTL P. & XIAOQING WU
3 ESA SP-361 // P 727 VOL. 2
4 -
5 PAPER IN PROC. OF THE 'SECOND ERS-1 SYMPOSIUM: SPACE AT THE SERVICE OF OUR ENVIRONMENT', PROCEEDINGS OF A SYMPOSIUM HELD IN HAMBURG, GERMANY, 11-14 OCTOBER 1993 (INDEXED UNDER 43)

* 940196E X SP 361 43
1 THE ORBIT DETERMINATION ACCURACY OF THE ERS-1 MISSION (JANUARY 1994)
2 SCHARROO R, WAKKER K.F. & METS G.J.
3 ESA SP-361 // P 735 VOL. 2
4 -
5 PAPER IN PROC. OF THE 'SECOND ERS-1 SYMPOSIUM: SPACE AT THE SERVICE OF OUR ENVIRONMENT', PROCEEDINGS OF A SYMPOSIUM HELD IN HAMBURG, GERMANY, 11-14 OCTOBER 1993 (INDEXED UNDER 43)

* 940197E X SP 361 43
1 ERS-1 ORBIT CALCULATION WITH THE GEOSAT SOFTWARE (JANUARY 1994)
2 AKSNES H. ET AL.
3 ESA SP-361 // P 741 VOL. 2
4 -
5 PAPER IN PROC. OF THE 'SECOND ERS-1 SYMPOSIUM: SPACE AT THE SERVICE OF OUR ENVIRONMENT', PROCEEDINGS OF A SYMPOSIUM HELD IN HAMBURG, GERMANY, 11-14 OCTOBER 1993 (INDEXED UNDER 43)

* 940198E X SP 361 43
1 PRECISE ORBIT ANALYSIS AND GLOBAL VERIFICATION RESULTS FROM ERS-1 ALTIMETRY (JANUARY 1994)
2 SHUM C.K. ET AL.
3 ESA SP-361 // P 747 VOL. 2
4 -
5 PAPER IN PROC. OF THE 'SECOND ERS-1 SYMPOSIUM: SPACE AT THE SERVICE OF OUR ENVIRONMENT', PROCEEDINGS OF A SYMPOSIUM HELD IN HAMBURG, GERMANY, 11-14 OCTOBER 1993 (INDEXED UNDER 43)

* 940199E X SP 361 43
1 IMPROVEMENT OF RADIAL POSITIONING OF ERS-1 THROUGH DUAL CROSSOVER ANALYSIS WITH TOPEX-POSEIDON (JANUARY 1994)
2 CARNOCHAN S. ET AL.
3 ESA SP-361 // P 753 VOL. 2
4 -
5 PAPER IN PROC. OF THE 'SECOND ERS-1 SYMPOSIUM: SPACE AT THE SERVICE OF OUR ENVIRONMENT', PROCEEDINGS OF A SYMPOSIUM HELD IN HAMBURG, GERMANY, 11-14 OCTOBER 1993 (INDEXED UNDER 43)

* 940200E X SP 361 43
1 REDUCING ERS-1 ORBIT ERROR USING TOPEX-POSEIDON DATA (JANUARY 1994)
2 LE TRAON P.Y. ET AL.
3 ESA SP-361 // P 759 VOL. 2
4 -
5 PAPER IN PROC. OF THE 'SECOND ERS-1 SYMPOSIUM: SPACE AT THE SERVICE OF OUR ENVIRONMENT', PROCEEDINGS OF A SYMPOSIUM HELD IN HAMBURG, GERMANY, 11-14 OCTOBER 1993 (INDEXED UNDER 43)

* 940201E X SP 361 43
1 ERS-1 ORBIT INFORMATION PROVIDED BY D-PAF (JANUARY 1994)
2 MASSMANN F-H. ET AL.
3 ESA SP-361 // P 765 VOL. 2
4 -
5 PAPER IN PROC. OF THE 'SECOND ERS-1 SYMPOSIUM: SPACE AT THE SERVICE OF OUR ENVIRONMENT', PROCEEDINGS OF A SYMPOSIUM HELD IN HAMBURG, GERMANY, 11-14 OCTOBER 1993 (INDEXED UNDER 43)

* 940202E X SP 361 43
1 IMPROVEMENT OF GLOBAL GRAVITY FIELD MODELLING FOR ERS-1 (JANUARY 1994)
2 SCHWINTZER P. ET AL.
3 ESA SP-361 // P 771 VOL. 2
4 -
5 PAPER IN PROC. OF THE 'SECOND ERS-1 SYMPOSIUM: SPACE AT THE SERVICE OF OUR ENVIRONMENT', PROCEEDINGS OF A SYMPOSIUM HELD IN HAMBURG, GERMANY, 11-14 OCTOBER 1993 (INDEXED UNDER 43)

* 940203E X SP 361 43
1 AERODYNAMIC FORCE REFINEMENT TO ERS-1 ORBITS USING ALONG-TRACK ACCELERATIONS FROM DORIS ON SPOT-2 (JANUARY 1994)
2 EHLERS S. & MOORE P.
3 ESA SP-361 // P 777 VOL. 2
4 -
5 PAPER IN PROC. OF THE 'SECOND ERS-1 SYMPOSIUM: SPACE AT THE SERVICE OF OUR ENVIRONMENT', PROCEEDINGS OF A SYMPOSIUM HELD IN HAMBURG, GERMANY, 11-14 OCTOBER 1993 (INDEXED UNDER 43)

* 940204E X SP 361 43
1 D-PAF SEA SURFACE MODELS GENERATED FROM DIFFERENT DATA SOURCES (JANUARY 1994)
2 ANZENHOFER M., GRUBER T. & RENTSCH M.
3 ESA SP-361 // P 783 VOL. 2
4 -
5 PAPER IN PROC. OF THE 'SECOND ERS-1 SYMPOSIUM: SPACE AT THE SERVICE OF OUR ENVIRONMENT', PROCEEDINGS OF A SYMPOSIUM HELD IN HAMBURG, GERMANY, 11-14 OCTOBER 1993 (INDEXED UNDER 43)

* 940205E X SP 361 43
1 M SUBSCRIPT 2 AND S SUBSCRIPT 2 OCEAN TIDE MODELS FOR THE NORTH ATLANTIC AND OCEAN ADJACENT SEAS FROM ERS-1 ALTIMETRY (JANUARY 1994)
2 ANDERSEN O.B.
3 ESA SP-361 // P 789 VOL. 2
4 -
5 PAPER IN PROC. OF THE 'SECOND ERS-1 SYMPOSIUM: SPACE AT THE SERVICE OF OUR ENVIRONMENT', PROCEEDINGS OF A SYMPOSIUM HELD IN HAMBURG, GERMANY, 11-14 OCTOBER 1993 (INDEXED UNDER 43)

* 940206E X SP 361 43
1 DETECTION OF RAIN CELLS IN ALTIMETER RETURNS (JANUARY 1994)
2 QUARTLY G.D., GUYMER T.H. & LAXON S.W.
3 ESA SP-361 // P 799 VOL. 2
4 -
5 PAPER IN PROC. OF THE 'SECOND ERS-1 SYMPOSIUM: SPACE AT THE SERVICE OF OUR ENVIRONMENT', PROCEEDINGS OF A SYMPOSIUM HELD IN HAMBURG, GERMANY, 11-14 OCTOBER 1993 (INDEXED UNDER 43)

* 940207E X SP 361 43
1 DETERMINATION OF WIND SPEED, WIND DIRECTION AND ATMOSPHERIC STRUCTURE USING ERS-1 SAR DATA DURING NORCSEX'91 (JANUARY 1994)
2 SHUCHMAN R. ET AL.
3 ESA SP-361 // P 805 VOL. 2
4 -
5 PAPER IN PROC. OF THE 'SECOND ERS-1 SYMPOSIUM: SPACE AT THE SERVICE OF OUR ENVIRONMENT', PROCEEDINGS OF A SYMPOSIUM HELD IN HAMBURG, GERMANY, 11-14 OCTOBER 1993 (INDEXED UNDER 43)

* 940208E X SP 361 43
1 HIGH LATITUDE MESOSCALE ATMOSPHERIC CIRCULATION FEATURES OBSERVED WITH THE ERS-1 SCATTEROMETER (JANUARY 1994)
2 LACHLAN-COPE T.A. ET AL.
3 ESA SP-361 // P 809 VOL. 2
4 -
5 PAPER IN PROC. OF THE 'SECOND ERS-1 SYMPOSIUM: SPACE AT THE SERVICE OF OUR ENVIRONMENT', PROCEEDINGS OF A SYMPOSIUM HELD IN HAMBURG, GERMANY, 11-14 OCTOBER 1993 (INDEXED UNDER 43)

* 940209E X SP 361 43
1 EXAMPLES OF MESOSCALE METEOROLOGY IN THE MEDITERRANEAN SEA USING ERS-1 SCATTEROMETER DATA (JANUARY 1994)
2 ZECCHETTO S. & BORTOLETTO M.
3 ESA SP-361 // P 815 VOL. 2
4 -
5 PAPER IN PROC. OF THE 'SECOND ERS-1 SYMPOSIUM: SPACE AT THE SERVICE OF OUR ENVIRONMENT', PROCEEDINGS OF A SYMPOSIUM HELD IN HAMBURG, GERMANY, 11-14 OCTOBER 1993 (INDEXED UNDER 43)

* 940210E X SP 361 43
1 WATER VAPOUR RETRIEVALS USING COMBINED ATSR INFRARED AND MICROWAVE DATA (JANUARY 1994)
2 BARTON I.J. ET AL.
3 ESA SP-361 // P 819 VOL. 2
4 -
5 PAPER IN PROC. OF THE 'SECOND ERS-1 SYMPOSIUM: SPACE AT THE SERVICE OF OUR ENVIRONMENT', PROCEEDINGS OF A SYMPOSIUM HELD IN HAMBURG, GERMANY, 11-14 OCTOBER 1993 (INDEXED UNDER 43)

* 940211E X SP 361 43
1 ANALYSIS OF ATMOSPHERIC LEE WAVES NEAR HOPEN (JANUARY 1994)
2 VACHON P.W., JOHANNESSEN O.M. & JOHANNESSEN J.A.
3 ESA SP-361 // P 825 VOL. 2
4 -
5 PAPER IN PROC. OF THE 'SECOND ERS-1 SYMPOSIUM: SPACE AT THE SERVICE OF OUR ENVIRONMENT', PROCEEDINGS OF A SYMPOSIUM HELD IN HAMBURG, GERMANY, 11-14 OCTOBER 1993 (INDEXED UNDER 43)

* 940212E X SP 361 43
1 QUANTITATIVE REMOTE SENSING IN THE 11-MICRON WAVELENGHT REGION USING ATSR (JANUARY 1994)
2 ZAVODY A.M. ET AL.
3 ESA SP-361 // P 829 VOL. 2
4 -
5 PAPER IN PROC. OF THE 'SECOND ERS-1 SYMPOSIUM: SPACE AT THE SERVICE OF OUR ENVIRONMENT', PROCEEDINGS OF A SYMPOSIUM HELD IN HAMBURG, GERMANY, 11-14 OCTOBER 1993 (INDEXED UNDER 43)

* 940213E X SP 361 43
1 ERS-1 SAR FOR MONITORING SOIL MOISTURE AND RIVER FLOODING (JANUARY 1994)
2 BLYTH K., BIGGIN D.S. & RAGAB R.
3 ESA SP-361 // P 839 VOL. 2
4 -
5 PAPER IN PROC. OF THE 'SECOND ERS-1 SYMPOSIUM: SPACE AT THE SERVICE OF OUR ENVIRONMENT', PROCEEDINGS OF A SYMPOSIUM HELD IN HAMBURG, GERMANY, 11-14 OCTOBER 1993 (INDEXED UNDER 43)

* 940214E E SP 361 43
1 USE OF ERS-1 SAR DATA FOR LAND APPLICATIONS (JANUARY 1994)
2 BORGEAUD M. ET AL.
3 ESA SP-361 // P 845 VOL. 2
4 -
5 PAPER IN PROC. OF THE 'SECOND ERS-1 SYMPOSIUM: SPACE AT THE SERVICE OF OUR ENVIRONMENT', PROCEEDINGS OF A SYMPOSIUM HELD IN HAMBURG, GERMANY, 11-14 OCTOBER 1993 (INDEXED UNDER 43)

* 940215E X SP 361 43
1 DETECTING SURFACE ROUGHNESS AND MOISTURE VARIATIONS IN DESERTS (JANUARY 1994)
2 CUDLIP W. ET AL.
3 ESA SP-361 // P 849 VOL. 2
4 -
5 PAPER IN PROC. OF THE 'SECOND ERS-1 SYMPOSIUM: SPACE AT THE SERVICE OF OUR ENVIRONMENT', PROCEEDINGS OF A SYMPOSIUM HELD IN HAMBURG, GERMANY, 11-14 OCTOBER 1993 (INDEXED UNDER 43)

* 940216E X SP 361 43
1 SOIL MOISTURE ESTIMATION USING ERS-1 SAR DATA (JANUARY 1994)
2 VENKATARATNAM L. ET AL.
3 ESA SP-361 // P 855 VOL. 2
4 -
5 PAPER IN PROC. OF THE 'SECOND ERS-1 SYMPOSIUM: SPACE AT THE SERVICE OF OUR ENVIRONMENT', PROCEEDINGS OF A SYMPOSIUM HELD IN HAMBURG, GERMANY, 11-14 OCTOBER 1993 (INDEXED UNDER 43)

* 940217E X SP 361 43
1 CORRELATION BETWEEN SOIL MOISTURE AND THE BACKSCATTERING COEFFICIENT OF ERS-1 DATA (JANUARY 1994)
2 ROMBACH M., DEMIRCAN A. & MAUSER W.
3 ESA SP-361 // P 861 VOL. 2
4 -
5 PAPER IN PROC. OF THE 'SECOND ERS-1 SYMPOSIUM: SPACE AT THE SERVICE OF OUR ENVIRONMENT', PROCEEDINGS OF A SYMPOSIUM HELD IN HAMBURG, GERMANY, 11-14 OCTOBER 1993 (INDEXED UNDER 43)

* 940218E X SP 361 43
1 SOIL MOISTURE BASED ON ERS-1 SAR DATA FOR BIOMASS ASSESSEMENT (JANUARY 1994)
2 DABROWSKA-ZIELINSKA K. ET AL.
3 ESA SP-361 // P 865 VOL. 2
4 -
5 PAPER IN PROC. OF THE 'SECOND ERS-1 SYMPOSIUM: SPACE AT THE SERVICE OF OUR ENVIRONMENT', PROCEEDINGS OF A SYMPOSIUM HELD IN HAMBURG, GERMANY, 11-14 OCTOBER 1993 (INDEXED UNDER 43)

* 940219E X SP 361 43
1 DONNEES MULTI-TEMPORELLES SAR ERS-1 POUR UNE ETUDE ENVIRONNEMENTALE: RECHERCHE DE LA MESURE D'UN PARAMETRE D'HUMIDITE DES SOLS EN ALSACE, FRANCE (JANUARY 1994)
2 FELLAH K. ET AL.
3 ESA SP-361 // P 869 VOL. 2
4 -
5 PAPER IN PROC. OF THE 'SECOND ERS-1 SYMPOSIUM: SPACE AT THE SERVICE OF OUR ENVIRONMENT', PROCEEDINGS OF A SYMPOSIUM HELD IN HAMBURG, GERMANY, 11-14 OCTOBER 1993 (INDEXED UNDER 43)

* 940220E X SP 361 43
1 SOIL MOISTURE ESTIMATION USING ERS-1 SAR DATA (JANUARY 1994)
2 MOHAN S. ET AL.
3 ESA SP-361 // P 875 VOL. 2
4 -
5 PAPER IN PROC. OF THE 'SECOND ERS-1 SYMPOSIUM: SPACE AT THE SERVICE OF OUR ENVIRONMENT', PROCEEDINGS OF A SYMPOSIUM HELD IN HAMBURG, GERMANY, 11-14 OCTOBER 1993 (INDEXED UNDER 43)

* 940221E X SP 361 43
1 REGIONALIZATION OF SOIL PHYSICAL PARAMETERS USING ERS-1 PRI SAR DATA (JANUARY 1994)
2 V. PONCET F. ET AL.
3 ESA SP-361 // P 879 VOL. 2
4 -
5 PAPER IN PROC. OF THE 'SECOND ERS-1 SYMPOSIUM: SPACE AT THE SERVICE OF OUR ENVIRONMENT', PROCEEDINGS OF A SYMPOSIUM HELD IN HAMBURG, GERMANY, 11-14 OCTOBER 1993 (INDEXED UNDER 43)

* 940222E X SP 361 43
1 ON THE RETRIEVAL OF SOIL MOISTURE FROM ERS-1 SAR DATA (JANUARY 1994)
2 LE TOAN T. ET AL.
3 ESA SP-361 // P 883 VOL. 2
4 -
5 PAPER IN PROC. OF THE 'SECOND ERS-1 SYMPOSIUM: SPACE AT THE SERVICE OF OUR ENVIRONMENT', PROCEEDINGS OF A SYMPOSIUM HELD IN HAMBURG, GERMANY, 11-14 OCTOBER 1993 (INDEXED UNDER 43)

* 940223E X SP 361 43
1 ERS-1 SAR DATA FOR GEOECOLOGICAL MONITORING OF A GRASSLAND AREA (JANUARY 1994)
2 PRIETZSCH C. & GROSS H.
3 ESA SP-361 // P 889 VOL. 2
4 -
5 PAPER IN PROC. OF THE 'SECOND ERS-1 SYMPOSIUM: SPACE AT THE SERVICE OF OUR ENVIRONMENT', PROCEEDINGS OF A SYMPOSIUM HELD IN HAMBURG, GERMANY, 11-14 OCTOBER 1993 (INDEXED UNDER 43)

* 940224E X SP 361 43
1 ERS'S SAR: AN AID FOR GEOLOGICAL MAPPING AND MINERAL EXPLORATION IN RAIN FOREST AREAS (JANUARY 1994)
2 DEROIN J-P. ET AL.
3 ESA SP-361 // P 897 VOL. 2
4 -
5 PAPER IN PROC. OF THE 'SECOND ERS-1 SYMPOSIUM: SPACE AT THE SERVICE OF OUR ENVIRONMENT', PROCEEDINGS OF A SYMPOSIUM HELD IN HAMBURG, GERMANY, 11-14 OCTOBER 1993 (INDEXED UNDER 43)

* 940225E X SP 361 43
1 GEOECOLOGICAL INVESTIGATIONS ON LANDSCAPE DEGRADATION IN S.E. PATAGONIA WITH ERS-1 SAR DATA (JANUARY 1994)
2 ENDLICHER W. & HOPPE P.
3 ESA SP-361 // P 903 VOL. 2
4 -
5 PAPER IN PROC. OF THE 'SECOND ERS-1 SYMPOSIUM: SPACE AT THE SERVICE OF OUR ENVIRONMENT', PROCEEDINGS OF A SYMPOSIUM HELD IN HAMBURG, GERMANY, 11-14 OCTOBER 1993 (INDEXED UNDER 43)

* 940226E X SP 361 43
1 APPLICATION OF ERS-1 AND OPTICAL DATA FOR MAPPING OF GEOLOGICAL FEATURES IN ARGENTINA (JANUARY 1994)
2 MEHL H., MILLER H. & REIMER W.
3 ESA SP-361 // P 907 VOL. 2
4 -
5 PAPER IN PROC. OF THE 'SECOND ERS-1 SYMPOSIUM: SPACE AT THE SERVICE OF OUR ENVIRONMENT', PROCEEDINGS OF A SYMPOSIUM HELD IN HAMBURG, GERMANY, 11-14 OCTOBER 1993 (INDEXED UNDER 43)

* 940227E X SP 361 43
1 ERS-1 SAR OBSERVATION OF SALT CRUST DEVELOPMENT IN SOUTHERN TUNISIA (JANUARY 1994)
2 MILLINGTON A.C., WADGE G. & ARCHER D.
3 ESA SP-361 // P 911 VOL. 2
4 -
5 PAPER IN PROC. OF THE 'SECOND ERS-1 SYMPOSIUM: SPACE AT THE SERVICE OF OUR ENVIRONMENT', PROCEEDINGS OF A SYMPOSIUM HELD IN HAMBURG, GERMANY, 11-14 OCTOBER 1993 (INDEXED UNDER 43)

* 940228E X SP 361 43
1 MARINE TERRACES IN PATAGONIA AND THEIR VISUALIZATION IN SATELLITE IMAGES (JANUARY 1994)
2 SCHWAN H. ET AL.
3 ESA SP-361 // P 917 VOL. 2
4 -
5 PAPER IN PROC. OF THE 'SECOND ERS-1 SYMPOSIUM: SPACE AT THE SERVICE OF OUR ENVIRONMENT', PROCEEDINGS OF A SYMPOSIUM HELD IN HAMBURG, GERMANY, 11-14 OCTOBER 1993 (INDEXED UNDER 43)

* 940229E X SP 361 43
1 GEOMORPHIC OBJECTS DETECTED BY ERS-1 SAR IMAGES IN DIFFERENT GEODYNAMIC CONTEXTS (JANUARY 1994)
2 CHOROWICZ J. ET AL.
3 ESA SP-361 // P 923 VOL. 2
4 -
5 PAPER IN PROC. OF THE 'SECOND ERS-1 SYMPOSIUM: SPACE AT THE SERVICE OF OUR ENVIRONMENT', PROCEEDINGS OF A SYMPOSIUM HELD IN HAMBURG, GERMANY, 11-14 OCTOBER 1993 (INDEXED UNDER 43)

* 940230E X SP 361 43
1 GEOLOGICAL POTENTIAL OF ERS-1 SAR DATA: OBSERVATIONS IN PARTS OF ARAVALLI AND THAR DESERT (WESTERN INDIA) (JANUARY 1994)
2 MEHTA N.S. ET AL.
3 ESA SP-361 // P 931 VOL. 2
4 -
5 PAPER IN PROC. OF THE 'SECOND ERS-1 SYMPOSIUM: SPACE AT THE SERVICE OF OUR ENVIRONMENT', PROCEEDINGS OF A SYMPOSIUM HELD IN HAMBURG, GERMANY, 11-14 OCTOBER 1993 (INDEXED UNDER 43)

* 940231E X SP 361 43
1 SIGNIFICATIVITY OF WAVE LENGTH COMPUTATION USING SPATIAL AUTOCORRELATION THEORY ON SAR IMAGE OF ERS-1 (JANUARY 1994)
2 CORNET Y, COMHAIRE A-L. & OZER A.
3 ESA SP-361 // P 941 VOL. 2
4 -
5 PAPER IN PROC. OF THE 'SECOND ERS-1 SYMPOSIUM: SPACE AT THE SERVICE OF OUR ENVIRONMENT', PROCEEDINGS OF A SYMPOSIUM HELD IN HAMBURG, GERMANY, 11-14 OCTOBER 1993 (INDEXED UNDER 43)

* 940232E X SP 361 43
1 MAPPING OF SEA BOTTOM TOPOGRAPHY WITH ERS-1 C-BAND SAR (JANUARY 1994)
2 VOGELZANG J. ET AL.
3 ESA SP-361 // P 945 VOL. 2
4 -
5 PAPER IN PROC. OF THE 'SECOND ERS-1 SYMPOSIUM: SPACE AT THE SERVICE OF OUR ENVIRONMENT', PROCEEDINGS OF A SYMPOSIUM HELD IN HAMBURG, GERMANY, 11-14 OCTOBER 1993 (INDEXED UNDER 43)

* 940233E X SP 361 43
1 ERS-1 SAR IMAGES A SLICK NEAR A SHELF SEA FRONT IN CARDIGAN BAY
2 MATTHEWS J.P., BROWNE D.P. & KENNEDY F.
3 ESA SP-361 // P 949 VOL. 2
4 -
5 PAPER IN PROC. OF THE 'SECOND ERS-1 SYMPOSIUM: SPACE AT THE SERVICE OF OUR ENVIRONMENT', PROCEEDINGS OF A SYMPOSIUM HELD IN HAMBURG, GERMANY, 11-14 OCTOBER 1993 (INDEXED UNDER 43)

* 940234E X SP 361 43
1 ERS-1 SAR DATA ANALYSIS OF THE FRENCH GUYANA COASTAL PLAIN: SOME THEMATIC ASPECTS (JANUARY 1994)
2 RUDANT J.P. ET AL.
3 ESA SP-361 // P 953 VOL. 2
4 -
5 PAPER IN PROC. OF THE 'SECOND ERS-1 SYMPOSIUM: SPACE AT THE SERVICE OF OUR ENVIRONMENT', PROCEEDINGS OF A SYMPOSIUM HELD IN HAMBURG, GERMANY, 11-14 OCTOBER 1993 (INDEXED UNDER 43)

* 940235E X SP 361 43
1 CAPABILITIES OF ERS-1 SAR FOR SNOW AND GLACIER MONITORING IN ALPINE AREAS (JANUARY 1994)
2 ROTT H. & NAGLER T.
3 ESA SP-361 // P 965 VOL. 2
4 -
5 PAPER IN PROC. OF THE 'SECOND ERS-1 SYMPOSIUM: SPACE AT THE SERVICE OF OUR ENVIRONMENT', PROCEEDINGS OF A SYMPOSIUM HELD IN HAMBURG, GERMANY, 11-14 OCTOBER 1993 (INDEXED UNDER 43)

* 940236E X SP 361 43
1 CAPABILITIES AND LIMITATIONS OF ERS-1 SAR DATA FOR SNOW COVER DETERMINATION IN MOUNTAINOUS REGIONS (JANUARY 1994)
2 HAEFNER H. ET AL.
3 ESA SP-361 // P 971 VOL. 2
4 -
5 PAPER IN PROC. OF THE 'SECOND ERS-1 SYMPOSIUM: SPACE AT THE SERVICE OF OUR ENVIRONMENT', PROCEEDINGS OF A SYMPOSIUM HELD IN HAMBURG, GERMANY, 11-14 OCTOBER 1993 (INDEXED UNDER 43)

* 940237E X SP 361 43
1 MICROWAVE REMOTE SENSING OF SNOW USING RADAR AND RADIOMETER (JANUARY 1994)
2 HALLIKAINEN M.
3 ESA SP-361 // P 977 VOL. 2
4 -
5 PAPER IN PROC. OF THE 'SECOND ERS-1 SYMPOSIUM: SPACE AT THE SERVICE OF OUR ENVIRONMENT', PROCEEDINGS OF A SYMPOSIUM HELD IN HAMBURG, GERMANY, 11-14 OCTOBER 1993 (INDEXED UNDER 43)

* 940238E X SP 361 43
1 DETECTING NATURAL WINTER-RELATED FEATURES USING ERS-1 SAR IMAGES (JANUARY 1994)
2 WEYDAHL D.J.
3 ESA SP-361 // P 983 VOL. 2
4 -
5 PAPER IN PROC. OF THE 'SECOND ERS-1 SYMPOSIUM: SPACE AT THE SERVICE OF OUR ENVIRONMENT', PROCEEDINGS OF A SYMPOSIUM HELD IN HAMBURG, GERMANY, 11-14 OCTOBER 1993 (INDEXED UNDER 43)

* 940239E X SP 361 43
1 SNOW-COVER DEVELOPMENT AS A COMPONENT OF THE LOCAL GEOSYSTEM ON POTTER PENINSULA, KING GEORGE ISLAND, ANTARCTICA (JANUARY 1994)
2 WUNDERLE S., GOSSMANN H. & SAURER H.
3 ESA SP-361 // P 987 VOL. 2
4 -
5 PAPER IN PROC. OF THE 'SECOND ERS-1 SYMPOSIUM: SPACE AT THE SERVICE OF OUR ENVIRONMENT', PROCEEDINGS OF A SYMPOSIUM HELD IN HAMBURG, GERMANY, 11-14 OCTOBER 1993 (INDEXED UNDER 43)

* 940240E X SP 361 43
1 CHARACTERISATION OF ERS-1 SCATTEROMETER MEASUREMENTS AND WIND RETRIEVAL (JANUARY 1994)
2 STOFFELEN A. & ANDERSON D.
3 ESA SP-361 // P 997 VOL. 2
4 -
5 PAPER IN PROC. OF THE 'SECOND ERS-1 SYMPOSIUM: SPACE AT THE SERVICE OF OUR ENVIRONMENT', PROCEEDINGS OF A SYMPOSIUM HELD IN HAMBURG, GERMANY, 11-14 OCTOBER 1993 (INDEXED UNDER 43)

* 940241E X SP 361 43
1 ERS-1 SCATTEROMETER ESTIMATES OF ANNUAL VARIATIONS OF ATLANTIC ITCZ AND PACIFIC NECC (JANUARY 1994)
2 HALPERN D., FREILICH M.H. & DUNBAR R.S.
3 ESA SP-361 // P 1003 VOL. 2
4 -
5 PAPER IN PROC. OF THE 'SECOND ERS-1 SYMPOSIUM: SPACE AT THE SERVICE OF OUR ENVIRONMENT', PROCEEDINGS OF A SYMPOSIUM HELD IN HAMBURG, GERMANY, 11-14 OCTOBER 1993 (INDEXED UNDER 43)

* 940242E X SP 361 43
1 IDENTIFICATION OF SEA ICE ZONES USING THE AMI-WIND: PHYSICAL BASES AND APPLICATIONS TO THE FDP AND CERSAT PROCESSING CHAINS (JANUARY 1994)
2 CAVANIE C. ET AL
3 ESA SP-361 // P 1009 VOL. 2
4 -
5 PAPER IN PROC. OF THE 'SECOND ERS-1 SYMPOSIUM: SPACE AT THE SERVICE OF OUR ENVIRONMENT', PROCEEDINGS OF A SYMPOSIUM HELD IN HAMBURG, GERMANY, 11-14 OCTOBER 1993 (INDEXED UNDER 43)

* 940243E X SP 361 43
1 SCATTEROMETER-RETRIEVED WINDS FROM THE ICELAND-FAEROE AREA (JANUARY 1994)
2 ESSEN H.H.
3 ESA SP-361 // P 1013 VOL. 2
4 -
5 PAPER IN PROC. OF THE 'SECOND ERS-1 SYMPOSIUM: SPACE AT THE SERVICE OF OUR ENVIRONMENT', PROCEEDINGS OF A SYMPOSIUM HELD IN HAMBURG, GERMANY, 11-14 OCTOBER 1993 (INDEXED UNDER 43)

* 940244E X SP 361 43
1 MAPPING ERS-1 WIND FIELDS OVER NORTH WEST ATLANTIC USING A VARIATIONAL OBJECTIVE ANALYSIS (JANUARY 1994)
2 SIEFRIDT L. ET AL.
3 ESA SP-361 // P 1017 VOL. 2
4 -
5 PAPER IN PROC. OF THE 'SECOND ERS-1 SYMPOSIUM: SPACE AT THE SERVICE OF OUR ENVIRONMENT', PROCEEDINGS OF A SYMPOSIUM HELD IN HAMBURG, GERMANY, 11-14 OCTOBER 1993 (INDEXED UNDER 43)

* 940245E X SP 361 43
1 METHOD TO DERIVE AVERAGE WIND FIELD FROM ERS-1 SCATTEROMETER MEASUREMENTS (JANUARY 1994)
2 BENTAMY A. ET AL.
3 ESA SP-361 // P 1023 VOL. 2
4 -
5 PAPER IN PROC. OF THE 'SECOND ERS-1 SYMPOSIUM: SPACE AT THE SERVICE OF OUR ENVIRONMENT', PROCEEDINGS OF A SYMPOSIUM HELD IN HAMBURG, GERMANY, 11-14 OCTOBER 1993 (INDEXED UNDER 43)

* 940246E X SP 361 43
1 THE VIERS-1 SCATTEROMETER ALGORITHM (JANUARY 1994)
2 JANSSEN P.A.E.M. ET AL.
3 ESA SP-361 // P 1033 VOL. 2
4 -
5 PAPER IN PROC. OF THE 'SECOND ERS-1 SYMPOSIUM: SPACE AT THE SERVICE OF OUR ENVIRONMENT', PROCEEDINGS OF A SYMPOSIUM HELD IN HAMBURG, GERMANY, 11-14 OCTOBER 1993 (INDEXED UNDER 43)

* 940247E X SP 361 43
1 APPLICATION OF ERS-1 35 DAY CYCLE ALTIMETRY DATA TO MEAN SEA LEVEL DETERMINATION IN SMALL OCEAN BASINS (JANUARY 1994)
2 FENOGLIO L. & GROTEN E.
3 ESA SP-361 // P 1041 VOL. 2
4 -
5 PAPER IN PROC. OF THE 'SECOND ERS-1 SYMPOSIUM: SPACE AT THE SERVICE OF OUR ENVIRONMENT', PROCEEDINGS OF A SYMPOSIUM HELD IN HAMBURG, GERMANY, 11-14 OCTOBER 1993 (INDEXED UNDER 43)

* 940248E X SP 361 43
1 AN ALTIMETRIC MEAN SEA SURFACE AND ITS SPECTRAL ANALYSIS (JANUARY 1994)
2 KIM M.C., SHUM C.K. & TAPLEY B.D.
3 ESA SP-361 // P 1047 VOL. 2
4 -
5 PAPER IN PROC. OF THE 'SECOND ERS-1 SYMPOSIUM: SPACE AT THE SERVICE OF OUR ENVIRONMENT', PROCEEDINGS OF A SYMPOSIUM HELD IN HAMBURG, GERMANY, 11-14 OCTOBER 1993 (INDEXED UNDER 43)

* 940249E X SP 361 43
1 MEAN SEA SURFACE COMPUTATION FROM ERS-1 DATA (JANUARY 1994)
2 WISSE E. ET AL.
3 ESA SP-361 // P 1053 VOL. 2
4 -
5 PAPER IN PROC. OF THE 'SECOND ERS-1 SYMPOSIUM: SPACE AT THE SERVICE OF OUR ENVIRONMENT', PROCEEDINGS OF A SYMPOSIUM HELD IN HAMBURG, GERMANY, 11-14 OCTOBER 1993 (INDEXED UNDER 43)

* 940250E X SP 361 43
1 ARCTIC GEODYNAMICS: ARCTIC SCIENCE AND ERS-1 SATELLITE ALTIMETRY (JANUARY 1994)
2 ANDERSON A.J. & SANDWELL D.T.
3 ESA SP-361 // P 1059 VOL. 2
4 -
5 PAPER IN PROC. OF THE 'SECOND ERS-1 SYMPOSIUM: SPACE AT THE SERVICE OF OUR ENVIRONMENT', PROCEEDINGS OF A SYMPOSIUM HELD IN HAMBURG, GERMANY, 11-14 OCTOBER 1993 (INDEXED UNDER 43)

* 940251E X SP 361 43
1 GEOID UNDULATIONS AND SEA SURFACE TOPOGRAPHY IN THE NORTH ATLANTIC FROM ALTIMETER DATA (JANUARY 1994)
2 ARENT N., HUCKELHEIM G. & KOCH K.R.
3 ESA SP-361 // P 1065 VOL. 2
4 -
5 PAPER IN PROC. OF THE 'SECOND ERS-1 SYMPOSIUM: SPACE AT THE SERVICE OF OUR ENVIRONMENT', PROCEEDINGS OF A SYMPOSIUM HELD IN HAMBURG, GERMANY, 11-14 OCTOBER 1993 (INDEXED UNDER 43)

* 940252E X SP 361 43
1 AN ALTIMETER-DERIVED GEOID IN THE ARCTIC OCEAN: FIRST RESULTS OF THE PEGASE PROJECT (JANUARY 1994)
2 BLANC F. ET AL.
3 ESA SP-361 // P 1071 VOL. 2
4 -
5 PAPER IN PROC. OF THE 'SECOND ERS-1 SYMPOSIUM: SPACE AT THE SERVICE OF OUR ENVIRONMENT', PROCEEDINGS OF A SYMPOSIUM HELD IN HAMBURG, GERMANY, 11-14 OCTOBER 1993 (INDEXED UNDER 43)

* 940253E X SP 361 43
1 SEA SURFACE TEMPERATURE AND BOUNDARY LAYER FLUXES FROM ERS-1/ATSR DATA (JANUARY 1994)
2 MATHUR A.K., ILANTHIRAYAN S. & AGARWAL V.K.
3 ESA SP-361 // P 1081 VOL. 2
4 -
5 PAPER IN PROC. OF THE 'SECOND ERS-1 SYMPOSIUM: SPACE AT THE SERVICE OF OUR ENVIRONMENT', PROCEEDINGS OF A SYMPOSIUM HELD IN HAMBURG, GERMANY, 11-14 OCTOBER 1993 (INDEXED UNDER 43)

* 940254E X SP 361 43
1 FILAMENTS AND FINE STRUCTURE OF SEA SURFACE TEMPERATURE IN ATSR IMAGE DATA (JANUARY 1994)
2 ROBINSON I.S. ET AL.
3 ESA SP-361 // P 1087 VOL. 2
4 -
5 PAPER IN PROC. OF THE 'SECOND ERS-1 SYMPOSIUM: SPACE AT THE SERVICE OF OUR ENVIRONMENT', PROCEEDINGS OF A SYMPOSIUM HELD IN HAMBURG, GERMANY, 11-14 OCTOBER 1993 (INDEXED UNDER 43)

* 940255E X SP 361 43
1 AN ASSESSMENT OF THE ACCURACY OF ATSR DUAL VIEW SEA SURFACE TEMPERATURE ALGORITHMS (JANUARY 1994)
2 THOMAS J.P. & TURNER J.
3 ESA SP-361 // P 1093 VOL. 2
4 -
5 PAPER IN PROC. OF THE 'SECOND ERS-1 SYMPOSIUM: SPACE AT THE SERVICE OF OUR ENVIRONMENT', PROCEEDINGS OF A SYMPOSIUM HELD IN HAMBURG, GERMANY, 11-14 OCTOBER 1993 (INDEXED UNDER 43)

* 940256E X SP 361 43
1 INTERCOMPARISON OF AVHRR AND ATSR DATA AND DATA PRODUCTS (JANUARY 1994)
2 BARTON I.J. ET AL
3 ESA SP-361 // P 1099 VOL. 2
4 -
5 PAPER IN PROC. OF THE 'SECOND ERS-1 SYMPOSIUM: SPACE AT THE SERVICE OF OUR ENVIRONMENT', PROCEEDINGS OF A SYMPOSIUM HELD IN HAMBURG, GERMANY, 11-14 OCTOBER 1993 (INDEXED UNDER 43)

* 940257E X SP 361 43
1 PROSPECTS FOR GLOBAL CHANGE DETECTION WITH SATELLITE SST OBSERVATIONS (JANUARY 1994)
2 ALLEN M.R. ET AL.
3 ESA SP-361 // P 1103 VOL. 2
4 -
5 PAPER IN PROC. OF THE 'SECOND ERS-1 SYMPOSIUM: SPACE AT THE SERVICE OF OUR ENVIRONMENT', PROCEEDINGS OF A SYMPOSIUM HELD IN HAMBURG, GERMANY, 11-14 OCTOBER 1993 (INDEXED UNDER 43)

* 940258E X SP 361 43
1 ERS-1 SCATTEROMETER MEASUREMENTS OVER THE SOUTHERN OCEAN (JANUARY 1994)
2 FREILICH M.H.
3 ESA SP-361 // P 1111 VOL. 2
4 -
5 PAPER IN PROC. OF THE 'SECOND ERS-1 SYMPOSIUM: SPACE AT THE SERVICE OF OUR ENVIRONMENT', PROCEEDINGS OF A SYMPOSIUM HELD IN HAMBURG, GERMANY, 11-14 OCTOBER 1993 (INDEXED UNDER 43)

* 940259E X SP 361 43
1 SURFACE WIND AND PRECIPITATION PATTERNS IN TROPICAL CYCLONES OBSERVED WITH THE ERS-1 SCATTEROMETER AND WITH THE SSM/I (JANUARY 1994)
2 QUILFEN Y. ET AL.
3 ESA SP-361 // P 1117 VOL. 2
4 -
5 PAPER IN PROC. OF THE 'SECOND ERS-1 SYMPOSIUM: SPACE AT THE SERVICE OF OUR ENVIRONMENT', PROCEEDINGS OF A SYMPOSIUM HELD IN HAMBURG, GERMANY, 11-14 OCTOBER 1993 (INDEXED UNDER 43)

* 940260E X SP 361 43
1 COMPARISON OF ERS-1 SCATTEROMETER AND FLORIDA STATE UNIVERSITY TROPICAL WINDS (JANUARY 1994)
2 LEGLER D.M. & O'BRIEN J.J.
3 ESA SP-361 // P 1123 VOL. 2
4 -
5 PAPER IN PROC. OF THE 'SECOND ERS-1 SYMPOSIUM: SPACE AT THE SERVICE OF OUR ENVIRONMENT', PROCEEDINGS OF A SYMPOSIUM HELD IN HAMBURG, GERMANY, 11-14 OCTOBER 1993 (INDEXED UNDER 43)

* 940261E X SP 361 43
1 ERS-1 SURFACE WIND OBSERVATIONS OVER A CYCLONE SYSTEM IN BAY OF BENGAL DURING NOVEMBER 1992 (JANUARY 1994)
2 KISHTWAL C.M. ET AL.
3 ESA SP-361 // P 1127 VOL. 2
4 -
5 PAPER IN PROC. OF THE 'SECOND ERS-1 SYMPOSIUM: SPACE AT THE SERVICE OF OUR ENVIRONMENT', PROCEEDINGS OF A SYMPOSIUM HELD IN HAMBURG, GERMANY, 11-14 OCTOBER 1993 (INDEXED UNDER 43)

* 940262E X SP 361 43
1 TROPICAL CYCLONE MONITORING USING ERS-1 SCATTEROMETER DATA (JANUARY 1994)
2 ROQUET H. & POITEVIN J.
3 ESA SP-361 // P 1133 VOL. 2
4 -
5 PAPER IN PROC. OF THE 'SECOND ERS-1 SYMPOSIUM: SPACE AT THE SERVICE OF OUR ENVIRONMENT', PROCEEDINGS OF A SYMPOSIUM HELD IN HAMBURG, GERMANY, 11-14 OCTOBER 1993 (INDEXED UNDER 43)

* 940263E X SP 361 43
1 ERS-1 SAR USE TO DETERMINE LAKE DEPTHS IN ARCTIC AND SUB-ARCTIC REGIONS (JANUARY 1994)
2 MELLOR J.C.
3 ESA SP-361 // P 1141 VOL. 2
4 -
5 PAPER IN PROC. OF THE 'SECOND ERS-1 SYMPOSIUM: SPACE AT THE SERVICE OF OUR ENVIRONMENT', PROCEEDINGS OF A SYMPOSIUM HELD IN HAMBURG, GERMANY, 11-14 OCTOBER 1993 (INDEXED UNDER 43)

* 940264E X SP 361 43
1 ERS-1 SCATTEROMETER DATA PROCESSING OVER THE MEDITERRANEAN SEA: ALGORITHM DEVELOPMENT AND VALIDATION ACTIVITIES AT I-PAF (JANUARY 1994)
2 BARTOLONI A. ET AL.
3 ESA SP-361 // P 1149 VOL. 2
4 -
5 PAPER IN PROC. OF THE 'SECOND ERS-1 SYMPOSIUM: SPACE AT THE SERVICE OF OUR ENVIRONMENT', PROCEEDINGS OF A SYMPOSIUM HELD IN HAMBURG, GERMANY, 11-14 OCTOBER 1993 (INDEXED UNDER 43)

* 940265E X SP 361 43
1 ERS-1 SATELLITE DATA IN COMPARISON WITH NUMERICAL WIND AND WAVE MODEL FORECAST RESULTS (JANUARY 1994)
2 BEHRENS A. & SCHRADER D.
3 ESA SP-361 // P 1155 VOL. 2
4 -
5 PAPER IN PROC. OF THE 'SECOND ERS-1 SYMPOSIUM: SPACE AT THE SERVICE OF OUR ENVIRONMENT', PROCEEDINGS OF A SYMPOSIUM HELD IN HAMBURG, GERMANY, 11-14 OCTOBER 1993 (INDEXED UNDER 43)

* 940266E X SP 361 43
1 OBSERVATIONS WITH THE ROWS INSTRUMENT DURING THE GRAND BANKS CALIBRATION/VALIDATION EXPERIMENTS (JANUARY 1994)
2 VANDEMARK D. & CHAPRON B.
3 ESA SP-361 // P 1161 VOL. 2
4 -
5 PAPER IN PROC. OF THE 'SECOND ERS-1 SYMPOSIUM: SPACE AT THE SERVICE OF OUR ENVIRONMENT', PROCEEDINGS OF A SYMPOSIUM HELD IN HAMBURG, GERMANY, 11-14 OCTOBER 1993 (INDEXED UNDER 43)

* 940267E X SP 361 43
1 CROSS CALIBRATION OF ERS-1 AND TOPEX AND GEOSAT WAVE HEIGHTS (JANUARY 1994)
2 COTTON P.D. & CARTER D.J.T.
3 ESA SP-361 // P 1165 VOL. 2
4 -
5 PAPER IN PROC. OF THE 'SECOND ERS-1 SYMPOSIUM: SPACE AT THE SERVICE OF OUR ENVIRONMENT', PROCEEDINGS OF A SYMPOSIUM HELD IN HAMBURG, GERMANY, 11-14 OCTOBER 1993 (INDEXED UNDER 43)

* 940268E X SP 361 43
1 ERS-1 SAR INVESTIGATIONS OF SNOW AND ICE FACIES ON ICE CAPS IN THE EUROPEAN HIGH ARCTIC (JANUARY 1994)
2 DOWDESWELL J.A., REES W.G. & DIAMENT A.D.
3 ESA SP-361 // P 1171 VOL. 2
4 -
5 PAPER IN PROC. OF THE 'SECOND ERS-1 SYMPOSIUM: SPACE AT THE SERVICE OF OUR ENVIRONMENT', PROCEEDINGS OF A SYMPOSIUM HELD IN HAMBURG, GERMANY, 11-14 OCTOBER 1993 (INDEXED UNDER 43)

* 940269E X SP 361 43
1 THE RASCALS SYSTEM: A TOOL FOR ERS-1 DATA PRODUCT QUALITY ANALYSIS AND SENSOR PERFORMANCE ASSESSMENT (JANUARY 1994)
2 EICHENHERR H. ET AL
3 ESA SP-361 // P 1177 VOL. 2
4 -
5 PAPER IN PROC. OF THE 'SECOND ERS-1 SYMPOSIUM: SPACE AT THE SERVICE OF OUR ENVIRONMENT', PROCEEDINGS OF A SYMPOSIUM HELD IN HAMBURG, GERMANY, 11-14 OCTOBER 1993 (INDEXED UNDER 43)

* 940270E X SP 361 43
1 CD-RECORDABLE AS NEW MEDIUM FOR THE DISTRIBUTION OF ERS-1 SAR PRODUCTS BY THE D-PAF (JANUARY 1994)
2 ENGEL H. & GREDEL J.
3 ESA SP-361 // P 1183 VOL. 2
4 -
5 PAPER IN PROC. OF THE 'SECOND ERS-1 SYMPOSIUM: SPACE AT THE SERVICE OF OUR ENVIRONMENT', PROCEEDINGS OF A SYMPOSIUM HELD IN HAMBURG, GERMANY, 11-14 OCTOBER 1993 (INDEXED UNDER 43)

* 940271E X SP 361 43
1 THE FRENCH PROCESSING AND ARCHIVING FACILITY: OVERVIEW AND STATUS (JANUARY 1994)
2 FARCY P., POULIQUEN S. & HARSCOAT M.
3 ESA SP-361 // P 1187 VOL. 2
4 -
5 PAPER IN PROC. OF THE 'SECOND ERS-1 SYMPOSIUM: SPACE AT THE SERVICE OF OUR ENVIRONMENT', PROCEEDINGS OF A SYMPOSIUM HELD IN HAMBURG, GERMANY, 11-14 OCTOBER 1993 (INDEXED UNDER 43)

* 940272E X SP 361 43
1 QUICK-LOOK OCEAN PRODUCTS GENERATION AT D-PAF (JANUARY 1994)
2 GRUBER T., ANZENHOFER M. & RENTSCH M.
3 ESA SP-361 // P 1191 VOL. 2
4 -
5 PAPER IN PROC. OF THE 'SECOND ERS-1 SYMPOSIUM: SPACE AT THE SERVICE OF OUR ENVIRONMENT', PROCEEDINGS OF A SYMPOSIUM HELD IN HAMBURG, GERMANY, 11-14 OCTOBER 1993 (INDEXED UNDER 43)

* 940273E X SP 361 43
1 OPERATIONAL PERFORMANCE OF THE GERMAN PROCESSING AND ARCHIVING FACILITY (JANUARY 1994)
2 GREDEL J.
3 ESA SP-361 // P 1197 VOL. 2
4 -
5 PAPER IN PROC. OF THE 'SECOND ERS-1 SYMPOSIUM: SPACE AT THE SERVICE OF OUR ENVIRONMENT', PROCEEDINGS OF A SYMPOSIUM HELD IN HAMBURG, GERMANY, 11-14 OCTOBER 1993 (INDEXED UNDER 43)

* 940274E X SP 361 43
1 GEOMORPHOLOGICAL MAPPING AND INVESTIGATION OF THE THAWING DYNAMICS AT POTTER PENINSULA (KING GEORGE ISLAND) (JANUARY 1994)
2 HOCHSCHILD V., STABLEIN G. & KLENKE M.
3 ESA SP-361 // P 1203 VOL. 2
4 -
5 PAPER IN PROC. OF THE 'SECOND ERS-1 SYMPOSIUM: SPACE AT THE SERVICE OF OUR ENVIRONMENT', PROCEEDINGS OF A SYMPOSIUM HELD IN HAMBURG, GERMANY, 11-14 OCTOBER 1993 (INDEXED UNDER 43)

* 940275E X SP 361 43
1 STEREO-RADARGRAMMETRIC EVALUATION OF ERS-1 SAR IMAGES: A CASE STUDY IN SOUTHERN ITALY (JANUARY 1994)
2 KAUFMANN V. ET AL.
3 ESA SP-361 // P 1211 VOL. 2
4 -
5 PAPER IN PROC. OF THE 'SECOND ERS-1 SYMPOSIUM: SPACE AT THE SERVICE OF OUR ENVIRONMENT', PROCEEDINGS OF A SYMPOSIUM HELD IN HAMBURG, GERMANY, 11-14 OCTOBER 1993 (INDEXED UNDER 43)

* 940276E X SP 361 43
1 MESOSCALE VARIATIONS IN THE ALASKA GYRE FROM ERS-1 ALTIMETER DATA (JANUARY 1994)
2 LAGERLOEF G. ET AL.
3 ESA SP-361 // P 1217 VOL. 2
4 -
5 PAPER IN PROC. OF THE 'SECOND ERS-1 SYMPOSIUM: SPACE AT THE SERVICE OF OUR ENVIRONMENT', PROCEEDINGS OF A SYMPOSIUM HELD IN HAMBURG, GERMANY, 11-14 OCTOBER 1993 (INDEXED UNDER 43)

* 940277E X SP 361 43
1 MOSAICKING ERS-1 IMAGES: DIFFICULTIES, SOLUTIONS AND RESULTS ON THE FRENCH GUYANA (JANUARY 1994)
2 ROSAZ J.M., MAITRE H. & RUDANT J.P.
3 ESA SP-361 // P 1221 VOL. 2
4 -
5 PAPER IN PROC. OF THE 'SECOND ERS-1 SYMPOSIUM: SPACE AT THE SERVICE OF OUR ENVIRONMENT', PROCEEDINGS OF A SYMPOSIUM HELD IN HAMBURG, GERMANY, 11-14 OCTOBER 1993 (INDEXED UNDER 43)

* 940278E X SP 361 43
1 GRAVITY FIELD OF THE ROSS SEA REGION FROM SATELLITE ALTIMETRY: GEODYNAMIC IMPLICATIONS FOR WEST ANTARCTICA (JANUARY 1994)
2 MCADOO D.C. ET AL.
3 ESA SP-361 // P 1227 VOL. 2
4 -
5 PAPER IN PROC. OF THE 'SECOND ERS-1 SYMPOSIUM: SPACE AT THE SERVICE OF OUR ENVIRONMENT', PROCEEDINGS OF A SYMPOSIUM HELD IN HAMBURG, GERMANY, 11-14 OCTOBER 1993 (INDEXED UNDER 43)

* 940279E X SP 361 43
1 THE VALIDATION OF ATSR MEASUREMENTS WITH IN SITU SEA TEMPERATURES (JANUARY 1994)
2 MINNETT P. & STANSFIELD K.L.
3 ESA SP-361 // P 1233 VOL. 2
4 -
5 PAPER IN PROC. OF THE 'SECOND ERS-1 SYMPOSIUM: SPACE AT THE SERVICE OF OUR ENVIRONMENT', PROCEEDINGS OF A SYMPOSIUM HELD IN HAMBURG, GERMANY, 11-14 OCTOBER 1993 (INDEXED UNDER 43)

* 940280E X SP 361 43
1 IMPLEMENTATION OF THE DLR/INPE SAR PROCESSOR FOR ERS-1 INTERFEROMETRY (JANUARY 1994)
2 MOREIRA J.R. & MURA J.C.
3 ESA SP-361 // P 1239 VOL. 2
4 -
5 PAPER IN PROC. OF THE 'SECOND ERS-1 SYMPOSIUM: SPACE AT THE SERVICE OF OUR ENVIRONMENT', PROCEEDINGS OF A SYMPOSIUM HELD IN HAMBURG, GERMANY, 11-14 OCTOBER 1993 (INDEXED UNDER 43)

* 940281E X SP 361 43
1 THE ALONG TRACK SCANNING RADIOMETER (ATSR) GLOBAL VALIDATION RESULTS (JANUARY 1994)
2 MUTLOW C.T. ET AL.
3 ESA SP-361 // P 1245 VOL. 2
4 -
5 PAPER IN PROC. OF THE 'SECOND ERS-1 SYMPOSIUM: SPACE AT THE SERVICE OF OUR ENVIRONMENT', PROCEEDINGS OF A SYMPOSIUM HELD IN HAMBURG, GERMANY, 11-14 OCTOBER 1993 (INDEXED UNDER 43)

* 940282E X SP 361 43
1 INTERFEROMETRIC SAR SIMULATOR (JANUARY 1994)
2 NIRCHIO F. & OLIVIERI A.
3 ESA SP-361 // P 1251 VOL. 2
4 -
5 PAPER IN PROC. OF THE 'SECOND ERS-1 SYMPOSIUM: SPACE AT THE SERVICE OF OUR ENVIRONMENT', PROCEEDINGS OF A SYMPOSIUM HELD IN HAMBURG, GERMANY, 11-14 OCTOBER 1993 (INDEXED UNDER 43)

* 940283E X SP 361 43
1 GEOMETRIC INTEGRATION OF MULTI-IMAGE INFORMATION (JANUARY 1994)
2 POHL C. & VAN GENDEREN J.L.
3 ESA SP-361 // P 1255 VOL. 2
4 -
5 PAPER IN PROC. OF THE 'SECOND ERS-1 SYMPOSIUM: SPACE AT THE SERVICE OF OUR ENVIRONMENT', PROCEEDINGS OF A SYMPOSIUM HELD IN HAMBURG, GERMANY, 11-14 OCTOBER 1993 (INDEXED UNDER 43)

* 940284E X SP 361 43
1 RELIEF ESTIMATION IN TROPICAL CONTEXT (FRENCH GUYANA) WITH SAR ERS-1 IMAGERY (JANUARY 1994)
2 TONON M. ET AL.
3 ESA SP-361 // P 1261 VOL. 2
4 -
5 PAPER IN PROC. OF THE 'SECOND ERS-1 SYMPOSIUM: SPACE AT THE SERVICE OF OUR ENVIRONMENT', PROCEEDINGS OF A SYMPOSIUM HELD IN HAMBURG, GERMANY, 11-14 OCTOBER 1993 (INDEXED UNDER 43)

* 940285E X SP 361 43
1 CONTRIBUTION OF ERS-1 SAR DATA TO HYDROLOGIC APPROACH IN TROPICAL AREA: EXAMPLE OF FRENCH GUYANA (JANUARY 1994)
2 LOINTIER M. ET AL.
3 ESA SP-361 // P 1267 VOL. 2
4 -
5 PAPER IN PROC. OF THE 'SECOND ERS-1 SYMPOSIUM: SPACE AT THE SERVICE OF OUR ENVIRONMENT', PROCEEDINGS OF A SYMPOSIUM HELD IN HAMBURG, GERMANY, 11-14 OCTOBER 1993 (INDEXED UNDER 43)

* 940286E X SP 361 43
1 EXPERIENCES WITH ERS-1 SAR DATA PROCESSING AND GEOCODING AT THE GERMAN PAF (JANUARY 1994)
2 SCHATTLER B., ROTH A. & KOSMANN D.
3 ESA SP-361 // P 1273 VOL. 2
4 -
5 PAPER IN PROC. OF THE 'SECOND ERS-1 SYMPOSIUM: SPACE AT THE SERVICE OF OUR ENVIRONMENT', PROCEEDINGS OF A SYMPOSIUM HELD IN HAMBURG, GERMANY, 11-14 OCTOBER 1993 (INDEXED UNDER 43)

* 940287E X SP 361 43
1 ESTIMATION OF SOIL MOISTURE BY USING ERS-1 DATA (JANUARY 1994)
2 SCHOENERMARK M. ET AL.
3 ESA SP-361 // P 1277 VOL. 2
4 -
5 PAPER IN PROC. OF THE 'SECOND ERS-1 SYMPOSIUM: SPACE AT THE SERVICE OF OUR ENVIRONMENT', PROCEEDINGS OF A SYMPOSIUM HELD IN HAMBURG, GERMANY, 11-14 OCTOBER 1993 (INDEXED UNDER 43)

* 940288E X SP 361 43
1 DETERMINATION OF PHASE ERRORS OF ERS-1 SAR (JANUARY 1994)
2 SEIFERT F.M. & MOREIRA J.R.
3 ESA SP-361 // P 1279 VOL. 2
4 -
5 PAPER IN PROC. OF THE 'SECOND ERS-1 SYMPOSIUM: SPACE AT THE SERVICE OF OUR ENVIRONMENT', PROCEEDINGS OF A SYMPOSIUM HELD IN HAMBURG, GERMANY, 11-14 OCTOBER 1993 (INDEXED UNDER 43)

* 940289E X SP 361 43
1 IN SEARCH OF THE FRANKLIN EXPEDITION WITH THE AID OF ERS-1 (JANUARY 1994)
2 WADHAMS P. & SAUVADET P.
3 ESA SP-361 // P 1285 VOL. 2
4 -
5 PAPER IN PROC. OF THE 'SECOND ERS-1 SYMPOSIUM: SPACE AT THE SERVICE OF OUR ENVIRONMENT', PROCEEDINGS OF A SYMPOSIUM HELD IN HAMBURG, GERMANY, 11-14 OCTOBER 1993 (INDEXED UNDER 43)

* 940290E X SP 361 43
1 SAR OCEAN WAVE IMAGERY: SPECTRA AND STATISTICS (JANUARY 1994)
2 IETILE F.
3 ESA SP-361 // P 1343 VOL. 2
4 -
5 PAPER IN PROC. OF THE 'SECOND ERS-1 SYMPOSIUM: SPACE AT THE SERVICE OF OUR ENVIRONMENT', PROCEEDINGS OF A SYMPOSIUM HELD IN HAMBURG, GERMANY, 11-14 OCTOBER 1993 (INDEXED UNDER 43)

* 940291E E SP 361 43
1 HIGH PRECISION ORBITS FOR ERS-1: 3 DAY AND 35 DAY REPEAT CYCLES (JANUARY 1994)
2 DOW J.M. ET AL.
3 ESA SP-361 // P 1349 VOL. 2
4 -
5 PAPER IN PROC. OF THE 'SECOND ERS-1 SYMPOSIUM: SPACE AT THE SERVICE OF OUR ENVIRONMENT', PROCEEDINGS OF A SYMPOSIUM HELD IN HAMBURG, GERMANY, 11-14 OCTOBER 1993 (INDEXED UNDER 43)

* 940292E E SP 361 43
1 GLOBAL OCEAN TIDE MAPPING AND DYNAMIC SEA SURFACE TOPOGRAPHY DETERMINATION USING ERS-1 ALTIMETRY (JANUARY 1994)
2 ROMAY-MERINO M.M. ET AL.
3 ESA SP-361 // P 1355 VOL. 2
4 -
5 PAPER IN PROC. OF THE 'SECOND ERS-1 SYMPOSIUM: SPACE AT THE SERVICE OF OUR ENVIRONMENT', PROCEEDINGS OF A SYMPOSIUM HELD IN HAMBURG, GERMANY, 11-14 OCTOBER 1993 (INDEXED UNDER 43)

* 940322E E B 0078 43
1 THE ESA EARTH-OBSERVATION GUIDE AND DIRECTORY SERVICE (MAY 1994)
2 TRIEBNIG G.
3 ESA BULLETIN NO. 78 // PP 65-73
4 SEE ESA BULLETIN NO. 78, INDEXED UNDER 99
5 -

Energy Production and Conversion 44

* 940070E CRP 3745 44
1 RFCS PHASE 3 - FINAL REPORT (NOVEMBER 1993)
2 DORNIER, GERMANY (CONTR NO. 7561/88/NL/US(SC))
3 ESA CR(P)-3745 // 230 PP
4 AVAIL MF

Life Sciences

Life Sciences (General) 51

* 940059E CRP 3736 51
1 AUTOMATED BIOLAB - EXECUTIVE SUMMARY (DECEMBER 1993)
2 CARLO GAVAZZI, ITALY (CONTR NO. 10060/92/NL/JSC)
3 ESA CR(P)-3736 // 63 PP
4 AVAILABLE MF & HARD COPY (ESA PRICE CODE E1)

Aerospace Medicine 52

* 940328E X J 1801 52
1 THE USE OF MEDICAMENTS IN SPACE - THERAPEUTIC MEASURES AND POTENTIAL IMPACT OF PHARMACOKINETICS DUE TO WEIGHTLESSNESS (MARCH 1994)
2 PAVY-LE TRAON A. ET AL.
3 ESA JOURNAL VOL. 18, NO. 1 // PP 33-50
4 SEE ESA JOURNAL. INDEXED UNDER 99
5 IN SUPPORT OF THE PREPARATORY PROGRAMME FOR THE EUROPEAN MANNED SPACE INFRASTRUCTURE, THE LONG-TERM PROGRAMME OFFICE (LTPO) WITHIN ESA'S SPACE STATION AND MICROGRAVITY DIRECTORATE INITIATED A SERIES OF STUDIES AIMED AT A BETTER UNDERSTANDING OF THE PHYSIOLOGICAL AND PSYCHOLOGICAL ASPECTS OF LIVING IN SPACE. IN THIS CONTEXT, IN 1991 MEDES (INSTITUT DE MEDECINE ET PHYSIOLOGIE SPATIALE) WAS CONTRACTED BY THE AGENCY TO INVESTIGATE THE TYPE AND EFFICACY OF DRUGS AVAILABLE FOR USE BY ASTRONAUTS DURING SPACE MISSIONS TO COUNTERACT THE EFFECTS OF WEIGHTLESSNESS OR FOR MEDICAL TREATMENTS. THIS PAPER SUMMARISES THE MAIN OUTCOME OF THIS RESEARCH, IN THE CONTEXT OF THE SO-CALLED 'PHARMEMSI STUDY'. THE FIRST PART IS DEDICATED TO THE CONTENT OF THE MEDICAL KITS USED BY ASTRONAUTS IN FLIGHT, WHILE THE SECOND DESCRIBES HOW WEIGHTLESSNESS CAN MODIFY THE ACTION OF DRUGS (I.E. PHARMACODYNAMICS AND PHARMACOKINETICS PARAMETERS) ON THE HUMAN BODY. RECOMMENDATIONS ARE GIVEN ON 'SPACE PHARMACOPOEIA' AS WELL AS THE AREAS OF RESEARCH NEEDED TO ADAPT MEDICATION TO THE WEIGHTLESS ENVIRONMENT.

Behavioral Sciences 53

* 940303E CRP 3760 53
1 COGNITIVE ACTIVITY ANALYSIS TOOL SET - 35355/1/TR.1 + 2 - FINAL REPORT AND EXECUTIVE SUMMARY (OCTOBER 1993)
2 AEROSYSTEMS, U.K. (CONTR NO. 9841/92/NL/FM(SC))
3 ESA CR(P)-3760 // 132 PP AND 6 PP
4 AVAIL MF AND HARD COPY (ESA PRICE CODE E2, E0)

Man/System Technology and Life Support 54

* 940068E STM 245 54
1 BODY POSTURE IN MICROGRAVITY (MARCH 1994)
2 VERGE-DEPRE K.
3 ESA STM-245 // VI + 39 PP
4 ESA PRICE CODE: E0
5 THIS REPORT DESCRIBES THE PLANNING, EXECUTION AND ANALYSIS OF A NUMBER OF EXPERIMENTS PERFORMED UNDER CONDITIONS OF WEIGHTLESSNESS DURING PARABOLIC AEROPLANE FLIGHTS. THE AIM OF THESE EXPERIMENTS WAS TO OBTAIN DATA FOR USE IN THE ERGOMAN COMPUTER SIMULATOR, WHICH IS USED IN THE DEVELOPMENT OF MANNED SPACECRAFT WORKING AREAS. THE NEED TO OBTAIN SUCH DATA AROSE BECAUSE OF UNCERTAINTY ABOUT THE RELIABILITY OF THE NASA DATA, WHICH HAD HITHERTO BEEN THE ONLY ONES AVAILABLE. THE RESULTS OF THE EXPERIMENTS WERE SOMEWHAT INCONCLUSIVE. THIS WAS DUE TO TWO MAIN DIFFICULTIES. IN THE FIRST PLACE THE PARABOLAS FLOWN TENDED TO VARY WITH REGARD TO THE LENGTH OF TIME THE WEIGHTLESS CONDITION WAS SIMULATED AND THE SMOOTHNESS OF THE FLIGHT. IN THE SECOND PLACE, THE NUMBER OF SUBJECTS TESTED WAS QUITE SMALL, WHILE DIFFERENCES IN THE MANNER IN WHICH THEY REACTED TO 0 G WERE QUITE LARGE.

* 940311E CRP 3761 54
1 SPECIFIC METHODS FOR MMI DESIGN - FINAL REPORT AND EXECUTIVE SUMMARY (JUNE 1993)
2 CRI, DENMARK (CONTR NO.9842/92/NL/FM(SC))
3 ESA CR(P)-3761 // 305 PP AND 41 PP
4 AVAIL MF AND HARD COPY (ESA PRICE CODE E3, E0)

Mathematical and Computer Sciences

Computer Operations and Hardware 60

* 940050E CRX 3727 60
1 SILICON COMPILER ASSESSMENT AND DESIGN TOWARDS EUROPEAN SPACE SCADES-I - FINAL REPORT (MARCH 1993)
2 IMEC, BELGIUM (CONTR NO. 8615/90/NL/PM(SC))
3 ESA CR(X)-3727 // 108 PP
4 AVAILABLE MF & HARD COPY (ESA PRICE CODE E2)

* 940321E E B 0078 60
1 EVOLUTION OF THE TECHNICAL COMPUTING SERVICES AT ESTEC (MAY 1994)
2 DE JONG E. ET AL.
3 ESA BULLETIN NO. 78 // PP 60-64
4 SEE ESA BULLETIN NO. 78, INDEXED UNDER 99
5 -

Computer Programming and Software 61

* 940055E CRP 3732 61
1 ADA PAYLOAD SUPPORT SOFTWARE FOR OBDH INTELLIGENT CONTROL UNIT FINAL REPORT (JANUARY 1993)
2 THARSYS, FRANCE (CONTR NO. 9517/91/NL/SF)
3 ESA CR(P)-3732 // 38 PP
4 AVAILABLE MF & HARD COPY (ESA PRICE CODE E0)

* 940299E CRP 3756 61
1 ESA-DDC 1.1 - EXECUTIVE SUMMARY (MARCH 1994)
2 MMS, FRANCE (CONTR NO. 9558/91/NL/JG-WO 12)
3 ESA CR(P)-3756 // 37 PP
4 AVAIL MF AND HARD COPY (ESA PRICE CODE E0)

Computer Systems 62

* 940323E E B 0078 62
1 THE COLUMBUS UTILISATION INFORMATION SYSTEM 'CUIS' (MAY 1994)
2 GENDREAU G. & WILLEKENS P.
3 ESA BULLETIN NO. 78 // PP 74-79
4 SEE ESA BULLETIN NO. 78, INDEXED UNDER 99
5 -

Social Sciences

Administration and Management 81

* 940316E E B 0078 81
1 THE ESA MODIFICATION PROCEDURE AS A TOOL FOR MANAGEMENT AND ENGINEERING CONTROL (MAY 1994)
2 KAHN S.G. & DURAN M.
3 ESA BULLETIN NO. 78 // PP 20-27
4 SEE ESA BULLETIN NO. 78, INDEXED UNDER 99
5 -

Economics and Cost Analysis 83

* 940314E E B 0078 83
1 REVIEW OF INDUSTRY/ESA BUSINESS PRACTICES WITHIN THE SCIENTIFIC PROGRAMME (MAY 1994)
2 DALE D., JAGTMAN F. & DEAK T.
3 ESA BULLETIN NO. 78 // PP 7-14
4 SEE ESA BULLETIN NO. 78, INDEXED UNDER 99
5 -

* 940315E E B 0078 83
1 LA POLITIQUE INDUSTRIELLE DE L'ESA - LE CONCEPT EVOLUTIF DU 'JUSTE RETOUR' (MAY 1994)
2 IMBERT P. & GRILLI G.
3 ESA BULLETIN NO. 78 // PP 16-19
4 SEE ESA BULLETIN NO. 78, INDEXED UNDER 99
5 -

Law and Political Science 84

* 940324E E B 0078 84
1 LA CONVENTION DE L'ESA A L'OEUVRE - ENSEIGNEMENTS DU PASSE (MAY 1994)
2 LAFFERRANDERIE G. & KAYSER V.
3 ESA BULLETIN NO. 78 // PP 80-82
4 SEE ESA BULLETIN NO. 78, INDEXED UNDER 99
5 -

Space Sciences

Lunar and Planetary Exploration 91

* 940317E E B 0078 91
1 COMET P/SHOEMAKER-LEVY 9 ON COLLISION COURSE WITH JUPITER (MAY 1994)
2 BILLEBAUD F. & LEBRETON J.-P.
3 ESA BULLETIN NO. 78 // PP 28-32
4 SEE ESA BULLETIN NO. 78, INDEXED UNDER 99
5 -

* 940330E X J 1801 91
1 SPACE-PLATFORM IMPACT PROBABILITIES - THE THREAT OF THE LEONIDS (MARCH 1994)
2 BEECH M. & BROWN P.
3 ESA JOURNAL VOL. 18, NO. 1 // PP 63-72
4 SEE ESA JOURNAL, INDEXED UNDER 99
5 COMET P/TEMPEL-TUTTLE PASSES PERIHELION ON 28 FEBRUARY 1998 AND IT IS HIGHLY LIKELY THAT IN THE TIME INTERVAL FROM 1997 TO 2000 THE EARTH WILL WITNESS AT LEAST ONE METEOR STORM FROM THE ASSOCIATED LEONID METOROID STREAM. THE VERY HIGH METEOROID FLUX, AND THE CONCOMITANT RISE IN THE SPACE-PLATFORM/METEOROID IMPACT PROBABILITY THAT COULD RESULT FROM A LEONID METEOR STORM, POSES A TANGIBLE THREAT TO ALL EARTH-ORBITING SPACE PLATFORMS.

General 99

* 940313E B 0078 99
1 ESA BULLETIN, MAY 1994
2 BATTRICK B. / GUYENNE T.D. / MATTOK C. (EDS.)
3 ESA BULLETIN NO. 78 // 100 PAGES
4 NO CHARGE
5 -

* 940325E J 1801 99
1 ESA JOURNAL, MARCH 1994
2 BATTRICK B. / GUYENNE T.D. (EDS.)
3 ESA JOURNAL VOL. 18, NO. 1 // 94 PAGES
4 NO CHARGE
5 -

IEEE

IEEE COMMUNICATIONS SOCIETY

FIRST EUROPEAN WORKSHOP ON MOBILE / PERSONAL SATCOMS

(EMPS'94)

AEI

Associazione Elettrotecnica ed Elettronica Italiana

PURPOSE

To focus on the state-of-the-art and perspectives of mobile/personal satellite commmunications in the framework of hand-held and vehicular land mobile developments.

To provide a technical forum to the main European actors in the field where to debate and identify the perspectives, and to improve the interactions.

Venue:
ESA / ESRIN
Via Galileo Galilei
Frascati, Roma (Italy)

Date:
October 13-14, 1994

WORKSHOP CO-CHAIRMEN

Prof. Fulvio Ananasso
Telespazio S.p.A.
Via Tiburtina, 965
00156 Roma, Italy
Phone: +39-6-4079-3428
Fax: +39-6-4079-3624

Prof. Francesco Vatalaro
Università di Roma Tor Vergata (DIE)
Via della Ricerca Scientifica
00133 Roma, Italy
Phone: +39-6-7259-4464
Fax: +39-6-7259-4464 or +39-6-2020519
e-mail: vatalaro@tovvx1.ccd.utovrm.it

WORKSHOP ADVANCE PROGRAMME

First day:
- Session 1: Services, markets and regulatory issues
  Chairman: **Dr. M. Lopriore**
- Session 2: Concepts, systems and key technologies
  Chairman: **Prof. B.G. Evans**
- Session 3: Processing and network aspects
  Chairman: **Prof. G. Maral**
- Panel discussion A: Market prospectives
  Chairman: **Mr. P. Verhoef**

Second day:
- Session 4: Channel and radiofrequency aspects
  Chairman: **Dr. E. Lutz**
- Panel discussion B: Systems alternatives
  Chairman: **Prof. E. Del Re**

TECHNICAL PROGRAMME COMMITTEE

Prof. Fulvio Ananasso
Telespazio S.p.A, Roma, Italy
Prof. Francesco Vatalaro
Università di Roma Tor Vergata, Italy
Prof. Ezio Biglieri
Politecnico di Torino, Italy
Prof. Barry G. Evans
University of Surrey, England
Prof. Enrico Del Re
Università di Firenze, Italy
Dr. Mario Lopriore
ESA/ESTEC, Noordwijk, The Netherlands
Dr. Erich Lutz
DLR, Oberpfaffenhofen, Germany
Prof. Gérard Maral
ENST- Paris, Toulouse, France
Dr. Roger Rogard
ESA/ESTEC, Noordwijk, The Netherlands
Prof. Guido Tartara
Politecnico di Milano, Italy
Dr. Pietro Porzio Giusto
CSELT, Torino, Italy
Prof. Francesco Valdoni
Università di Roma Tor Vergata, and IIC, Italy
Mr. Paul Verhoef
European Commission, Bruxelles, Belgium

FOR REGISTRATIONS AND RESERVATIONS CONTACT THE WORKSHOP SECRETARIAT

IIC, Via Pertinace, Villa Piaggio 16125 Genova (Italy)
Tel. +39-10-2722383, Fax +39-10-2722183

PAPERS (subject to confirmation)

F. Ananasso, "Service, market and regulatory aspects for satellite PCN"
P. Verhoef, "European Commission views on satellite personal communication networks"
P. Porzio Giusto, G. Quaglione, "Technical alternatives for satellite mobile networks"
H. Kuhlen, "Multi-media satellite mobile services and systems"
J. Benedicto, "Key technologies for future mobile and personal satellite communications"
M. Lisi, M. Piccinni, A. Vernucci, "Payload design alternatives for geostationary personal communications satellites"
R. De Gaudenzi, T. Garde, F. Giannetti, M. Luise, "An overview of CDMA techniques for mobile and personal satellite communications"
E. Del Re, "Interworking procedures between satellite and terrestrial systems"
P. Dondl, "Integration between satellite and cellular: the ETSI point of view "
A. Böttcher, G.E. Corazza, E. Lutz, F. Vatalaro, M. Werner, "Aspects of satellite constellation and system connectivity analysis"
C. Cuellen, A. Sammut, H. Xiaoping, W. Zhao, R. Tafazzuoli, B.G. Evans, "Network and signalling aspects of satellite personal communication networks (S-PCN)"
B.G. Evans, G. Butt, M.A.N. Parks, "Channel models for mobile/personal satellite communication systems"
P. Capodieci, R. Del Ricco, A. Vernucci, "Gateway earth stations for future LEO communications satellite systems"
E. Biglieri, "Advances in modulation and coding for the satellite mobile channel"
G.E. Corazza, A. Jahn, E. Lutz, F. Vatalaro, "Channel characterization for mobile satellite communications"
G. Di Bernardo, A. Rallo, E. Damosso, L. Stola, M. Sforza, "Propagation models for the land mobile satellite channel: validation aspects"

PANELISTS (subject to confirmation)

A) **Mr. G. Berretta** (EUTELSAT), **Ms. C. Johnson** (Iridium Inc.), **Mr. H. Kuhlen** (Deutsche Aerospace), **Mr. J. Yeomans** (KPMG)

B) **Mr. J. Huber** (Siemens), **Mr. C. Mastracci** (Alenia Spazio), **Mr. D. Rouffet** (Alcatel Espace), **Prof. G. Stette** (ETSI) and a **ESA representative**

SPONSORS

- Università di Roma Tor Vergata
- Telespazio
- ESA - European Space Agency
- IIC - Istituto Internazionale delle Comunicazioni
- Alenia Spazio

COOPERATING ORGANIZATIONS

- AEI - Associazione Elettrotecnica ed Elettronica Italiana
- IEEE Communications Society
- IEEE Region 8
- IEEE Satellite and Space Communications Committee
- ETSI - European Telecommunications Standards Institute
- European Commission, DG XIII - Satellite policy (approval pending)

Publications Available from ESA Publications Division

Publication	Number of issues per year	Scope/Contents	Availability	Source
Periodicals				
ESA Bulletin	4	ESA's primary magazine	Free of charge	ESA Publications Division, ESTEC, 2200 AG Noordwijk, The Netherlands
ESA Journal	4	ESA's learned journal	..	
Earth Observation Quarterly (English or French)	4	Remote-sensing newspaper	..	..
ECSL News	4	Newspaper of the European Centre for Space Law (under the auspices of ESA)	..	..
Reaching for the Skies	4	Space Transportation Systems newspaper	..	..
Microgravity News (English with French summaries)	3	Microgravity Programme newspaper	..	..
Preparing for the Future	4	Technology Programme newspaper	..	..
Monographs	**Code**			
Conference Proceedings	(SP-xxx)	Volumes of specific Conference papers	Prices below	ESA Publications Division, ESTEC, 2200 AG Noordwijk, The Netherlands
Scientific/Technical Monographs	(SP-xxxx)	Specific/detailed information on graduate-level subjects	..	
ESA Brochures	(BR-xxx)	Summaries of less than 50 pages on a specific subject	..	..
ESA Folders	(F-xxx)	'Folders' giving short descriptions of subjects for the space-interested layman	Free of charge	..
Scientific & Technical Reports	(STR-xxx)	Graduate level — reflecting ESA's position on a given subject	Prices below	..
Scientific & Technical Memoranda	(STM-xxx)	Graduate level — latest but not finalised thinking on a given subject	..	..
Procedures, Standards & Specifications	(PSS-xxx)	Definitive requirements in support of contracts	..	..
Other Publications				
Training Manuals	(TM-xxx)	Series for education of users or potential users of ESA programmes, services or facilities	..	..
Technical Translations	(TT-xxx)	Translations of national space-related documents — (Microfiche or photocopy only)	Prices from ESRIN	ESRIN, Via Galileo Galilei, CP64, 00044 Frascati, Italy, or ESA/IRS Office, 8-10 Mario Nikis 75738 Paris 15, France
Public-relations material		General literature, posters photographs, films, etc.		ESA Public Relations Service 8-10 rue Mario-Nikis 75738 Paris 15, France

Charges for printed documents	E0	E1	E2	E3	E4
Number of pages in document	1–50	51–100	101–200	201–400	401–600
Price (Dutch Guilders)	35	50	70	80	100

Note from Head of ESA Publications Division:

In the last three years we have left the price of our publications unchanged. Costs have risen in that time, particularly postal charges, and from 1 January 1994 new prices will be charged as shown above.

To compensate for this increase two discounts will be possible:

a. *All orders over Dfl. 110 – discount of 10%.*
b. *All orders for addresses outside Europe over Dfl. 110 – no extra payment for airmail.*

Order Form for ESA Publications

IMPORTANT

1. Orders must be accompanied by a Cheque or International Banker's Draft, in Dutch Guilders, made payable to 'ESA Publications Division'. No publications will be sent before receipt of payment.
2. Within Europe mailing is free-of-charge. Outside Europe airmail is free-of-charge for orders over Dfl. 110; smaller orders are sent sea mail.

RETURN TO: FINANCE DIVISION (EFA/P)
ESTEC, POSTBUS 299
2200 AG NOORDWIJK
THE NETHERLANDS

No. of copies	ESA reference	Title	Price per copy, Dfl.	Total Dfl.

Total:

Discount for orders over Dfl. 110: 10% of total: . . . .

Total amount enclosed: Dfl. . . . .

MAILING ADDRESS (Print carefully)

Name . . . .

Function . . . .

Organisation . . . .

Mailing Address . . . .

. . . .

Town & Postal Code . . . .

Country . . . .

Date . . . . Signature . . . .

METHOD OF PAYMENT (Please tick box)

[ ] Cheque
[ ] International Banker's Draft

enclosed, made payable to ESA Publications Division'.

NOTES FOR CONTRIBUTORS

Contributions, which should be original papers, should be addressed to ESA Publications Division (attn. B. Battrick), c/o ESTEC, Noordwijk, The Netherlands.

Manuscripts and Illustrations

The manuscript should be neatly typed on one side of the paper only, with double spacing and an adequate left-hand margin. Mathematics, where not typed, should be very clearly written.

Diagrams and illustrations should be separate from the typescript and of sufficient quality to permit distinct reproduction. Line drawings should be clear, with lettering large enough to be legible when reduced for printing. Glossy photographs (approx. 18×24 cm) permit the best quality of reproduction. A separate list of captions and legends should be submitted, with a clear indication of which illustration they must accompany.

Abstract

This should be as brief as possible (normally not more than 150 words) and should summarise the conclusions of the paper. It should be self-explanatory and not require reference to the paper itself. It should be provided in both English and French where possible.

References

Bibliographical references should be numbered and listed at the end of the paper, and noted in the text with Arabic indices.

For periodicals, the author's name, year of publication, title of the article, abbreviated name of the periodical, volume number, issue number and page numbers should be quoted. For books, the author's or editor's name, year of publication, title of the book, volume (where applicable), page numbers, name and location of publisher should be given.

RECOMMANDATIONS AUX AUTEURS

Le Journal publie des articles orginaux; ces derniers doivent être adressés à l'ESA, Division des Publications, ESTEC, Noordwijk, Pays-Bas (à l'attention de B. Battrick).

Textes et illustrations

Les textes doivent être correctement dactylographiés, au recto seulement, avec double interligne et une marge suffisante à gauche. Les formules mathématiques qui ne sont pas dactylographiées doivent être soigneusement écrites à la main.

Les illustrations originales (dessins, photographies . .), qui seront fournies sur des feuilles séparées du texte, doivent être d'une qualité suffisante pour permettre une reproduction claire. Les dessins doivent être assez nets et comporter des annotations assez grandes pour rester lisibles après réduction. Les photographies sur papier glacé (format 18×24 cm) permettent les meilleures reproductions. Une liste des légendes sera fournie sur une feuille séparée, avec indication précise de la figure que chacune d'elles accompagne.

Résumé

Chaque texte est accompagné d'un résumé succinct (pas plus de 150 mots) qui fait ressortir avec concision les points saillants et les conclusions de l'étude. Ce résumé sera fourni, dans la mesure du possible, en anglais et en français.

Références

Les références bibliographiques doivent être numérotées et regroupées dans une liste à la fin du texte.

Pour les périodiques, on indiquera dans l'ordre: nom(s) de(s) auteur(s), année de publication, titre de l'article, nom du périodique en abrégé, numéros du volume et du fascicule, nombre de pages. Pour les livres, on indiquera: nom(s) de(s) auteur(s) ou responsable(s) de la publication, année de publication, titre du livre, tome, pages concernées, éditeur et lieu de parution.

european space agency / agence spatiale européenne
8-10 rue Mario Nikis
75738 Paris 15 France